Nitrogen Isotopic Variation in Irons and Other Fe-Ni Metal Rich Meteorites

Thesis

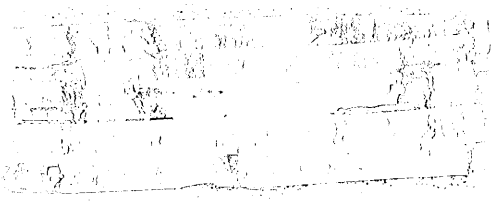

Nitrogen Isotopic Variation in Irons and Other Fe-Ni Metal Rich Meteorites.

by

Ian Franchi, B.Sc. St.And.

A dissertation submitted for the degree of
DOCTOR OF PHILOSOPHY
at the Open University

March 1988

Department of Earth Sciences,
Open University

Date of submission: 25 March 1988

Date of award: 14 July 1988

ProQuest LLC
789 East Eisenhower Parkway
P.O. Box 1346
Ann Arbor, MI 48106 - 1346

ABSTRACT

An investigation of the nitrogen concentration, its distribution, location and isotopic composition in iron meteorites and the anomalous metal-rich mesosiderite Bencubbin has been undertaken with the use of a high sensitivity mass spectrometer. Existing stepped heating extraction systems were modified for the types of material analysed in this study and a laser microprobe technique was developed for the purpose of analysing well characterised sample areas of the Bencubbin meteorite with high spatial resolution.

The irons display a range in $\delta^{15}N$ values which is to too large to be the result of fractionation processes in the nebula. An explanation involving primordial heterogeneity is favoured, with the iron meteorite parent bodies having sampled at least four isotopically distinct nitrogen reservoirs. One of the factors controlling the $\delta^{15}N$ variation may be an input of ^{15}N-rich nitrogen, together with ^{26}Al, from a nova event prior to solar nebula collapse. The behaviour of nitrogen during core formation processes is also considered and compared with the observed nitrogen variation in the non-magmatic group IAB. Other secondary processes affecting nitrogen in the iron meteorites are also identified. The isotopic composition of nitrogen has been used to identify genetic links between iron and stony meteorites, thereby enhancing the normal technique based on oxygen isotopic composition (prohibited by the rarity of oxygen bearing minerals).

A second factor influencing the primordial nitrogen isotopic variability has been identified in the unusual polymict breccia Bencubbin. This meteorite contains two nitrogen components, N_α and N_β, with a $\delta^{15}N$ value $\approx +1000‰$ (twice the ^{15}N content of atmospheric nitrogen), present in the metal clasts and probably in the silicate clasts and matrix also. The carrier phase of N_α appears to be a chromium-rich sulphide ($(Cr_{0.67}, Fe_{0.33})_2S_3$) with a structure similar to pseudo-hexagonal pyrrhotite, containing sulphur slightly depleted in ^{34}S. N_β may be associated with carbon showing a small enrichment of ^{13}C. The data gathered so far indicate that these components formed from a supernova.

ACKNOWLEDGEMENTS

For his initiation of this work, and his supervision and guidance throughout this study I am indebted to Dr. Colin T. Pillinger. The supervisory role of Dr. Ian P. Wright is also gratefully appreciated. Both "supervisors" are particularly thanked for their stimulating discussion of the results of this work as well as their critical reviews of this thesis.

Little work, if any, would have been possible without the willingness of the curators of meteorite collections to supply samples. I would especially like to thank Dr. Robert Hutchison and Dr. Carlton Moore for the samples they provided. I would also like to thank R. Hutchison, and Alex Bevan, for their guidance in petrographic matters of meteoritic material, as well as their well informed discussion of many aspects of this work.

I would like to thank Dr. Conel O. M. Alexander for the ATEM work performed at the Univ. of Essex, much wide ranging discussions and copious distractions. Dr. Peter W. van Calstren for preparation of some of the acid residues. Dr. Simon Kelley is also thanked for the use of unpublished data and discussion of some problems associated with the Bencubbin meteorite and development of the laser microprobe technique.

I would like to thank Simon J. Prosser, Andrew D. Morse and Steve Nichols for prompt repair and reconstruction of faulty magic boxes (electronics). The good humor, interest and help of other members of the Planetary Sciences Unit, past and present, is gratefully acknowledged. I would particularly like to thank S.J.P. for his deft handling of a life-line.

I am indebted to Jim, Conel and Richard for their choice of personal transport system, Fiona for just being there, Stuart for assistance with the mass spectrometer control software and Sarah for being so generous with her whiskey. The friendship and help of other students and staff of the Dept. of Earth Sciences, too numerous to mention, is also gratefully acknowledged.

Financial support from the Science and Engineering Research Council, my family and the Clydesdale Bank plc. is also greatly appreciated.

TABLE OF CONTENTS

LIST OF FIGURES

LIST OF TABLES

CHAPTER 1
INTRODUCTION

1.1 GENERAL INTRODUCTION

As a guide to its initial abundance in the early solar system, the photosphere of the sun indicates that nitrogen was the sixth most abundant element, constituting approximately 5% of the mass of the elements in the solar nebula, excluding hydrogen and helium (Cameron, 1982). However, the volatile nature of molecular nitrogen (which is relatively stable, both chemically and thermally) has meant that the processes involved in planetary formation and differentiation have resulted in the the vast bulk of planetary material, *i.e.* that from the interior of the planets and meteorite parent bodies, now having very low nitrogen abundances (the bulk nitrogen content of the Earth's mantle is believed to be <20ppm (*e.g.* Sweeney *et al.*, 1978; Letolle, 1980)). The atmophile behaviour of nitrogen is well expressed on the surface of the Earth where it constitutes 78% of the atmosphere and is abundant (≈1wt.%) in the biomass.

The abundance of nitrogen in a geological sample is, to a certain extent, dependent on the history of that sample, being particularly influenced by events such as heating/melting and interaction with the biosphere. However, a more informative record of the geological history of a sample will be retained in the isotopic composition of some of the elements. Isotopic variation can be brought about in a number of different ways, the most common being through radioactive decay of unstable nuclei, nuclear reactions *in situ*, isotopic fractionation or even from an initial heterogeneity.

Radioactive decay

Of the isotopes of nitrogen (^{12}N to ^{19}N) only ^{14}N and ^{15}N are stable, present in the terrestrial atmosphere with a $^{14}N/^{15}N$ ratio of 272.0 (*e.g.* Mariotti, 1983).

The most stable of the other isotopes is ^{13}N, with a half-life of only 9.96 minutes. Such a time scale is totally insignificant when dealing with most planetary processes. Similarly, of the unstable nuclei of other elements which decay to produce stable nuclei of nitrogen, the most stable is that of ^{14}C (half-life = 5370 years), which through the loss of a β^- particle produces ^{14}N. Although significantly more stable than any of the unstable nuclei of nitrogen the time scale of the decay is still short compared to many geological processes and its abundance, at least on the surface of the Earth, is so low that it can have no measurable effect on the $^{14}N/^{15}N$ ratio.

Nuclear reactions

Spallation reactions on oxygen atoms in silicate rocks exposed to Galactic cosmic rays (high energy particles (>5MeV) originating from outside the solar system) can produce significant changes in the $^{14}N/^{15}N$ ratio of a sample (*e.g.* Becker *et al.*, 1976). Evidence of exposure to cosmic rays indicates that the sample must have resided within 2 - 3m of the surface of a body with little or no atmosphere (Wasson, 1985). The production rate of spallogenic ^{15}N in lunar soils has been calculated to be 3.6×10^{-12}g g^{-1} my^{-1}* (Becker *et al.*, 1976). The production rate of ^{14}N is roughly similar (Armstrong and Alsmiller, 1971) and therefore, even with exposure ages of 10^9 years, spallogenic production of ^{15}N will have little effect on the nitrogen concentration of a sample. However, as the $^{14}N/^{15}N$ ratio of this spallogenic nitrogen is approximately 1 a significant change in the $^{14}N/^{15}N$ ratio of the sample (typically >200) can occur, particularly in low nitrogen samples. Table 1.1 shows the effect of spallogenic production of nitrogen on the $\delta^{15}N$ value of samples with different initial nitrogen concentrations.

* Footnote - The Moon shields a sample on its surface from half the cosmic ray flux, therefore, as a significant proportion of the cosmic rays can pass through small meteorites (<3m) the production rates in these bodies will be twice that of lunar samples.

	Exposure time (x 10^6 years)			
	10	50	100	500
Initial N (ppm)	$\Delta\ \delta\ ^{15}N$ (‰)			
2	+10	+50	+100	+500
10	+2	+10	+20	+100
50	+0.4	+2	+4	+20

Table 1.1 Effect of spallogenic production of nitrogen on $\delta^{15}N$ value. This table shows the calculated $\delta^{15}N$ values at different times for three samples initially containing a nitrogen concentration of 2, 10 and 50ppm and a $\delta^{15}N$ value of 0‰ exposed to a normal cosmic ray flux. The calculation is according to that of Kung and Clayton (1978) who determined that the change in $\delta^{15}N = 2 \times (t/\text{ppm N})$, where t is the exposure time in millions of years and ppm N is the initial nitrogen concentration.

Isotopic fractionation

Isotopic fractionation of nitrogen isotopes can occur through a variety of processes, the most common being when nitrogen is diffusing through a phase or across a phase boundary (including evaporation) and during chemical reactions, including simple isotope exchange processes (Hoefs, 1987). Fractionation during diffusion is a function of the molecules with the different isotopes moving at different speeds (kinetic fractionation), the molecule with the heavier isotope moving more slowly than those with the lighter isotope. Therefore, provided such processes do not proceed to completion, any residual nitrogen will be enriched in ^{15}N (O'Neil, 1986). Such fractionations are independent of temperature.

Partitioning of the two isotopes of nitrogen between co-existing phases in equilibrium can also result in isotopic variation. If the two phases are then mechanically separated the fractionation is irreversible. The magnitude of such fractionations is temperature dependent, with increasing effects as the temperature

approaches 0K (Hoefs, 1987). For most types of reaction the effect of equilibrium fractionation is small (*e.g.* Richet *et al.*, 1977) although non-equilibrium processes involving extreme conditions can produce more pronounced effects, *e.g.* reaction between excited forms of molecular nitrogen and oxygen at low temperatures (77K) can produce large enrichments of ^{15}N in the products (Manuccia and Clark, 1976).

With such a wide range of processes which can fractionate the two stable isotopes of nitrogen, measurement of the $^{14}N/^{15}N$ ratio, and comparison with that of the probable initial values, should yield valuable information on the history of the sample analysed. Within the context of this study the solar nebula can be thought of as the initial reservoir, the meteorites and their parent bodies being derived from this reservoir.

Initial heterogeneity

Isotopic variation in the present day solar system may result if the reservoir from which the solar system and its constituent parts formed (*i.e.* the solar nebula) was itself not thoroughly mixed. However, the scale of the heterogeneity in the primordial reservoir will be important in determining whether any isotopic heterogenity survives to the present day, as variations on a small scale may well be homogenised during planetary processes. Heterogeneity in the solar nebula would most probably be due to admixtures of components with distinctive isotopic compositions. Such isotopic compositions could be the result of fractionation processes in the interstellar medium such as ion-molecule reactions (Adams and Smith, 1981) or from different nucleosynthetic sources (Arnould, 1988). ^{14}N and ^{15}N are produced in different nucleosynthetic environments, nitrogen rich in ^{14}N being synthesised during the red giant or planetary nebula stage of stellar evolution and ^{15}N-rich nitrogen during novae or supernovae events (Wannier and Werner, 1985).

1.2 DETERMINATION OF NITROGEN ISOTOPE RATIOS

1.2.1 Isotopic Analysis

To permit comparisons of nitrogen isotopic compositions determined in different laboratories, the $^{14}N/^{15}N$ ratio of the sample is compared against that of an internationally accepted standard (atmospheric nitrogen) and is expressed as the δ value in per mil variation according to

$$\delta^{15}N_{AIR} = \left(\frac{(^{14}N/^{15}N)_{AIR}}{(^{14}N/^{15}N)_{sample}} - 1 \right) \times 1000$$

Conventionally, nitrogen isotopic measurements are performed on molecular nitrogen using a dual inlet dynamic vacuum gas source mass spectrometer based on the design of Nier (1947). The use of a special 4 way valve, called a change-over valve, permits rapid and repeated comparisons of equal sized aliquots of unknown sample and reference gas, thereby permitting very precise determination of $\delta^{15}N$, a typical standard error being ±0.026‰ (*e.g.* Mariotti, 1984).

The amount of gas required by a dynamic vacuum mass spectrometer is typically >0.1μmoles nitrogen. The need for such a sample size is due to relatively inefficient use of the sample gas, the gas being expanded into an inlet section and then bled through a narrow bore capillary tube into the mass spectrometer, which is open to a diffusion pump at all times (Figure 1.1). Therefore, most of the sample gas either remains in the inlet section or goes directly to the pumps. Given that many geological specimens contain small amounts of nitrogen, typically a few tens of ppm (Table 1.2) then the need for 0.1μmoles or more of sample gas to perform an analysis requires an initial sample size of the order of a gram. Although not an excessively large sample requirement for many applications it is prohibitive for certain types of precious

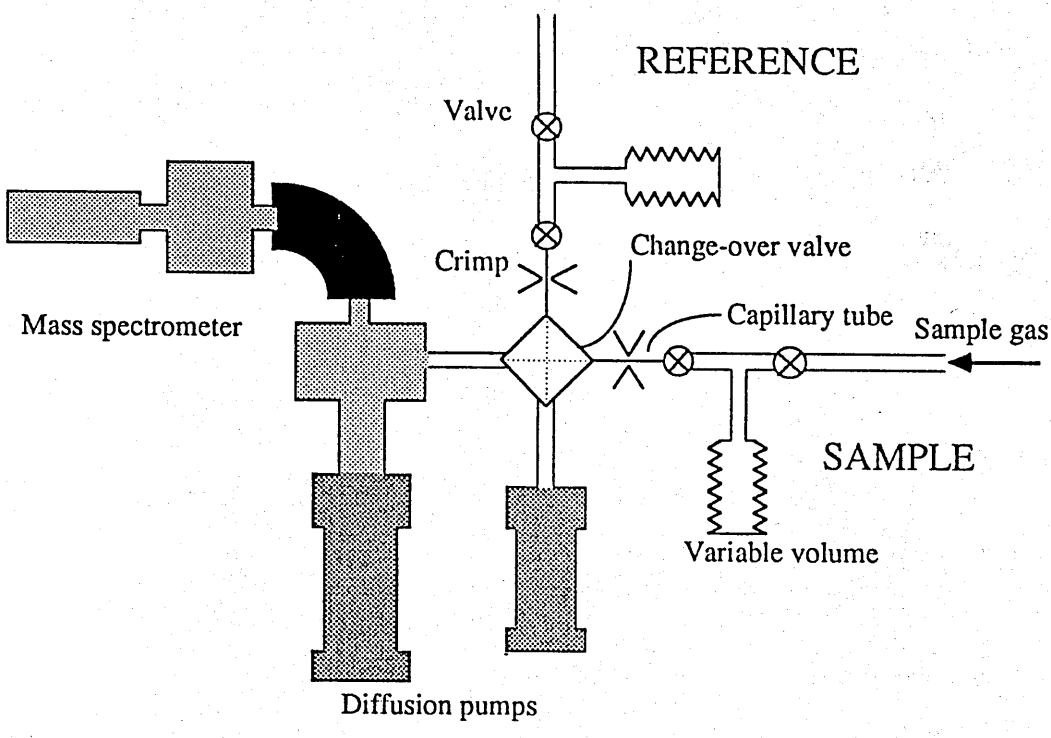

Figure 1.1 Schematic diagram of a dynamic vacuum mass spectrometer. The most characteristic feature of such an instrument is the change-over valve which allows rapid and repeated switching of the destination of gas from both sides of the inlet section. When gas from the sample side of the inlet section is being bled slowly into the mass spectrometer (which is open to a pump) gas from the reference side is bled at the same rate directly to a different pump and *vice versa*. The pressure of gas on both sides of the inlet section must be equal (by adjusting the variable volume reservoirs) and so must the rate at which gas is bled through the change-over valve (by adjustment of the crimps on the capillary tubes) to minimise instrumental effects.

materials (*e.g.* extra-terrestrial samples) or hard-won minor components (*e.g.* separates of minor minerals concentrated by physical or chemical means).

To reduce the sample size requirements an obvious improvement would be to make more efficient use of the sample gas during the analysis. Irako *et al.* (1975) and later Gardiner and Pillinger (1979) suggested employing a static vacuum mass spectrometer, developed by Reynolds (1956) for noble gas analyses, for the determination of small amounts of nitrogen and other active gases. Fallick *et al.*

(1980) proposed its use for nitrogen isotopic determination which was demonstrated by Brown and Pillinger (1981) and Frick and Pepin (1981).

To perform an analysis on a static vacuum mass spectrometer the instrument is isolated from the pumps prior to the sample gases being admitted through a high conductance valve (Figure 1.2). Following analysis of the sample gas the mass spectrometer is evacuated and an aliquot of reference gas admitted for analysis which is then used in the calculation of the $\delta^{15}N$ value. Such a configuration permits isotopic analysis of 0.1nmoles of nitrogen with a precision of ±0.24‰, *i.e.* a 1000 fold decrease in sample size against only a ten fold increase in analytical uncertainty (Wright *et al.*, 1988). The increased analytical uncertainty of the static vacuum mass spectrometers is still small compared to the errors introduced due to sample heterogeneity, sample gas extraction and purification of these gases, which introduce an uncertainty of up to ±0.7‰ for a typical conventional system (Minagawa *et al.*, 1984).

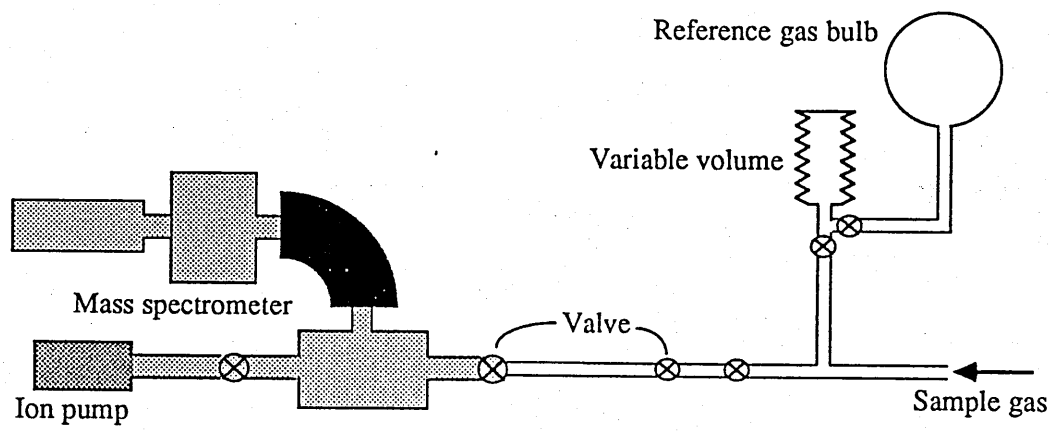

Figure 1.2 Schematic diagram of a static vacuum mass spectrometer. The operation of this instrument is simpler than that described in Figure 1.1. With the mass spectrometer isolated from the ion pump sample gas is simply expanded from the unshaded part of the inlet section into the mass spectrometer. Following the analysis the gas in the mass spectrometer is removed using the ion pump before a comparative analysis of the reference gas is made. Using the variable volume aliquottter, an aliquot of reference gas is metered out such that when it is admitted to the mass spectrometer it matches the pressure of the aliquot of sample gas.

1.2.2 Nitrogen Extraction

The most common method used to extract nitrogen from samples is to heat them, normally *in vacuo*, to temperatures at which they will either melt or decompose, although a pressure of oxygen may be introduced to promote oxidation of the sample. However, almost all samples treated in this manner will liberate two nitrogen components - nitrogen indigenous to the sample and nitrogen which can be considered a contaminant phase (trapped atmospheric gas, inorganic weathering products and organic contamination such as spores, dust, *etc.*) (Chang *et al.*, 1974). Because the abundance of nitrogen in most geological samples is very low (Table 1.2) compared to the atmosphere (78%) and biosphere (up to 14% of an individual amino acid) contamination can cause a large shift in the measured $\delta^{15}N$ value from the true value of the sample. Fortunately, most of the contamination can be removed from the sample at temperatures below 600°C while many geological samples do not liberate any nitrogen until higher temperatures. The absorbed gases will be mostly removed if the sample is heated to about 300°C and the organic material should oxidise at temperatures below 500°C. Therefore, application of a stepped heating programme allows discrimination of gases indigenous to the sample with various forms of contamination (*e.g.* Des Marais, 1978).

The principle of stepped heating to resolve indigenous nitrogen from contamination may be extended to permit identification of different indigenous nitrogen components within the same sample (Becker and Clayton, 1975). Different phases would be expected to melt/decompose/oxidise at different temperatures and therefore the nitrogen release temperature should be indicative of the nature of the carrier phase. However, where the contamination could be resolved using only 2 or 3 steps (*e.g.* Des Marais, 1978), many more steps are required to distinguish different components within a sample. As each step should liberate sufficient gas to perform an isotopic analysis, the minimum sample size requirements are considerably larger (x10) than those used in whole-

	ppm N
Meteorites	
Carbonaceous chondrites	1850
LL-group chondrites	48
L-group chondrites	21
H-group chondrites	24
Achondrites	38
Irons	18*
Igneous rocks	
Granites and granodiorites	21
Gabbros and diorites	11
Ultramafics	14
Metamorphic rocks	
Slates and phyllites	326
Schists	114
Gneisses	36
Sedimentary rocks	
Shales	1870
Greywackes	180
Sandstones	120
Limestones	73
Cherts	210

Table 1.2 Mean nitrogen concentration of typical planetary material. The data are the mean of numerous analyses summarised by Wlotzka (1974) except * which is a median value.

rock determinations. Therefore, use of a high sensitivity static vacuum mass spectrometer (as opposed to the more conventional dynamic vacuum mass spectrometers) greatly facilitates the application of this technique.

1.2.3 Microprobe Techniques

As an extension to the philosophy of determining the distribution and isotopic variation of nitrogen within samples (the purpose of high resolution stepped heating extractions) two different types of microprobe technique have been

developed, allowing spatial resolution and better characterisation of the sample. The first technique is that of the laser microprobe used by Norris *et al.* (1981). This technique involved using a laser beam to melt a sample in order to liberate the gases. The sample was sealed in an evacuated capillary tube for laser extraction, the tube then being cracked open within the inlet section of a static vacuum mass spectrometer for analysis of the evolved gases. However, although capable of detecting small amounts of nitrogen released from lunar agglutinates Norris *et al.* (1981) did not report any isotopic measurements.

The second microprobe technique to be used for nitrogen analysis is the ion probe. This method involves using a primary ion beam, normally Cs^+, to bombard an area on the surface of a sample (spot size 5 - 10μm) causing sputtering of the sample. Secondary ions from the sample generated during this process are drawn into an analytical mass spectrometer directly above the sample where the intensity of appropriate ion beams can be measured (McKeegan *et al.*, 1985). Nitrogen is analysed as CN^- and therefore analysis of nitrogen using an ion probe is limited to samples which contain both carbon and nitrogen in close spatial association. The errors on $\delta^{15}N$ measurements using such instruments are typically around ±30 to ±40‰ (*e.g.* Zinner *et al.*, 1987a), which are very large compared to more conventional mass spectrometric techniques. Therefore, the application of the ion probe is also curtailed for the present to samples where such errors are insignificant, *i.e.* those with unusual or anomalous nitrogen isotopic compositions.

1.3 NITROGEN ISOTOPIC VARIATION IN THE SOLAR SYSTEM

As can be seen in Figure 1.3 nitrogen in whole-rock samples of solar system materials displays a wide range in $\delta^{15}N$ values, from -177 to +973‰. Most measurements have been performed on samples in the laboratory, either on

terrestrial and meteoritic material or returned lunar samples, with the data for the other planets being gathered remotely by mass spectrometers aboard unmanned space probes or from high resolution infra-red spectra.

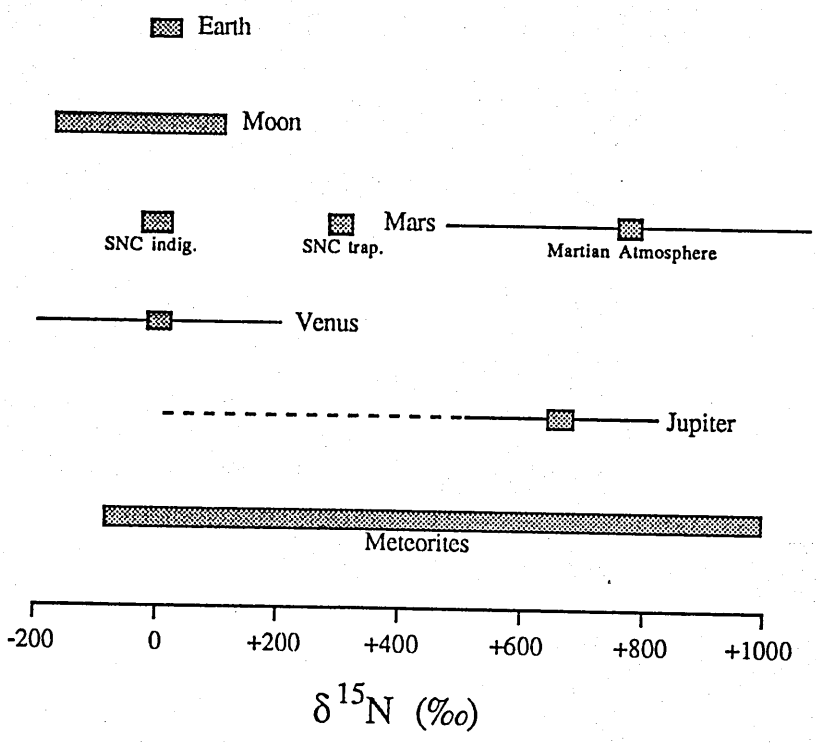

Figure 1.3 Nitrogen isotopic variation in the solar system. The $^{14}N/^{15}N$ ratio of nitrogen in a number of solar system bodies (expressed as the $\delta^{15}N$ value relative to terrestrial atmosphere). Data taken from Kaplan, 1975; Nier *et al.*, 1976; Hoffman *et al.*, 1979; Tokunaga *et al.*, 1979; Clayton and Thiemens, 1980; Becker and Pepin, 1984; Hoefs, 1987.

1.3.1 The planets

Earth and Venus

The nitrogen isotopic composition of the bulk Earth is not known, although the $\delta^{15}N$ value of the atmosphere is 0‰ (by definition) and that of mantle derived rocks ranges from -11 to +20‰ (*e.g.* Javoy *et al.*, 1984; Javoy and Pineau, 1986; Exley *et al.*, 1987; Boyd *et al.*, 1988). Such a range is very limited compared to that displayed by solar system material in general. The atmosphere of Venus, a planet very similar to Earth in many respects, also appears to contain

nitrogen with a $\delta^{15}N$ value very similar to that of the Earth, around 0‰, although as the measurement was from infra-red spectra the errors are rather large, around ±200‰ (Hoffman *et al.*, 1979).

Mars

The atmosphere of Mars is highly enriched in ^{15}N, the mass spectrometers aboard the Viking landers reporting $\delta^{15}N$ values of +770±300‰ (Nier *et al.*, 1976). However, rather than this value being the original $\delta^{15}N$ value of the nitrogen in Mars when the planet formed it is believed to be due to preferential loss of fast atoms of ^{14}N produced in the martian exosphere (McElroy *et al.*, 1976). The nitrogen isotopic composition of the SNC meteorites (shergottites, nakhlites and Chassigny), which are believed to originate from Mars (*e.g.* McSween, 1984), contain magmatic nitrogen with a $\delta^{15}N$ value of between -40 and 0‰, as well as small amounts of a trapped atmospheric component in glassy material with a $\delta^{15}N$ value of at least +310‰ (Becker and Pepin, 1984;Weins *et al.*, 1986). The light component presumably was present in the rock when it originally crystallised, and represents the isotopic composition of nitrogen in the interior of Mars (Becker and Pepin, 1984), and as such is similar to that on Earth and Venus.

Jupiter

The measurement of the $^{14}N/^{15}N$ ratio of ammonia in the Jovian atmosphere ($\delta^{15}N$ = +660‰) suggests that nitrogen in this planet is also enriched in ^{15}N (Tokunaga *et al.*, 1979). However, Tokunaga *et al.* noted a high degree of saturation of the $^{14}NH_3$ lines in the infra-red spectra used for the measurements. Such an effect could result in an apparent enrichment of ^{15}N and therefore the $\delta^{15}N$ value of nitrogen in the atmosphere of Jupiter is by no means at this stage fixed.

Moon

Rock samples collected during the Apollo missions contain low nitrogen concentrations (<5ppm) and have $\delta^{15}N$ values of up to +193‰ (Becker and Clayton, 1975). The nitrogen isotopic composition of lunar breccias and soils have lighter $\delta^{15}N$ values (Figure 1.3), with whole-rock values from -177‰ to +100‰ and higher nitrogen concentrations, up to 120ppm (Kaplan, 1975; Clayton and Thiemens, 1980). Most of this nitrogen, with its wide range in $\delta^{15}N$ values (almost 300‰), has an extra-lunar origin.

The isotopically heavy nitrogen in the lunar rocks (and also that liberated from soils at high temperatures during stepped heating) is due to spallogenic production of nitrogen in these samples when exposed on the lunar surface to cosmic ray bombardment. It is generally believed that most of the nitrogen on the lunar surface has a solar origin, being implanted solar wind particles - energetic ions which have escaped from the solar corona (*e.g.* Kerridge, 1982a). Soils with recent exposure to the solar wind have $\delta^{15}N$ values up to +156‰ (Norris *et al.*, 1983) but the much older soils, fossilised in breccias, have $\delta^{15}N$ values down to -278‰ (Carr *et al.*, 1985). There are two different explanations to account for these variations. Either there has been a secular increase in the $^{14}N/^{15}N$ ratio of the solar wind over the past 3 x 10^9 years or the isotopic composition of the solar wind has remained constant with time and a light nitrogen component has been mixed in. Becker and Clayton (1975) have suggested that this component could have been out gassed from the moon and retrapped in the soils.

Geiss and Bochsler (1982) question the ability of any possible mechanism changing the $^{14}N/^{15}N$ ratio of the solar wind over the necessary time scale ($\approx$3 x 10^9 years) and favour a model involving an admixture of variable amounts of isotopically heavy solar nitrogen and small amounts of isotopically light planetary nitrogen. However, despite detailed studies of the distribution of nitrogen in

lunar soils (Norris *et al.*, 1983; Carr *et al.*, 1985) it is not yet possible to unambiguously determine whether the light nitrogen has a solar or lunar origin.

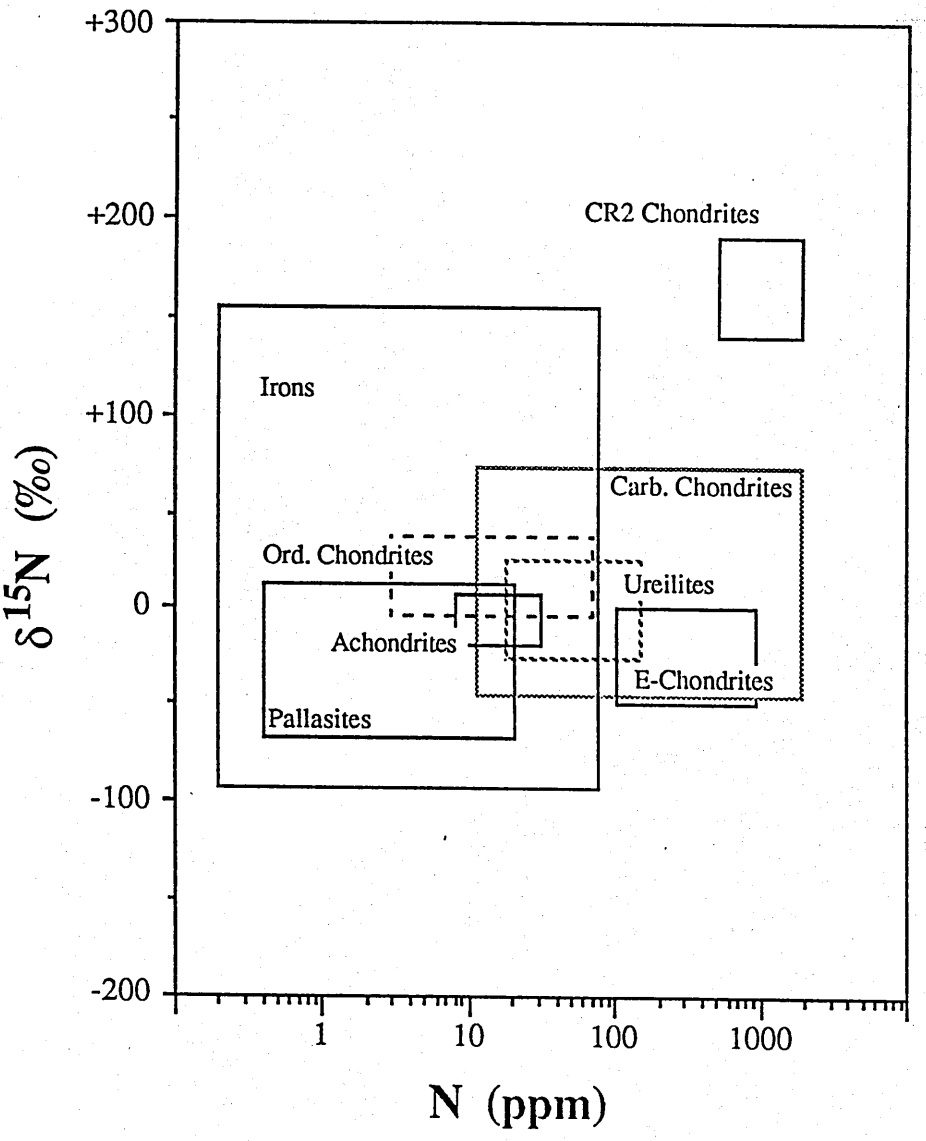

Figure 1.4 Nitrogen abundance and isotopic variation in meteorite groups. Each field defines the range of nitrogen concentration and isotopic composition displayed by "normal" members of each group. Data taken from Kung and Clayton, 1978; Prombo, 1984; Kerridge, 1985; Grady *et al.*, 1985; Grady *et al.*, 1986.

1.3.2 Nitrogen Isotopic Variation in Meteorites

As can be seen in Figure 1.3 the total range in $\delta^{15}N$ values of whole-rock meteoritic material is in excess of that displayed by the rest of the solar system. This is partly a reflection of the very diverse nature of meteorites. The following, with reference to Figures 1.4 and 1.5, is a summary of the nitrogen isotopic composition determinations in meteorites, dealing with each family of meteorites individually.

Carbonaceous chondrites

Although numerically a rather small group of meteorites, these meteorites are important samples as their composition and mineralogy indicate they have suffered very little planetary processing and so record details of the composition of the solar nebula and the processes operating within it. Because of this they are perhaps the most intensively studied meteorites (McSween, 1987). Isotopic measurements of meteoritic nitrogen are no exception to this rule, although this may partly be due to the high concentrations of nitrogen (<1890ppm) and the wide spectrum of $\delta^{15}N$ values (-45 to +190‰) which would greatly facilitate the early measurements. The most recent survey of nitrogen in the carbonaceous chondrites by Kerridge (1985) shows that different types of carbonaceous chondrites have relatively narrow ranges in $\delta^{15}N$ value (<40‰). However, Kerridge also found considerable intra-meteorite variability, *e.g.* Allende samples have yielded $\delta^{15}N$ values from -43 to +24‰ but with the abundance only varying from 18 to 30ppm. These intra-meteorite variations indicate an isotopically heterogeneous distribution of nitrogen within the specimens. A small grouplet of carbonaceous chondrites, the CR2s, contain nitrogen which is particularly enriched in ^{15}N, with $\delta^{15}N$ values up to +190‰ (Kung and Clayton, 1978; Kerridge, 1985).

The vast bulk of the nitrogen in most of the carbonaceous chondrites is present in organic molecules, from complex macromolecular kerogen-like

material to low molecular weight amino acids and amines. The solvent-insoluble macromolecular material tends to be enriched in ^{15}N, with $\delta^{15}N$ values typically around +40‰, although careful analysis by Gilmour *et al.* (1986) has shown that some of this nitrogen is more ^{15}N-enriched ($\delta^{15}N$ = +80‰). The isotopic composition of nitrogen from the amino acids is also heavy with maximum $\delta^{15}N$ values of +90‰ recorded (Becker and Epstein, 1982; Epstein *et al.*, 1987). The signature of isotopically heavy nitrogen in the amino acids, and other organic material, together with deuterium (δD = +1370‰) and ^{13}C ($\delta^{13}C$ = +23‰) enrichments is believed to have been imparted during formation in the interstellar medium (Epstein *et al.*, 1987).

Two of the more unusual nitrogen components in carbonaceous chondrites are contained in Cδ (diamonds) and Cβ (silicon carbide). The small diamonds (5 x 10^{-9}m) contain anomalous xenon (Xe-HL) as well as isotopically light nitrogen (Lewis *et al.*, 1987), with the minimum $\delta^{15}N$ value reported to date -375‰ (Ash *et al.*, 1987). The silicon carbide crystals contain the noble gas components Ne-E(H) and s-process Xe as well as exceptionally heavy carbon ($\delta^{13}C$ values up to +7300‰) and yield a wide spectrum of $\delta^{15}N$ values from -856 to +3200‰ (Zinner *et al.*, 1987a; Tang *et al.*, 1988). Both these components are believed to be circumstellar condensates, having formed around carbon rich stars. The favoured history of Cδ is one involving condensation from the envelope of a red-giant star followed by ion-implantation of the nitrogen and noble gases during a supernova event (Lewis *et al.*, 1987). The silicon carbide grains on the other hand may require a number of different nucleosynthetic events to produce the observed wide range of nitrogen, carbon, silicon and noble gas isotopic compositions (Zinner *at al.*, 1987a; Tang *et al.*, 1988).

Ordinary chondrites

Nitrogen in ordinary chondrites has not been studied in great detail, despite the fact that they are numerically more abundant than the carbonaceous chondrites

(by a factor of 20). One controlling aspect is the low abundance of nitrogen in these meteorites, typically <30ppm (*e.g.* Kothari and Goel, 1974). The ordinary chondrites have a rather limited range in $\delta^{15}N$ values, from -10 to +20‰ (Kung and Clayton, 1978), very similar to that displayed by terrestrial rocks (Figures 1.3 and 1.4). There are too little data to determine if any differences in nitrogen isotopic composition exist between the L-, LL- and H-group chondrites. Recently, Alexander *et al.* (1988) have identified unusual $\delta^{15}N$ values in the most unequilibrated ordinary chondrites, similar to the carbonaceous components Cδ and the macromolecular organic material present in carbonaceous chondrites.

Enstatite chondrites

These meteorites are particularly nitrogen rich, with up to 970ppm (Kung and Clayton, 1978; Grady *et al.*, 1986). Their high nitrogen content is due to the occurrence of nitrogen as two nitrides - osbornite (TiN) and sinoite (Si_2N_2O) as well as substitution of O^{2-} by N^{3-} in the silicate lattice (Grady *et al.*, 1986).

The isotopic composition of nitrogen in the enstatite chondrites is depleted in ^{15}N, with $\delta^{15}N$ values typically between -45 and -20‰ (Injerd and Kaplan, 1974; Kung and Clayton, 1978) although a few meteorites have $\delta^{15}N$ values up to 0‰ (Grady *et al.*, 1986). Part of the range in $\delta^{15}N$ values may be accounted for by isotopic fractionation between sinoite and osbornite and the variable proportions of each in the different samples (Grady *et al.*, 1986). One of the enstatite chondrites, Abee, contains a minor, relatively labile component highly enriched in ^{15}N, with a $\delta^{15}N$ value of +269‰ (Grady *et al.*, 1986). The identity of the carrier of this nitrogen component is not known, although it may be associated with the volatile-rich carbonaceous component "mysterite", which Ganapathy and Larimer (1980) have suggested is present in this meteorite

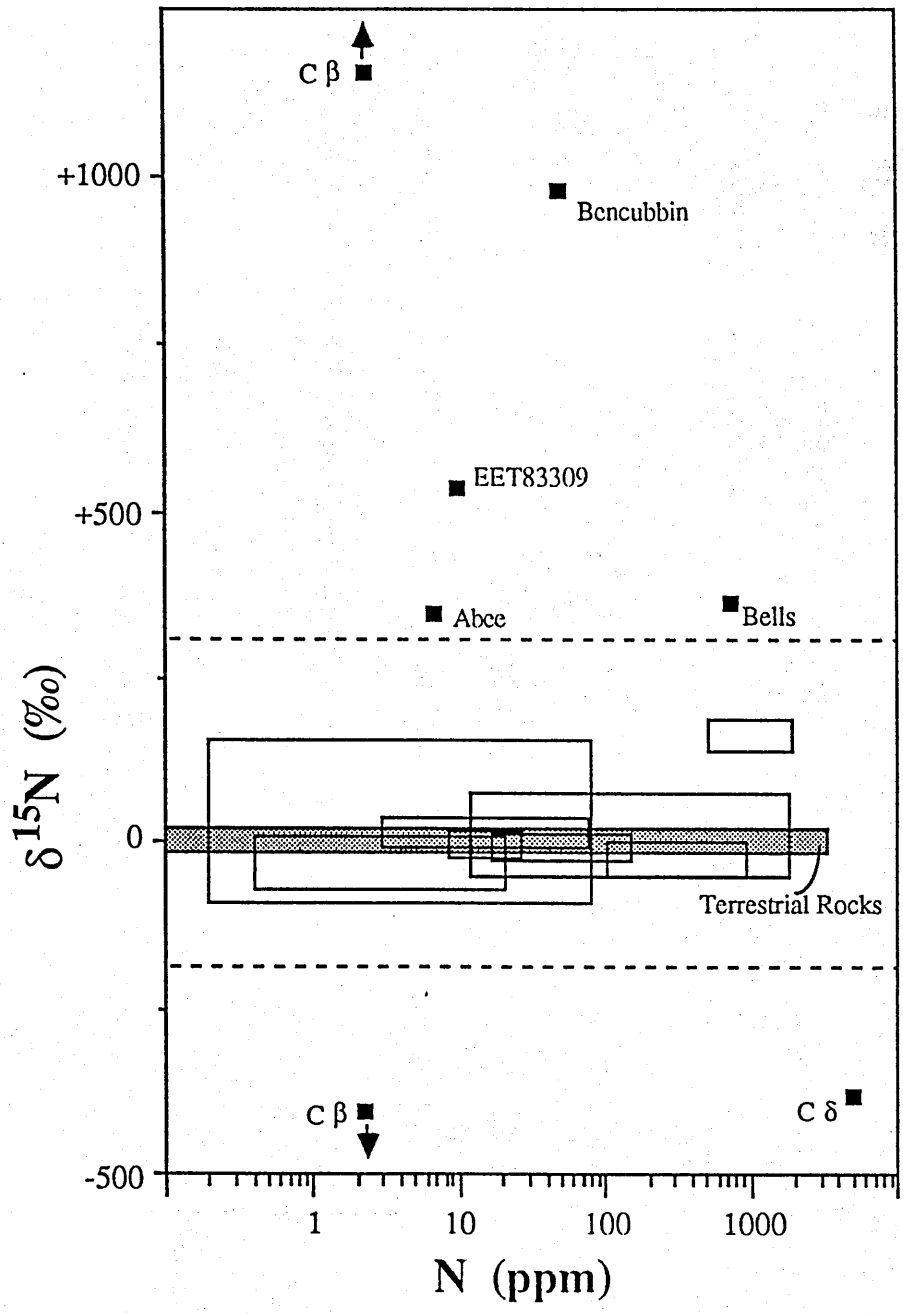

Figure 1.5 Meteorites containing extreme nitrogen isotopic compositions. The range of $\delta^{15}N$ values shown in Figure 1.4 is that between the dotted lines. The Bencubbin and Bells data are whole-rock values, the other points are the maximum/minimum values recorded during stepped heating extractions and ion probe measurements. The unlabelled boxes are those labelled in Figure 1.4. Data taken from Prombo and Clayton, 1985; Grady *et al.*, 1986; Ash *et al.*, 1987; Becker, 1987; Hoefs, 1987; Grady and Pillinger, 1988; Tang *et al.*, 1988.

Achondritic meteorites

The differentiated meteorites include the HED assemblage (the howardites, eucrites, diogenites and mesosiderites) as well as the enstatite achondrites and the ureilites. As with most other types of meteorites the number of nitrogen isotopic analyses are rather limited. Two enstatite achondrites have yielded $\delta^{15}N$ values of +4 and -24‰ (Kung and Clayton, 1978; Grady *et al.*, 1986), one eucrite has a $\delta^{15}N$ value of +5‰ (Kung and Clayton, 1978) and the metal phase of one mesosiderite has a $\delta^{15}N$ value of -8‰ (Prombo, 1984). With so few analyses it is impossible to make generalisations.

Five main group ureilites (unusual carbon-rich ultramafic meteorites) have $\delta^{15}N$ values between -25 and +26‰ (Kung and Clayton, 1978; Grady *et al.*, 1985). This range is heavier than displayed by the other achondritic meteorites, but is similar to that of the carbonaceous chondrites. This is in agreement with the observation of Clayton *et al.* (1976) who noted that the oxygen isotopic composition of the ureilites falls on a mixing line between the inclusions of C2 and C3 carbonaceous chondrites.

Three brecciated polymict ureilites have been analysed for nitrogen by Grady and Pillinger (1988). EET83309, Nilpena and North Haig all contain one, and possibly two nitrogen components enriched in ^{15}N, with $\delta^{15}N$ values up to +600‰ (Figure 1.5). The origin of the ^{15}N enrichment is unclear but may have been introduced during the brecciation event experienced by these meteorites.

Two anomalous mesosiderites, Bencubbin and Weatherford, have also been analysed for nitrogen and these two meteorites have been found to contain exceptionally heavy nitrogen, with whole-rock $\delta^{15}N$ values up to +973‰ (Prombo and Clayton, 1985; Keeling *et al.*, 1987). The complex nature of these meteorites (both are polymict breccias) and the wide range in $\delta^{15}N$ values reported from different samples of the meteorites (+414 to +973‰) indicate a complex distribution of nitrogen, and possibly the presence of a minor component even more highly enriched in ^{15}N (Prombo and Clayton, 1985).

Prombo and Clayton believe that the ^{15}N enrichment may be the result of presolar processes, probably the product of a nova explosion prior to the formation of the solar nebula or isotopic fractionation under extreme non-equilibrium conditions.

Pallasites

The metal phase of these stony-iron meteorites contains relatively low concentrations of nitrogen, from 0.4 to 21ppm and the silicate portions between 1.2 and 4.6ppm (Prombo, 1984). The $\delta^{15}N$ values measured from these samples ranged from -66 to +13‰ for the metal phase and +19 to +30‰ for the silicate phases. With only 5 analyses Prombo and Clayton (1984) were unable to infer much from the results of the metal samples but suggested that with the long cosmic ray exposure ages of the pallasites (180 to 230 x 10^6 years) spallogenic production of nitrogen in the silicates may account for the difference in the $\delta^{15}N$ value of the metal and silicate portions.

Iron meteorites

The iron meteorites, composed almost entirely of Fe-Ni metal, contain the widest range of $\delta^{15}N$ values (-92 to +153‰) displayed by any family of meteorites and they also contain the lowest nitrogen concentrations, down to 0.2ppm (Prombo, 1984). Different types of iron meteorite tend to have distinctive nitrogen isotopic compositions (Prombo and Clayton, 1983), and therefore may be useful in determining the genetic relationships between iron meteorite groups and also between iron and stony meteorites. Indeed, some of the iron and stony meteorite groups believed to be related on the basis of oxygen isotopic composition and trace element geochemistry have very similar nitrogen isotopic compositions (Prombo and Clayton, 1983). However, despite the highly differentiated nature of these meteorites, there appears to be some heterogeneity of the nitrogen, with samples from the same meteorite displaying

large ranges in $\delta^{15}N$, *e.g.* 5 analyses of Toluca have produced $\delta^{15}N$ values of -62, -55, -54, -41 and -14‰ (Pepin and Becker, 1982; Prombo, 1984).

1.3.3 Cause of Nitrogen Variation in Meteorites

The range in the isotopic composition of nitrogen displayed by whole-rock samples of meteoritic material is possibly greater than that of any other element. A number of workers have addressed the problem of explaining the range in observed $\delta^{15}N$ values (Kung and Clayton, 1978; Kerridge, 1982b; Geiss and Bochsler, 1982). One of the first problems in attempting to model the behaviour of nitrogen in the solar nebula is identifying an isotopic composition for this primordial reservoir. As most fractionation processes tend to produce enrichments of the heavier isotope Kerridge (1982b) considered starting from isotopically light values ranging from that of the ancient solar wind ($\delta^{15}N$ = -200‰) to that of the enstatite chondrites ($\delta^{15}N$ = -40‰). However, Kerridge believed neither starting composition was capable of producing the observed range of $\delta^{15}N$ values by any plausible mechanisms. Kung and Clayton (1978) had earlier come to a similar conclusion, and suggested that the more extreme variations reflected the signature of different nucleosynthetic events.

Geiss and Bochsler (1982) suggested that the mean $\delta^{15}N$ value of nitrogen in the solar system has a $\delta^{15}N$ value of +90±80‰ and that this represents an admixture of two, or possible more, components. One of these components, called "heavy lunar nitrogen", represents the dominant form of nitrogen in the solar system and has an isotopic composition comparable with present day solar wind nitrogen. The other component, which they term "light planetary nitrogen", is much less abundant and has a $\delta^{15}N$ value of ≤-500‰.

1.4 RESEARCH OBJECTIVES

The first objective of this study is to investigate further the variations of nitrogen isotopic composition in meteoritic material. The range of $\delta^{15}N$ values considered by Geiss and Bochsler (1982) and other workers who have tackled the problem of explaining the nitrogen isotopic variation in meteorites only extended from about -180 to +190‰, which at the time was considered very large. The discovery of a number of meteorites with $\delta^{15}N$ values of up to +1000‰, as well as the extreme $\delta^{15}N$ values found in the Cβ and Cδ components present in the carbonaceous chondrites greatly extends this range. The earlier models, which suggest that nitrogen in the nebula was never homogeneous do not specify the exact causes of that heterogeneity. As the median $\delta^{15}N$ values found in meteorites are probably representative of well homogenised solar nebula nitrogen it is those meteorites containing unusual nitrogen which may shed light on the origin of the $\delta^{15}N$ variations.

The main thrust of this work therefore concentrates on those meteorites with the lightest and heaviest whole-rock $\delta^{15}N$ values, *i.e.* the iron meteorites and the polymict breccia Bencubbin. An effort will be made to correlate the $\delta^{15}N$ variations of the iron meteorites with the variations in elemental abundance patterns of the different groups. This should permit an insight into the behaviour of nitrogen, and its isotopic composition, during condensation. As for Bencubbin, the relatively high abundance of isotopically anomalous nitrogen in this meteorite (≈50ppm) should greatly facilitate the process of locating and identifying any nitrogen carriers. The nature of such components should provide clues as to at least some of the processes influencing the nitrogen isotope variations in the solar system, as well as the conditions within the solar nebula which are necessary to permit the survival of unusual carriers.

The use of a high sensitivity static vacuum mass spectrometer will allow detailed examination of the nitrogen variation within individual samples, on a

scale not possible using conventional instruments, and on samples unsuitable for ion probe investigation. Such a study should not only yield information on the history of the meteorites but also the nitrogen systematics in solar system material, which should then permit a better understanding of the information contained in previous whole-rock determinations.

Iron meteorites

The relatively simple mineralogy and differentiated composition of the iron meteorites has permitted a reasonably complete understanding of many aspects of their formation history, making them suitable for initiating a detailed study of nitrogen in the early solar system. The oxygen content of the iron meteorites is generally exceptionally low and therefore spallogenic production of nitrogen in these meteorites should be virtually negligible, allowing direct measurement of the isotopic signature of the nitrogen present when the meteorite cooled at 4.5Ga. However, it is generally believed that the differentiated nature of the iron meteorites indicates that their parent bodies have suffered considerable heating, and that each group of iron meteorites belongs to a separate parent body. Therefore, to understand the inter-meteorite-group variations (imparted from the solar nebula?) it is necessary to examine the variations within the groups to understand the effects of parent body processes. The problem of variations within individual irons reported by earlier workers must also be addressed, as this has serious consequences regarding the significance of the observed inter-meteorite variations.

Determining the distribution and isotopic variation of nitrogen in the irons is facilitated by the solubility of the metal phase in weak mineral acids allowing relatively easy isolation of minor components. Chapter 3 describes the results of analyses of whole-rock and acid residue samples of iron meteorites and examines the distribution and isotopic composition of nitrogen within individual irons, their parent bodies and the solar nebula.

The choice of iron meteorites does not limit this work to simply a study of nitrogen isotopic variation. Although a great deal is known about the formation of the irons considerable gaps still remain in our knowledge. For example:

(1) The relationships between some types of iron meteorites and stony meteorites have been established on the basis of oxygen isotopic composition but this work is severely hampered by the lack of oxygen bearing minerals in iron meteorites. The use of nitrogen isotopes, present in both irons and stones, may facilitate such work and, therefore, one aspect of this study is to increase the scope for making genetic assessments.

(2) Although the formation history of most iron meteorites is well understood, some iron meteorite groups have unusual trace element abundance patterns and contain numerous silicate inclusions which cannot be readily explained by the same processes which formed most of the irons. A comparison of nitrogen isotopic variation in these groups with that in the more normal iron meteorite groups may help constrain the available models.

(3) The classification scheme currently used for iron meteorites fails to classify 14% of the irons, the use of $\delta^{15}N$ values may be of considerable use in indicating possible relationships which could then be further explored.

Bencubbin

Although many of the components in Bencubbin are coarse in size, a number of features are very small and difficult to sample. For this reason Prombo and Clayton (1985) were unable to fully explore the nitrogen systematics of the meteorite, as their minimum sample requirements was ≈1g or even larger. The use of high sensitivity static vacuum mass spectrometers provides the opportunity to advance along three different routes not open to Prombo and Clayton. Firstly,

it allows sampling of well characterised areas of the meteorite, helping establish the distribution of nitrogen within the breccia, and therefore timing of introduction. Secondly, the use of high resolution stepped heating extraction techniques on whole-rock and acid-residue samples, without resorting to excessively large sample sizes, will also yield more information on the nature of the location or carrier phase(s) of the heavy nitrogen. Finally, the nature of this meteorite is ideally suited to an investigation by a microprobe technique, the development of which is greatly facilitated by the ability of the static vacuum mass spectrometer to analyse nanogram quantities of nitrogen gas. Chapter 4 describes the application of high resolution stepped heating to whole-rock and acid residue samples of this meteorite and related meteorites along with results of a laser microprobe examination. The location and distribution of nitrogen in the meteorite and the origin of the ^{15}N enrichment are discussed in light of the results of these experiments.

A study of the distribution of nitrogen in the Bencubbin meteorite may yield information regarding the formation history of this unusual meteorite, which is a mixture of metal clasts (with possibly primitive compositions), achondritic silicate clasts (with chondritic compositions), and unusual chondritic clasts (Kallemeyn *et al.*, 1978; Hutchison, 1986). The formation of the clasts, the brecciation and melting events and Bencubbin's relationship to other meteorites are still poorly understood. A detailed study of the distribution of the isotopically unusual nitrogen in this meteorite may help to improve the situation.

To undertake all the studies described above, new techniques were developed and existing ones modified substantially. Chapter 2 describes the mass spectrometer used, its operation and performance in the configuration adopted for this study. The extraction system, for stepped heating and laser microprobe analyses, developed to cope with the types of material and small amounts of gas analysed is also described and evaluated.

CHAPTER 2
ANALYTICAL AND SAMPLE GAS PREPARATION TECHNIQUES

2.1 INTRODUCTION

The extraction techniques and analytical instrument used in this study for the purpose of determining nitrogen abundances and stable isotope ratios in metallic samples are, in a number of ways, non-conventional. The instrument used was a static vacuum mass spectrometer with a single Faraday bucket collector which achieves a gain in sensitivity of 2 to 3 orders of magnitude over conventional, dynamic vacuum mass spectrometers. Associated with any decrease in the sample size requirements of a mass spectrometer there must be a parallel reduction in the blank levels of the sample preparation technique; this has also been achieved. Other analytical techniques were also employed in this study but were generally of a more conventional nature except for the instrument used for carbon isotopic determinations which is very similar to that used for the nitrogen analyses.

Details of the nitrogen mass spectrometer are given by Wright *et al.* (1988) and a thorough description and evaluation of the extraction and purification technique by Boyd *et al.* (1988). The extraction and analytical technique used for carbon analyses is reported in detail by Carr (1985) and Carr *et al.* (1986). Therefore, this chapter will concentrate on describing and explaining the main points of the technique for nitrogen analyses and a general description of the technique for carbon. The design and operational protocol of the equipment and the technique are not constant, both being continually updated and modified as problems are encountered and solutions devised. In the interest of brevity only

the most recent design and protocol are discussed although earlier versions will be mentioned which are particularly relevant to the discussion in later chapters.

The mass spectrometer determines the isotopic composition of nitrogen by measuring the 28/29 ratio, *i.e.* that of molecular nitrogen. However, it is conventional to relate absolute data in terms of $^{15}N/^{14}N$, which is equivalent to 0.5 times the reciprocal of the 28/29 ratio. To circumvent problems of absolute calibration of different mass spectrometers, and also long term instability of individual instruments the results are expressed in the standard δ notation (see Section 1.2.1). The choice of atmospheric nitrogen as the international standard is obviously very convenient, replicate analysis from many studies having shown that the isotopic composition of atmospheric nitrogen is homogeneous, both geographically (including industrial centres) and with height above the Earth's surface (*e.g.* Dole *et al.*, 1954; Junk and Svec, 1958; Mariotti, 1983). Due to the large amounts of oxygen, carbon dioxide and other species in air a secondary working reference gas of pure nitrogen is employed, the isotopic composition being calibrated against purified aliquots of atmospheric nitrogen. It is then necessary to correct the measured $\delta^{15}N$ value for any offset between the working reference gas and AIR to obtain a true $\delta^{15}N_{AIR}$ measurement.

A number of different extraction techniques have been employed throughout this study. Stepped heating has been used extensively for both the removal of terrestrial contamination as well as characterisation of different indigenous components within samples. A description of the main types of stepped heating programmes used in this study are given in Section 2.5.

One aspect of this study was to develop a laser microprobe extraction technique. This work was initiated by Norris *et al.* (1981). These workers developed an off-line technique for nitrogen extraction, *i.e.* the laser was fired at a sample contained in a sealed evacuated quartz tube, and to analyse the evolved gas

the tube was cracked open in the inlet section of the mass spectrometer. Section 2.7 describes and evaluates an on-line laser microprobe extraction technique, *i.e.* one in which the sample chamber is connected directly to a high sensitivity static mass spectrometer.

2.2 THE MASS SPECTROMETER

2.2.1 General Description

A schematic diagram of the main components of the static vacuum, single collector mass spectrometer and the necessary electronic control/data acquisition units is shown in Figure 2.1. The actual mass spectrometer is based on a V.G. Micromass 601-type analyser head which has a 6.2cm radius flight tube and a 90°C deflection. An operational vacuum of better than 5.10^{-9} torr is maintained by the ion pump with valve VA closed, the diffusion pump and rotary pump only being used when the pressure is $>10^{-5}$ torr. All the valves on the mass spectrometer are high conductance CR-38 valves which allow rapid equilibration of gases admitted to the mass spectrometer and evacuation following analysis of these gases.

The Faraday bucket which collects the impinging ion beam is connected directly to a remote head amplifier. This converts the ion beam current signals into voltages with a basic sensitivity of 1V for every 10^{-10}A input and then transmits the signal to one of the second stage amplifiers. AMP#1 and AMP#2 are used in the normal operational mode, the former with a set gain of x1 and the latter with a gain of x100. The third second stage amplifier (AMP#3) has a variable gain from x1 to x3000 and is connected to a chart recorder to facilitate peak shape and sensitivity optimisation. Signals from AMP#1 and #2 are sent

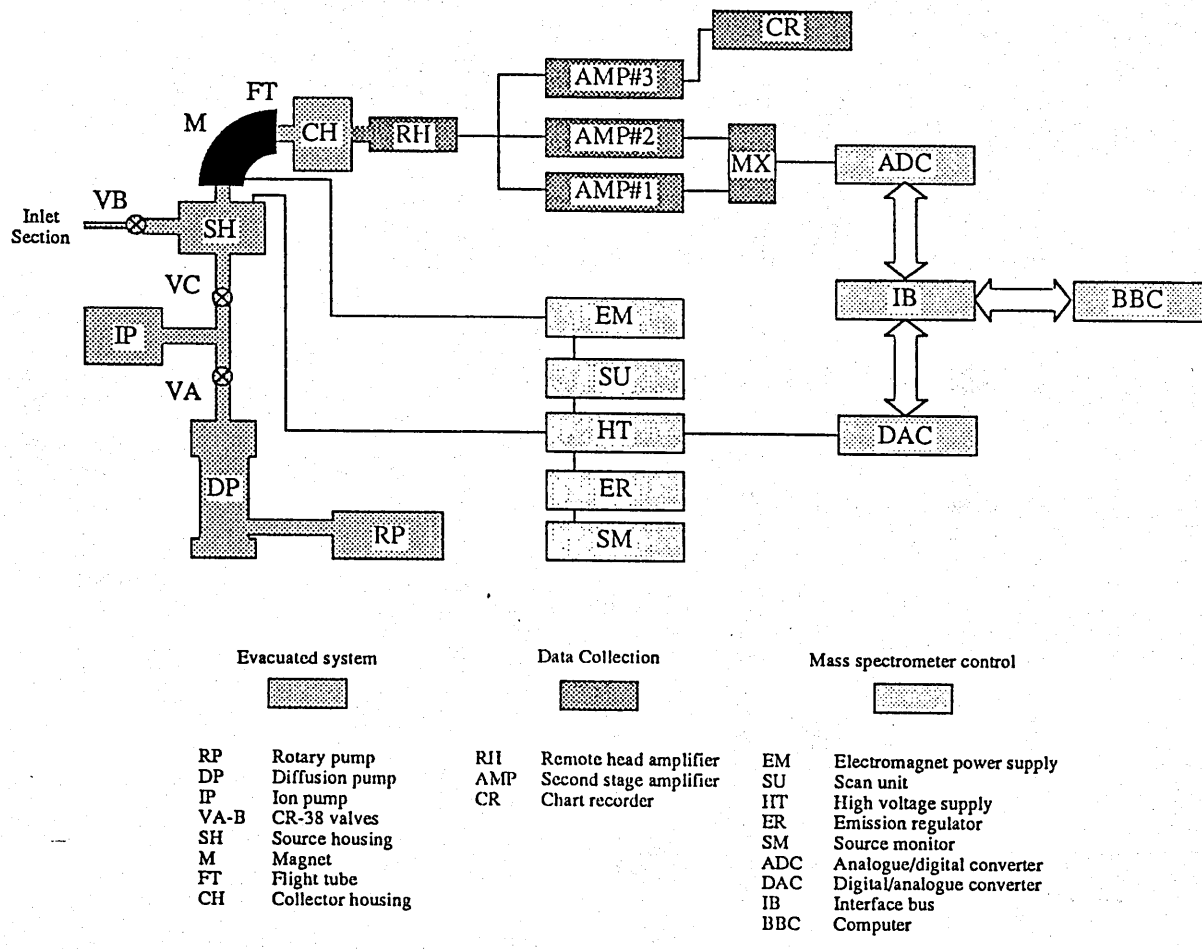

Figure 2.1 Schematic diagram of static vacuum mass spectrometer. The three main shaded regions show evacuated parts of the instrument, the data collection hardware and the units which control the mass spectrometer.

through a 16-bit analogue-to-digital converter via a multiplexor unit, and monitored by the BBC computer.

Control of the mass spectrometer is also performed by the computer. Signals from the computer, via a 2x12-bit digital-to-analogue converter control the output of the 0-5kV high voltage supply. By increasing the accelerating voltage the ion beam can be swept across the Faraday bucket. Both the accelerating voltage and the current to the electromagnet can also be controlled manually or with the scan control unit. The full range of choice of the accelerating voltage and magnetic field strength enables the collection of mass spectrometric data from m/z 1 up to 60.

2.2.2 Operation of the Instrument

With valve VC closed (Figure 2.1), the software control is initiated to coincide with opening of VB, allowing gas stored in the inlet section to pass into the mass spectrometer. The pressure of gas is allowed to equilibrate for 60 seconds before VB is once again closed. During the first half of the equilibration period, continuous monitoring of the intensity of the m/z 28 ion beam permits coarse, incremental adjustments to be made to the pressure of gas in the mass spectrometer, provided there is a reserve of nitrogen contained in the inlet section. The second half of the equilibration period is used to scan the mass range 60 to 25 to assess the purity of the gases.

To acquire isotopic data the m/z 29 and 28 ion beams are swept over the Faraday bucket 15 times. The intensity of each beam is corrected for baseline offsets and the m/z 29 beam is also adjusted for tailing of the m/z 28 beam (abundance sensitivity at m/z 29 = 60ppm of the m/z 28 beam). As there is no measurable variation in the 28/29 ratio over the time scale of an analysis (7 minutes) the mean of the measured values is calculated rather than the ratio at t=0

(time of admission). Upon completion of each analysis the mass spectrometer is pumped out through VC by the ion pump. The pump out period between successive analyses during a stepped heating or bulk extraction is approximately 8 minutes.

2.3 THE GLASS LINE

The glass line is essentially constructed of pyrex glass (o.d. 8mm, i.d. 6mm) except where high temperatures are required, in which case quartz glass (o.d. 6mm, i.d. 4mm) is employed. The valves used are mostly the "backed" valves described by McNaughton *et al.* (1983), although a number of normal valves are also employed. Operation of the valves occasionally allows small "bursts" of atmosphere into the glass line, resulting in irreproducible blanks. The backed valves maintain a separate vacuum between the atmosphere and the sample handling parts of the system therefore alleviating this problem. Initially the backs of these valves were pumped by the same diffusion pump that pumped the main part of the glass line. The number of valves in the system affects the ultimate vacuum, presumably due to small continuous leaks across the backs of the valves. As the ultimate vacuum affects the size of the blank contribution an independent pumping system was introduced to pump the backing line and parts of the laser system (see Section 2.7). With the dual pumping system a normal working pressure of 5×10^{-7} torr is achieved in the main glass line.

To facilitate pumping, and minimise the blank, it has been found necessary to keep the glass line hot (150°C). This is achieved by wrapping insulated heater tapes around all parts of the glass line through which sample gases pass. Certain parts of the glass line, however, require temperatures in excess of 150°C, *e.g.* copper oxide, sample, platinum fingers, *etc.* (Figure 2.2). To heat these fingers

Figure 2.2 Schematic diagram of the main glass line. For simplicity three sections of the glass line are not shown. (i) the section of glass line from V5 to the laser-port (Figure 2.7), (ii) the mercury manometer and aliquoting system used to refill the reference gas bulb and (iii) the line which shadows the main line for pumping backed valves - referred to as the backing line.

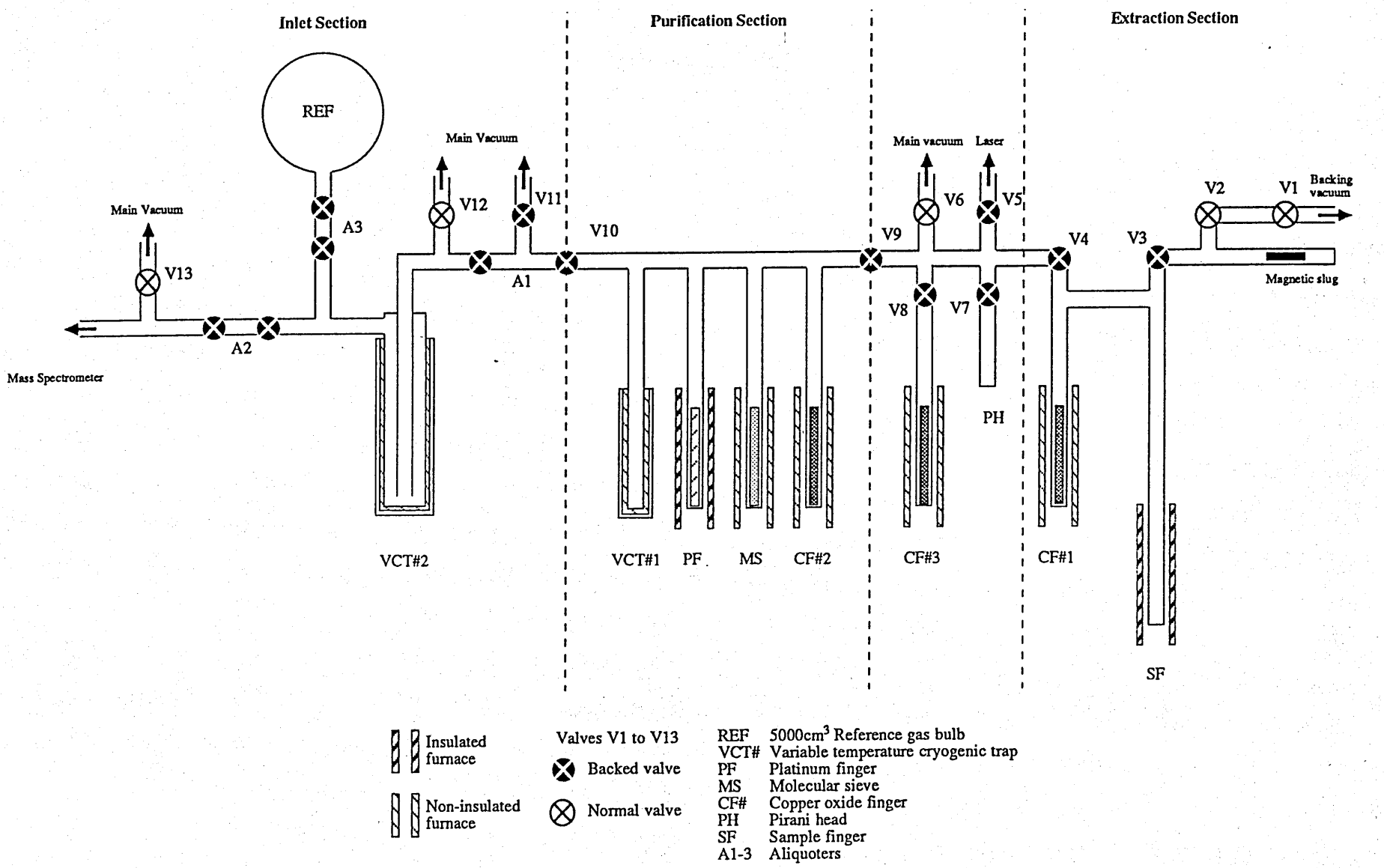
Inlet Section
Purification Section
Extraction Section
REF
Main Vacuum
Main Vacuum
Main vacuum
Laser
Backing vacuum
V13
A3
V12
V11
V10
V9
V6
V5
V4
V3
V2
V1
A2
A1
V8
V7
Magnetic slug
Mass Spectrometer
PH
VCT#2
VCT#1
PF
MS
CF#2
CF#3
CF#1
SF
Insulated furnace
Non-insulated furnace
Valves V1 to V13
Backed valve
Normal valve
REF 5000cm3 Reference gas bulb
VCT# Variable temperature cryogenic trap
PF Platinum finger
MS Molecular sieve
CF# Copper oxide finger
PH Pirani head
SF Sample finger
A1-3 Aliquoters

two types of furnace are used, termed insulated and non-insulated. The former are capable of attaining temperatures up to 1300°C but have considerable thermal inertia. The non-insulated furnaces are simply wire spirals shielded by a quartz glass sleeve. They can only achieve temperatures up to 1000°C but have the ability to change temperature very quickly (*e.g.* 450 to 850°C in 90 seconds).

The glass line can be divided into three principle sections (Figure 2.2). Firstly, there is the sample loading and extraction section, in which gases are liberated from the solid sample. These gases are transferred into the purification section, where any nitrogen bearing compounds are converted to molecular nitrogen and interfering species oxidised and separated from the nitrogen. Finally, the nitrogen from the purification section is expanded into the inlet section where it is measured out into aliquots of gas suitable for analysis in the mass spectrometer. This final section is also used to meter out suitable sized aliquots of reference gas. Each section will now be described in more detail below.

2.3.1 Sample Loading and Gas Extraction

Samples, in platinum buckets, are loaded by removing valve V2 with V1 and V3 shut (Figure 2.2). The loading arm is then evacuated through the backing line, thereby maintaining high vacuum in the main glass line. Removal of the previous sample from the bottom of the sample vessel is also achieved without loss of vacuum by carefully collapsing the quartz glass immediately above the expended sample before drawing out the glass. Prior to analysis the sample is degassed at 150°C overnight (pressure = 10^{-6} torr) and the bottom of the sample vessel heated at 1200°C.

When the sample is to be analysed its furnace is lowered to the appropriate temperature and the sample manipulated past V3 with the aid of the magnetic slug. In the case of iron meteorite specimens the magnetic slug is superfluous.

Extraction of gases is performed with V3 and V4 closed. The copper oxide finger CF#1 (wire form Cu(II)O wrapped in platinum foil) supplies oxygen to the sample if its temperature is raised to 850°C. Towards the end of each step (normally 31 minutes) oxygen is resorbed back onto the copper oxide at 600°C for 5 minutes and 450°C for 1 minute. At the end of each step the gases are transferred to the purification section through V4 and V9 with V5 to V8 and V10 shut.

Prolonged periods at high temperature with the non-insulated furnace on CF#1 in the vertical position resulted in the spacing between the winds of the wire spiral becoming uneven, due to the effect of gravity, producing "hot spots" in the furnace. Although the copper oxide is protected from reacting with the glass by a platinum foil sheath these hot spots can cause melting of oxygen depleted Cu(II)O, which flows easily through the loosely folded foil, reacts with the quartz glass and results in catastrophic loss of vacuum. With CF#1 positioned horizontally rather than vertically the life of the furnace is greatly prolonged.

2.3.2 Purification of the Sample Gases

A detailed discussion of the reactions involved in the purification of the nitrogen can be found in Boyd *et al.* (1988), the following is simply a basic outline of "what-is-happening-where". Transfer of the sample gases is accomplished by cooling the 5Å molecular sieve to liquid nitrogen temperature (-196°C) which will trap all gases except H_2, He and Ne. To liberate the gases from the molecular sieve the temperature is raised to 200°C. Excess oxygen is resorbed onto copper oxide finger CF#2, which is maintained in an oxygen-depleted state.

The interfering species which must be removed from the nitrogen include CO, CO_2, CH_4 and other organic molecules. CO_2 is readily removed from nitrogen

by cooling the variable temperature cryogenic trap (VCT#1) to -180°C (at liquid nitrogen temperatures small amounts of N_2 are also condensed). However, CO and CH_4 are permanent gases at the pressures involved and have to be oxidised to CO_2 in order that they may be removed. CH_4 is rapidly oxidised to CO in the presence of the platinum finger (1150°C) and CF#2 (450°C) with a half life of a few seconds (Boyd *et al.* 1988). CO is also oxidised in the presence of these two fingers to form CO_2, which can then be condensed out on VCT#1. It is unlikely that much CO and CH_4 is transferred from the extraction section as the presence of copper oxide and platinum (CF#1) at 850°C would rapidly oxidise any such species liberated or formed during heating of the sample. Other species which are removed by the crogenic trap at this stage are H_2O and SO_2.

The conversion of any oxides of nitrogen to molecular nitrogen is equally important. Failure to do so would lead to low yields and possible fractionation of the isotopes, as N_2O, NO and NO_2 are condensible species. N_2O has a very low stability in the purification section, with conversion to its molecular constituents complete in 15 seconds (Boyd *et al.*, 1988). NO_2 is reduced to NO quite rapidly but, unfortunately, the latter species has considerable stability in the purification section, with a half life of about 20 minutes.

However, it is unlikely that detectable quantities of NO or NO_2 are produced from combustion of iron meteorites. Nitrogen oxides are most readily formed by the breakdown of nitro- compounds (*e.g.* nitrates or nitro-benzene) or from reaction of oxygen with nitrogen bearing molecules in which nitrogen is bound to another species such as hydrogen in ammonia or carbon in organic compounds (*e.g.* Bowman, 1976). Formation of oxides of nitrogen from reaction of oxygen and molecular nitrogen on the other hand is extremely difficult, the same also appears to be true for substituted atomic nitrogen in diamonds (Boyd *et al.*, 1988). Therefore, as nitrogen in metal also exists as atomic nitrogen, or nitrides,

(Fast, 1965) it is considered that it would be very difficult for NO or NO_2 to form during combustion of metallic samples.

The normal purification procedure employed during this study lasts 11 minutes. Upon completion of the transfer of gases into the purification section (2 minutes) the molecular sieve is warmed up to 200°C (4 minutes) and the variable temperature cryotrap cooled to -175°C (4 minutes). After 10 minutes the nitrogen, plus any noble gases, are expanded into the isolated inlet section through V10 (Figure 2.2). After 1 minute V10 is closed.

The work on the Bencubbin meteorite (Chapter 4) and a few of the iron meteorites (Chapter 3) was performed without copper oxide finger CF#1. For these experiments oxygen for the combustion was derived from CF#3 and simply expanded into the extraction section at the start of each step. Such a system also offers the possibility of performing simple pyrolyses (*i.e.* the sample is heated up *in vacuo*). The lack of a finger containing hot platinum and copper oxide in the extraction section and the possibility of oxygen depletion during heating resulted in the need for an extended purification procedure. This involved cycling the copper oxide CF#2 up to 850°C for 6 minutes, then resorbing oxygen at 600°C for 6 minutes and at 450°C for 10 minutes to ensure complete combustion of any reduced species and the removal of high pressures of excess oxygen often present at the end of each step.

Although the above technique was adequate for the analysis of exceptionally heavy nitrogen in the Bencubbin meteorite from high resolution stepped heating extractions it was found to introduce unacceptable errors for the higher precision necessary in the study of whole rock samples of iron meteorites. The reason for the increased errors were due to problems in extracting the gas from the samples, which usually required repeated combustions at 1250°C. This produced two problems, firstly the blank at the maximum temperature of the system is higher

than at lower temperatures and is less predictable so close to the bake-out temperature. Secondly, there is a significant fractionation of the nitrogen isotopes due to diffusion out of the sample (Figure 2.3). Therefore, if there is incomplete recovery of the nitrogen, significant errors in the measured isotopic composition are introduced. These errors are compounded by the errors introduced by the variable blanks, which are magnified even further when corrections for blank contribution are attempted.

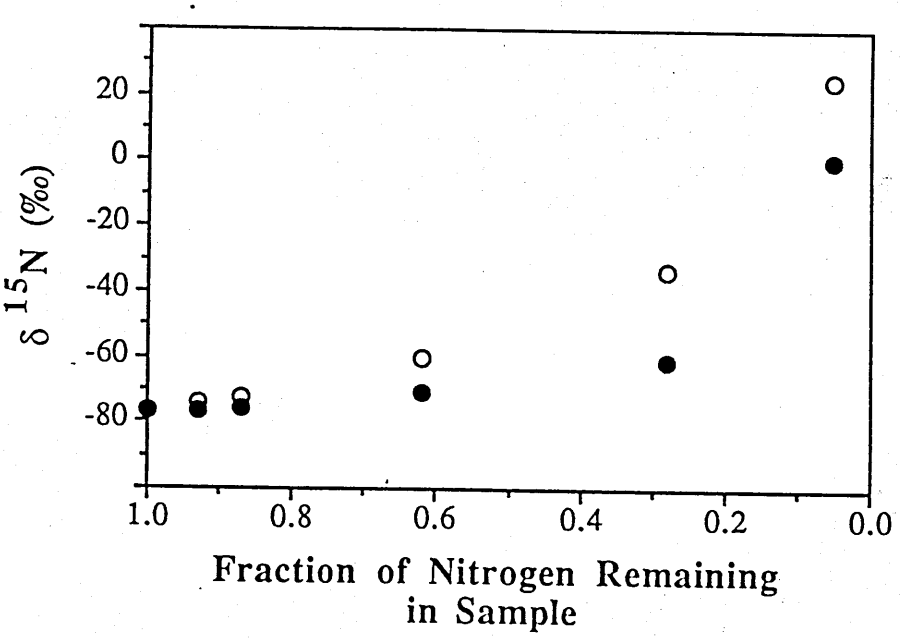

Figure 2.3 Fractionation of nitrogen during combustion of an iron meteorite. The filled circles show the isotopic composition of nitrogen remaining in the sample after each step from 900 to 1300°C during a stepped combustion of the Cape York iron meteorite. The sample was two chips - 3.2 and 5.7mg. The $\delta^{15}N$ value of the gas remaining in the sample behaves in a similar manner to that predicted if the nitrogen was simply diffusing out of the sample (open circles). The difference between the two curves is due to some of the nitrogen being released from the sample without fractionation due to oxidation of the metal. The large number of steps required to liberate all the nitrogen introduce large errors into the final $\delta^{15}N$ value. To reduce these errors samples are cut into smaller chips (<1mg), the extractions performed only at 1250°C (see Section 2.5) and a contiuous oxygen supply introduced - copper oxide finger CF#1 (Figure 2.2).

Introduction of copper oxide finger CF#1, increasing the initial step size to 60 minutes and chopping the samples into as small a chip as possible (0.1 - 0.2mm^3) (see Section 3.2) had the result of liberating about 99% of the nitrogen in one step, the remainder being recovered in a second 30 minute step at the same temperature (see Section 2.5.1).

2.3.3 Sample and Reference Gas Handling in the Inlet Section

Once expansion of the sample gases into the inlet section is complete (V10 shut) a crude estimate of the pressure of gas in the inlet section can be obtained by opening V9 (Figure 2.2) and monitoring the deflection on a Penning gauge attached to the main glass line. Armed with this first approximation, use of the two aliquotters A1 and A2 and the valves to the pumps (V11-13) it is then possible to reduce large samples to a size within the capabilities of the mass spectrometer. Any condensible species which may have evaded condensation on VCT#1 have to pass through the larger, and cooler VCT#2 (-185°C). After a total of two minutes in the inlet section the gas is expanded into the mass spectrometer.

The static vacuum mass spectrometer, as with conventional dynamic instruments, requires that the source pressure of the sample and reference gases are equal. The purpose of this is to ensure that any instrumental effects are cancelled out in the comparison of the isotopic ratio of the sample and reference gases. To deliver precisely metered aliquots of reference gas to the mass spectrometer a small, variable volume aliquotter (A3) similar in design to that described by Carr *et al.* (1986) is placed between a 5000cm^3 reference gas reservoir and the main part of the inlet section (Figure 2.2). With careful calibration of A3 and the aid of aliquotters A1 and A2 any pressure within the range of the mass spectrometer can be prepared with a precision of ±2%. The reference gas in the 5000cm^3 bulb is filled from a detachable 2000cm^3 bulb.

Introduction of a pressure of gas into the reference bulb compatible with the sensitivity of the mass spectrometer is achieved by a second aliquotting system attached to a mercury manometer on the far side of the bulb (not shown in Figure 2.2).

2.4 TECHNIQUE APPRAISAL

2.4.1 Reproducibility

The cornerstone to any geochemical technique is the stability and precision of the analytical instrument. Table 2.1 shows the results of 13 analyses of 9ng aliquots of reference gas performed during an eight hour period. Although these

Run No.	m/z 28	28/29	$\delta^{15}N$ (‰)
1	3.212	139.083	
2	3.202	139.065	+0.46
3	3.182	139.017	+0.08
4	3.208	138.992	+0.52
5	3.144	139.113	-0.44
6	3.172	139.110	+0.02
7	3.165	139.114	+0.25
8	3.189	139.187	-0.16
9	3.156	139.215	-0.14
10	3.187	139.205	+0.22
11	3.153	139.152	+0.22
12	3.172	139.161	-0.24
13	3.188	139.103	
	3.179±0.021	139.129±0.075	+0.04±0.30

Table 2.1 Reproducibility of nitrogen abundance and isotopic composition measurements. The intensity of the m/z 28 ion beam (used to determine yields), the 28/29 ratio and the zero enrichment $\delta^{15}N$ value from a set of 13 aliquots of reference gas performed throughout the analysis of an unknown sample are shown. The size of each aliquot of gas was 9ng. The $\delta^{15}N$ values are derived by comparing each analyses with the mean of the analyses on either side, referred to as a zero enrichment.

measurements were not consecutive analyses (they are interspersed with analyses of an unknown sample) the reproducibility is very good. The height of the m/z 28 peak, used to determine the yield of nitrogen, has a 1σ error of ±0.67% about the mean. The ability to measure the 28/29 ratio is even better, the mean value having a 1σ error of ±0.075, equivalent to about ±0.5‰. In terms of calculating the isotopic composition of the gas, conversion to $\delta^{15}N$ values (comparison of each ratio with the mean of the two on either side) gives a 1σ error of ±0.30‰. Although such an error may be an order of magnitude larger than that obtainable on a conventional dynamic instrument about 3 orders of magnitude less sample is required. Also, for most of the purposes of this study the errors can be considered insignificant, as iron meteorites display a range in $\delta^{15}N$ values from -95 to +155‰ and Bencubbin contains nitrogen with a $\delta^{15}N$ value of up to +1000‰.

Reducing the sample size has two effects. Firstly the errors associated with each measurement increase, albeit very slightly down to sample sizes of 3ng. However, below 3ng the errors increase sharply to ±3‰ for a sample size of 1ng. The second effect of sample sizes is on the measured 28/29 ratio - which decreases with decreasing sample sizes. Once again, for large samples (>5ng) the effect is rather limited but below 5ng there is a large shift in the ratio, which from 5ng down to 1ng would be equivalent to almost 20‰. The cause of this effect is not clearly understood but is most probably due to small amounts of interfering species in the mass spectrometer such as CO or some hydrocarbons or even due to the formation of N_2H (Wright *et al.*, 1988). Fortunately this effect is highly reproducible and applies to both sample and reference gas equally. Therefore, by precisely matching the pressure of nitrogen during the analysis of the reference gas to that of the preceding unknown sample gas using the aliquotting system in

the inlet section (Figure 2.2) the effect is cancelled out in the calculation of the $\delta^{15}N$ value.

2.4.2 Calibration of the Instrument

Initially, the absolute sensitivity of the mass spectrometer was achieved using a fixed volume aliquotter attached to the reference bulb. However, the errors associated with the pressure of nitrogen in the bulb were not accurately known. A much more satisfactory technique is to use accepted standards. The standard materials chosen were NBS steels SRM 133a and SRM 368, which contain 320 and 100ppm nitrogen respectively. The nitrogen is extracted in exactly the same manner as from the whole rock iron meteorite samples (see Section 2.5.1). The yields obtained are then normalised to the known concentration of nitrogen in the samples. Table 2.2 shows the results of five consecutive analyses of the two steels; the results are reproducible, with an error of ±4.1% of the mean correct value.

The reference gas used is cylinder nitrogen (White Spot Grade, British Oxygen Corporation, Ipswich, U.K.). The isotopic composition of the reference gas is also calibrated against standard materials. However, there are only two

Sample	$\delta^{15}N$ (‰)	ppm N
SRM 368	-0.3	101.8
SRM 368	+0.4	96.2
SRM 368	-1.4	99.7
SRM 133a	-2.9	308.0
SRM 133a	-1.8	338.4

Table 2.2 Nitrogen in standard steels. Bulk nitrogen concentration and isotopic compositions from NBS standard steels SRM 368 and SRM 133a. The concentrations have been normalised to the mean value of all five runs (corrected for different absolute concentrations).

NBS standards available, NBS-N1 and NBS-N2, both of which are anhydrous ammonium sulphates. Unfortunately, such compounds are not ideally suited to the extraction technique designed for metal and silicate geological samples, it being very difficult to achieve full conversion to nitrogen gas. A much more convenient standard to use is local air. The variation in the isotopic composition of nitrogen in the atmosphere from a range of sample sites encompassing the globe, including industrial centres and up to an altitude of 51.6km is smaller than the errors of the static mass spectrometer (Dole *et al.*, 1954; Junk and Svec, 1958; Mariotti, 1983). Therefore, use of local air, which by definition has a $\delta^{15}N$ value of 0‰, is a perfectly satisfactory standard for the purposes of this study. Also, its cost is very low and delivery time negligible.

A small bulb (50cm^3) with an aliquotter and a B10 cone adaptor is evacuated to a base pressure of about 10^{-5} torr. An aliquot of local air (sampled clear of any obvious immediate sources of pollution) is admitted to the evacuated bulb. The bulb is then attached to the glass line at the B10 socket adjacent to the laser port (see Figure 2.7). Once base pressure is achieved, aliquots of local air, including CO_2, O_2 and Ar are transferred into the clean up section and purified using the extended procedure described in Section 2.3.2. The gas can then be treated in the same manner as any other unknown sample gas.

The reference gas in the bulb attached to the inlet section is replaced regularly and following loss of vacuum. Each bulb of fresh reference gas is calibrated against local air. The results of one typical calibration are shown in Table 2.3. From these results the mean $\delta^{15}N$ value of local air is 1.1‰ lighter than the reference gas, *i.e.* the $\delta^{15}N$ value of the reference gas is +1.1‰. Equipped with such a calibration, all $\delta^{15}N$ measurements of unknown samples performed with that particular bulb of reference gas are corrected for such an offset.

Run No.	$\delta^{15}N$ (‰)
1	-1.17
2	-1.38
3	-0.74
	-1.10±0.33

Table 2.3 $\delta^{15}N$ value of local air. Three consecutive analyses of local air showing the $\delta^{15}N$ value of local air relative to the reference gas. As there are no reported variations in the nitrogen isotopic composition of the atmosphere these results indicate that the $\delta^{15}N$ value of the reference gas is +1.1‰.

The results of Wright *et al.* (1988) show that the static mass spectrometer is linear in the range 0 to +20‰. Outside this limited range of $\delta^{15}N$ values there are no accepted standard materials and therefore it is impossible to determine whether this linearity extends any further. However, results from a wide range of materials are very similar to those from other laboratories (Wright *et al.*, 1988), showing that, even if linearity is not guaranteed, the effects must be similar to those in the other laboratories and so the results obtained are at least comparable with those of other workers.

2.4.3 Nitrogen Contribution from the System

During any extraction of gases from a sample, by the time the nitrogen is admitted to the mass spectrometer it will contain a component acquired from the the system, completely unrelated to the sample and termed the "blank". For samples with a different isotopic composition to the blank the measured $\delta^{15}N$ value of the sample will be drawn towards that of the blank. The blank is derived from a number of sources but over the years it has been found that once a base level has been reached (approximately 7-10 days after exposure to atmosphere)

the total blank from the glass line and hot fingers remains reasonably constant. With a predictable blank contribution it is then possible to perform corrections on the measured isotopic composition to determine the true $\delta^{15}N$ value of the sample gas. One problematic area, however, is the platinum bucket which contains the sample. As the size of the bucket is very variable any nitrogen contribution from this source will therefore also be variable.

A number of techniques involving prolonged heating at 1200°C (always in batches of 10 to 20 buckets) have been tried in an attempt to remove all the nitrogen from the platinum buckets. Variations including heating under vacuum and in air were found to be unsatisfactory. Because samples are loaded into the bucket in air a component of adsorbed atmospheric nitrogen will always exist. However, the application of a stepped heating program readily removes this

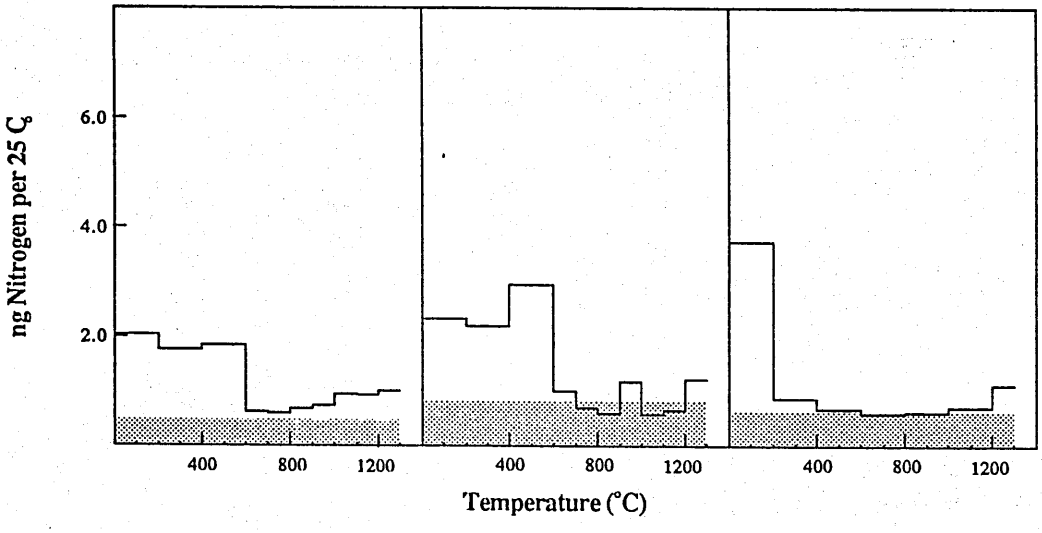

Figure 2.4 Nitrogen contribution from platinum buckets. The total nitrogen liberated during stepped combustions of three platinum buckets pre-baked in different ways. (a) heated for 12 hours at 1200°C under vacuum (10^{-5} torr), (b) heated for 12 hours open to the atmosphere and (c) heated for 12 hours at 1100°C under vacuum but cooled under a pressure of pure oxygen (20 torr). The shaded area in each represents the amount of blank predicted from the first steps of the day performed on an empty sample finger.

component by 300°C (see Section 2.5) and much larger amounts of trapped atmosphere may be released from the sample itself up to 300°C. Most geological materials will not liberate any indigenous nitrogen until the temperature is above 600°C, but above 600°C the amount of gas being liberated by the platinum buckets pre-baked under vacuum and in air is still variable and temperature dependant (Figures 2.4a and b).

The release profile from a platinum bucket in Figure 2.4c shows a much more constant release of nitrogen over the temperature range of interest. The trapped atmospheric component is still present but above 400°C there is no detectable change in the amount of blank until above 1200°C. The quartz tube had only been heated to 1200°C and it can be shown that most of this increased blank does infact originate from the tube rather than the platinum bucket. The preparation for this bucket involved heating it to about 1100°C for 12 hours at 10^{-5} torr (at 1200°C the buckets tend to fuse together), exactly as was done for the bucket in Figure 2.4a. However, rather than cooling under vacuum a pressure of oxygen (20 torr) was generated from a copper oxide finger before the buckets were cooled to room temperature. It is not entirely clear what the effect of the oxygen is, one possibility is that the surface of the cooled platinum strongly adsorbs, or even absorbs gas, so that if the first gas it is exposed to is air, many of the available sites are filled with nitrogen. By cooling the buckets under oxygen these sites are already occupied when the bucket is exposed to air.

At the start of every heating programme one or two temperature steps are performed before the sample is dropped down into the sample vessel (Figure 2.2). This allows the amount of blank evolved from the isolated sample vessel over the time of a typical step and from processing the gas through the glass line to be estimated. The shaded areas in Figure 2.4 are the amount of blank from the glass line predicted from the first two blank steps of that day. In Figure 2.4c it is

clear that no detectable quantities of nitrogen are liberated from the platinum bucket over the temperature range 400 to 1200°C. Therefore, it is possible to predict the size of the blank over the temperature range at which most geological samples liberate their indigenous nitrogen.

To correct the measured $\delta^{15}N$ value for blank contribution, not only must the amount of blank be known, but also the isotopic composition. Normally the amount of blank is too small (<0.7ng) for an accurate isotopic measurement, although when the blank is high (>2ng) measurements have been performed, the $\delta^{15}N$ value being very close to 0‰. It is possible that this value does not apply to much smaller blanks, but without the means of measuring the isotopic composition it will have to suffice as an approximation.

2.5 STEPPED HEATING PROGRAMMES

Stepped heating of a sample to liberate indigenous gases can be employed for two different purposes. The first reason is to discriminate between gases indigenous to the sample and the various forms of contamination (*e.g.* atmospheric gases, organic contamination and inorganic weathering products), first introduced for geological samples by Chang *et al.* (1974). The second application of stepped heating is that it offers the possibility of identifying gases released from different sites within the same sample (Becker and Clayton, 1975). For the purpose of analysing nitrogen in geological samples it is almost always necessary to employ a stepped heating programme of some sort due to the high abundance of nitrogen in the atmosphere and the low abundance in geological samples. However, it is always worthwhile limiting the number of steps to the minimum necessary for the purpose of the analysis as this reduces the amount of sample required and the time involved to perform the extraction. For these

reasons two different types of stepped heating programmes were employed in this study, one for bulk contents of whole rock samples and one for identifying different components within whole rock samples and acid residues.

2.5.1 Bulk Nitrogen Extractions

This programme is designed to quickly remove surface contamination from metal samples (iron meteorites and standard steels) and then extract all the indigenous gas in as few steps as possible. This reduces the possibility of losing nitrogen indigenous to the sample with the surface contamination and minimises errors introduced due to incomplete recovery of the nitrogen. It must be added that this particular variation has only been evaluated for the analysis of metallic iron specimens and its suitability for other materials is as yet untested.

At the start of each day the copper oxide finger CF#1 (Figure 2.2) is heated to 900°C for 10 minutes and then the oxygen resorbed at 600 and the 450°C for 15 minutes, during which time the sample finger is raised from its overnight temperature of 1200°C to almost 1300°C. The purpose of these two steps is to remove any nitrogen from the copper oxide and the surrounding glass which may be liberated during the first step and to minimise the extra blank observed above 1200°C in Figure 2.4c. The amount of blank from the system with the sample furnace at 1250°C is then determined.

The temperature of the sample furnace is lowered to 700°C and the sample dropped into the sample finger. Once the pressure is better than 10^{-6} torr the sample is combusted for 20 minutes and the gases removed, purified and analysed. The yield of nitrogen from this step is almost always less than 3ng with a $\delta^{15}N$ value close to 0‰, and is taken to be contamination. If a second step is performed at this temperature no gas is evolved and is therefore not normally included in the programme. After the clean-up step the furnace temperature is

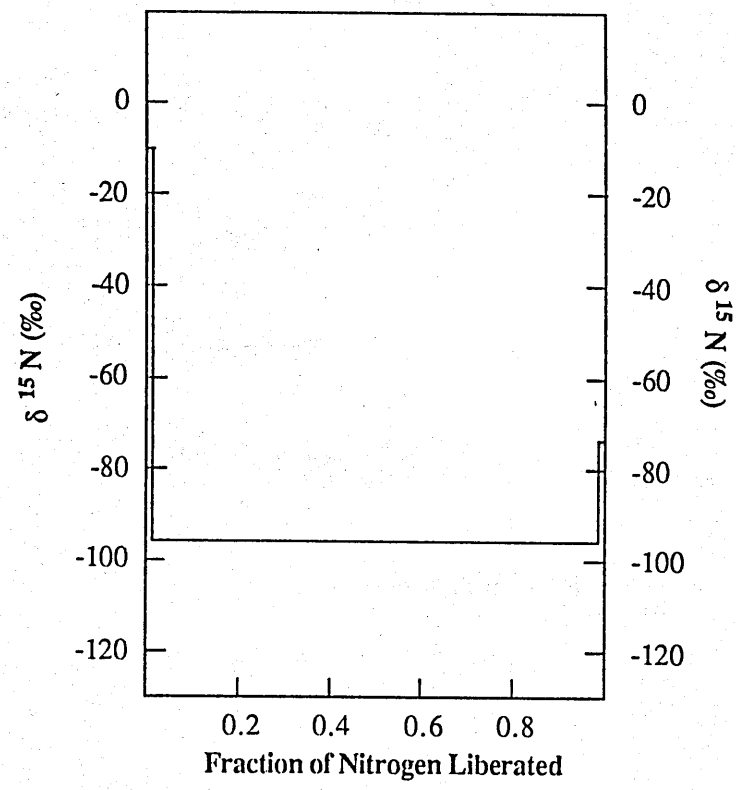

Figure 2.5 Bulk combustion of the iron meteorite Uwet. Typical release from an iron meteorite employing a heating programme with a single step at 700°C and then repeated steps at 1250°C, the first of 61 minutes duration, with subsequent steps 31 minutes long. The gases released in the first step (700°C) have a $\delta^{15}N$ value close to 0‰, indicative of terrestrial contamination.

raised to 1250°C and the sample combusted for 60 minutes. The gases are then removed and processed in the normal manner. Following transfer, a second combustion at 1250°C is started immediately, lasting 31 minutes, after which the gases are removed and analysed as before. By performing a series of 31 minute steps with selected samples it has been determined that for the iron meteorites and NBS SRM 368 only one 31 minute step, after the initial 60 minute step, is required to extract all the nitrogen, but for NBS SRM 133a at least two repeated steps are necessary. The results from a typical run, that of the IIAB iron meteorite Uwet are shown in Figure 2.5, with 99% of the gas liberated above 700°C doing so in a single step.

2.5.2 High Resolution Stepped Heating Extractions

The second heating programme is longer, but much simpler than that used for the bulk nitrogen determinations. At the start of the day copper oxide finger CF#1 is heated to 900°C as above and the sample furnace temperature lowered to about 100°C. The blank levels are then determined in a step(s) up to 200°C. From 200 to 1200°C, or even hotter, a series of 31 minute steps are performed in immediate succession. The size of each temperature increment is determined by a number of factors. At low temperatures (<600°C), particularly for whole rock samples large temperature increments are employed, the gases liberated over this temperature range generally having all the characteristics of terrestrial contamination. However, in the acid residues, particularly those of Bencubbin (see Section 4.3), some of the gas liberated below 600°C is indigenous to the sample.

Provided sufficient gas for analysis is being liberated smaller temperature increments are normally employed over the temperature range at which gas indigenous to the sample is being evolved. The size of the temperature steps over the main releases of nitrogen are typically 50°C, although sometimes they can be smaller (usually 25°C). A similar pattern of temperature increments were employed for the determination of carbon and its isotopic composition in the Bencubbin samples.

2.6 CARBON EXTRACTION AND ANALYSIS

Stepped heating extractions for carbon analysis were performed on whole rock samples and acid residues of the Bencubbin meteorite (see Chapter 4). For these measurements another static vacuum mass spectrometer was used. Details of this instrument, and the extraction/purification system coupled to it are

described by Carr (1985) and Carr *et al.* (1986). The following is a brief summary of these two reports.

The instrument is very similar in design to the one described in Section 2.2, exceptions being that it has a 9cm radius flight tube and three Faraday buckets to monitor the ion beams. The extra buckets allow the three ion beams of interest , m/z 44, 45 and 46, to be monitored simultaneously, necessary because of the very short half-life of CO_2 in a static vacuum mass spectrometer (≈35 seconds). The errors on $\delta^{13}C$ values, determined in precisely the same manner as for the $\delta^{15}N$ values on the nitrogen instrument, are <±1‰ on sample sizes of 12ng of carbon as CO_2 (Carr *et al.*, 1986). The yield measurements are determined by trapping the CO_2 into a small volume and measuring the pressure of gas using a capacitance manometer. The errors on the yield measurements are approximately ±0.5%.

The glass line used is comparable in design to that of nitrogen, however, the combustion and purification technique is slightly modified. The oxygen for the combustion of the sample is derived from a copper oxide finger, but before being exposed to the sample it is frozen onto a molecular sieve. This has two purposes, firstly it allows a higher pressure of oxygen to be generated (≈200 torr). Secondly, if the molecular sieve is only warmed to room temperature the oxygen will be liberated but and CO_2 blank from the copper oxide will remain trapped. The molecular sieve and copper oxide are valved off from the combustion section except when oxygen is being transferred. The purification of the gases is also straight forward, with a platinum finger at 1150°C on line to the sample to ensure complete oxidation of any CO and CH_4 generated. CO_2 produced is simply frozen out of the system and the excess oxygen trapped back down onto the

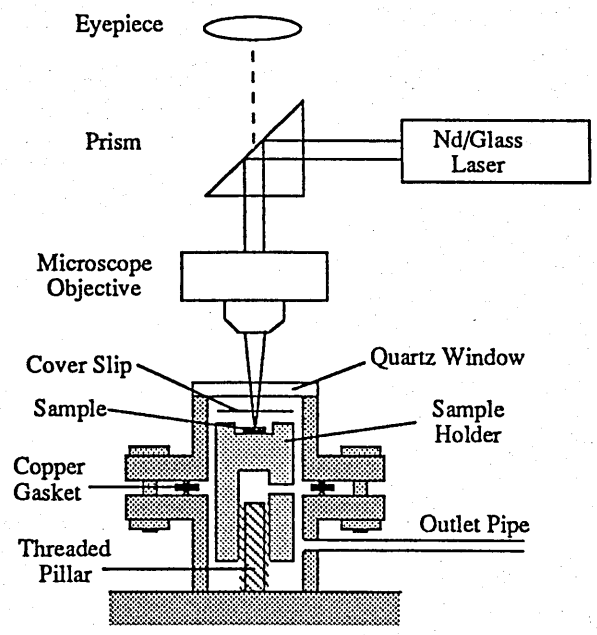

Figure 2.6 Schematic diagram of the laser-port.

molecular sieve*. Any residual non-condensible species are simply pumped away before the CO_2 is cryogenically separated from the other condensible species (*i.e.* SO_2 and H_2O) using a variable temperature cryogenic trap similar to VCT#1 in Figure 2.2.

2.7 LASER MICROPROBE EXTRACTION

2.7.1 General Description for Nitrogen Extraction

A full description of this technique is presented in Franchi *et al.* (1986a), the following is only a summary of the more important features and those particularly

* Footnote - Recently it has been shown that small amounts of carbon dioxide are removed during resorption of the oxygen onto the molecular sieve, resulting in low yields (≈50%). However, the isotopic composition of the carbon does not appear to be unduely affected (Ash, pers. comm., 1987).

relevant to this study. The laser used is a neodymium-glass pulsed laser (non Q-switched) which operates at 1064nm wavelength. It can deliver a 0.1 to 5J pulse with a duration of 300μsec, giving a power density range of 10^7 to 10^{10}Wcm^{-2}. The laser beam is focused on to solid surfaces through a microscope objective lens (x5) to produce small pits up to 120μm across and 200μm deep. The same optics are used to view the sample, permitting accurate targeting of the laser beam. The samples can be illuminated by either transmitted or reflected light using a "cold" light source.

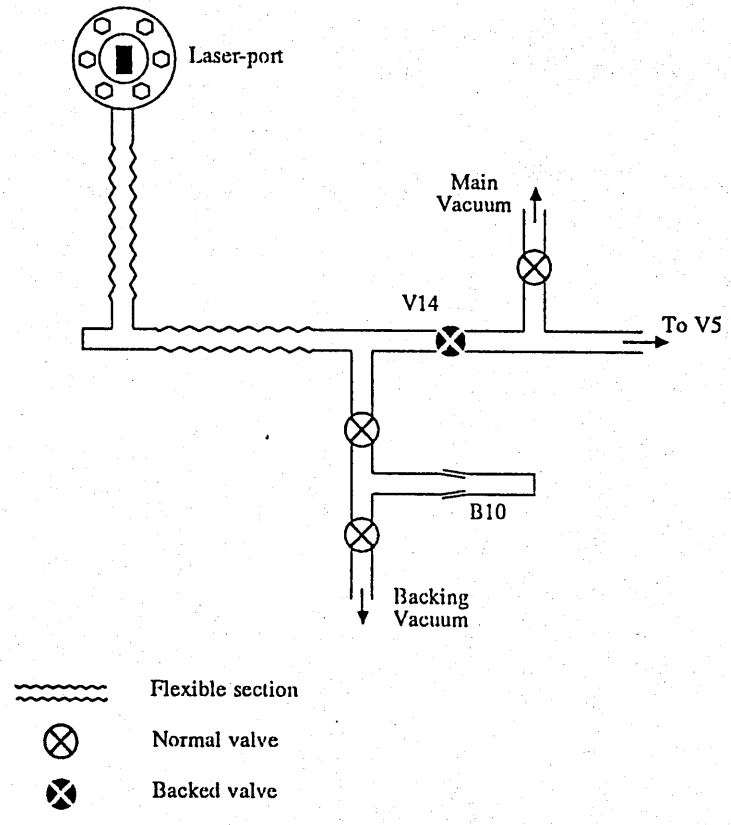

Figure 2.7 Schematic diagram of glass line to laser-port. Evacuation of atmosphere is through backing line - preserving vacuum in main glass line, through V5 (Figure 2.2). The B10 cone and socket is used to attach a small bulb of local air for calibration of the reference gas (see Section 2.4.2).

A diagram of the sample containing chamber (laser-port) most often used is shown in Figure 2.6. It is constructed from two 70mm stainless steel flanges, the lower one welded to a base plate, with a threaded pillar and an outlet pipe, the upper one containing a quartz window through which the sample can be viewed and the laser beam transmitted. Samples are mounted in stainless steel holders, the height of which can be adjusted on the threaded pillar. A 1 inch diameter glass cover slip is placed above the sample, its purpose being to protect the quartz window from molten material ejected from the laser pits. As the position of the laser is fixed the sample port is attached to the glass line by two stainless steel flexible tubes welded at 90° to each other (Figure 2.7) permitting movement in the x, y and z directions, achieved using three micrometers. The second laser-port is composed of three 70mm flanges, the top and bottom flanges containing quartz windows, permitting the sample to be viewed in transmitted light. The sample holders are mounted on the middle flange along with the outlet pipe.

Sample preparation was very sample specific, the rule being to clean the sample as thoroughly as possible without harming the sample. Metal and non-friable silicate samples were washed with methanol in ultrasound to remove surface contamination, but lunar breccias and carbonaceous chondrites could only be handled with care, no cleaning being possible. With the samples mounted in the laser-port the chamber was evacuated using the backing line vacuum, through valve V14 (Figure 2.7). To achieve base pressure the sample was pumped for at least 48 hours, wrapped in heater tapes maintaining a temperature of up to 300°C. The bake out temperature is sample specific as samples such as carbonaceous chondrites contain labile indigenous organic nitrogen which may be lost at 300°C. It was eventually discovered that the illumination of the sample also reduced the blank level, although the reason why is unclear, and therefore it is also necessary to illuminate the sample chamber for several hours during the pump out period. A

similar effect and operating protocol has also been observed in conjunction with a system designed for the study of argon (S. Kelley, 1986, pers. comm.).

Gases extracted from the sample by the laser are trapped onto the molecular sieve in the purification section through V5 (Figure 2.2). Thereafter, an extended purification procedure is employed before the gases are admitted to the inlet section (see Section 2.3.2). The amount of nitrogen present in most geological samples is so low that multiple pulses of the laser are usually required to liberate sufficient gas for isotopic analysis. The blank levels for a typical laser extraction are generally around 0.5ng.

2.7.2 Evaluation of Laser Microprobe Technique for Nitrogen

A number of different materials have been analysed using the laser microprobe in order to evaluate the viability of the technique.

(a) Titanium nitride

Artificially produced titanium nitride (TiN) in the form of aggregates of 100μm crystals, was analysed 5 times from three different areas. Each analysis was easily performed on the gases liberated from a single pulse due to the high nitrogen content of the sample (22wt.% N) The results, shown in Table 2.4, display a number of interesting features. The isotopic composition of the gas liberated from the three different target areas shows some variation, although analyses from the same region (target area 3) are all very similar. This shows that the laser microprobe is capable of providing reproducible isotopic compositions and that there is some isotopic heterogeneity in the titanium nitride sample. The mean isotopic composition of the three target areas ($\delta^{15}N$ = -4.6‰) compares very favourably with the $\delta^{15}N$ value of -3.8‰ obtained from a piece of the sample analysed using a conventional stepped heating extraction.

The yield of nitrogen from each pulse is also quite variable. This time it is the three analyses from target area 3 which show the largest variation, the yields from target areas 1 and 2 and that from the first analysis of area 3 all being in excellent agreement. The three analyses for target area 3 were all performed on the same spot, the second and third pulses being focused into the pit formed by the first pulse. Two effects may have been occurring simultaneously to account for the

Target area	No. of Pulses	Yield (ng N)	Yield (wt.% N)	$\delta^{15}N$ (‰)
1	1	153.9	15.4	-4.7
2	1	156.2	15.6	-2.0
3	1	147.4	14.7	-7.5
3	1	64.5	6.4	-6.5
3	1	22.9	2.3	-7.5

Table 2.4 Laser microprobe analysis of titanium nitride. The results of analyses of nitrogen liberated from artificial osbornite (TiN) using a single pulse of the laser. Output energy = 5J. The first three analyses were from different target areas, the last two were from the same pit as the first pulse at target area 3.

observed fall in yield with each repeated pulse. The first effect is that when a pit is formed molten material is ejected out of the pit, coating the underside of the cover slip. This makes focusing difficult on subsequent shots and some of the laser beam may be absorbed when passing through this coating, resulting in attenuation of the beam at the sample surface. The second effect is possibly due to molten titanium, with little or no nitrogen, falling back into the pit. Therefore, some of the energy delivered in the second and third pulses is wastefully used heating metal devoid of nitrogen. Therefore, it is necessary to focus the laser on a fresh surface for each pulse if reproducible results are to be achieved.

The concentration of nitrogen liberated from each target area can only be approximately determined as the dimensions of each pit are estimated using a calibrated graticule in the eyepiece. The best determinations of the pit size in the titanium nitride (50μm diameter, 100μm deep) suggest that the sample only contains about 15.5wt.% nitrogen. However, the sample is known to contain 22wt.% nitrogen, indicating a recovery rate of about 70%. Full recovery of reference gas expanded into the laser-port shows that this is not a problem associated with trapping the gases into the purification section. The most likely explanation is that some of the nitride originally in each pit was melted but did not decompose to titanium and nitrogen.

(b) Murchison meteorite

The CM2 carbonaceous chondrite is composed of a suite of various refractory light inclusions and chondrules surrounded by a dark, volatile rich matrix (Fuchs *et al.*, 1973)). The meteorite is also ideally suited for microprobe study as it contains between 350 and 850ppm nitrogen (Kerridge, 1985 and refs. therein) with a number of distinct isotopic components (*e.g.* Lewis *et al.*, 1983). The

Target area	No. of Pulses	Yield (ng N)	Yield (ppm N)	$\delta^{15}N$ (‰)
1	5	12.6	790	+41.7
2	8	16.5	650	+44.7
3	9	18.6	650	+43.0
4	10	19.7	620	+38.5
5	10	22.3	700	+44.0

Table 2.5 Laser microprobe analysis of the dark matrix in the Murchison meteorite. The concentration and isotopic composition of nitrogen extracted from the dark matrix of the Murchison meteorite by the laser microprobe are shown. The results of bulk whole rock determinations employing conventional techniques are 450 to 850ppm and +36 to +44‰ (Kerridge, 1985). Output energy = 5J.

laser microprobe was used to extract nitrogen from a number of matrix sites and some of the inclusions. The results from the areas of dark matrix are shown in Table 2.5. The $\delta^{15}N$ values obtained from 5 analyses of the dark matrix range from +38.5 to +44.7‰, with a mean value of +42.4±2.2‰. This is in excellent agreement with published whole rock $\delta^{15}N$ values which vary from +36 to +44‰ (Kerridge, 1985). As most of the nitrogen in the meteorite is present in the dark matrix it would therefore appear that the laser microprobe is capable of liberating nitrogen from a geological sample, albeit a relatively nitrogen rich one, without affecting the nitrogen isotopic composition.

The size of the pits produced by the laser were approximately 60μm x 120μm. Therefore the calculated concentration of nitrogen liberated from the matrix of the Murchison meteorite varied from 620 to 790ppm. Once again, these are in good agreement with values obtained using conventional techniques (350 to 850ppm nitrogen, (Kerridge, 1985)). These results show a much higher recovery rate (close to 100%) than was obtained from the titanium nitride (70% yield). Figure

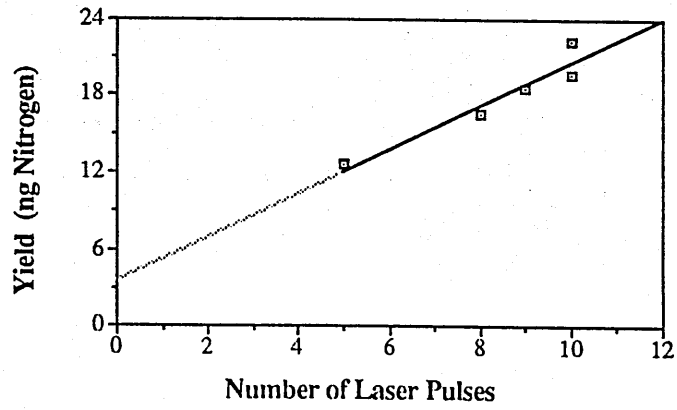

Figure 2.8 Nitrogen yield from Murchison matrix versus number of laser pulses. For five pulses or more there is a linear relationship between yield and number of pulses. However, this cannot apply to a smaller number of pulses as the relationship defined does not pass through the origin.

2.8 shows that there is a linear relationship between the number of pulses and the yield of nitrogen for samples obtained with 5 or more pulses. However, the line does not pass through the origin, indicating that for a larger number of pulses relatively less gas is released per pulse. As each pulse was focused on a fresh surface of the sample the effect of laser energy being absorbed by volatile depleted material redeposited in the pit cannot be responsible for the observed drop in yield. However, the problems associated with coating of the cover slip with ejected material will get worse with increasing number of pulses and so could account for the results from the Murchison meteorite matrix.

The results from the light coloured inclusions in Murchison (Table 2.6) show a much wider range of $\delta^{15}N$ values (+12.4 to +60.6‰) and lower nitrogen concentrations (80 to 420ppm). It should be noted that the inclusions with the lowest nitrogen concentrations (target areas 6 and 9) have $\delta^{15}N$ values farthest from the matrix values. Due to the small size of the inclusions (<2mm) the large

Target area	No. of Pulses	Laser Energy (J)	Yield (ng N)	Yield (ppm N)	$\delta^{15}N$ (‰)
6	15	5	5.8	80	+60.6
7	10	5	19.6	420	+41.0
8	6	5	10.1	360	+34.5
9	11	1	1.2	160	+12.4
10	18	1	2.6	220	+51.9
11	14	0.7	1.7	290	+30.8
12	15	0.3	0.8	370	nm

Table 2.6 Laser microprobe analysis of the light coloured inclusions in the Murchison meteorite. The concentration and isotopic composition of nitrogen extracted from light coloured refractory inclusions in the Murchison meteorite using the laser microprobe are shown. The errors on the yield determinations from the last four analyses are 5x greater than the others due to the much smaller, variable sized pits produced at lower output energies. The results from target areas 7 and 8 are close to the values obtained from the dark matrix (Table 2.5) suggesting that these inclusion were completely penetrated and that matrix material was sampled.

number of pulses employed in these extractions may have resulted in some inclusions being completely penetrated to sample the surrounding matrix giving the observed high nitrogen yields. Therefore, a truer reflection of the nitrogen isotopic variation of the light coloured inclusions in Murchison is shown by the inclusions with the least amount of nitrogen (target areas 6, and 9 to 11). It thus becomes very interesting that two different isotopic signatures were obtained from different inclusions.

(c) Uwet iron meteorite

The IIAB iron meteorite Uwet is known to contain 13.9 ppm nitrogen with a $\delta^{15}N$ value of -95.6‰ (see Table 3.7). The mineralogy of this iron meteorite is quite simple, being composed of a single kamacite crystal containing phosphides ($(Fe,Ni)_3P$) and a few very small (<5μm) carlsbergite crystals (CrN). The phosphides are present as both large (<5x0.1mm) schreibersite crystals and numerous small (<20μm) rhabdites. The nitrides in this meteorite are concentrated in the schreibersite crystals (A. Bevan, 1986, pers. comm.). Therefore, a comparison of the nitrogen in the kamacite with that in the schreibersite was attempted. The possibility of individual nitride crystals biasing the results does not exist as their size dictates that over thirty crystals need to be sampled to liberate sufficient gas to perform an isotopic measurement.

The results from the study are shown in Table 2.7. Unfortunately, the amount of gas is so low that isotopic measurements could only be made on 3 of the 4 schreibersite crystals analysed and no measurements could be performed on the kamacite target areas. The measured $\delta^{15}N$ value of the schreibersite crystals ranged from -76 to -66‰. This is more than 20‰ heavier than that measured on schreibersite and carlsbergite crystals from this meteorite using stepped heating

Target phase	No. of Pulses	Yield (ng N)	Yield (ppm N)	$\delta^{15}N$ (‰)
Schreibersite	12	3.4	62	-66
Schreibersite	21	1.6	17	-67
Schreibersite	25	1.6	14	-76
Kamacite	30	0.6	3	nm
Kamacite	25	0.7	4	nm

Table 2.7 Laser microprobe analysis of the iron meteorite Uwet. Due to the low concentration of nitrogen in this sample (whole rock = 13.9ppm) isotopic analyses could only be performed on three of the schreibersite ($(Fe,Ni)_3P$) crystals. Laser output energy = 5J.

techniques (Figure 2.9). The problem appears to stem from the amount of gas liberated from the sample, each analysis being performed on 3.4ng of N_2 or less. With the large number of pulses used for each analysis, each pulse on a fresh surface, the cumulative effect of trace quantities of terrestrial nitrogen on the sample surface could be affecting the measured $\delta^{15}N$ value.

The yields of nitrogen from the schreibersite crystals range from 13 to 64ppm. Only the first crystal analysed was broad enough for the pits to sample only the phosphide, the other crystals were narrower (<50μm), and as the pits were approximately 70μm across, some nitrogen poor kamacite was also sampled. However, the concentration of nitrogen in the schreibersites determined by stepped heating is 165ppm, indicating that no more than 40% of the total nitrogen was recovered by the laser microprobe. The recovery rate from the kamacite is even worse - only 3 to 4ppm nitrogen was recovered from the kamacite, yet the kamacite must contain approximately 12.5ppm nitrogen, implying a recovery rate of less than 30%. If some of the nitrogen analysed is terrestrial contamination then the recovery rates are in fact much lower than 30%.

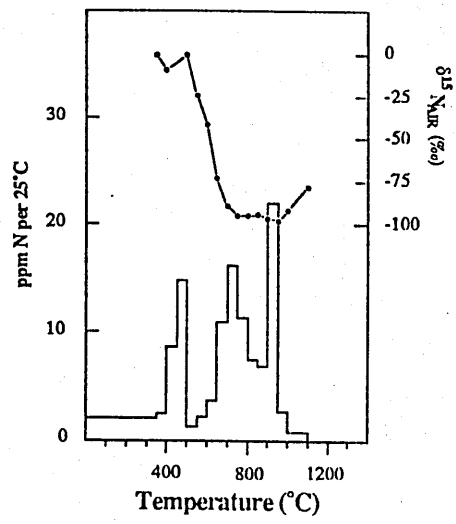

Figure 2.9 Nitrogen profile from stepped combustion of a 6M HCl residue of Uwet. Three components are distinguishable, although the one around 450°C with a $\delta^{15}N$ value of around 0‰ is probably terrestrial contamination. The other two releases are believed to be from the phosphide phases, shreibersite and rhabdites, (around 750°C) and the nitride carlsbergite (950°C). Above 600°C the residue contains 165ppm nitrogen with a $\delta^{15}N$ value of -93.7‰.

The general conclusion from this study is that for samples with low nitrogen concentrations, particularly metallic samples, the laser microprobe has limited application with the current blank and mass spectrometer sensitivity levels. For samples with a known isotopic composition and a moderately coarse mineralogy the laser microprobe can readily be used to map out the distribution of the nitrogen. Samples with relatively high nitrogen concentrations allow the laser microprobe to produce informative data on the distribution and isotopic composition of nitrogen on the scale of 1mm. Recently, it has been shown that the ion-probe can also be employed to determine the isotopic composition of nitrogen with a high degree of spatial resolution and sample characterisation

(Zinner *et al.*, 1987a). However, unlike a conventional mass spectrometer, the ion-probe can only succesfully analyse nitrogen as CN^- and therefore it is restricted to samples in which nitrogen is intimately associated with at least comparable concentrations of carbon. The power of the laser microprobe is that it can extract nitrogen for analysis from any material which will melt or vapourise under the focussed laser beam (3-4000°C). However, the laser microprobe requires to be interfaced to a more sensitive mass spectrometer in order that the nitrogen isotopic composition of geological materials can be detemined on gas extracted from only one laser pulse.

2.7.3 Evaluation of The Laser Microprobe Extraction Technique for Carbon

Carbon exists in geological samples in a number of forms, as reduced organic matter, graphitic carbon and diamonds, oxidised gaseous carbon dioxide in fluid inclusions and as the carbonate mineral. The initial work has been confined to samples containing the highest concentrations of carbon - carbonates and pure graphitic carbon.

The mass spectrometer used is the one described in Section 2.6. The gases extracted were split into two fractions, CO_2 and H_2O were trapped into a cold finger at -196°C and the non-condensible gases, including CO, trapped into a purification section on a 5Å molecular sieve. The CO_2 is simply separated from the water on a variable temperature cryogenic trap before being analysed. The CO on the other hand is oxidised to CO_2 over hot (450°C) copper oxide before being cryogenically separated from the other species.

Carbonates

A sample of pure calcite ($CaCO_3$) was used for this initial study. The energy from the laser beam is not very efficiently absorbed by colourless materials such as calcite, thus melt pits could not be easily formed in this material. Occasionally larger yields were obtained, particularly in cloudy regions of the crystals which absorb the laser energy much better. In an attempt to enhance the absorption of the laser energy a sample of calcite was coated in a thin coat of gold, the hope being that the energy would be absorbed by the gold, causing thermal decrepitation of the underlying calcite. However, the gold was quickly melted and stripped off a large area of the surface without transmitting very much heat to the calcite and so the pits formed in the gold coated calcite were little different to those in the uncoated samples.

The results from the calcite samples are shown in Table 2.8. The yield of CO_2 is highly variable, from 9ng to 128ng per pulse. The reasons for the variation are not known, it being impossible to notice any peculiarities in the calcite under the gold coat. Some possible explanations may be degassing along fractures or decrepitation of fluid inclusions. The isotopic composition of the gas liberated is also highly variable, although ignoring the CO analysis from target area 5 and the one obviously anomalous CO_2 analysis (target area 4) the mean $\delta^{13}C$ value is -0.6±1.3‰. This compares reasonably well with the true $\delta^{13}C$ value of the calcite (+1.8‰). The mean $\delta^{18}O_{PDB}$ value for the analyses is -16.8±4.8‰ which is considerably lighter than the true value of -2.5‰.

The most probable cause of the light $\delta^{13}C$ and $\delta^{18}0$ values from the laser extractions is the presence of small amounts of contamination and/or blank. As the blank for these extractions was somewhat variable a correction for an arbitrary amount of blank cannot be justified. As the $\delta^{13}C$ value of the blank varied from -20 to -50‰, and any organic contamination is around -25‰ this may explain

Target area	No. of Pulses	Species of gas	Yield (ng C)	$\delta^{13}C$ (‰)	$\Delta\delta^{13}C$ (‰)	$\delta^{18}0$ (‰)	$\Delta\delta^{18}O$ (‰)
1	6	CO_2+CO	677	-2.3	-4.1	-*	-*
2	1	CO_2	8.7	+0.5	-1.3	-23.6	-21.1
3	1	CO_2	4.8	-1.8	-3.6	-15.8	-13.3
4	1	CO_2	11.4	+10.1	+12.9	-14.0	-11.5
5	1	CO_2	53.5	-0.8	-2.4	-25.4	-23.9
		CO	1.9	-26.7	-28.5	-*	-*
6**	4	CO_2	517	+1.2	-0.6	-16.5	-14.0

Table 2.8 Laser microprobe analysis of calcite. The isotopic composition of carbon and oxygen liberated from a calcite sample by the laser microprobe and the difference from the true value ($\delta^{13}C$ = +1.8‰, $\delta^{18}O$ = -2.5‰).are shown. * To analyse CO the gas is oxidised to CO_2 over hot copper oxide and so the oxygen isotopic signature is lost. ** this sample was coated in a thin film of gold in an attempt to assist absorption of the laser energy by the colourless calcite. Output energy = 5J.

the small shift in the measured $\delta^{13}C$ values. However, on the limited amount of data it is impossible to explain the large offset in the measured $\delta^{18}O$ value. The small amount of CO recovered from target area 5 with a $\delta^{13}C$ value of -28.‰ is probably almost entirely blank.

Graphitic Carbon

These analysis were performed on gas extracted from a graphite rod ($\delta^{13}C$ = -25.5‰) in an atmosphere of oxygen (150 torr). The oxygen was generated and purified in exactly the same manner as described in Section 2.6. The results of two analyses are shown in Table 2.9. Most of the gas liberated was in the form of CO rather than CO_2. With pits approximately 70μm across and over 100μm deep almost 1000ng of carbon must have been vaporised from each pulse. With only 20 to 30ng of CO_2 generated from 6 pulses this is obviously a very

inefficient means of oxidising carbon. Two factors in particular must be contributing to this low yield. One is the short duration of the experiment, each pulse lasting a nominal 300μsec. The pressure of oxygen will also have an effect, with higher pressures increasing the probability of oxidising the carbon and so producing higher yields.

The isotopic composition of the two species generated is different. The $\delta^{13}C$ value of the CO_2 has a mean of -27.2‰, once again close to that of the true value ($\delta^{13}C$ = -25.5‰) but that of the CO (-33.5‰) is 8‰ lighter and the total $\delta^{13}C$ value of the two extractions (CO + CO_2) are -31.5 and -32.6‰, 6 to 7‰ lighter

Target area	No. of Pulses	Species of gas	Yield (ng C)	$\delta^{13}C$ (‰)	$\delta^{13}C_{total}$ (‰)	$\Delta\delta^{13}C_{total}$ (‰)
1	6	CO_2	3.8	-26.5	-31.5	-6.0
		CO	20.1	-32.5		
2	6	CO_2	7.7	-28.0	-32.6	-7.1
		CO	19.1	-34.4		

Table 2.9 Laser induced oxidation of graphitic carbon. The true $\delta^{13}C$ value of the graphite is -25.5‰ and the last column shows the difference between the true $\delta^{13}C$ value and that of the sum of the CO_2 and CO liberated from each target area. Output energy = 5J.

than the true value. Gas generated from 100 pulses of the laser into the same graphite rod and analysed on a conventional dynamic mass spectrometer had a $\delta^{13}C$ value of -29.2‰ (Franchi *et al.*, 1986a), similar to the fractionation observed in the much smaller sample sizes employed in this study. As the blank is predominantly from the purification and oxygen generation it is similar for the two sets of experiments which means that in the large scale extraction the blank

would be almost negligible. Therefore, the observed offset in $\delta^{13}C$ values cannot be entirely due to a contribution of isotopically light blank and so must reflect a true isotopic fractionation.

Although the total carbon extracted from the graphite is fractionated the analysis of the CO_2 does give a much closer indication of the isotopic composition of the carbon rod. Even if small isotopic fractionations do exist for the CO_2 liberated from calcite and graphite it may be that they are reproducible and corrections could easily be made by comparing the analysis of an unknown with gas extracted in the same manner from a similar standard material. However, the poor understanding about the sources of the blank and the lack of application to the main aspects of this thesis curtailed further exploration of the many problems still to be resolved in the development of a laser microprobe technique for carbon.

CHAPTER 3
NITROGEN IN THE IRON METEORITES

3.1 INTRODUCTION

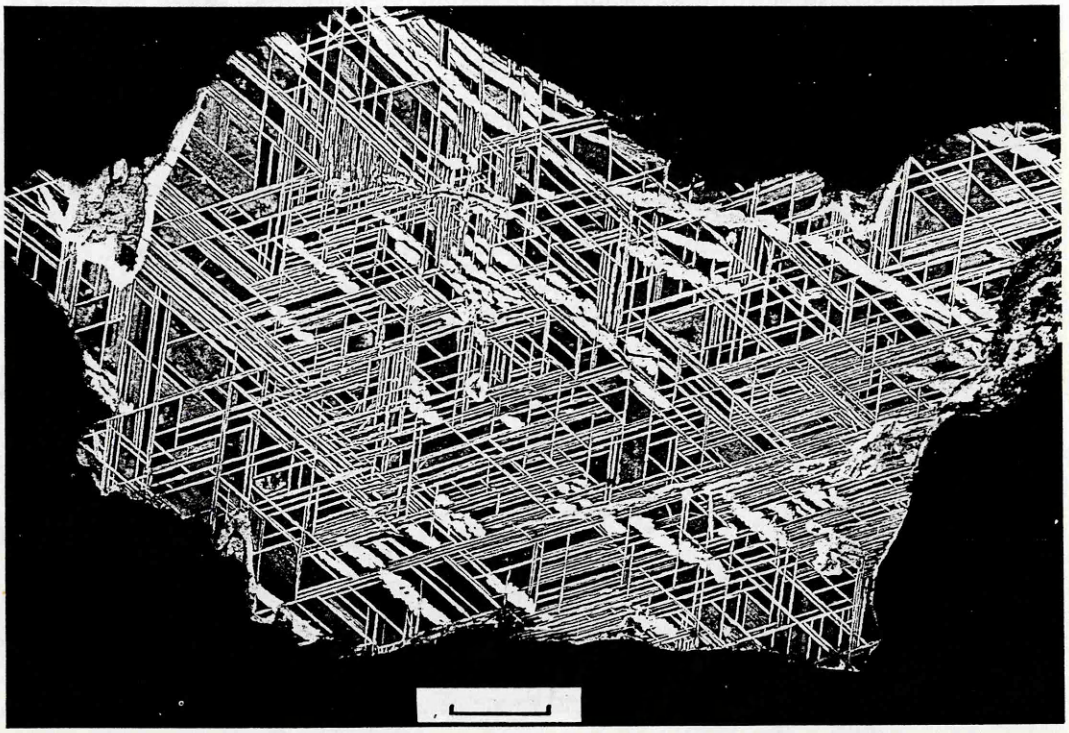

Figure 3.1 The Widmannstätten pattern in iron meteorites. On this macroscopic photograph of a polished and etched slice of the Edmonton (Kentucky) iron meteorite (group IIIAB), three of the kamacite orientations which produce the Widmannstätten pattern can be clearly seen. The fourth orientation is sub-parallel to the cut surface, appearing as thick, irregular light coloured plumes. Photograph taken from Buchwald (1975). Scale bar = 2cm.

Excluding those meteorites recovered in the past decade from the Antarctic ancient ice fields, approximately 25% of all meteorites in the world's collections are iron meteorites and by mass they constitute over 90wt.% (Buchwald, 1975; Graham *et al.*, 1985). However, this relative abundance of iron meteorites is not a true reflection of the composition of the early solar system. The mechanical strength of the irons makes them much more resistant to space attrition (*i.e.* during impacts with other bodies) than stony meteorites (Kracher and Wasson, 1982). Their survival in the solar system is reflected in their cosmic ray exposure

ages, which extend beyond 10^9 years, whereas the stony meteorites rarely exceed 50 x 10^6 years (McSween, 1987). The unusual nature of the iron meteorites compared to terrestrial rocks or stony meteorites greatly facilitates their recovery as meteorite "finds". A much better picture of the relative importance of iron meteorites comes from recorded falls which suggests they make up about 4.6% of the population (Graham *et al.*, 1985).

Whatever their abundance the irons remain important samples. By their very nature they obviously contain a different record of aspects of the formation processes operating on the meteorite parent bodies to that carried by the stony meteorites. They may provide valuable insight into the important process of core formation; samples of the cores of the Earth and other terrestrial planets will probably never be available for direct examination.

3.1.1 Mineralogy and Structure

To date, more than 40 minerals have been identified in iron meteorites; a summary of the more common and those relevant to this study are listed in Table 3.1. Iron meteorites are primarily composed of the Fe-Ni alloys kamacite and taenite, analogous to body centred cubic α-iron and face centred cubic γ-iron respectively (Buchwald, 1975). Kamacite is normally observed as an intricate and regular pattern of crystal intergrowths, called the Widmanstätten pattern, with the taenite filling interstitial sites (Figure 3.1). This structure is produced by solid state growth of kamacite at temperatures below 1100K. For metal with a composition typical of iron meteorites (5 to 20wt.% Ni) the Fe-Ni phase diagram (Figure 3.2) predicts that taenite will crystallise from molten metal at around 1800K and it is not until the metal has cooled to less than 1100K that kamacite begins growing.

Troilite, graphite and silicate inclusions in the iron meteorites formed at temperatures above the solidus from molten metal, either because they were immiscible with the metal or they formed in small pockets of liquid trapped in the

Mineral	Composition
Kamacite	Fe,Ni (<7.5wt.% Ni)
Taenite*	Fe,Ni (>30wt.% Ni)
Graphite	C
Cohenite	$(Fe,Ni)_3C$
Haxonite*	$(Fe,Ni)_{23}C_6$
Schreibersite*	$(Fe,Ni)_3P$
Carslbergite*	CrN
Roaldite	$(Fe,Ni)_4N$
Troilite*	FeS
Sphalerite	ZnS
Daubréelite*	$FeCr_2S_3$
Chromite	$FeCr_2O_3$
Chlorapatite	$Ca_5(PO_4)_3Cl$
Whitlockite	$Ca_3(PO_4)_2$
Olivine	$(Mg,Fe)_2SiO_4$
Orthopyroxene	$(Mg,Fe)SiO_3$
Clinopyroxene	$(Mg,Fe,Ca)SiO_3$
Plagioclase	$NaAlSi_3O_8$ - $CaAl_2Si_2O_8$

Table 3.1 Minerals present in iron meteorites. Only the more common minerals and those most relevant to this study are shown - more than half the total number of minerals found to date are not listed. Those marked with an * have no known terrestrial occurrence. Information taken from Buchwald (1977) and Nielsen and Buchwald (1981).

crystallising metal (Buchwald, 1975; Kracher and Wasson, 1982). Almost all the other minerals present in the iron meteorites grew by solid state diffusion (Comerford, 1969; Buchwald and Scott, 1971), although some large phosphide inclusions may have crystallised from liquid metal in P-rich irons (Doan and Goldstein, 1969).

The growth of kamacite by solid state diffusion is controlled by the diffusion rates in the parental and crystallising phases, and the time available before diffusion is effectively ceased around 750K (Buchwald, 1975). Therefore, it is possible to estimate the cooling rate from one or two simple parameters in each

meteorite. There are a number of different techniques for calculating the cooling rate, but methods based on cooling rate curves calculated from central taenite Ni contents and the width of the taenite fields (Wood, 1964) are generally the most accurate (Saikumar and Goldstein, 1987). The variation in the cooling rates of iron meteorites between 1050 and 700K vary from about 1 to 250K My^{-1} (Wood, 1979), although Narayan and Goldstein (1985) have suggested that the cooling rates are in fact much faster (75 to 80000K My^{-1}) after redetermining the diffusion rates of Ni.

3.1.2 Classification of Iron Meteorites

Prior to the development of routine high sensitivity analytical techniques the classification of iron meteorites was based on the bandwidth of the kamacite crystals (Table 3.2). This scheme divides the irons into 8 categories plus a number of anomalous samples. The 8 categories described by Buchwald (1975) range from ataxites (no structure visible with a hand lens) through 6 types of octahedrites (characteristic Widmanstätten pattern with kamacite crystals ranging

Structural Class	Symbol	Bandwidth (mm)	Total
Hexahedrites	H	-	50
Coarsest Octahedrites	Ogg	>3.3	20
Coarse Octahedrites	Og	1.3-3.3	90
Medium Octahedrites	Om	0.5-1.3	210
Fine Octahedrites	Of	0.2-0.5	55
Finest Octahedrites	Off	<0.2, continuous	7
Plessitic Octahedrites	Opl	<0.2, spindles	20
Ataxites	D	-	33
Anomalous		All	40
			525

Table 3.2 Structural classification of iron meteorites. After Buchwald (1975).

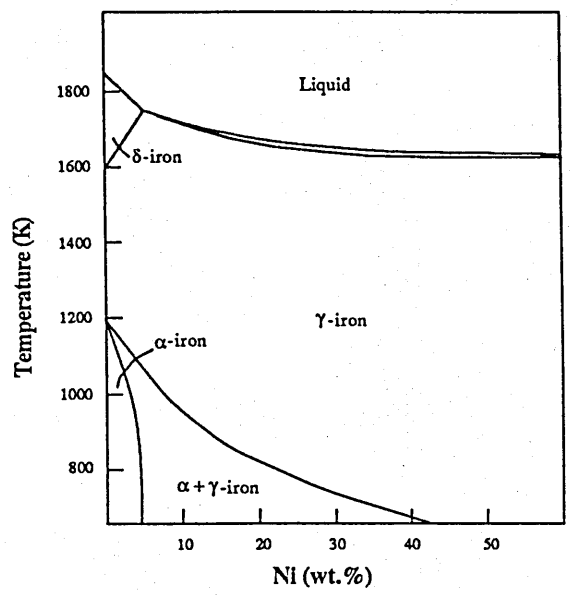

Figure 3.2 The Fe-Ni phase diagram. The structure of the solidus and liquidus (1700 to 1900K) is relatively straightforward. During cooling of the iron meteorites (typically 5 to 20wt.% Ni) the first metal to crystallise from the liquid will be depleted in Ni relative to the liquid and become progressively enriched in Ni as crystallisation progresses. Below 1200K there is a two phase region through which iron meteorites with typical Ni contents must cool. The compositional boundaries of this two phase region are up to 7wt.% Ni and 40wt.% Ni, defining the composition of kamacite and taenite respectively. Although there is considerable structure in the Fe-Ni phase diagram below 700K the diffusion rate of Ni below 750K is so slow as to effectively terminate the development of any large scale structures. Taken from Wasson (1985) and Chuang *et al.* (1986).

from <0.2mm to >3.3mm wide) and the hexahedrites (each meteorite is a single kamacite crystal). However, this is purely a descriptive classification and cannot be used as a genetic indicator. A much more powerful scheme has been developed over the past 20 years based on the trace element and Ni content of the meteorites, although textural information is still necessary to resolve ambiguities.

Using the variation of the Ga and Ge abundances with Ni content (Figure 3.3) the iron meteorites can be divided into 13 groups (*e.g.* Scott and Wasson, 1975) - see Table 3.3. For all iron meteorites the concentration of Ga varies by a factor of 2000 and that of Ge by 40000, yet the variation within individual

Class	Structure	Total
IAB	Og-Om	107
IC	Og	11
IIAB	H-Ogg	68
IIC	Opl	7
IID	Om-Of	15
IIE	Om-Of	14
IIF	Opl-D	5
IIIAB	Og-Om	197
IIICD	Of-D	21
IIIE	Og	13
IIIF	Ogg-Om	6
IVA	Of	56
IVB	D	12
IRANOM	All	78
Unclassified	All	115
		725

Table 3.3 Chemical classification of iron meteorites. After Wasson and co-workers. Data taken from Graham (1985).

groups, excluding groups IAB and IIICD, is very restricted, varying by less than a factor of 1.6 (Wasson, 1985). The trace element and Ni variations displayed by the irons are believed to be the product of at least two fractionation events. The differences between the groups reflecting a primary fractionation event which occurred during condensation (Scott, 1978) and the variations shown within groups due to geological processing on the meteorite parent bodies (Scott, 1972).

Groups IAB and IIICD, in contrast to the other groups, display wide ranges in Ni, Ga and Ge (Scott and Wasson, 1975). They are also unusual in that almost 25% of them contain silicate and graphite inclusions, normally very rare in iron meteorites, as well as numerous large phosphide and carbide inclusions (Buchwald, 1975). Groups IAB and IIICD clearly did not form under normal igneous conditions; they are referred to as non-magmatic groups. Irons in the small group IIE also contain silicate inclusions (Buchwald, 1975) and recently Wasson and Wang (1986) proposed that the trace element/Ni variations were indicative of formation processes similar to those of groups IAB and IIICD.

3.1.3 Formation of the Iron Meteorites

The mean elemental abundances in each iron meteorite group are a function of the composition of metal incorporated into each parent body and therefore the differences between groups are due to fractionation during condensation and/or heterogeneity in the solar nebula (Scott, 1978). The abundances in the groups depleted in the relatively volatile elements Ga, Ge, Cu and Au (*i.e.* groups IIIF, IVA and IVB) suggest equilibration of Fe-Ni metal with nebular gases at 1200 to 1300K assuming a total pressure of 10^{-5}atms (Kelly and Larimer, 1977). Other groups indicate lower temperatures of 600 to 800K (Sears, 1978). However, the nature of these fractionation processes during condensation are not well understood due to further fractionation of many of the trace elements during secondary processing in the parent bodies.

The Magmatic Groups

The nature of the formation processes of the magmatic iron meteorites, which produced the secondary elemental fractionations, are relatively well understood. The variations in the trace element/Ni ratios from each group approximate those expected from fractional crystallisation of a large pool or core of molten iron (Scott, 1972). The Fe-Ni phase diagram (Figure 3.2) predicts that, for bulk compositions of between 5 and 20wt.% Ni, the first metal to crystallise from the molten phase upon cooling will be depleted in Ni relative to the initial bulk composition of the liquid. With decreasing temperature the Ni content of the residual liquid will increase which results in that of the crystallising phase doing so also. Ni has a partition coefficient (K_d) of 0.9 to 1.0 (*i.e.* it shows only a slight preference for the liquid phase) and therefore during fractional crystallisation the Ni content of the residual liquid will not normally increase by more than a few wt.% except for the final few percent of liquid to crystallise.

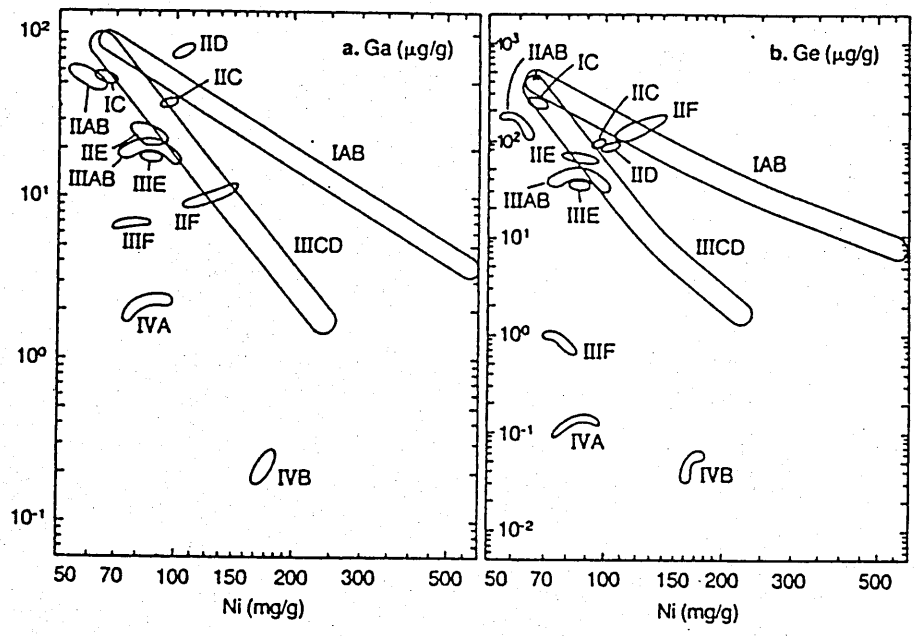

Figure 3.3 Plots of Ga and Ge versus Ni content of the iron meteorite groups. The range in the concentration of Ga, Ge and Ni in most groups is very limited compared to the range displayed by all irons (note log scales). The differences between groups are due to a primary fractionation event, probably during condensation in the solar nebula, the variation within groups due to secondary processing on the parent bodies. The small intra-group variations of Ga, Ge and Ni are very characteristic of fractional crystallisation of individual pools of molten metal, the three elements having K_d values close to 1. However, two groups (IAB and IIICD) cover wide ranges in these three elements, probably the result of different formation processes. The IABs and IIICDs, together with the IIEs are often refered to as the non-magmatic groups (c.f. all the other groups are generally considered to have formed by magmatic processes). Schematic diagram taken from Wasson (1985).

Elements such as Ga and Ge have K_d values close to 1 and so also display limited ranges in concentration within groups (Figure 3.3). Elements with K_d values much greater than 1, *e.g.* Ir, Ru, Rh, Pt and Os, display a strong preference for the solid phase and thus they become concentrated in the early crystallising, low-Ni metal and very depleted in the later, high-Ni metal (*e.g.* Figure 3.4). Au, P, As, Sb, Pb and Mo have K_d values of less than 1 (*i.e.* they prefer to exist in the liquid) and they are depleted in the low-Ni metal and enriched in the high-Ni metal (*e.g.* Figure 3.5). Fractional crystallisation from a

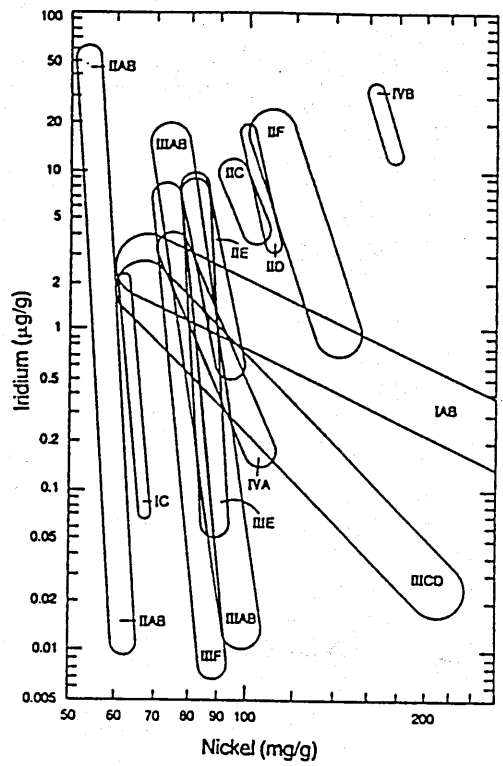

Figure 3.4 Plot of Ir versus Ni content of the iron meteorite groups. The sharp decrease in Ir with increasing Ni is characteristic of the behaviour of compatible elements ($K_d > 1$) during fractional crystallisation. Other elements in this catagory include Ru, Rh, Pt and Os. Once again, the two non-magmatic groups (IAB and IIICD) behave differently to the magmatic groups. Schematic diagram taken from Wasson (1985).

large pool of molten metal is also consistent with the lack of silicate inclusions from almost all magmatic iron meteorites, as the large density difference between liquid metal and silicate would lead to rapid segregation of the two phases even in a very weak gravity field (Wasson, 1970a).

Although it is generally believed that each iron meteorite group is derived from a different parent body there is some uncertainty as to whether aggregation of the liquid metal proceeded to complete core formation. If metal aggregation was arrested at an earlier stage then a number of smaller "mini-cores" at different depths in the parent body could be produced, the result referred to as a raisin-bread structure (McSween, 1987). Figure 3.6 shows two possible structures for

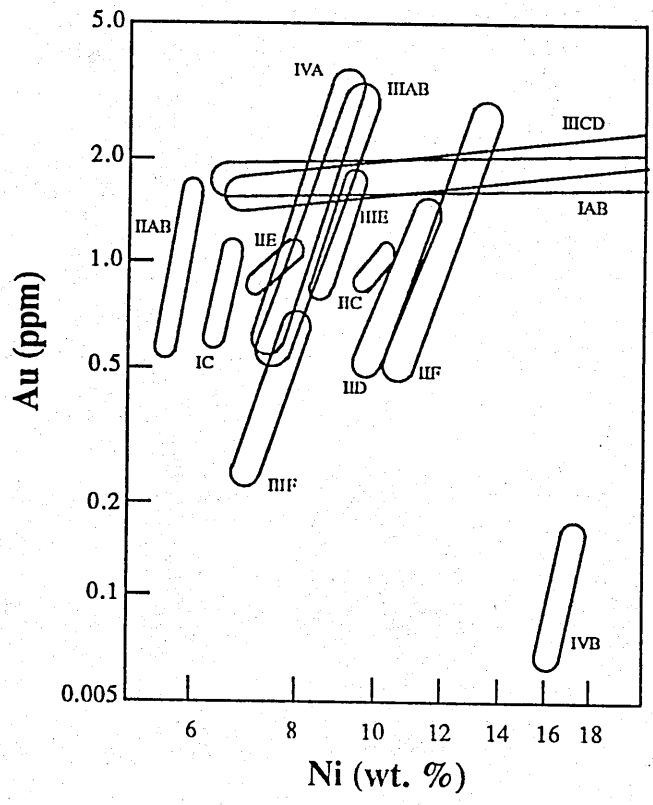

Figure 3.5 Plot of Au versus Ni content of the iron meteorite groups. The increase in Au with increasing Ni is characteristic of the behaviour of incompatible elements ($K_d < 1$) during fractional crystallisation. Other elements wich behave similarly include P, Sb, As and S. Once again the two non-magmatic groups (IAB and IIICD) behave differently to the magmatic groups. Schematic diagram taken from Scott and Wasson (1975), Kracher *et al.* (1980), Wasson *et al.* (1980), Malvin *et al.* (1984) and Wasson and Wang (1986).

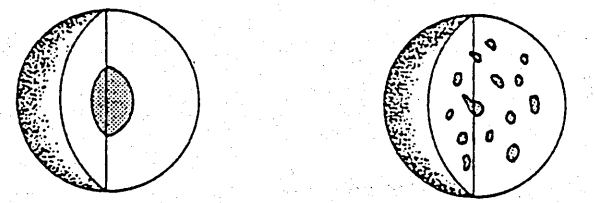

(a) Central core (b) Raisin-bread structure

Figure 3.6 Structure of iron meteorite parent bodies. (a) Temperature and time were sufficient to permit development of a fully differentiated parent body with a central core. (b) Prior to aggregation of the molten metal to a central core the temperature falls below the freezing point of the metal, trapping it as a large number of small bodies throughout the interior of the planetesimal - the raisin-bread structure. Diagram taken from McSween (1987).

iron meteorite parent bodies. Uniform cooling rates determined from some iron meteorite groups (*e.g.* group IIIAB displays a range of 1 to 10K My^{-1}) suggests that they were from a single body of metal whereas other groups have a wider range in cooling rates (*e.g.* group IVA varies between 3 and 200K My^{-1}) (Wood, 1979) indicating that they may have formed in a number of pools, probably within the same parent body (Moren and Goldstein, 1978).

A number of recent observations show that although the basic framework of the formation processes of the magmatic groups is reasonably well understood some important details remain to be established. In groups IIIAB, IVA and possibly IIAB the concentration of Ga and Ge correlate positively with that of Ni over most of the range of Ni concentrations (Figure 3.3) but in samples with a high-Ni content the Ga and Ge concentrations decrease with increasing Ni (Scott and Wasson, 1975). This may be due to the partition coefficients of Ga and Ge increasing, from <1 to >1 as the concentrations of volatile elements such as S, P and C increase (Willis and Goldstein, 1982; Jones and Drake, 1983). Unfortunately, experimental results have been unable to precisely match the observed trends in the iron meteorite groups without resorting to unreasonable volatile concentrations. Deviations from the refractory element (*e.g.* Ru, Re, Os, Pt and Ir)/Ni correlations have been observed in high-Ni samples of groups IIAB and IIIAB. These effects are too great to be the result of changing K_d values but they may record contamination of the last liquids to crystallise with small amounts of late stage primitive melt from the surrounding mantle (Pernicka and Wasson, 1987).

The Non-Magmatic Groups

The formation processes of the non-magmatic groups, IAB, IIE and IIICD are poorly understood, as is reflected by the wide range in models used to account for the structural and compositional features of these meteorites. The ranges in Ni, Ga and Ge are almost an order of magnitude greater than those

displayed by any of the magmatic groups (Figure 3.3), although in group IAB only two meteorites contain more than 15wt.% Ni and more than 90% of the IABs have Ni contents between 6.4 and 8.9wt.%. In contrast to the magmatic groups the range in refractory siderophile trace elements, such as Ir, are much more restricted (Figure 3.4) and are comparable with the variation displayed by Ga and Ge (Wasson *et al.*, 1980).

Another unusual feature of the non-magmatic group iron meteorites is that 25% of them contain large silicate inclusions, exceptionally rare in irons from magmatic groups (Buchwald, 1975). This suggests that these meteorites were never completely molten, otherwise the silicates and metal would have separated due to the large density difference (Wasson, 1970a). It is possible that the non-magmatic iron meteorites simply represent an early phase of normal core development, but for some reason it was never completed, in which case earlier fractionation processes are responsible for the observed trends (McSween, 1987). Alternatively, the formation processes may have been distinctly different, or at least modified, from those which produced the magmatic irons.

A broad outline of the formation and evolution of an iron meteorite parent body is condensation, accretion, melting, segregation and crystallisation during cooling (Kelly and Larimer, 1977). Therefore, if the non-magmatic irons are from a partially differentiated parent body then only the first three processes can be considered to have produced the observed trace element/Ni trends. Kelly and Larimer (1977) suggested that the refractory trace element/Ni trends in group IAB iron meteorites were produced by partial fractional melting of the parent body and that the maximum temperature barely exceeded that of the eutectic of the metal phase. Therefore, although there was enough heat to initiate segregation it was insufficient to drive it to completion and so the irons formed as a large number of separate, small melt pools, their composition related to the degree of melting. However, it is difficult to explain the behaviour of Ga and Ge within the framework of this model as these two elements display very similar variations in

concentration to Ir yet they have a K_d value of about 1 whereas that of Ir is approximately 20 (Wasson *et al.*, 1980).

A number of models have also been proposed which appeal to fractionation processes in the solar nebula to account for the silicate inclusions and the compositional trends in the non-magmatic groups. Wasson (1970b) suggested that group IAB irons formed "non-igneously" by heterogeneous accretion and segregation of large (>1m diameter) metallic bodies, trapping chondritic silicates in the process. The metal bodies were then stored in a large parent body where they were heated to <1400K and then slowly cooled to produce the observed Widmanstätten structure and recrystallisation of the silicate inclusions.

To explain the variations in the trace element concentrations Scott and Bild (1974) proposed a two-component mixing model,

(1) that high-Ni and low-Ni metal grains condensed in different locations with different refractory element concentrations and were simply mixed together in varying proportions to produce the observed trends or

(2) that both high-Ni and low-Ni metal condensed in the same location depleted in the refractory siderophile trace elements The low-Ni grains were larger, having been nucleated on refractory-rich oxide grains. Late stage partial equilibration increased the refractory content of the large, low-Ni metal grains to produce the observed trends.

However, Wasson *et al.* (1980) point out that, assuming equilibrium condensation sequences give a reasonable approximation to the condensation of the metal grains, a two-component model is too simple and that a larger number of components are necessary to explain all the observed trace element variations .

Just as inter-element effects on the K_d values were used to try to explain the trace element variations within some magmatic groups, similar models have been proposed for the non-magmatic groups. Kracher (1982) suggested that the trace element/Ni concentrations in group IAB irons were produced by fractional crystallisation. This model involves only partial melting of the parent body to

produce a very sulphide-rich parent liquid, the high sulphur content having a pronounced effect on the K_d values of trace elements. The silicate inclusions could have been incorporated into the sulphur-rich melt as aggregates containing large amounts of residual metal from the mantle (Kracher, 1985). Crystallisation of this partial melt should produce 10 times more sulphide than metal. However, in over 100 known IAB iron meteorites only one very sulphur-rich meteorite, Mundrabilla, has been recovered (Graham *et al.*, 1985). Similarly, only six winonaites (see Section 3.1.4) have been found, yet these should have been by far the most dominant materials on the parent body (Graham *et al.*, 1985). The apparent over-abundance of iron meteorites from this parent body may be due to their greater resistance to space attrition and the susceptibility of sulphide to corrosion of the surface of the Earth (Kracher, 1985).

As an alternative to the classical approach to explaining the origin of the non-magmatic iron meteorite groups, Wasson *et al.* (1980) proposed that they were produced by shock melting of a mega-regolith with a composition comparable with the most unequilibrated ordinary chondrites, each meteorite representing a single melt pool. Early melting followed by equilibrium crystallisation during the prolonged meteoritic bombardment at the start of the solar system produced Ni-rich melts from Ni-rich sulphides. With increased bombardment, higher temperatures resulted, inducing melting of Fe-rich sulphides and Fe-Ni metal which led to the formation of the Ni-poor members of the group. To explain the observed range in Ga and Ge abundances and also that of the refractory siderophiles, Ir, Re, Rh, W, and Os, Wasson *et al.* suggest that these elements condensed as refractory oxide phases, upon which early nucleation of Fe-rich Fe-Ni metal occurred. Equilibration of these large metal oxide grains produced the low-Ni, refractory-rich members of the group. The metal which condensed later did not nucleate on oxide grains and so were richer in Ni and depleted in refractory elements; these were the precursors to the high-Ni members.

3.1.4 Light Elements and Noble Gases in Iron Meteorites

For a number of different reasons studies of the light elements, and particularly their isotopic composition, have been somewhat limited. The following is a brief survey of these earlier studies.

Oxygen

Oxygen isotopes are useful for establishing the genetic relationships between different types of meteorites (*e.g.* Clayton *et al.*, 1976). Therefore, it would obviously be advantageous to know the isotopic composition of oxygen in the irons to study the relationships between iron and stony meteorite groups. Unfortunately, by their very nature (highly reduced Fe-Ni metal) the abundance of oxygen in iron meteorites is extremely low. Silicate inclusions in the non-magmatic irons, groups IAB, IIE and IIICD, are ideal for analysis but the occurrence of silicate inclusions in the magmatic groups is very rare (Buchwald, 1975). However, the trace mineral chromite ($FeCr_2O_4$) and some phosphates are present in a number of iron meteorite groups and they can be used as a source of oxygen.

Clayton *et al.* (1983) and Clayton *et al.* (1986) measured the isotopic composition of oxygen in 23 iron meteorites from 5 different groups (Figure 3.7). The results, plotted on a three isotope plot show that some of the iron meteorite groups may have originated from the same oxygen reservoir as some of the stony and stony-iron meteorite parent bodies. Groups IAB and IIICD have indistinguishable oxygen isotopic compositions and fall on the same fractionation line as the winonaites. Similarly, group IVA irons may be related to the L- or LL- group chondrites and IIE irons to the H-group chondrites. Such relationships are also indicated by other parameters, Scott and Bild (1974) having suggested that the mineralogical and structural composition of groups IAB and IIICD and the winonaites indicated that they formed in neighbouring parts of the solar nebula and the concentration of Ni, Ga, Ge and Ir in the metal phase of the

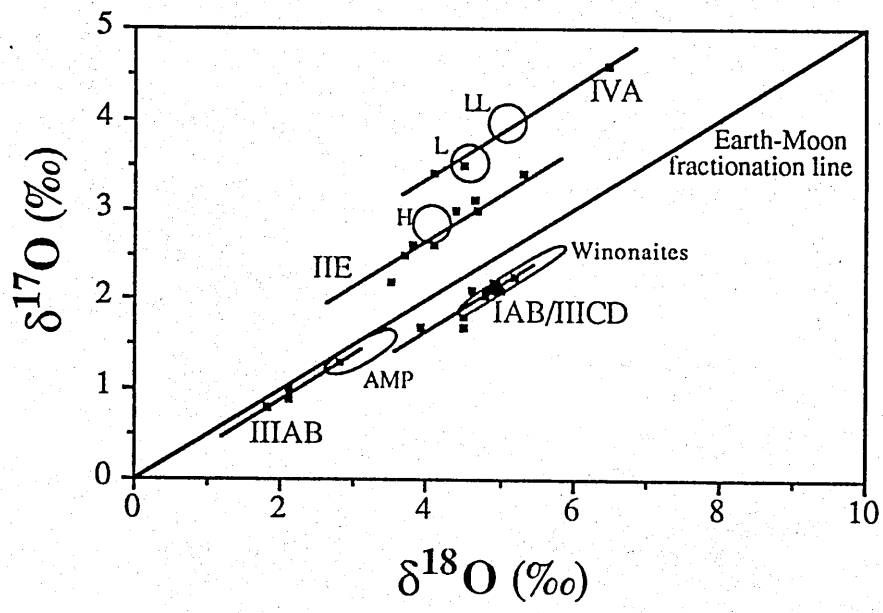

Figure 3.7 Oxygen isotopic composition of iron and stony meteorites. Fractionation lines (slope = 0.5) have been drawn through data from individual iron meteorite groups and the approximate fields of related stony meteorite groups. The data show that groups IAB and IIICD may have formed from the same oxygen reservoir as the winonaites, similarly the IIEs may be related to the H group chondrites, the IIIABs with the howardites, diogenites, eucrites, mesosiderites or pallasites and the IVAs with the L or LL group chondrites. Trace element data indicates that the IIIABs may be related to the pallasites as well as indicating similarities in the metal of the H group chondrites with that of the IIEs. Data taken from Clayton *et al.* (1983) and Clayton *et al.* (1986).

IIEs and the H-group chondrites form very small and overlapping ranges (Clayton *et al.*, 1983). However, the relationship between these iron meteorite groups and the chondritic meteorites is unclear, as no differentiated silicates appear to have been sampled from these iron meteorite parent bodies.

The IIIAB irons fall on the same fractionation line as differentiated stony and stony-iron meteorites such as the pallasites, mesosiderites, eucrites, howardites and diogenites (Figure 3.7) (Clayton *et al.*, 1986). The similarity in the siderophile trace element concentrations between the IIIAB irons and the metal phase of the pallasites lend further support to such an association (Scott, 1977). The prospect of more work on the oxygen isotopic composition of iron meteorites

is limited due to the difficulty of obtaining suitable samples, although as trace amounts of chromite and phosphates are found and the application of ion-probe techniques (*e.g.* Zinner *et al.*, 1987b) are established more data should be forthcoming.

Carbon

The carbon distribution within an iron meteorite can be very heterogeneous, being highly dispersed as dissolved carbon in kamacite and taenite, and concentrated in graphitic inclusions as well as the carbides cohenite and haxonite (Buchwald, 1975). The concentration of carbon in bulk samples of iron meteorites ranges from 0.002 to 0.185wt.% (Moore *et al.*, 1969) and the total range in $\delta^{13}C$ values is from -30.3 to -4.0‰ (Deines and Wickman, 1973). It is noteworthy that there is a fractionation of the carbon isotopes between the co-existing phases, with graphitic carbon typically 10 to 15‰ heavier than carbon in the carbide and metal phases (Deines and Wickman, 1975). As the range in $\delta^{13}C$ values for different components from a single iron meteorite can be 50% of the total range observed from all irons, obtaining representative samples of each meteorite is of paramount importance. However, as the grain size of most irons is relatively coarse, the size of representative samples is prohibitively large. Thus, it is necessary to perform analyses of separated phases in order to evaluate the carbon isotopic composition of iron meteorites. The early identification of this problem by Craig (1953) appears to have dissuaded most workers from analysing carbon in iron meteorites.

Sulphur

Sulphur suffers from a heterogeneous distribution similar to that observed for carbon, being found dissolved in the metal and also as large, irregularly distributed sulphide inclusions (Buchwald, 1975). The concentration of sulphur in iron meteorites ranges from 0.001 to 0.575wt.% (Moore *et al.*, 1969),

although two sulphide-rich irons are known, Mundrabilla containing approximately 8wt.% and Soroti 12wt.% sulphur (Buchwald, 1975). The isotopic composition of sulphur in iron meteorites has a very restricted range, with $\delta^{34}S$ values of between -0.45 and +0.55‰ (Burgess, 1987). Given that the precision of the analytical techniques are generally no better than ±0.1‰ the relatively narrow range in $\delta^{34}S$ values greatly limits their usefulness as generic indicators or isotopic tracers. However, the possibility of determining the relative abundance of all the stable isotopes of sulphur, by analysing the gas as SF_6 instead of SO_2 (Burgess, 1987), could prove to be much more powerful.

Noble Gases

The abundance of primordial noble gases in iron meteorites is very low, and moreover, the long cosmic ray exposure ages typical of irons has resulted in significant production of cosmogenic noble gases (Schultz *et al.*, 1971) to mask the primordial gases. The abundance of these cosmogenic nuclides permits the exposure ages of the meteorites to be determined, which range up to 2275×10^6 years (Voshage, 1967). However, such results have only a limited application to the study of the formation processes of iron meteorites as the breakdown of parent bodies to meteorites would normally be a complex, multiple event process. Attempts have been made to measure the isotopic composition of noble gases indigenous to the iron meteorites but this limits the choice of samples to those with very low concentrations of spallation products. The abundance of non-spallogenic noble gases in iron meteorites is so low that analyses are difficult and often incomplete (*e.g.* Hennecke and Manuel, 1977).

Murty *et al.* (1983) reported considerable depletions of ^{124}Xe and ^{126}Xe relative to atmospheric Xe in the non-magnetic fraction of acid residues of iron meteorites. Large variations in the $^{190}Os/^{184}Os$ ratios from residues of some iron meteorites have also been detected and it has been proposed that such anomalies indicate the presence of pre-solar material (Goel, 1986).

Nitrogen

The concentration of nitrogen in the iron meteorites has been the subject of a number of studies, revealing a range of 0.4 to 216ppm nitrogen (*e.g.* Nash and Baxter, 1947; Buchwald, 1961; Gibson and Moore, 1971; Shulka and Goel, 1981). However, the most recent studies, which incorporate a stepped heating extraction and isotopic analyses have found a more restricted range of 0.2 to 78ppm nitrogen (Pepin and Becker, 1982; Prombo and Clayton, 1983; Prombo, 1984). However, there is still a wide range in concentrations from irons in the same group and even from within the same iron meteorite (Table 3.4). For example Toluca, a group IAB iron, has liberated 41.5, 48.2 and 69.2ppm nitrogen (Prombo, 1984) as well as 5.7 and 4.8ppm (Pepin and Becker, 1982).

The isotopic composition of nitrogen in iron meteorites spans a wide range of $\delta^{15}N$ values from -91.8 to +153.2‰ (Prombo, 1984). However, the $\delta^{15}N$ values from individual irons are variable, *e.g.* the Toluca samples mentioned above had $\delta^{15}N$ values of -54.3, -54.9 and -61.9‰ (Prombo, 1984) and -40.9 and -13.5‰ (Pepin and Becker, 1982). Some reproducible results have been obtained, *e.g.* two analyses of Cape York, group IIIAB, yielded 35.4 and 38.1ppm nitrogen both with a $\delta^{15}N$ value of -84.6‰ (Prombo, 1984). However, Pepin and Becker (1982) reported only 20.6ppm with a $\delta^{15}N$ value of -32.3‰ from Cape York. The variations in the nitrogen abundance in the iron meteorites may be due to concentration of the nitrogen in specific phases such as the nitrides carlsbergite (CrN) and roaldite ($(Fe,Ni)_4N$). Isotopic fractionation of the isotopes of nitrogen between co-existing phases similar to that observed for carbon may account for the range in $\delta^{15}N$ values from each meteorite.

The concentration of nitrogen in acid residues of iron meteorites is generally greater than the concentration in the bulk sample, indicating that nitrogen is indeed concentrated in minor, acid-insoluble phases (Murty *et al.*, 1983). These workers found that 33% of the nitrogen in group IIIAB irons and 18% of the

Sample	Group	Prombo (1984) N (ppm)	Prombo (1984) $\delta^{15}N$ (‰)	Becker and Pepin (1982) N (ppm)	Becker and Pepin (1982) $\delta^{15}N$ (‰)
Canyon Diablo	IAB	20.2	-68.9		
		45.0	-49.9		
		48.8	-66.7		
		mean = 38.0±15.5	-61.8±10.4		
Colfax	IAB	77.8	-63.7		
Toluca	IAB	48.2	-54.9	4.8	-40.9
		69.2	-61.9	5.7	-13.5
		41.5	-54.3		
		mean = 52.9±4.2	-57.0±14.4		
Zacatecas 1792	IAB	7.7	-60.2		
Bendego	IC	15.1	-84.9		
Coahuila	IIAB	10.2	-91.8		
		7.2	-86.7		
		mean = 8.7±2.1	-89.2±3.6		
Hex River Mtns.	IIAB	11.1	-80.5		
Navajo	IIAB	3.5	-82.7		
Sikhote Alin	IIAB	13.2	-82.2		
Ballinoo	IIC	4.1	+125.3		
Perryville	IIC	4.4	+144.6		
Unter Massing	IIC	10.5	+153.2		
Needles	IID	27.8	+7.2		
		28.1	+7.8		
		mean = 27.9±0.2	+7.5±0.4		
Arlington	IIE	0.9	+14.6		
Weekeroo Stn.	IIE	2.7	+46.7		
Monahans	IIF	15.7	+7.1		
Bella Roca	IIIAB	16.1	-82.3		
Cape York	IIIAB	35.4	-84.6	20.6	-32.3
		38.1	-84.6		
		mean = 36.7±1.9	-84.6±0.01		
Grant	IIIAB	23.8	-84.6		
Henbury	IIIAB	28.0	-83.2		
Kenton Co.	IIIAB	4.6	-79.7		
Welland	IIIAB	20.5	-75.6		
Carlton	IIICD	32.4	-60.2		
Dayton	IIICD	69.0	-66.1	15.0	-55.5
Staunton	IIIE	12.1	-75.5		
Nelson Co.	IIIF	1.4	+8.6		
Gibeon	IVA	4.8	-3.4		
Hoba	IVB			0.8	+7.5
Tlacotepec	IVB	0.4	+3.3	2.1	+12.9

Table 3.4 Previous nitrogen isotopic composition determinations of grouped iron meteorites.

Data taken from Pepin and Becker (1982) and Prombo (1984).

Sample	Prombo (1984) N (ppm)	Prombo (1984) $\delta^{15}N$ (‰)	Pepin and Becker (1982) N (ppm)	Pepin and Becker (1982) $\delta^{15}N$ (‰)
Bacubirito	8.1	+127.4		
Bocaiuva	0.6	+11.2		
Butler	1.9	-32.8		
Cambria	0.3	+20.6		
Illinois Gulch	2.5	+33.6		
Kendall Co.	1.2	+0.9		
Kofa	3.8	-87.1		
Mbosi	16.0	+4.8		
Nedagolla	0.8	+2.5		
N'Goureyma	0.4	+19.3		
Nordheim	0.2	+49.1		
Piedade do Bagre	8.2	-25.1		
Pinõn			6.6	+14.7
Reed City	0.4	-0.5		
Santa Catharina	7.4	-18.4		
Sombrerete	0.6	+37.3		
Soper	0.2	+10.5		
Tombigbee River	0.2	-4.3		
Tucson	0.3	+8.2		
Washington Co.			3.2	-54.3

Table 3.5 Previous nitrogen isotopic composition determinations of ungrouped iron meteorites. Data taken from Pepin and Becker (1982) and Prombo (1984).

nitrogen in group IAB irons is concentrated in 4M H_2SO_4 resistant phases. However, as the analytical technique was instrumental neutron activation analysis (INAA) the small amounts of residue produced were radioactive and so prevented any characterisation of the carrier phases. Murty *et al.* (1983) suggested that the nitrogen carriers were primary condensates from the solar nebula, some of which may also be the carriers of isotopically anomalous Xe. They also proposed that the iron meteorites, both magmatic and non-magmatic, formed directly from the solar nebula and without the need for melting and segregation in a parent body.

Despite the uncertainties in the results some interesting features in the nitrogen concentration and isotopic composition of the irons are identifiable. Pepin and Becker (1982) noted that the nitrogen concentration is lowest in those irons with an ataxitic structure and depleted in volatile siderophile trace elements, although Prombo and Clayton (1983) also found low nitrogen concentrations in irons with high volatile siderophile concentrations. Prombo and Clayton (1983) noted that

the isotopic composition of nitrogen in iron meteorites falls into three general clusters;

(1) low $\delta^{15}N$ values in the range -90 to -60‰

(2) $\delta^{15}N$ values around 0‰ and

(3) high $\delta^{15}N$ values around +140‰

with each iron meteorite group falling into one cluster (*e.g.* IAB irons all fall in the first cluster). Ungrouped irons (Table 3.5) generally have $\delta^{15}N$ values around 0‰ (-32.8 to +49.1‰). The nitrogen isotopic composition of the ungrouped iron Bacubirito ($\delta^{15}N$ = +127.4‰) is very similar to that of the unusual IIC irons ($\delta^{15}N$ = +125.3 to +153.2‰), suggesting that the two may possibly be related (Prombo and Clayton, 1983).

The genetic relationships between the iron meteorite groups IIE and IVA with the H-group and the L- or LL-group chondrites respectively, established on the basis of oxygen isotopic compositions and trace element abundances is further strengthened by the $\delta^{15}N$ values from the two groups (Prombo and Clayton, 1983). The metal from two IIEs has a $\delta^{15}N$ value of +14.6 and +46.7‰ (Prombo, 1984) which is similar to that of the H-group chondrites, +14.0 to +36.2‰ (Kung and Clayton, 1978). Similarly, the $\delta^{15}N$ value from a IVA, -3.4‰ (Prombo and Clayton, 1983) is within the range reported by Kung and Clayton (1978) for the L- and LL-chondrites which have $\delta^{15}N$ values between -3.5 and +29‰.

3.2 SAMPLES AND PRE-ANALYTICAL TREATMENT

The 27 iron meteorites analysed in this study, and the sources from which they were obtained are listed in Appendix 1. Prior to investigation at least one surface of each sample was prepared for petrographic examination to establish the degree and distribution of any weathering of the sample and to determine the mineralogy of that particular piece of each meteorite. Using a small hacksaw a

thin wafer, approximately 0.2 x 10 x 10mm was sawn from a fresh part of the sample. The metal was cleaned using a corundum industrial abrasive unit and then washed with acetone agitated by ultrasound for 15 minutes. The wafer was then cut into small blocks, 0.1 to 0.2mm^3 using a pair of wire cutters and then washed once more with acetone for 15 minutes. From this sample of approximately 100 small chips, aliquots of 3 to 7mg (4 - 8 chips) were taken for each nitrogen isotopic analysis. The extraction technique used was one employing a continuous oxygen supply, although two early analyses (Odessa and Clark County) were performed using aliquots of pure oxygen (see Section 2.3.2).

Acid-residues of 12 of the iron meteorites were prepared using hydrochloric acid. The samples for acid-dissolution were taken from the same block as that used for the whole-rock nitrogen analyses. The crust of the sample and any interior region of weathering were excluded or removed and the samples cleaned with the corundum abrasive and ultrasonically cleaned with acetone. The samples were dried and weighed before being treated with 200ml of 3M HCl at 70°C for 24 hours, after which most of the sample had been dissolved and all visible reaction had ceased. All but the last 50ml of the supernatant liquid was removed using a pipette. The remaining acid plus residue was centrifuged before the last 50ml were removed to ensure that no residue was lost. The residue was then washed with distilled water until the wash had a pH of 7, after which it was rinsed in methanol and dried overnight at 100°C. The residues were then weighed. Except for Odessa and Cape York a magnetic separation was performed on each residue. A cylinder of soft iron (20 x 5mm) wrapped in clean aluminium foil was placed in contact with a magnet attached to a micrometer. The micrometer was then adjusted to bring the sample, in an optically flat dish with ≈5ml of methanol to within 5mm of the magnetised soft iron (Gardiner *et al.*, 1977). Once separated, full recovery of the sample was achieved by removing the soft iron from the magnet and the foil from the iron over a clean dish. The

	Initial mass (grams)	Recovered mass (mg) Magnetic (%)	Non-magnetic (%)
Group IAB			
ALH77250	7.426	60.254 (0.81)	2.153 (0.03)
Bischtube	5.035	353.453 (7.02)	nm
Four Corners	3.953	77.031 (1.95)	258.160 (6.53)
Odessa	0.892	94.583 (10.6)	
Toluca	6.095	146.351 (2.40)	0.605 (0.01)
Youndegin	8.541	123.253 (1.44)	0.744 (0.01)
Group IIIAB			
Cape York	1.258	5.726 (0.46)	
Henbury	14.768	3.356 (0.02)	nm
Narraburra	2.749	38.310 (1.39)	nm
Sacramento Mtns.	8.585	nm	13.179 (0.15)
Sanderson	1.911	11.743 (0.61)	nm
Thunda	4.604	15.644 (0.34)	0.180 (.004)

Table 3.6 Starting and recovered masses of acid dissolutions of iron meteorites. The Odessa and Cape York residues were not separated magnetically. The values in parenthesis are the mass of residue expressed as a percentage of the starting mass.

samples were then dried and the mass of the two fractions determined, although in some instances the mass of the non-magnetic fraction was too small to weigh accurately (<1μg). The starting and recovered masses from each acid-dissolution and magnetic separation are listed in Table 3.6.

Small aliquots of the residues were analysed for their nitrogen content and its isotopic composition using the stepped combustion technique described in Section 2.5.2. The residues of Cape York and Odessa were combusted using the earlier technique employing aliquots of pure oxygen rather than a continuous oxygen supply.

3.3 RESULTS AND DISCUSSION

3.3.1 Whole-rock δ^{15}N and N Concentration

The nitrogen concentration and δ^{15}N values of the iron meteorites analysed are shown in Table 3.7 and Figure 3.8. The results display a wide range in nitrogen concentration, from 0.4 to 117.6ppm and δ^{15}N values which vary from -95.8‰ to +155.6‰. Replicate analyses of a number of the iron meteorites show that the results are quite reproducible. Multiple analyses of Bischtube, Four Corners (both IAB) and Henbury (IIIAB) produced the same δ^{15}N value within ±0.5‰ (Table 3.8). The results from ALH77250 (IAB) produced a scatter of ±1.5‰ about the mean value, probably the result of greater analytical uncertainty due to the small amounts of gas released from this sample. A relatively high degree of isotopic heterogeneity, due to secondary processing (see Section 3.3.4), is present in this meteorite and and may also contribute to the observed spread in the results. Therefore, the standard errors on each analysis are approximately 0.5‰, although for low nitrogen samples (<10ppm) the errors can be larger by up to a factor of three, which is similar to the errors found from analyses of standard materials (Section 2.4.1). The main source of error from low nitrogen samples is the difficulty of accurately assessing the blank contribution. For samples with an isotopic composition similar to that of the contamination (δ^{15}N = 0‰) these errors will be less significant.

Replicate analyses of the nitrogen concentration produced more variable results than those of the isotopic composition. The results from ALH77250 (3.6±0.6ppm N) and Bischtube (34.0±3.7ppm N) are fairly consistent, but given that the uncertainty in nitrogen content determinations for standard materials is <±5% then much of this variation can be ascribed to sample heterogeneity. The results from Henbury (16.9 and 32.5ppm N) and Four Corners (44.9 and

Sample	Group	wt (mg)	$\delta^{15}N_{air}$(‰)	N (ppm)	Ni (wt.%)	Ref.
ALH77250	IAB		-53.3	3.6	7.0	(1)
ALH77283	IAB	6.53	-60.2	21.0	7.3	(2)
Bischtube	IAB		-42.8	33.8	7.9	(3)
Four Corners	IAB		-55.0	81.2	8.9	(3)
Odessa	IAB	8.29	-60.1	85.5	7.2	(3)
San Cristobal	IAB	5.11	-64.4	40.3	25.0	(4)
Toluca	IAB	4.82	-63.3	13.0	8.1	(3)
Youndegin	IAB	5.02	-59.7	62.7	6.4	(5)
Chihuahua City	IC	3.51	-87.5	67.5	6.7	(3)
Uwet	IIAB	6.10	-95.8	13.9	5.6	(6)
Kumerina	IIC	6.66	+155.6	16.9	9.7	(6)
Wallapai	IID	7.19	+12.5	16.3	11.3	(6)
Barranca Blanca	IIE	5.21	+20.7	2.7	8.1	(7)
Monahans	IIF	4.41	+14.4	23.7	10.6	(6)
Cape York	IIIAB	5.81	-80.0	20.7	7.6	(4)
Henbury	IIIAB		-85.8	24.7	7.5	(4)
Narraburra	IIIAB	5.41	-74.2	32.8	10.1	(4)
Sacramento Mtns.	IIIAB	5.59	-38.1	2.1	7.8	(4)
Sanderson	IIIAB	5.64	-74.5	13.8	9.8	(4)
Thunda	IIIAB	3.37	-78.7	43.9	8.1	(4)
Tamarugal	IIIAB	4.35	-79.1	15.6	8.4	(4)
Carlton	IIICD	5.47	-62.3	38.7	13.0	(8)
Willow Creek	IIIE	6.10	-33.3	5.8	8.8	(4)
Clark County	IIIF	7.82	-16.3	5.1	6.8	(7)
Putnam County	IVA	12.89	+18.0	0.4	8.0	(9)
Tlacotopec	IVB	4.16	+10.0	1.3	15.8	(9)

Table 3.7 Nitrogen concentration and $\delta^{15}N$ value of iron meteorites. Samples for which no sample weight are given have been analysed more than once, the results being the mean of the results from the multiple analyses. The replicate analyses are shown in Table 3.8. The references for the Ni contents are: (1) Kracher *et al.*, 1980; (2) Clark *et al.*, 1980; (3) Wasson, 1970a; (4) Scott *et al.*, 1973; (5) Wasson, 1974; (6) Wasson, 1969; (7) Scott and Wasson, 1976; (8) Wasson and Schaudy, 1971; (9) Schaudy *et al.*, 1972.

Sample	wt. (mg)	This work		Other work		
		$\delta^{15}N$(‰)	N (ppm)	$\delta^{15}N$(‰)	N (ppm)	Refs.
ALH77250	5.25	-53.9	2.9			
	5.47	-51.6	4.1			
	5.57	-54.6	3.8			
		-53.3	3.6			
Bischtube	5.09	-42.9	36.6			
	3.48	-42.8	31.3			
		-42.8	33.8			
Canyon Diablo				-68.9	20.2	(1)
				-49.9	45.0	(1)
				-66.7	48.8	(1)
Toluca	4.82	-63.3	13.0	-54.9	48.2	(1)
				-61.9	69.2	(1)
				-40.9	41.5	(1)
				-13.5	5.7	(2)
				-40.9	4.8	(2)
Four Corners	3.53	-54.5	44.9			
	2.00	-55.4	117.6			
		-55.0	81.2			
Cape York	5.81	-80.0	20.7	-84.6	38.1	(1)
				-84.6	35.4	(1)
				-32.3	20.6	(2)
Henbury	1.42	-86.2	16.9	-83.2	27.9	(1)
	4.58	-85.5	32.5			
		-85.8	24.7			
Carlton	5.47	-62.3	38.7	-60.2	32.4	(1)
Tlacotepec	4.15	+10.0	1.3	+3.3	0.4	(1)
				+12.7	2.1	(2)

Table 3.8 Replicate analyses of iron meteorites. For comparison replicate analyses from other studies are also shown as well as samples which have been analysed during this and other studies. References - (1) Prombo (1984); (2) Pepin and Becker (1982). The sample sizes used by Prombo ranged from 0.7 to 8.6g and those of Pepin and Becker from 7 to 48mg.

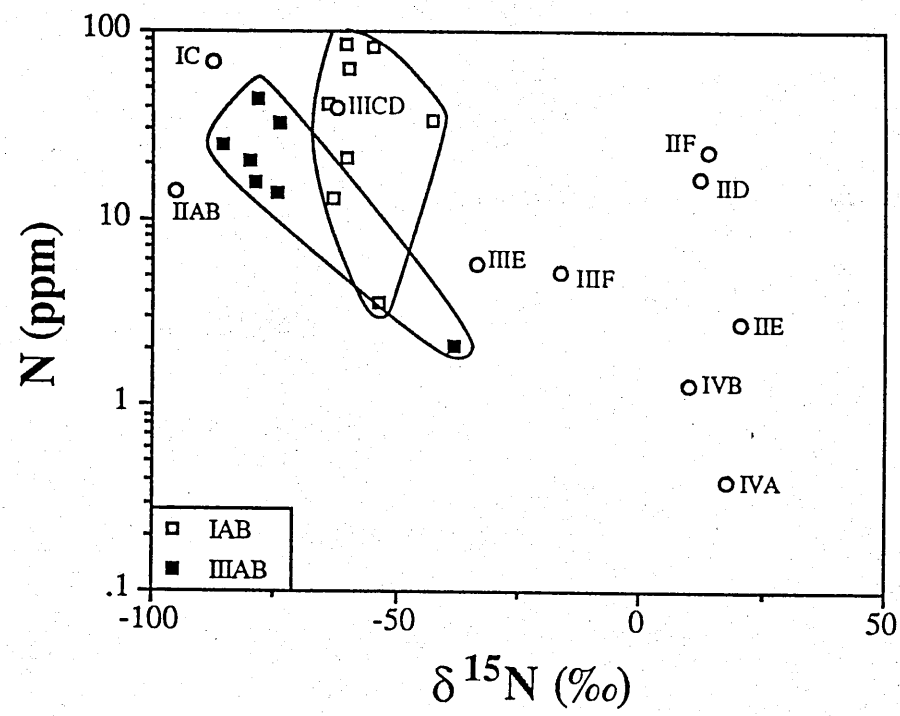

Figure 3.8 Plot of nitrogen concentration versus $\delta^{15}N$ value of iron meteorites. 26 iron meteorites analysed in this study are shown A further sample, Kumerina (IIC) which contains 16.9ppm nitrogen with a $\delta^{15}N$ value of +155.6‰ is not shown. Irons from groups IAB and IIIAB, from which several have been analysed, show a limited range in $\delta^{15}N$ values compared to that displayed by all irons.

117.6ppm N) demonstrate that nitrogen is indeed distributed very irregularly within iron meteorites. However, this variation appears to have little or no effect on the nitrogen isotopic composition, *e.g.* the two analyses of Four Corners had $\delta^{15}N$ values of -54.5 and -55.4‰.

The large range of $\delta^{15}N$ values from iron meteorites (-95.8 to +155.6‰) means that analytical errors of ±0.5‰ can be considered as insignificant. The two groups from which a large number of samples were analysed (IAB and IIIAB) display quite restricted ranges in nitrogen concentration and isotopic composition compared to all iron meteorites (Figure 3.8). However, a few irons from these groups have $\delta^{15}N$ values and/or nitrogen concentrations much lower than other members of those two groups. Similarly, the nitrogen in the IIIE iron

analysed, Willow Creek (5.8ppm, $\delta^{15}N$ = -33.3‰), is considerably heavier than that from Staunton (12.1ppm, $\delta^{15}N$ = -73.5‰), which was analysed by Prombo and Clayton (1983). To determine the cause of these variations within groups it is first necessary to establish their frequency and extent, which is aided by a comparison with published data.

3.3.2 Comparison with Previous Results

The results of replicate analyses from Prombo (1984) (performed on a conventional mass spectrometer; sample size = 0.7 to 8.6g) and Pepin and Becker (1982) (performed on a modified noble gas mass spectrometer; sample size = 7 to 48mg) and samples for which repeat analyses were performed in this study are presented in Table 3.8. There are are a number of observations which can be made from a comparison of the two data sets:

(1) in general, the results from this study agree much more closely with the results of Prombo (1984) than with those of Pepin and Becker (1982),

(2) the variations in the $\delta^{15}N$ values from replicate analyses in this study are considerably less than those observed by either Pepin and Becker (1982) or Prombo (1984)

(3) the variations in nitrogen concentration from replicate analyses in this study were usually similar to, although occasionally larger, than the variations observed by other workers, *e.g.* Gibson and Moore (1971), Shulka and Goel (1981), Pepin and Becker (1982) and Prombo (1984), despite using the smallest sample sizes.

From these observations it appears that the precision of the results from this study are at least comparable with, if not superior, to those published previously. In order to assist with the interpretation of the data from this study they will be combined with the results from Prombo (1984). The extent of the ranges in $\delta^{15}N$ values and nitrogen concentration from the two data sets are very similar (Figure 3.9), the maximum and minimum $\delta^{15}N$ values being +155.6 and

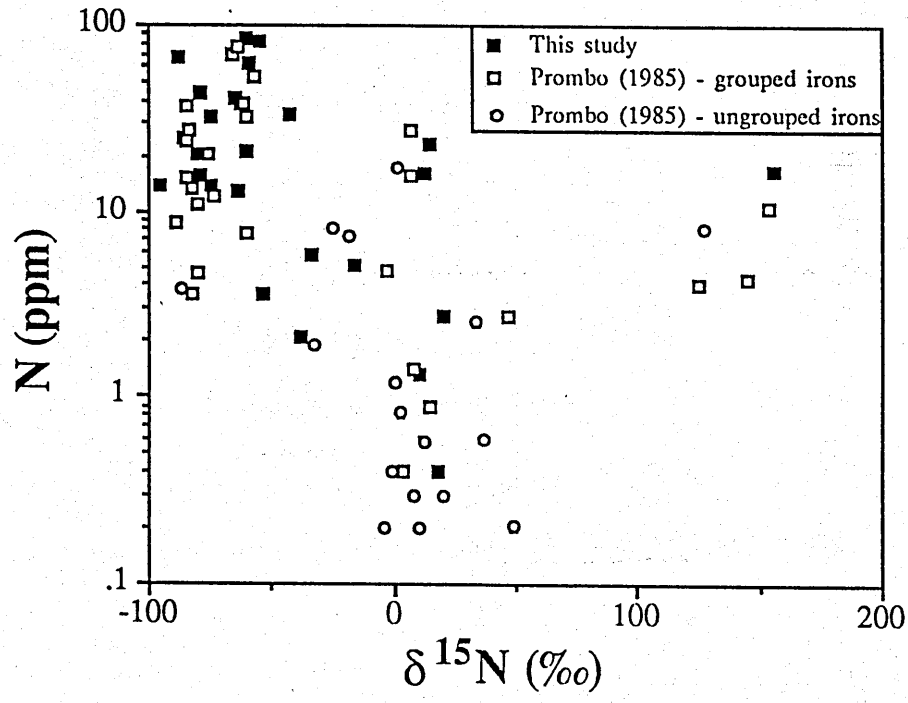

Figure 3.9 Plot of nitrogen concentration versus $\delta^{15}N$ value of iron meteorites - comparison with data from Prombo (1984). The total range of nitrogen concentrations and $\delta^{15}N$ values from the two data sets are very similar, as is the overall co-variation of these two parameters.

-95.8‰ from this study compared to a fractionally narrower range of +153.2 and -91.8‰ from Prombo (1984). Similarly, the variations in nitrogen concentration were 0.4 to 85.5ppm and 0.2 to 77.8ppm nitrogen respectively. The large disparity between the results of Pepin and Becker (1982) with those of both this study and Prombo (1984) suggest that certain unseen analytical problems may have been encountered by Pepin and Becker during extraction or analysis of the nitrogen.

The increased number of data points resulting from combining the results of Prombo (1984) with those of this study helps define the range of $\delta^{15}N$ values displayed by most members of groups IAB and IIIAB and also the unusual nature of the three meteorites from these two groups with much heavier $\delta^{15}N$ values

(Figure 3.10). It is also now clear that a number of other groups display wide ranges in $\delta^{15}N$ values, particularly the IIEs, IIIEs and IIIFs.

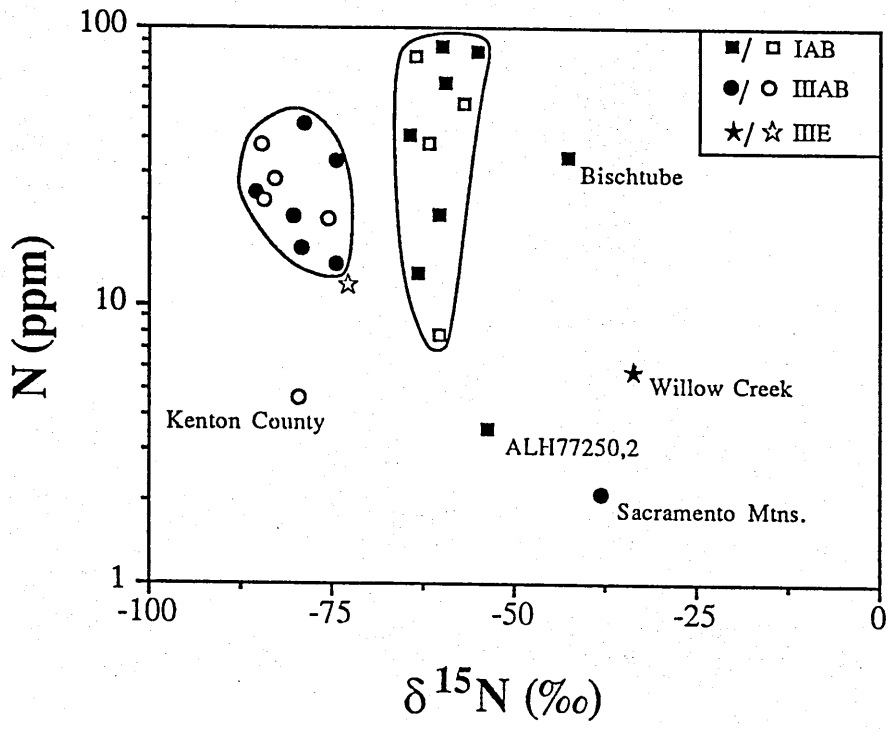

Figure 3.10 Plot of nitrogen concentration versus $\delta^{15}N$ value of iron meteorites - unusual members of groups IAB, IIIAB and IIIE. The five meteorites named have low nitrogen concentrations and/or heavy $\delta^{15}N$ values compared to other members in their respective groups. ALH77250, Sacramento Mtns. and Willow Creek have low nitrogen concentrations and heavy $\delta^{15}N$ values whereas for Kenton County only the concentration is low and Bischtube has only a heavy $\delta^{15}N$ value compared to other members of the group. Nelson County (IIIF) can also be included in the first catagory. The filled symbols are from this study, the open symbols from Prombo (1984).

3.3.3 The Effects of Shock and Recrystallisation on Nitrogen Content.

A range in deformation textures in the metal phase are produced when an iron meteorite is exposed to high shock pressures. For instance Neumann bands (mechanical twin planes) are formed in kamacite at relatively low pressures while conversion of α-iron (kamacite) to ε-iron (cross-hatched iron) is caused at shock pressures above 130kbar (Buchwald, 1975). Reheating of shock-deformed iron

causes stress relief, recovery, polygonisation and recrystallisation, the extent of which is a function of the degree of deformation, annealing time and temperature as well as the composition of the metal (Leslie *et al.*, 1962). The effect of shock events, usually due to orbital collisions, on the nitrogen in the metal phase of iron meteorites is limited. It may be expected that sudden shock pressures of a small body in space may cause a loss of nitrogen but the time scale of such events are extremely short and therefore opportunity for movement of the nitrogen is limited. Although over 50% of the iron meteorites analysed show some evidence of shock deformation, on the whole each group displays a limited range of nitrogen isotopic compositions and concentrations.

As noted in Section 3.3.2, three meteorites had lower nitrogen concentrations and heavier $\delta^{15}N$ values than other members of their respective groups, viz. ALH77250, Sacramento Mtns. and Willow Creek (Figure 3.10). These three meteorites all display annealing effects - in the case of ALH77250 and Willow Creek this is manifested as extensive polygonisation and recrystallisation of the kamacite (Buchwald, 1975). Sacramento Mtns. has suffered much milder annealing, resulting in decomposition and precipitation of minor phases along Neumann bands. However, this meteorite is very unusual in that it has been thoroughly deformed in a style which Buchwald (1975) suggests is the product of geological processes on the parent body followed by secondary shock deformation and cosmic reheating. The time scale of the reheating events, which cause the annealing, is far longer than the collision events and therefore may have a greater effect on the nitrogen in the metal. Schultz *et al.* (1971) noted that compared to IIIAB irons which had not suffered cosmic reheating Ruff's Mountain (IIIAB) was depleted in ^{4}He, ^{20}Ne and ^{36}Ar by a factor of approximately 10. Therefore, the observed depletion of nitrogen in cosmically-reheated iron meteorites may simply be due to diffusive gas loss from the metal during the heating and associated recrystallisation, together with a similar loss of noble gases.

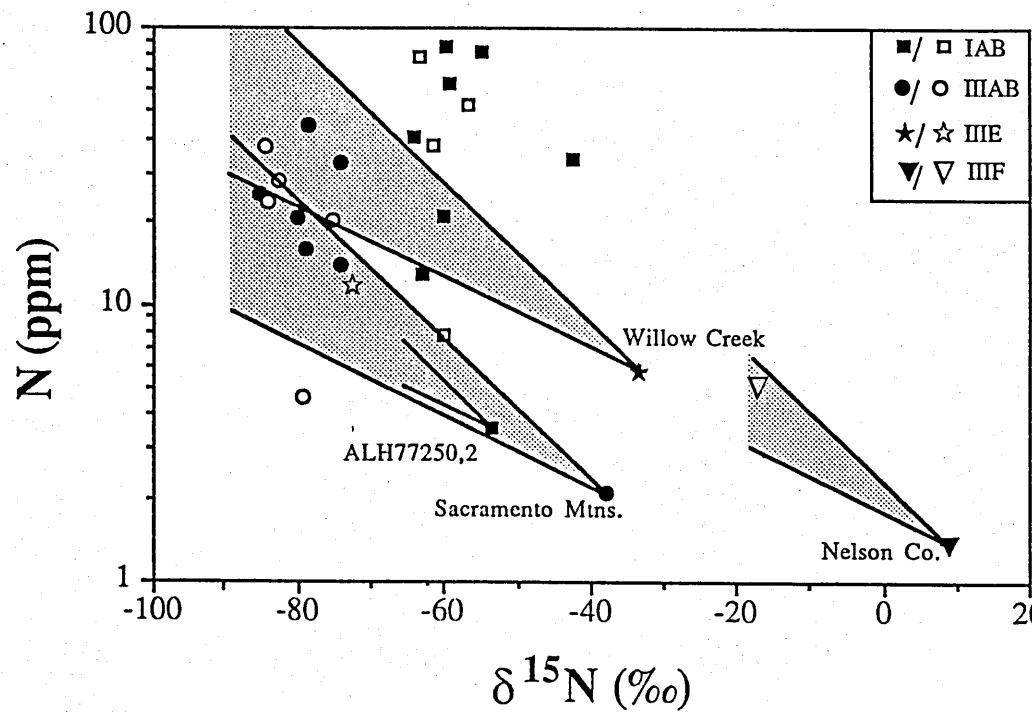

Figure 3.11 Plot of nitrogen concentration versus $\delta^{15}N$ value of iron meteorites - effects of shock and recrystallisation. The four named iron meteorites show evidence of extensive shock and recrystallisation, which may have led to gas loss. The shaded areas define the fractionation paths the nitrogen in these meteorites could have followed if degassing had caused the low concentrations and ^{15}N enriched isotopic composition. The upper boundaries are for only loss of molecular nitrogen, the lower boundary for diffusion of atomic nitrogen. In reality some combination of these two effects would be expected. Filled symbols from this study, open symbols from Prombo (1984).

If the nitrogen from the reheated meteorites has been lost by diffusion out of the metal then an associated isotopic fractionation may be expected. Nitrogen is normally dissolved in metal as atomic nitrogen (Fast, 1965) and if it is to be lost as a gas it will have to aggregate to molecular nitrogen at some point, most probably in the surface layers. Therefore, assuming a very simple model of kinetic isotopic fractionation based on diffusion/evaporation the degree of the fractionation should lie somewhere between that expected for atomic and molecular nitrogen. Figure 3.11 shows the fields of possible fractionation paths nitrogen in the three reheated meteorites may have taken given their present

nitrogen concentration and isotopic composition. The fractionation paths for Sacramento Mtns. pass through most of the IIIAB field although those from Willow Creek and ALH77250 pass above and below the other members of their groups respectively. However, due to the large uncertainties of the nitrogen concentration data, possibly due to sampling problems (see Section 3.3.4) such problems may not be real, particularly in the case of the IIIEs where more analyses may reveal a broader range of nitrogen concentrations.

The IIIF Nelson County has also suffered cosmic reheating and contains 1.4ppm nitrogen with a $\delta^{15}N$ value of +8.6‰ (Prombo and Clayton, 1983). Clark County, a IIIF which has not suffered any annealing (Buchwald, 1975), contains 5.1ppm nitrogen with a $\delta^{15}N$ value of -16.3‰ and this falls in the field of possible fractionation paths leading to Nelson County (Figure 3.11). There appears to exist a strong dependence of relatively low nitrogen concentrations and associated heavy $\delta^{15}N$ values (compared to other members of the same group) with iron meteorites which have experienced cosmic reheating events. Therefore, despite the limited amount of data, there is good evidence that cosmic reheating of shocked iron meteorites causes a substantial loss of nitrogen (60 to 90%) with an associated isotopic fractionation. With more data it may well be possible to use the nitrogen content and isotopic composition of shocked and recrystallised iron meteorites to quantitively determine the degree of reheating experienced by such meteorites.

The Bischtube meteorite (group IAB) has a $\delta^{15}N$ value of -42.8‰, almost 20‰ heavier than other members of the group. However, unlike the meteorites mentioned above Bischtube has a nitrogen concentration comparable to the rest of the group. The structure and geochemistry of this meteorite shows no evidence for extensive shock deformation or recrystallisation (Buchwald, 1975). It is possible that some other, as yet unidentified, secondary process has affected the nitrogen isotopic composition of this meteorite.

3.3.4 Distribution of Nitrogen in Iron Meteorites

To investigate some of the problems identified in the preceeding sections, particularly the distribution of nitrogen and associated isotopic fractionations between the two co-existing metal phases, mechanical separates of kamacite and taenite from the IIIAB iron Mount Edith were performed. As with the normal sampling procedure a thin (0.25x10x10mm) wafer was cut from this high-Ni, medium octahedrite. The wafer was then polished and etched on both sides to permit selection of suitable sampling sites. Taenite-rich areas (mostly plessite - a fine grained intergrowth of α- and γ-iron) and areas of predominantly kamacite were then carefully cut from the wafer using a pair of wire cutters.

To determine the distribution of nitrogen in the minor phases and the extent of any isotopic fractionations between such phases and the Fe-Ni metal, acid residues of 12 of the iron meteorites were prepared. The effect of hot (70°C) 3M HCl on iron meteorites is to selectively dissolve the kamacite, and to a slightly lesser extent the taenite, together with any troilite inclusions. Minor phases such as phosphides, nitrides, carbides, graphite and silicate inclusions are thus concentrated in an acid-insoluble residue under such conditions. The mass of residue recovered from each sample was variable, from 0.02 to 10.6% (Table 3.6). In general the highest recovery rates are from group IAB irons (mean = 5.1%) with those from group IIIAB a factor of 10 less (mean = 0.5%). This is consistent with the much higher abundance of inclusions in the non-magmatic IAB irons compared to all other groups (Buchwald, 1975).

Kamacite - taenite separation

Replicate analyses of the kamacite and taenite separates from Mount Edith (Table 3.9) reveal that the concentration of nitrogen in taenite (86.9, 90.4ppm) is considerably larger than that in kamacite (53.2, 30.7ppm). The isotopic composition in the two phases was also different, taenite having $\delta^{15}N$ values of

	Kamacite		Taenite	
	$\delta^{15}N$ (‰)	ppm N	$\delta^{15}N$ (‰)	ppm N
	-80.8	53.2	-82.9	86.9
	-77.7	30.7	-81.7	90.4
mean =	-79.2	41.9	-82.3	88.7

Table 3.9 Nitrogen concentration and $\delta^{15}N$ value of kamacite and taenite separates of Mount Edith. The taenite separates were virtually pure plessite but the kamacite samples contained small ribbons of taenite. Differeing proportions of taenite in the two kamacite samples may account for the more variable results from the kamacite. Using the second kamacite analysis, assuming 30% taenite in the meteorite gives a whole-rock nitrogen content of 48.1ppm and a $\delta^{15}N$ value of -80.2‰.

-82.9 and -81.7‰ whereas those in the kamacite were -80.8 and -77.7‰. It is apparent that the taenite data were more reproducible than that for the kamacite samples. This is because the taenite samples were more pure than the kamacite sampled which contained small ribbons of taenite. From these results it is clear that taenite contains at least 2 to 3 times more nitrogen than kamacite and therefore small amounts of taenite in the kamacite samples could account for the observed variations. If this is so, the kamacite sample with the lower nitrogen concentration will be more representative of the concentration and isotopic composition of nitrogen in pure kamacite. If taenite containing 2 to 3 times more nitrogen than kamacite is the norm for iron meteorites then this may also account for some of the difficulties associated with obtaining reproducible nitrogen concentrations (Table 3.8). Different mixes of kamacite and taenite in whole-rock samples would have different concentrations of nitrogen, but the overall isotopic composition of the nitrogen would be little affected.

The reason for the heterogeneous nitrogen distribution between the two metal phases is probably related to its solubility in the different lattice structures. This is primarily controlled by the size of the available sites. Taenite, with a face centred cubic lattice has interstitial octahedral sites with a radius of 0.054nm whereas in kamacite, which has a body centred cubic lattice, the sites are only 0.019nm. As the nitrogen atom has a radius of 0.074nm it can be accommodated in taenite with far less lattice distortion than it can in kamacite (Gibson and Moore, 1971). This has a considerable bearing on the maximum solubility of nitrogen, which in taenite is 28000ppm at 650°C but in kamacite is only 1000ppm at 590°C (Sims, 1963). As the metal cools, some of the nitrogen initially present in the taenite is not accommodated in the newly forming kamacite. Either this nitrogen diffuses out of the metal altogether or it can diffuse into the taenite zone. Some nitrogen undoubtedly is used in the formation of nitrides, they would be sampled along with the kamacite metal as the nitrides are very small, typically <20 x 5 x 1μm (Buchwald, 1975) and so would apparently increase the measured nitrogen concentration of the metal. If nitrogen diffuses through the different phases, an isotopic fractionation might be expected.

With a 70% loss of nitrogen a much larger isotopic effect than that observed could be achieved assuming diffusion of atomic nitrogen is the controlling factor. However, given that the mobility of nitrogen within the metal is such that nitrogen can escape from the kamacite it should be expected that some isotopic equilibrium is established between the nitrogen in the kamacite with that in the taenite. Whether the observed fractionation is the result of an equilibrium isotopic fractionation between kamacite and taenite or simply partial equilibration is unresolved.

Acid residues

The results of high resolution stepped combustions of the acid residues are shown in Figures 3.12 and 3.13, with a summary of the data shown in Table

3.10 (the full results are listed in Appendix 2). Typical of most residues is a bimodal release of nitrogen with a low temperature release from room temperature to *ca.* 500°C and a high temperature release anywhere between 500 and 1200°C. The amount of nitrogen in the low temperature release is variable, and occasionally it cannot be resolved from a large release of indigenous nitrogen at slightly higher temperatures. In such cases the $\delta^{15}N$ values of the first few temperature steps are generally around, or tending towards 0‰, indicating the presence of this component, *e.g.* Cape York, (Figure 3.12). The high temperature release is not well defined in the high-Ni members of group IIIAB, *e.g.* Thunda (Figure 3.12), whereas some samples liberate two nitrogen components at elevated temperatures, *e.g.* Youndegin (Figure 3.13).

The isotopic composition ($\delta^{15}N$ tending towards 0‰) and release temperature (25 to 500°C) of the low temperature nitrogen components in all the residues strongly suggests that this component may be a terrestrial contaminant. In some of the residues the $\delta^{15}N$ value of this component is much less than 0‰, but this may simply be due to small amounts of isotopically light nitrogen from components which predominantly degrade at higher temperature, possibly from acid etched surfaces.

The concentration of total nitrogen in the residues ranges from 4.6ppm (Narraburra magnetic) to 4.86wt.% (Henbury) and if only the high temperature releases are considered the range is 1.2ppm (Carlton magnetic) to 4.75wt.% (Henbury) (Appendix 2). If the concentration of nitrogen in the residues is corrected for the mass loss experienced during acid treatment then the concentration of acid-insoluble nitrogen is obtained. This ranges from 0.004 (Carlton magnetic) to 10.638ppm (Henbury) (Table 3.10). Most of the residues contain ≤1% of the total nitrogen recovered from the whole-rock samples (Table 3.11). Exceptions to this are ALH77250, Sacramento Mtns., Henbury and Cape York. ALH77250 and Sacramento Mtns. have experienced a cosmic reheating event which has caused a loss of nitrogen (see Section 3.3.3). The absolute

Figure 3.12 Stepped combustion profiles of the acid residues of the IIIAB irons. The yield axis (histogram) shows the concentration of acid resistant nitrogen in the whole rock (note the different scale on the bottom two diagrams). The low Ni members of this group (the meteorites are arranged in order of increasing whole rock Ni content) contain the highest concentration of acid-resistant nitrogen, with over 10ppm nitrogen in Henbury. The high Ni irons contain virtually no acid-resistant nitrogen. The $\delta^{15}N$ value of the nitrogen in the residues at low temperatures is generally close to 0‰, suggesting terrestrial contamination, but at high temperatures, the isotopic composition is more variable. In the low-Ni irons the $\delta^{15}N$ value is very similar to the whole-rock values (Table 3.7) but in the high-Ni irons the nitrogen remains close to 0‰. It is impossible to determine whether the latter is indigenous to the meteorite or simply trace amounts of contamination, possibly introduced during sawing. Sacramento Mtns , which has an intermediate Ni content, has a concentration of acid-resistant nitrogen and $\delta^{15}N$ which is intermediate between the high and low Ni members of the group. The high absolute concentration of nitrogen in the Henbury residue (≈5wt.%) and the release temperature indicate that the carrier is a nitride. However, the release temperature of nitrogen from the Cape York and Sacramento Mtns. residues is more similar to that of phosphides.

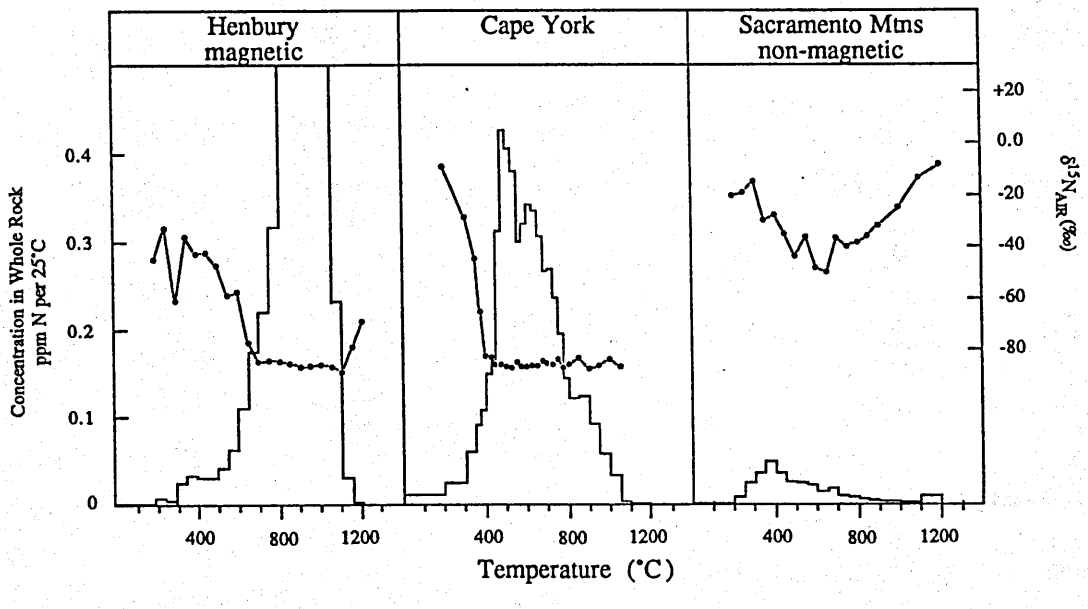
Henbury
magnetic
Cape York
Sacramento Mtns
non-magnetic
Concentration in Whole Rock
ppm N per 25°C
0.4
0.3
0.2
0.1
0
+20
0.0
-20
-40
-60
-80
δ15NAIR (‰)
400
800
1200
Temperature (°C)

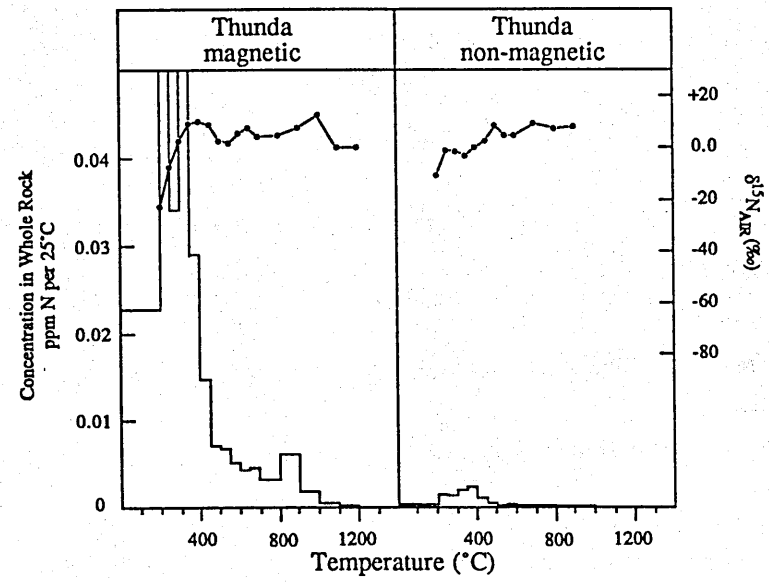
Thunda
magnetic
Thunda
non-magnetic
Concentration in Whole Rock
ppm N per 25°C
0.04
0.03
0.02
0.01
0
+20
0.0
-20
-40
-60
-80
δ15NAIR (‰)
400
800
1200
Temperature (°C)

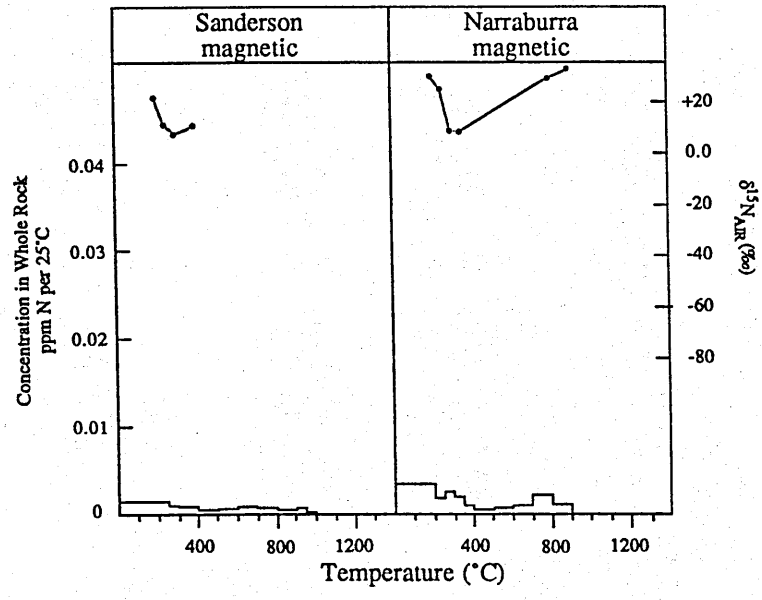
Sanderson
magnetic
Narraburra
magnetic
Concentration in Whole Rock
ppm N per 25°C
0.04
0.03
0.02
0.01
0
+20
0.0
-20
-40
-60
-80
δ15NAIR (‰)
400
800
1200
Temperature (°C)

Figure 3.13 Stepped combustion profiles of the acid residues of the IAB irons. (continued on the following page) The yield axis (histogram) shows the concentration of acid-resistant nitrogen in the whole rock. The IAB irons all contain similar concentrations of acid resistant nitrogen, approximately an order of magnitude less than the IIIAB irons, although this tends to be concentrated in either the magnetic or the non-magnetic separate of each residue. The $\delta^{15}N$ value of the nitrogen released below 600°C tends towards 0‰, indicating that it is most probably terrestrial contamination. At high temperatures the isotopic composition of the nitrogen is very similar to that released from the whole rock samples, *c.f.* the IIIABs. The release temperature of the nitrogen in the magnetic fractions are characteristic of phosphides and possibly nitrides, except the Odessa release which was from a carbide. The nitrogen in the non-magnetic fractions is predominantly released from graphitic carbon, although in the Four Corners residue small amounts of exceptionally heavy nitrogen ($\delta^{15}N = >+1000‰$) are released above 1100°C. This is spallogenic nitrogen from the abundant silicates present in this meteorite. Smaller quantities of spallogenic nitrogen may also be present in the non-magnetic fractions of Youndegin and ALH77250.

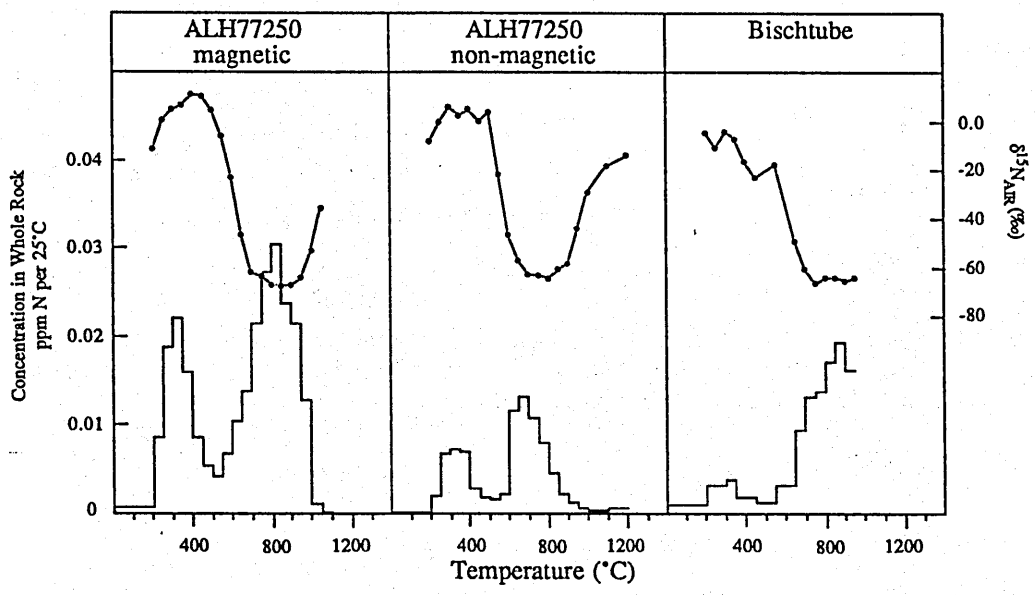
ALH77250
magnetic
ALH77250
non-magnetic
Bischtube
Concentration in Whole Rock
ppm N per 25°C
0.04
0.03
0.02
0.01
0
0.0
-20
-40
-60
-80
$\delta^{15}N_{AIR}$ (‰)
400
800
1200
Temperature (°C)

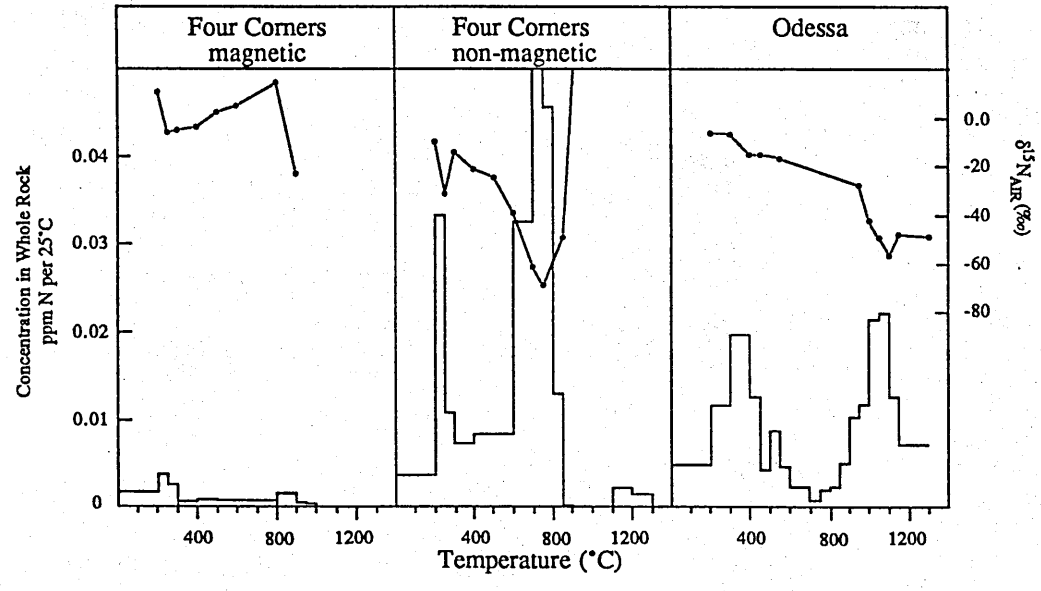
Four Corners
magnetic
Four Corners
non-magnetic
Odessa
Concentration in Whole Rock
ppm N per 25°C
0.04
0.03
0.02
0.01
0
0.0
-20
-40
-60
-80
$\delta^{15}N_{AIR}$ (‰)
400
800
1200
Temperature (°C)

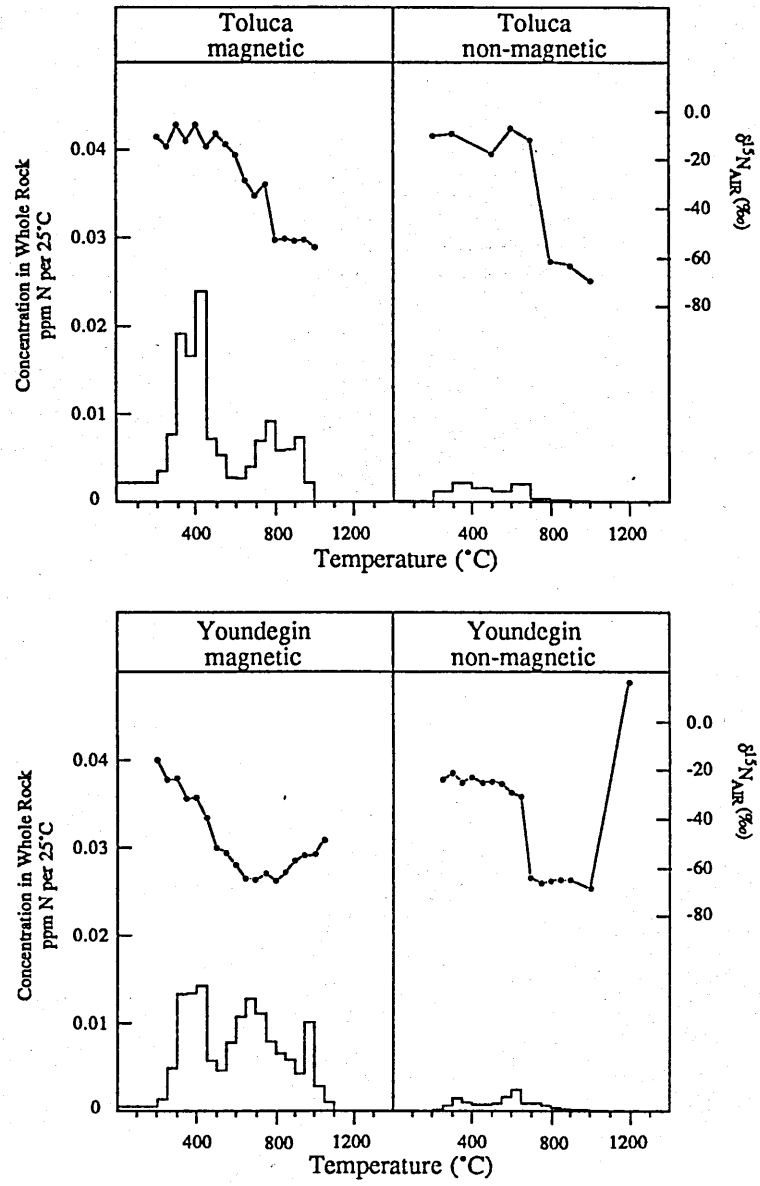
Toluca
magnetic
Toluca
non-magnetic
Youndegin
magnetic
Youndegin
non-magnetic
Concentration in Whole Rock
ppm N per 25°C
0.04
0.03
0.02
0.01
0
400
800
1200
Temperature (°C)
0.0
-20
-40
-60
-80
δ15NAIR (‰)

	BULK		LOW TEMP			HIGH TEMP		
	Conc. (ppm N)	$\delta^{15}N$ (‰)	Max. T. (°C)	Conc. (ppm N)	$\delta^{15}N$ (‰)	Temp (°C)	Conc. (ppm N)	$\delta^{15}N$ (‰)
GROUP IAB								
ALH77250 mag	1.021	-38.9	600	0.372	+3.6	600-1100	0.649	-63.3
ALH77250 non-mag	0.341	-37.8	550	0.117	+1.7	550-1000	0.216	-60.0
BISCHTUBE mag	0.461	-54.2	550	0.080	-10.4	550-950	0.381	-63.4
FOUR CORNERS mag	0.099	+0.7	500	0.065	+2.2	800-900	0.013	-23.1
FOUR CORNERS non-mag	1.243	-26.5	500	0.360	-22.9	500-1300	0.853	-61.4
ODESSA	0.907	-28.8	600	0.449	-11.6	850-1300	0.428	-46.6
TOLUCA mag	0.557	-22.3	600	0.380	-11.2	750-1000	0.122	-52.9
TOLUCA non-mag	0.073	-16.6	700	0.067	-11.1	700-1200	0.006	-62.8
YOUNDEGIN mag	0.592	-50.1	500	0.231	-34.2	500-1100	0.361	-59.7
YOUNDEGIN non-mag	0.051	-35.2	650	0.037	-25.6	650-1000	0.013	-63.7
GROUP IIIAB								
CAPE YORK	6.472	-83.0	375	0.394	-37.2	375-1200	6.078	-86.0
HENBURY mag	11.113	-84.2	600	0.475	-49.1	600-1200	10.638	-85.8
NARRABURRA mag	0.064	+28.6	500	0.044	+26.4	500-900	0.020	+32.3
SACRAMENTO MTNS mag	0.640	-31.6	450	0.309	-27.0	450-900	0.266	-41.3
						1000-1200	0.065	-13.2
SANDERSON mag	0.035	+17.0	400	0.020	+17.0	400-1000	0.015	-
THUNDA mag	0.686	-3.1	450	0.583	-4.6	450-1200	0.120	+5.7
THUNDA non-mag	0.025	-0.2	500	0.020	-1.7	500-1100	0.005	+6.8

Table 3.10 Summary of nitrogen extracted from acid residues of iron meteorites. All the concentrations are expressed as the concentration of acid insoluble nitrogen in the initial whole-rock sample. The data are displayed as three units: the column labelled BULK is the sum of all the nitrogen released from the sample, the column labelled LOW TEMP is the nitrogen released below the indicated temperature - the majority of which is deemed to be of terrestrial origin and the third column, labelled HIGH TEMP is the nitrogen released over the indicated temperature range considered to be indigenous to the sample. The exact cut-off temperature between the low and high temperature components is determined by the shape of the release profile and the isotopic composition of the gas being liberated, usually coinciding with a minimum in the release profile and/or a change in the $\delta^{15}N$ value.

Sample	Whole Rock		Insoluble N			$\Delta\delta^{15}N$	
	$\delta^{15}N$ (‰)	Conc. (ppm N)	$\delta^{15}N$ (‰)	Conc. (ppm N)	%	wr-insol (‰)	wr-sol (‰)
GROUP IAB							
ALH77250 mag	-53.3	3.6	-63.3	0.649	18.03	-10.0	+2.2
ALH77250 non-mag			-60.0	0.216	6.00	-6.7	
BISCHTUBE mag	-42.8	33.8	-63.4	0.381	1.13	-20.6	+0.2
FOUR CORNERS mag	-55.0	81.2	-23.1	0.013	0.02	+31.9	0.0
FOUR CORNERS non-mag			-61.4	0.853	1.05	-6.4	
ODESSA	-60.1	85.5	-46.6	0.428	0.50	+13.5	-0.1
TOLUCA mag	-63.3	13.0	-52.9	0.122	0.94	+10.4	-0.1
TOLUCA non-mag			-62.8	0.006	0.05	+0.4	
YOUNDEGIN mag	-59.7	62.7	-59.7	0.361	0.58	0.0	0.0
YOUNDEGIN non-mag			-63.7	0.013	0.02	-4.0	
GROUP IIIAB							
CAPE YORK	-80.0	20.7	-86.0	6.078	29.36	-6.0	+1.7
HENBURY mag	-85.8	24.7	-85.8	10.638	43.07	0.0	0.0
NARRABURRA mag	-74.2	32.8	+32.3	0.020	0.06	+106.5	-0.1
SACRAMENTO MTNS. mag	-38.1	2.1	-41.3	0.266	12.67	-3.2	+0.4
SANDERSON mag	-74.5	13.8	-	0.015	0.11	-	-
THUNDA mag	-78.7	43.9	+5.7	0.120	0.27	+84.8	-0.2
THUNDA non-mag			+6.8	0.005	0.01	+85.5	

Table 3.11 Comparison of nitrogen in the acid residues with that in the whole-rock samples. Only the nitrogen deemed to be indigenous to the acid-residue is considered (from the column labelled HIGH TEMP in Table 3.10). The two columns under $\Delta\delta^{15}N$ are the difference in the isotopic composition between the nitrogen in the whole-rock sample and that which is in acid-insoluble phases (wr-insol) and calculated to be present in the acid-soluble (wr-sol) phases.

concentration of the total amounts of nitrogen in the acid residues of ALH77250 (1.362ppm) and Sacramento Mtns. (0.640ppm) are comparable with that displayed by other members of these groups, 0.461 to 1.342ppm and 0.064 to 11.113ppm respectively. Therefore, although cosmic heating and recrystallisation of the metal causes a major loss of nitrogen from the whole-rock, this is primarily from the acid soluble phases and possibly the acid-insoluble nitrogen is not affected by these events.

Murty *et al.* (1983) used INAA to determine the nitrogen concentration in 4M H_2SO_4 residues of three IIIAB iron meteorites (Table 3.12) and found similar concentrations of acid resistant nitrogen to those above despite using stronger

	Flakes (ppm N)	Mag. (ppm N)	Non-mag. (ppm N)	Total (ppm N)	Whole rock (ppm N)
Group IAB					
Canyon Diablo	0.7	3.3	1.1	5.1	3.7 - 94
Odessa	1.9	3.5	2.6	8.0	4.9 - 109
Toluca	9.5	1.2	2.1	12.8	49 - 96
Group IIIAB					
Cape York	19.8	0.3	0.2	20.3	36 - 54
Davis Mtns.	2.0	4.1	3.6	9.7	18 - 66
Henbury	0.9	1.4	1.4	3.7	8 - 18

Table 3.12 Previous acid-insoluble nitrogen concentrations for groups IAB and IIIAB. These results were determined using INAA on residues prepared with 4M H_2SO_4. Whole-rock determinations from the same laboratory using the same technique are also presented for comparison. Acid-residue data taken from Murty *et al.* (1983). Whole-rock data taken from Kothari and Goel (1974) and Shulka and Goel (1981).

acids. The concentrations of acid insoluble nitrogen in the IABs are considerably lower than those reported by Murty *et al.* (1983), who found values of 5.1 to 12.8ppm in three IAB irons. Although this is lower than the concentration in the IIIABs it is still more than 10 times the values reported here. The identity of the carrier phase in the 4M H_2SO_4 residues is uncertain as they are present in the

flake, magnetic and non-magnetic fractions (Table 3.12). It may be that one or more of the carrier phases Murty *et al.* (1983) separated is resistant to their 4M H_2SO_4 treatment but was unstable in hot 3M HCl.

The isotopic composition of the nitrogen in 10 of the 19 acid residues is within ±10‰ of that of the parental whole-rock sample (Figure 3.14). However, a number of residues have large differences between the $\delta^{15}N$ value of the whole-rock and the acid-insoluble nitrogen, particularly the high-Ni members of group IIIAB (Thunda, Sanderson and Narraburra). When plotted against the concentration of acid-insoluble nitrogen then it can be seen that the difference in $\delta^{15}N$ value between the whole-rock and acid-insoluble nitrogen ($\Delta\delta^{15}N_{wr\text{-}insol}$) is largest in residues which contain less than 0.5% of the total nitrogen (Figure 3.15).

The largest $\Delta\delta^{15}N_{wr\text{-}insol}$ values from residues containing more than 1% of the whole-rock nitrogen are from ALH77250 (-10.0‰), Cape York (-6.0‰) and Bischtube (-20.6‰). The reason for the large $\Delta\delta^{15}N_{wr\text{-}insol}$ values for

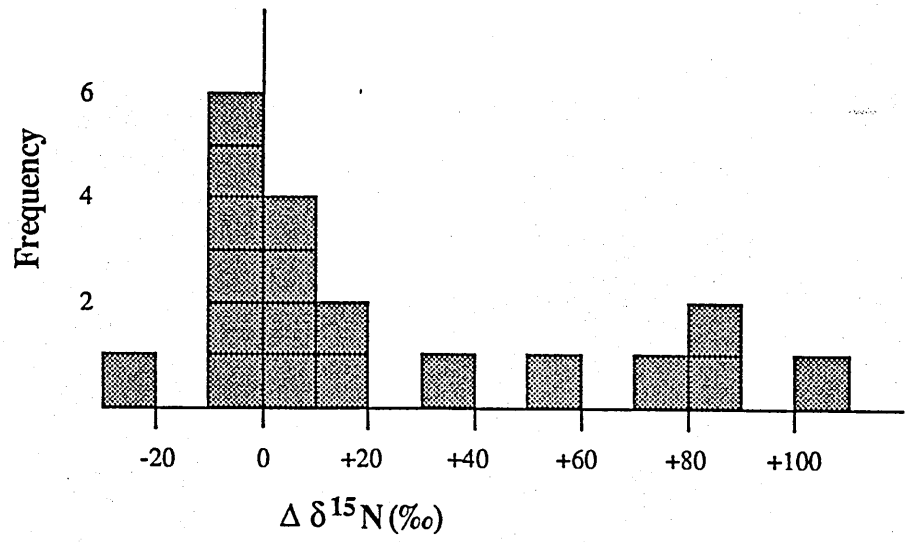

Figure 3.14 Frequency histogram of $\Delta\,\delta\,^{15}N_{wr\text{-}insol}$ values. 10 out of 19 meteorites have $\Delta\delta^{15}N_{wr\text{-}insol}$ values (the difference in the $\delta^{15}N$ value of the whole-rock and acid-resistant nitrogen) of less than ±10‰. However, some meteorites have $\Delta\delta^{15}N_{wr\text{-}insol}$ values of up to +100‰, particularly the high Ni IIIABs.

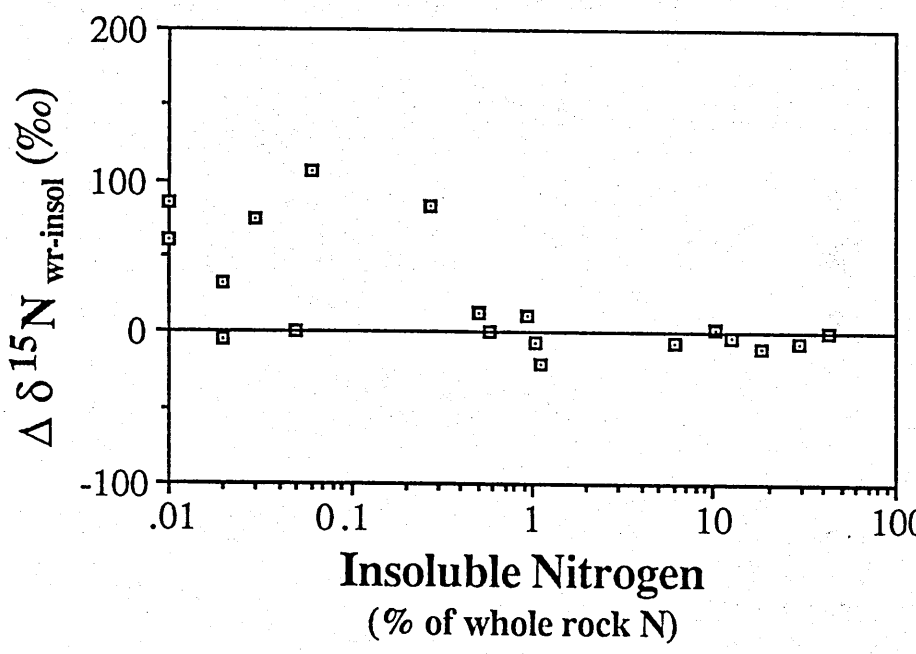

Figure 3.15 Plot of $\Delta\,\delta\,^{15}N_{wr\text{-}insol}$ versus concentration of acid insoluble nitrogen. For meteorites containing more than 0.5% of their nitrogen in an acid resistant phase the $\Delta\delta^{15}N_{wr\text{-}insol}$ values are generally very low, the largest values belonging to Bischtube and ALH77250 which have unusual whole rock $\delta^{15}N$ values (see text). All the meteorites with high $\Delta\delta^{15}N_{wr\text{-}insol}$ contain only very small quantities of acid resistant nitrogen.

ALH77250 can be attributed to preferential loss of nitrogen from the Fe-Ni metal during cosmic reheating (see Section 3.3.3), with an associated isotopic fractionation but with little, if any loss from the acid resistant phases. The Cape York whole-rock analysis may be in error as two analyses of Cape York by Prombo (1984) gave $\delta^{15}N$ values of -84.6‰, closer than the value given here to that of Henbury ($\delta^{15}N$ = -85.8‰), which is related to the Cape York meteorite (Buchwald, 1975). The whole-rock value for Cape York obtained by Prombo (1984) would give a $\Delta\delta^{15}N_{wr\text{-}insol}$ value of only -1.4‰. The whole-rock $\delta^{15}N$ value of Bischtube is considerably heavier than any of the other IAB irons and appears to be somewhat anomalous although the isotopic composition of the residue ($\delta^{15}N$ = -63.4‰) indicates that initially it was the same as the other IABs, the whole-rock value being due to some secondary process (see Section 3.4.3) which affected only the acid soluble nitrogen.

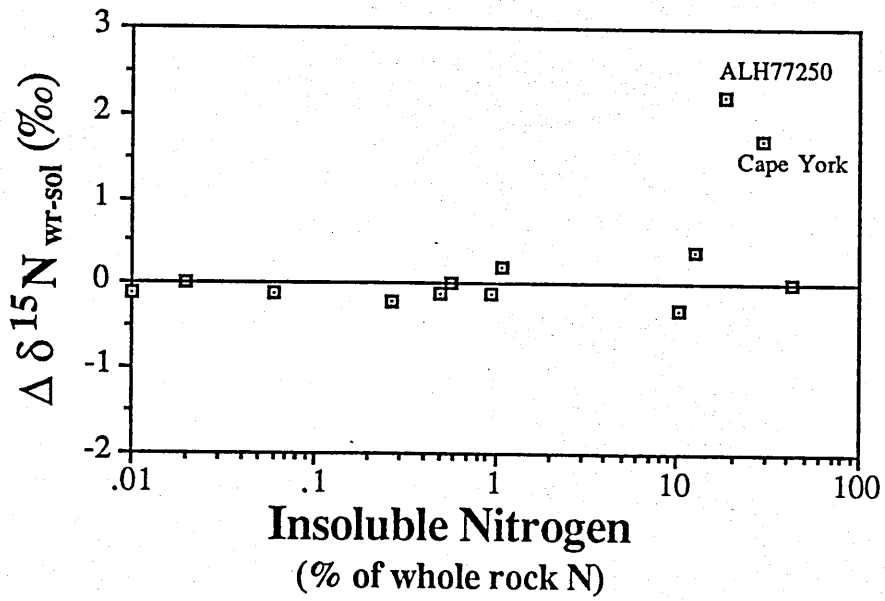

Figure 3.16 Plot of $\Delta\,\delta\,^{15}N_{wr\text{-}sol}$ versus concentration of acid insoluble nitrogen. With the exception of Cape York and ALH77250 the $\Delta\delta^{15}N_{wr\text{-}sol}$ values are all less than ±0.5‰, comparable to the analytical error. As the sampling technique employed for the whole rock samples attempted to exclude large inclusions (*i.e.* only sampling Fe-Ni metal) the effects of the large $\Delta\delta^{15}N_{wr\text{-}insol}$ values in some meteorites (Figure 3.15) are insignificant. Therefore, the results obtained should be representitive of the isotopic composition of the whole meteorite. The ALH77250 meteorite is one of the recrystallised irons (see text). The Cape York whole rock sample ($\delta^{15}N$ = -80.0‰) may have suffered from trace amounts of high temperature contamination, lowering the $\delta^{15}N$ value by 4 - 5‰ as Prombo (1984) reported two analyses, each with a $\delta^{15}N$ value of -84.6‰, which would give a $\Delta\delta^{15}N_{wr\text{-}sol}$ value of +0.4‰.

The degree to which the whole-rock $\delta^{15}N$ value is affected by the acid-insoluble nitrogen can be judged by the difference in the $\delta^{15}N$ value between the whole-rock and the acid-soluble nitrogen ($\Delta\delta^{15}N_{wr\text{-}sol}$). The $\delta^{15}N$ value of the acid-soluble nitrogen, which is assumed to arise from kamacite and taenite, is calculated from a mass balance of the mean isotopic composition of the acid residues and that of the whole-rock sample analysis (Table 3.11). On a plot of $\Delta\delta^{15}N_{wr\text{-}sol}$ against the concentration of acid-insoluble nitrogen all but two irons have $\Delta\delta^{15}N_{wr\text{-}sol}$ values in the range -0.3 to +0.4‰ (Figure 3.16), which is within the range of analytical uncertainty. The two irons with larger $\Delta\delta^{15}N_{wr\text{-}sol}$

values are Cape York, possibly the result of an inaccurate whole-rock value (see above) and ALH77250 which has suffered cosmic reheating (see Section 3.3.3). Those irons with the largest $\Delta\delta^{15}N_{wr\text{-}insol}$ values have more than 99% of their nitrogen dissolved in the metal phase and thus obviously the $\delta^{15}N$ value of the acid-soluble component is very close to the whole-rock value. When a significant percentage of the total nitrogen is concentrated in minor phase(s) the isotopic composition of the acid-insoluble nitrogen has a more pronounced effect on the $\delta^{15}N$ value of the whole-rock sample, but as the $\Delta\delta^{15}N_{wr\text{-}insol}$ of these samples is relatively small the net effect on the whole-rock $\delta^{15}N$ value is negligible.

As the sampling technique employed in this study tended to exclude large inclusions it can be concluded that the effects of isotopic heterogeneity between the minor (acid-insoluble) and major (acid-soluble) phases in iron meteorites has little effect on the results of the whole-rock $\delta^{15}N$ analyses. This is because the samples were predominantly kamacite and taenite which contain almost all the nitrogen with an isotopic composition very close to the average $\delta^{15}N$ value of the meteorite. It is not clear whether the large $\Delta\delta^{15}N_{wr\text{-}insol}$ values observed in some samples indicate the presence of trace quantities of a minor phase with a distinct isotopic composition due to equilibrium fractionation or the presence of pre-solar grains (suggested by Murty *et al.*, 1983) or are simply the result of contamination problems introduced during the sawing, cleaning or acid-dissolution of the sample.

3.3.5 Relationships Between Different Iron Meteorite Groups

In Section 3.3.3 (Figure 3.11) the effects of secondary heating on the nitrogen concentration and isotopic composition in iron meteorites were shown to be considerable, with ALH77250, Sacramento Mtns, Willow Creek and Nelson County all showing such effects. In the following discussion only primary processes will be considered and therefore these four meteorites will be excluded. Having established that large isotopic fractionations between co-existing phases

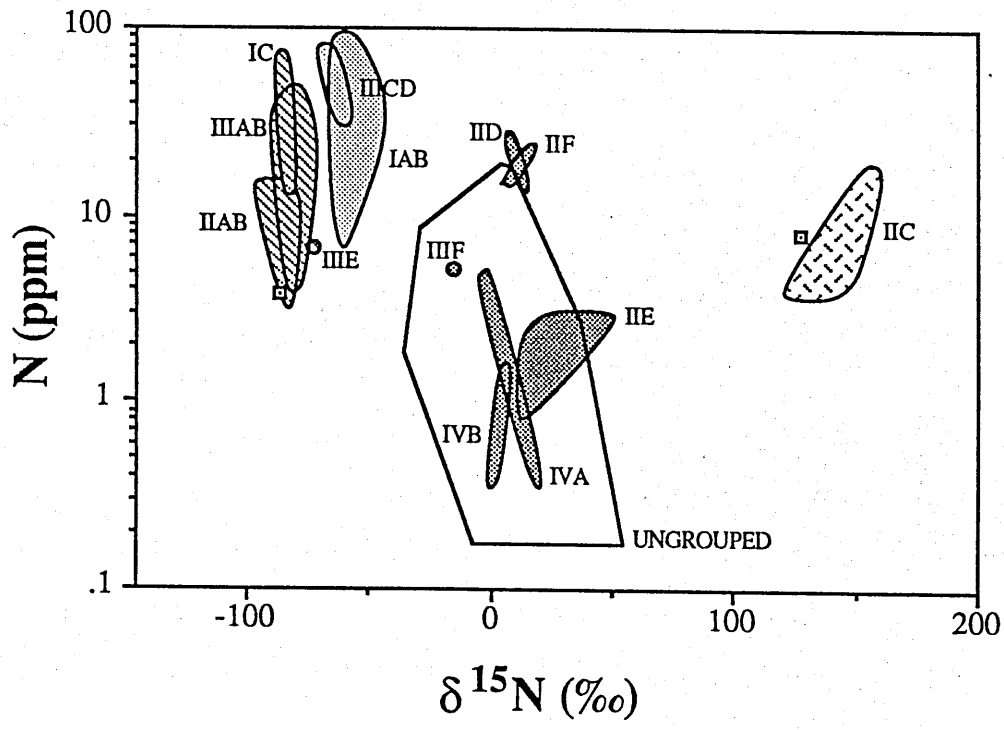

Figure 3.17 Summary plot of nitrogen concentration versus $\delta^{15}N$ value of iron meteorites. The results of Prombo (1984) are added to the results of this study, with the exception of the shocked and recrystallised irons (see Section 3.3.3), to show the overall variation in nitrogen concentration and isotopic composition within and between different groups. The iron meteorite groups can be split into four clusters (different shading) on their nitrogen concentration and isotopic composition (see text). The ungrouped irons from Prombo (1984) are also plotted, more than 90% falling in the large unshaded field around 0‰. However, one ungrouped iron plots adjacent to the IIC field and another on the margin of the IIAB field. Although chemically distinct, it is likely that there is some connection between these particular ungrouped (open squares) and grouped iron meteorites.

do not seriously influence the whole-rock nitrogen isotopic composition determinations (see previous Section) it is now possible to attempt to define and interpret any variations which may be present.

On the basis of their $\delta^{15}N$ values the iron meteorite groups can be divided into four clusters (Figure 3.17), *cf.* Prombo and Clayton (1983) only identified three clusters. The $\delta^{15}N$ value ranges of these four clusters and the groups present in each are:

(1) -96 to -74‰, groups IC, IIAB, IIIAB and IIIE,

(2) -66 to -43‰, groups IAB and IIICD, although apart from Bischtube all these irons fall in the much more restricted range of -66 to -55‰,

(3) -16 to +46‰, groups IID, IIE, IIF, IIIF, IVA and IVB, although, with the exception of the IIE Weekeroo Station these irons have $\delta^{15}N$ values of between -16 to +18‰ and

(4) +125 to +156‰, group IIC.

Of the 18 ungrouped iron meteorites analysed by Prombo (1984) 16 fall in the range -33 to +49‰. The two ungrouped irons which do not fall in this range are Kofa (3.8ppm; $\delta^{15}N$ = -87.1‰) and Bacubirito (8.1ppm; $\delta^{15}N$ = +127.4‰), which have $\delta^{15}N$ values very similar to the first and fourth clusters respectively.

The plot of all the individual data from the iron meteorites (Figure 3.9) shows that in general, irons with high nitrogen concentrations tend to have the lightest $\delta^{15}N$ values and those with lower concentrations tend to have heavier $\delta^{15}N$ values. Although this is suggestive of isotopic fractionation associated with diffusive loss of nitrogen the scatter of the data is too great to be the result of a simple fractionation of an initially homogeneous reservoir, although if the IIC irons are ignored it may be feasible. Parent body processes undoubtedly play a role in modifying the original nitrogen inventory through further degassing and diffusion, which would also impart a pattern of lower nitrogen abundances and heavier isotopic compositions. During melting of the parent bodies, mixing with other components with different isotopic compositions such as organic nitrogen-bearing compounds formed at lower nebular temperatures (Geiss and Bochsler, 1982) may produce a wider range in $\delta^{15}N$ values. However, the extent to which such processes operate and their relevance to the final nitrogen isotopic composition is unknown. Therefore, the range in nitrogen isotopic compositions between different clusters of iron meteorites is most probably due to initial heterogeneity in the solar nebula, in keeping with the conclusions of workers

studying nitrogen in stony meteorites (*e.g.* Kung and Clayton, 1978; Geiss and Bochsler, 1982).

3.3.6 Nitrogen in the Solar Nebula - Evidence from Iron Meteorites

The nitrogen isotopic compositions of the two non-magmatic iron meteorite groups, IAB and IIICD, are indistinguishable (Figure 3.17). The limited range in $\delta^{15}N$ values from the two groups shows that nitrogen in the formation region of the IAB and IIICD parent bodies was isotopically homogeneous. The metallographic structure of irons from these two groups is also very similar (Buchwald, 1975), as are the unusual trace element/Ni trends they define (*e.g.* Figures 3.3, 3.4 and 3.5) (Scott, 1972), all of which indicate that these two groups formed by very similar processes (Scott and Bild, 1974). The oxygen isotopic composition of the silicate inclusions from members of these two groups also fall in the same region in $\delta^{17}O/\delta^{18}O$ space (Figure 3.7) and suggests they formed in a restricted part of the solar system (Clayton *et al.*, 1983). Although very similar, the differences in the trace element variations with Ni and the nature of the silicate inclusions in the meteorites suggest that the IABs and IIICDs probably formed on separate parent bodies (Wasson *et al.*, 1980).

If nitrogen existed as extensive, isotopically homogeneous reservoirs within parts of the nebula, then the other clusters of iron meteorite groups shown in Figure 3.17 may also have genetic significance. The cluster of meteorite groups with $\delta^{15}N$ values between -96 and -74‰ may be from parent bodies which formed in close proximity. This cluster includes the two main magmatic groups, IIAB and IIIAB as well as the minor groups IC and IIIE, which together comprise 75% of all the grouped magmatic iron meteorites. These four iron meteorite groups all have very similar metallographic structures as well as trace element and Ni abundances, *e.g.* Ga/Ni, Ge/Ni and Ir/Ni plots (Figures 3.3 and 3.4) (Buchwald, 1975; Scott and Wasson, 1975). Therefore, the trace element and nitrogen data suggest that the four magmatic groups IC, IIAB, IIIAB and

IIIE, have a common origin, perhaps forming in a distinct region of the solar nebula. However, there is no evidence to suggest they did not belong to separate parent bodies. Indeed, it is probably necessary to invoke two nitrogen reservoirs with slightly different isotopic compositions as on most trace element/Ni plots the four groups are readily resolved into two pairs, groups IC and IIAB and groups IIIAB and IIIE. This pairing is reflected in the $\delta^{15}N$ values, groups IC and IIAB having a range of $\delta^{15}N$ values of -96 to -81‰, slightly lighter than those from groups IIIAB and IIIE, which range from -86 to -74‰ (Figure 3.17).

The variation of nitrogen isotopic compositions and its relationship with the cosmochemistry of the siderophile elements in the solar nebula is not necessarily straightforward. Group IIC irons have Ni contents comparable with group IIIAB and IIIE and trace element concentrations intermediate between groups IIAB and IIIAB yet the IICs have uniquely heavy nitrogen isotopic compositions ($\delta^{15}N \approx$ +150‰). To produce such an enrichment in ^{15}N from nitrogen with an initial $\delta^{15}N$ value of 0‰ by some fractionation process in the solar nebula involving equilibrium or non-equilibrium reactions low temperatures (<100K) are required (Geiss and Bochsler, 1982). However, the metal phases should condense from the nebula at relatively high temperatures, around 1370K (*e.g.* Larimer, 1974). As the lowest calculated equilibrium temperatures between metal and solar nebula gas is about 600K (Sears, 1978) it is probable that the metal was accreted at temperatures far higher than 100K. Therefore, producing the ^{15}N enrichment observed in the IIC iron meteorites by equilibrium isotopic fractionation processes in the solar nebula is not considered likely. The alternative explanation is that, isotopically, nitrogen had a heterogeneous distribution within the solar nebula.

The final cluster of iron meteorite groups, *i.e.* those with $\delta^{15}N$ values around 0‰, is comprised of group IVA (8% of all irons) plus five small groups, IID, IIF, IIIF, IVB and the non-magmatic group IIE (Figure 3.17). Over 90% of all the ungrouped meteorites analysed also have $\delta^{15}N$ values around 0‰. If the

controlling the cooling rate. Further exploration of this relationship is certainly merited, particularly to determine whether the relationship is real or merely fortuitous.

One parameter which may control the cooling rate and could conceivably be linked to the nitrogen isotopic composition of the parent bodies is the abundance of short lived radionuclides. ^{26}Al, with a half life of 7.2×10^5 years, has been proposed by a number of workers as the main heat source for melting of the meteorite parent bodies (*e.g.* Fish *et al.*, 1960). Meteorites with different thermal histories could have had different initial concentrations of this nuclide (Sonett and Reynolds, 1979). Irons with the highest ^{26}Al abundances would have the slowest cooling rates, and it is those irons which have the largest enrichments of ^{14}N. The most commonly proposed site of ^{26}Al synthesis is in the envelope of a nova explosion (Arnould, 1988), but this would also produce an abundance of ^{15}N (Trimble, 1975). This is in direct contrast to the observed distribution of nitrogen isotopes and iron meteorite cooling rates, suggesting that ^{26}Al and nitrogen are in fact decoupled.

However, because of the complex controls of meteorite parent body cooling rates it may still be possible to explain the observed cooling rate and $\delta^{15}N$ variations within the framework of an input of ^{15}N and live ^{26}Al into the solar nebula. By considering the effects of the insulation of parent bodies Wood (1979) has shown that for small parent bodies (radius <20km) with a high degree of sintering it is necessary to have an excess (>40%) of ^{26}Al over normal solar system abundances to achieve melting of the interior. In such a parent body extensive melting occurs during the first half-life of ^{26}Al, but thereafter cooling is fast, reaching values of ≈200K My^{-1} over the temperature range of Widmannstätten pattern formation. Such a cooling rate is directly comparable with that displayed by the IIC irons, typically 100 to 250K My^{-1} (Wood, 1979).

Due to its short half life, ^{26}Al must have been injected into the nebula shortly before accumulation into large bodies (<7×10^6 years) if it is to be considered as

general statements concluded about the other three clusters are correct then it can be assumed that all these groups also formed from a region of the solar nebula with a well defined nitrogen isotopic composition. As these meteorites cover a large, and relatively complete range in trace element and Ni abundances it should be possible to determine if there is any variation in the nitrogen isotopic composition during condensation.

Figure 3.18 is a plot of $\delta^{15}N$ value against Ga/Ni ratio, normalised to the CI chondrite value, the latter being a measure of the degree of equilibrium condensation from an initially homogeneous nebula (Scott, 1978). For those irons with $\delta^{15}N$ values around 0‰ there is no systematic departure away from the mean $\delta^{15}N$ value with increasing Ga/Ni ratio. Therefore, assuming that all

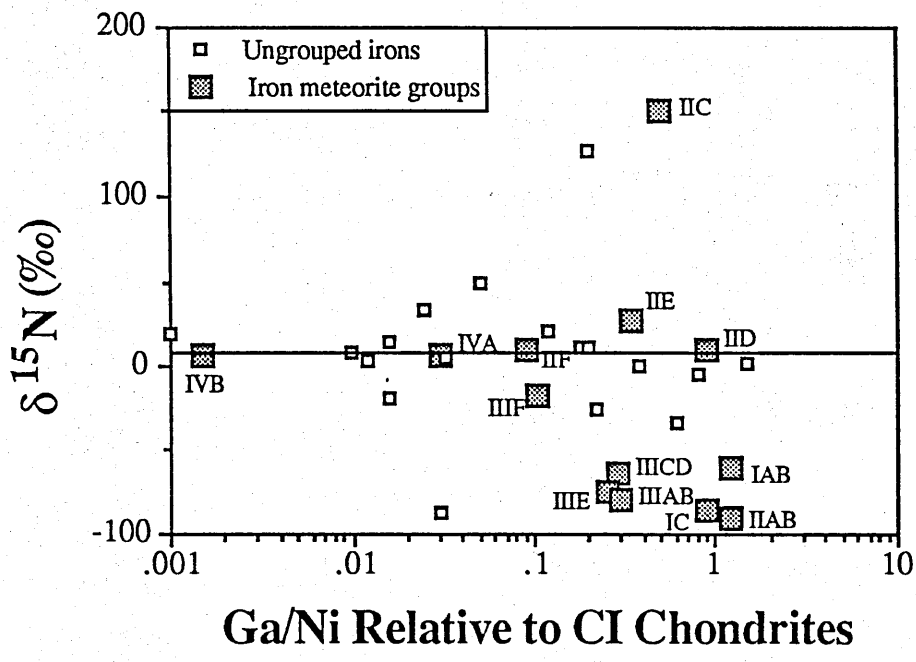

Figure 3.18 Plot of $\delta^{15}N$ value versus CI chondrite normalised Ga/Ni ratio. The open boxes are individual ungrouped iron meteorites, the larger filled boxes the mean values of each iron meteorite group. The Ga/Ni ratio is a measure of fractionation during equilibrium condensation. Although there is a wide range in $\delta^{15}N$ values and Ga/Ni ratios, if the iron meteorites are split into the four clusters from Figure 3.17 then it can be seen that within each cluster there is no systemmatic variation in the $\delta^{15}N$ value with the Ga/Ni ratio. Ga/Ni ratios taken from Scott (1978) and the ungrouped iron meteorite data from Prombo (1984).

these irons did form from a single homogeneous portion of the solar nebula, there is no fractionation of nitrogen isotopes during condensation. Although there is a scatter around the mean $\delta^{15}N$ value (+9‰) this may be due to processing on the parent bodies, as a similar scatter of trace element/Ni ratios around fractionation lines suggest that these ungrouped irons all experienced processes similar to those of the grouped irons (Scott, 1978). It may be that two nitrogen reservoirs are represented by this main central cluster as two of its members, groups IIE and IVA have different oxygen isotopic signatures. Alternatively, this may signify that there were more variations in the solar nebula of the isotopic composition of oxygen, relative to the total range displayed by meteorites than the equivalent range displayed by nitrogen. In contrast, the differences in the $\delta^{15}N$ values of the non-magmatic irons, groups IAB and IIICD, with those from groups IC, IIAB, IIIAB and IIIE are also matched by differences in the oxygen isotopic composition (Clayton *et al.*, 1983), indicating that there can be co-variation of both elements.

3.3.7 Variation of $\delta^{15}N$ Value and Cooling Rates in Iron Meteorites

Using the cooling rates in the review by Wood (1979), Figure 3.19 suggests that there is a positive correlation between cooling rate and $\delta^{15}N$ value. The cooling rates range from 1K My^{-1} for irons with a $\delta^{15}N$ value of around -90‰ up to 250K My^{-1} for group IIC with its $\delta^{15}N$ values of around +150‰. A plot of cooling rate versus nitrogen concentration (Figure 3.20) indicates that for most irons the nitrogen concentration is independant of the cooling rate, although iron meteorites with fast cooling rates (>10K My^{-1}) tend to have low nitrogen concentrations. Such trends are consistent with loss of nitrogen from the hot metal. However, as discussed in previous sections it is unlikely to be possible to account for the $\delta^{15}N$ variations of all iron meteorites evolving from a single homogeneous reservoir. Therefore, it appears that some other process may be controlling the $\delta^{15}N$ value of iron meteorites, and related or coupled to a process

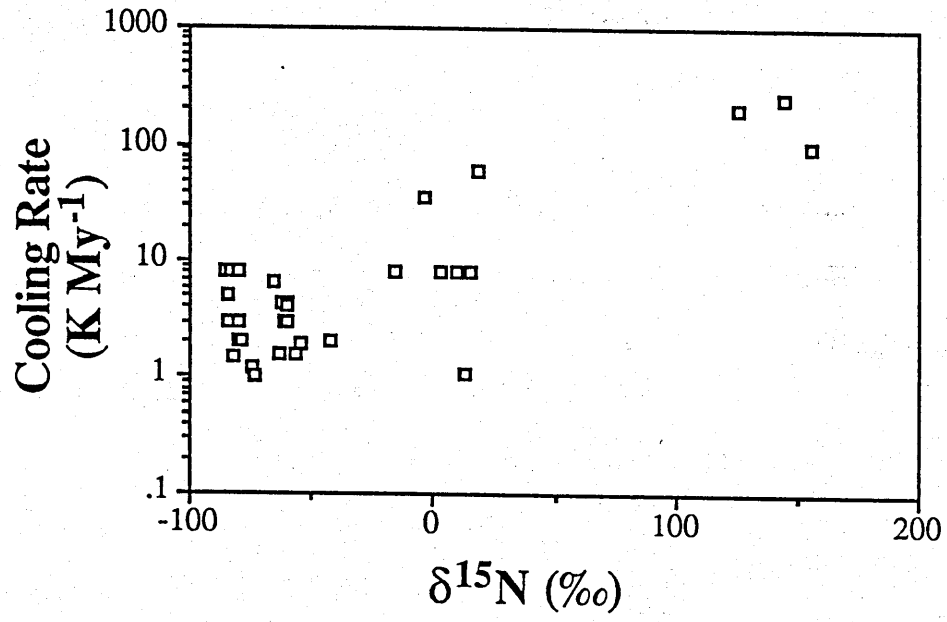

Figure 3.19 Plot of iron meteorite group cooling rate versus $\delta^{15}N$ value. Published cooling rates are available for 30 of the iron meteorites which have been analysed in this study or by Prombo (1984). Only group IIF is not represented on this plot. There appears to be a positive correlation. The cooling rate data are from Wood (1979).

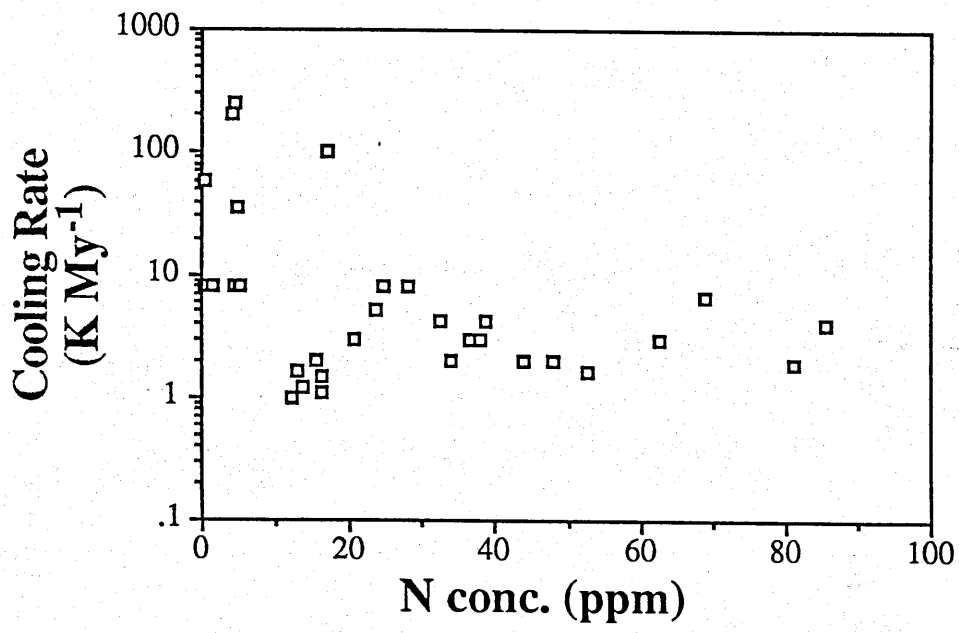

Figure 3.20 Plot of iron meteorite group cooling rate versus nitrogen concentration. The data are for the same meteorites shown in Figure 3.19. The cooling rate data are from Wood (1979).

controlling the cooling rate.. Further exploration of this relationship is certainly metritted, particularly to determine whether the relationship is real or merely fortuitous.

One parameter which may control the cooling rate and could conceivably be linked to the nitrogen isotopic composition of the parent bodies is the abundance of short lived radionuclides. ^{26}Al, with a half life of 7.2×10^5 years, has been proposed by a number of workers as the main heat source for melting of the meteorite parent bodies (*e.g.* Fish *et al.*, 1960). Meteorites with different thermal histories could have had different initial concentrations of this nuclide (Sonett and Reynolds, 1979). Irons with the highest ^{26}Al abundances would have the slowest cooling rates, and it is those irons which have the largest enrichments of ^{14}N. The most commonly proposed site of ^{26}Al synthesis is in the envelope of a nova explosion (Arnould, 1988), but this would also produce an abundance of ^{15}N (Trimble, 1975). This is in direct contrast to the observed distribution of nitrogen isotopes and iron meteorite cooling rates, suggesting that ^{26}Al and nitrogen are in fact decoupled.

However, because of the complex controls of meteorite parent body cooling rates it may still be possible to explain the observed cooling rate and $\delta^{15}N$ variations within the framework of an input of ^{15}N and live ^{26}Al into the solar nebula. By considering the effects of the insulation of parent bodies Wood (1979) has shown that for small parent bodies (radius <20km) with a high degree of sintering it is necessary to have an excess (>40%) of ^{26}Al over normal solar system abundances to achieve melting of the interior. In such a parent body extensive melting occurs during the first half-life of ^{26}Al, but thereafter cooling is fast, reaching values of $\approx$200K My^{-1} over the temperature range of Widmannstätten pattern formation. Such a cooling rate is directly comparable with that displayed by the IIC irons, typically 100 to 250K My^{-1} (Wood, 1979).

Due to its short half life, ^{26}Al must have been injected into the nebula shortly before accumulation into large bodies ($<7 \times 10^6$ years) if it is to be considered as

a possible heat source (Fish *et al.*, 1960). Because of the short time interval before formation of the parent bodies, ^{15}N enriched nitrogen, injected in along with the live ^{26}Al, may have been unable to fully homogenise with the original nebula nitrogen. Unfortunately, the structure and composition of the iron meteorite parent bodies are not well defined, and therefore it is difficult to place any certainty on interpretations of the cooling rate and $\delta^{15}N$ variations.

3.3.8 Relationships Between Iron and Stony Meteorites

Primarily on the basis of their oxygen isotopic composition, 5 of the iron meteorite groups can be linked to different types of stony and stony-iron meteorites (Clayton *et al.*, 1983; Clayton *et al.*, 1986). However, it is entirely possible that in a heterogeneous nebula two unrelated reservoirs may have similar isotopic compositions. Therefore, a genetic indicator independent of the oxygen isotopic composition could greatly assist in unraveling the inter-meteorite group relationships and be applicable to irons which do not contain measurable quantities of oxygen.

The nitrogen isotopic compositions of stony and iron meteorites which can be "related" on the basis of oxygen isotopic composition are shown in Figure 3.21. The IIEs and the H-group chondrites and the IVAs and the L- and LL-group chondrites display very similar ranges in nitrogen isotopic composition as noted by Prombo and Clayton (1983). However, the IAB/IIICDs and the winonaites, in contrast to their similar oxygen isotopic compositions, have very different nitrogen isotopic compositions. These iron meteorite groups have $\delta^{15}N$ values generally between -66 and -55‰ whereas a stepped combustion of Winona revealed only 4.2ppm nitrogen with a $\delta^{15}N$ value of +14‰ above 600°C (Figure 3.22). Below 600°C there is a release of isotopically light nitrogen with a $\delta^{15}N$ value of -27‰. However, as this sample is known to release a large amount of carbon (0.2wt.%) over the same temperature range with an isotopic composition indicative of terrestrial contamination (Grady and Pillinger, 1986) it is probable

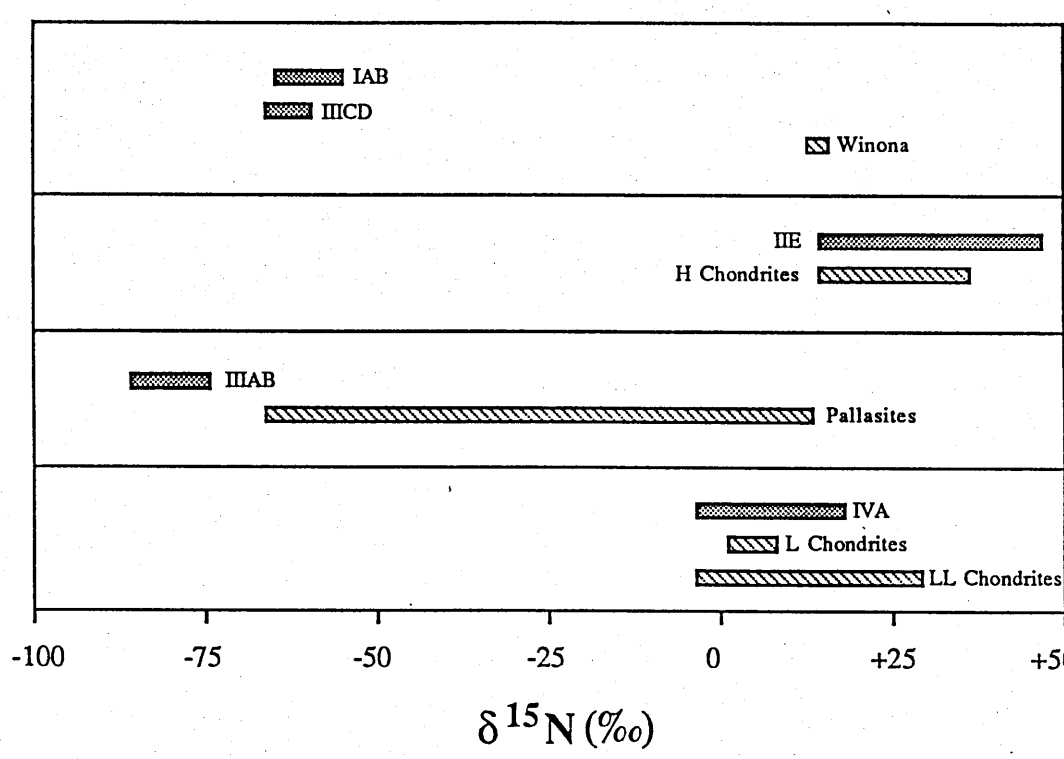

Figure 3.21 Comparison of the $\delta^{15}N$ value of "related" iron and stony meteorites. The IAB and IIICD irons and the winonaites have indistinguishable oxygen isotopic compositions. The H-group chondrites and the IIE irons fall on the same oxygen isotope fractionation line, as do the IIIABs and the pallasites and the IVAs and the L- and LL-group chondrites (Figure 3.7).

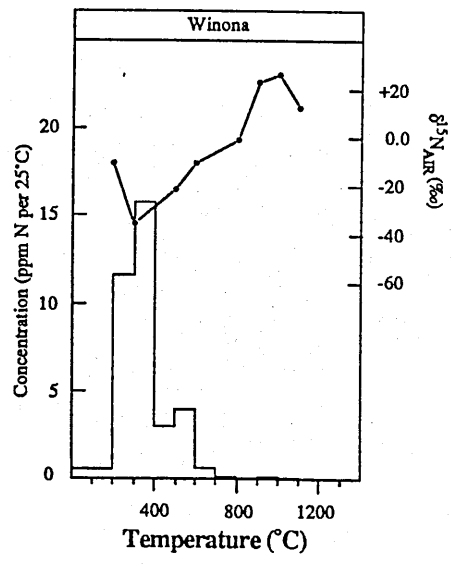

Figure 3.22 Stepped combustion profile of a whole-rock sample of Winona. The large release of isotopically light nitrogen may be indigenous, however, Grady and Pillinger (1986) reported large amounts of terrestrial carbon over the same temperature range, which would normally be expected to be accompanied by some nitrogen.

that a large proportion of the low temperature nitrogen is also terrestrial. If there is a component of nitrogen with a $\delta^{15}N$ value of -60‰ (≈70ppm) its low release temperature is characteristic of organic material.

If the more refractory phases in Winona (*e.g.* metal and silicates) did initially have a $\delta^{15}N$ value similar to that of the IABs, nitrogen loss during the brief heating/melting event suffered by the meteorite (Bild, 1977) may have fractionated the nitrogen present. The scale of the ^{15}N enrichment relative to the IABs is such that to leave 4ppm nitrogen with a $\delta^{15}N$ value of +14‰ in Winona necessitates that the initial nitrogen concentration was greater than 500ppm, assuming a $\delta^{15}N$ value of -60‰. Analyses of the other winonaites may reveal whether such a mechanism is responsible for the large difference in isotopic compositions between Winona and the IABs. It is possible that the $\delta^{15}N$ value has been modified by cosmic rays producing spallogenic nitrogen. However, assuming an initial $\delta^{15}N$ value of -60‰, a minimum cosmic ray exposure age of over 150 x 10^6 years is required to change the $\delta^{15}N$ value to +14‰ using the equation described by Kung and Clayton (1978). The cosmic ray exposure age of Winona is around 50 x 10^6 years (Mason and Jarosewich, 1967), which could only shift the $\delta^{15}N$ value to -35‰.

Group IIIAB irons and the pallasites also have different $\delta^{15}N$ values, the IIIABs falling between -85.8 and -74.2‰ whereas the metal phase of seven pallasites display a much wider range from -66.2 to +12.2‰ (Table 3.13) (Prombo, 1984). The pallasites are believed to have originated at the core-mantle boundary of the IIIAB parent body (*e.g.* Scott, 1977). The exact formation mechanism, however, is not well established, but probably involves mechanical mixing of originally separate liquid metal and solid silicate portions. The mixing/brecciation event may have been the result of a large asteroidal impact with the parent body or collapse of a void at the core-mantle boundary produced by contraction during cooling (Wasson, 1985). The metal phase of the main group pallasites is highly fractionated, with very low Ir concentrations and

Sample	N (ppm)	$\delta^{15}N$ (‰)
Ahumada	13.1	-54.3
Brenham	21.0	-66.2
Finmarken	6.6	-59.1
Glorieta Mtn.	9.7	-51.0
Marjalahti	2.5	-27.9
Pavlodar	0.4	+12.2
Springwater	3.8	-54.8

Table 3.13 Nitrogen concentration and $\delta^{15}N$ value of the metal phase of Pallasites. Data are from Prombo (1984).

high-Ni contents extending beyond the range of the high-Ni IIIABs. This is taken to show that they crystallised at a very late stage in the solidification of the IIIAB parent body core (Scott, 1977). Within such a scheme the spread of $\delta^{15}N$ in the pallasites and the difference between them and the IIIAB irons can be readily explained by loss of nitrogen.

On a plot of nitrogen concentration against $\delta^{15}N$ value the pallasites define a progression to low concentrations and heavier isotopic compositions which can be traced back to the composition of the IIIAB irons (Figure 3.23). The variation in nitrogen isotopic composition and concentration from the IIIABs through the pallasites very closely follows the path predicted for fractional loss of molecular nitrogen from the metal. The range in $\delta^{15}N$ values and nitrogen concentration is much more restricted in the IIIABs than in the pallasites which suggests that the major nitrogen loss event was a late stage event associated with pallasite formation. The violent agitation of the metal during the collapse or brecciation event which produced the pallasites may have been sufficiently thorough to cause the observed loss of nitrogen.

Glorieta Mountains and Pavlodar have distinctive trace element abundances implying that they had a different formation history to the rest of the main group

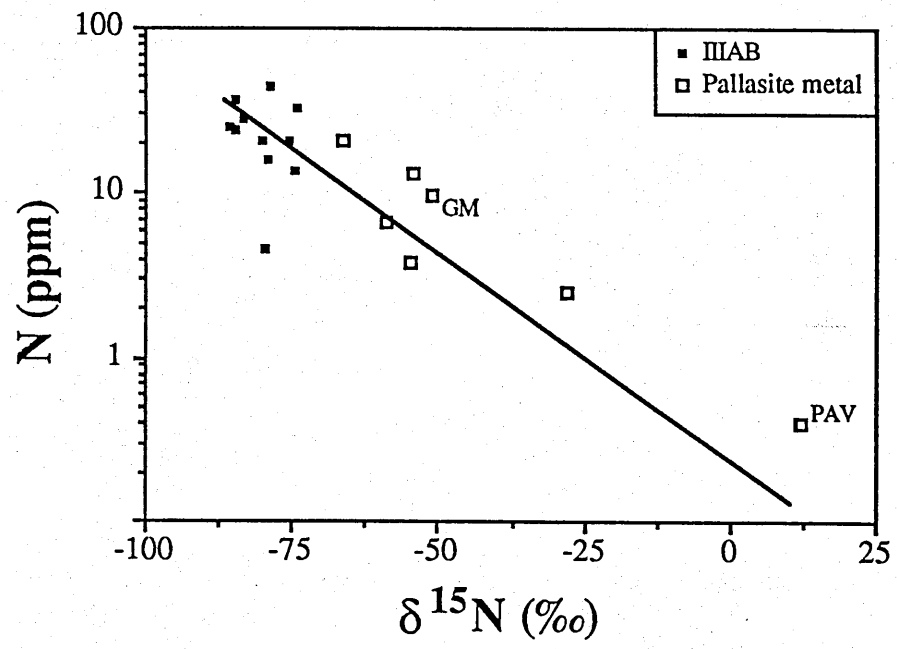

Figure 3.23 Plot of nitrogen concentration versus $\delta^{15}N$ value of the pallasites. The IIIAB irons, possibly related to the pallasites, are also shown on this plot. With increasing $\delta^{15}N$ value the concentration of nitrogen systematically falls, with the IIIAB irons plotting at the high nitrogen concentration/low $\delta^{15}N$ value end of the sequence. The line shown is for Rayleigh fractionation during degassing of metal with an initial nitrogen concentration of 25ppm and $\delta^{15}N$ value of -85‰. GM = Glorieta Mountain and PAV = Pavlodar (see text). Pallasite data from Prombo (1984).

pallasites (Scott, 1977). The oxygen isotopic composition of their silicates however is indistinguishable from the other pallasites (Clayton and Mayeda, 1978a). The nitrogen data suggest that the metal phase of all the main group pallasites may indeed be related. The relatively high trace element abundances in Pavlodar may be the result of a late stage input of primitive metal melt from the surrounding mantle, similar to the process proposed by Pernicka and Wasson (1987) to account for small enrichments observed in the high-Ni IIIABs. However, it is not clear how some of the very low trace element abundances in Glorieta Mountains could be produced from IIIAB metal.

The published isotopic composition of nitrogen in most of the remaining stony meteorite groups is shown in Figure 3.24. Almost all the groups display

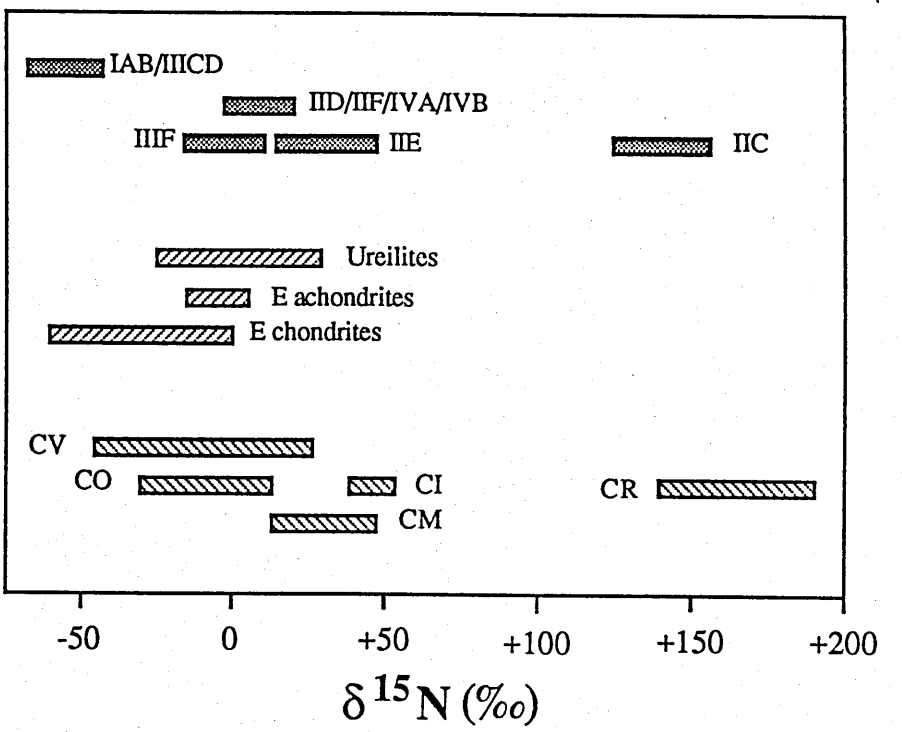

Figure 3.24 Comparison of $\delta^{15}N$ value of "unrelated" iron and stony meteorites. The range of nitrogen isotopic compositions in stony meteorite groups which have not been linked to iron meteorite groups are shown. Most of the groups display wide ranges of $\delta^{15}N$ values around 0‰, making it almost impossible to match any up with the 6 iron meteorite groups also found in this range. Only the unusual CRs and the IIC iron meteorites show any clear similarities. Data for stony meteorites taken from Kung and Clayton (1978), Kerridge (1985), Grady *et al.* (1985) and Grady *et al.* (1986).

wide ranges in $\delta^{15}N$ values (≈50‰) and are largely confined in the range -50 to +50‰. Such large ranges in $\delta^{15}N$ make it difficult to identify any close matches with one of the 6 iron meteorite groups which also cluster around 0‰. Two of the stony meteorite groups do have restricted ranges of $\delta^{15}N$ values, the CIs (+39 to +52‰) and the enstatite achondrites (-16 to +4‰). The CI range overlaps with the heaviest value recorded from group IIE and that of the enstatite achondrites matches the range displayed by the IIIFs (including the recrystallised meteorite Nelson County). However, although such results merit further investigation, only two meteorites have been analysed from each group and with

more analyses broader ranges in the $\delta^{15}N$ values comparable to the other stony meteorite groups may be revealed. Also, most of the nitrogen in the CI chondrites is present in the organic material, and therefore direct comparison with the nitrogen in the much more refractory metal of the iron meteorites should be treated with caution. It is intriguing to note that during stepped heating of the enstatite chondrites nitrogen libertated above has $\delta^{15}N$ values as low as -60‰ (Grady *et al.*, 1986), comparable with that in the IAB and IICD irons.

The CR carbonaceous chondrites have heavy $\delta^{15}N$ values (+140 to +190‰), which are very similar to those displayed by the IIC iron meteorites (+125 to +156‰). Although the match is not perfect the unusual nature of the nitrogen within the two types of meteorite suggests that they could have formed in the same region of the solar nebula. However, as noted for the relationship between the ordinary chondrites and the IIE and IVA irons, the exact significance of primitive chondritic meteorites and irons (highly differntiated meteorites) having the same $\delta^{15}N$ value is unclear. In such cases a much better understanding of the relationship between iron and chondritic material would be possible if related differentiated silicates also existed.

3.4 COMPARISON OF THE NITROGEN VARIATION IN MAGMATIC AND NON-MAGMATIC GROUPS

To compare the variations of nitrogen isotopic composition and concentration in the magmatic and non-magmatic groups the largest, and possible the most extensively studied groups were selected, with group IIIAB being taken as representative of the magmatic irons and IAB for the non-magmatic irons. As with Section 3.3 the meteorites which have suffered high shock pressures and recrystallisation are excluded from the discussion.

3.4.1 Nitrogen in Group IIIAB Iron Meteorites

The whole-rock analyses display a range in concentrations from 13.8 to 48.1ppm nitrogen and $\delta^{15}N$ values from -85.8 to -74.2‰ (Table 3.7). As noted earlier these results are in good agreement with the results of Prombo (1984) who found a similar range of isotopic compositions ($\delta^{15}N$ = -84.6 to -75.6) and concentrations, although one sample, that of Kenton County, was found to contain only 4.6ppm nitrogen. In order to determine if there is any change in the nitrogen concentration or isotopic composition with evolution of the parent body it is useful to plot the nitrogen data against the Ni content of the meteorite. In general, each magmatic iron meteorite group is believed to have formed on a different parent body, solidifying by fractional crystallisation of a single homogeneous pool of molten metal. In such an environment the Fe-Ni phase diagram (Figure 3.2) predicts that the first metals to solidify will be relatively depleted in Ni and that as fractional crystallisation continues the crystallising metal will become progressively enriched in Ni. Therefore, any variation with Ni concentration should indicate that the nitrogen is affected by processes operating during cooling of the parent body.

The results of this study (filled symbols in Figure 3.25a) show that the lowest $\delta^{15}N$ values in group IIIAB are from irons with the lowest Ni content and with increasing Ni the nitrogen isotopic composition becomes heavier. Most of the results of Prombo (1984) follow a similar pattern although two, Bella Roca and Grant, have relatively low $\delta^{15}N$ values compared to other members of the group with similar Ni contents. On a plot of nitrogen concentration against Ni content (Figure 3.25b) the data points fail to resolve any systematic variation. The results from Prombo (1984), with the exception of Kenton County with its unusually low nitrogen concentration, suggest that there may be a decrease in nitrogen concentration with increasing Ni content. Prombo's data was acquired from much larger sample (1000 times larger than those employed in this study) and

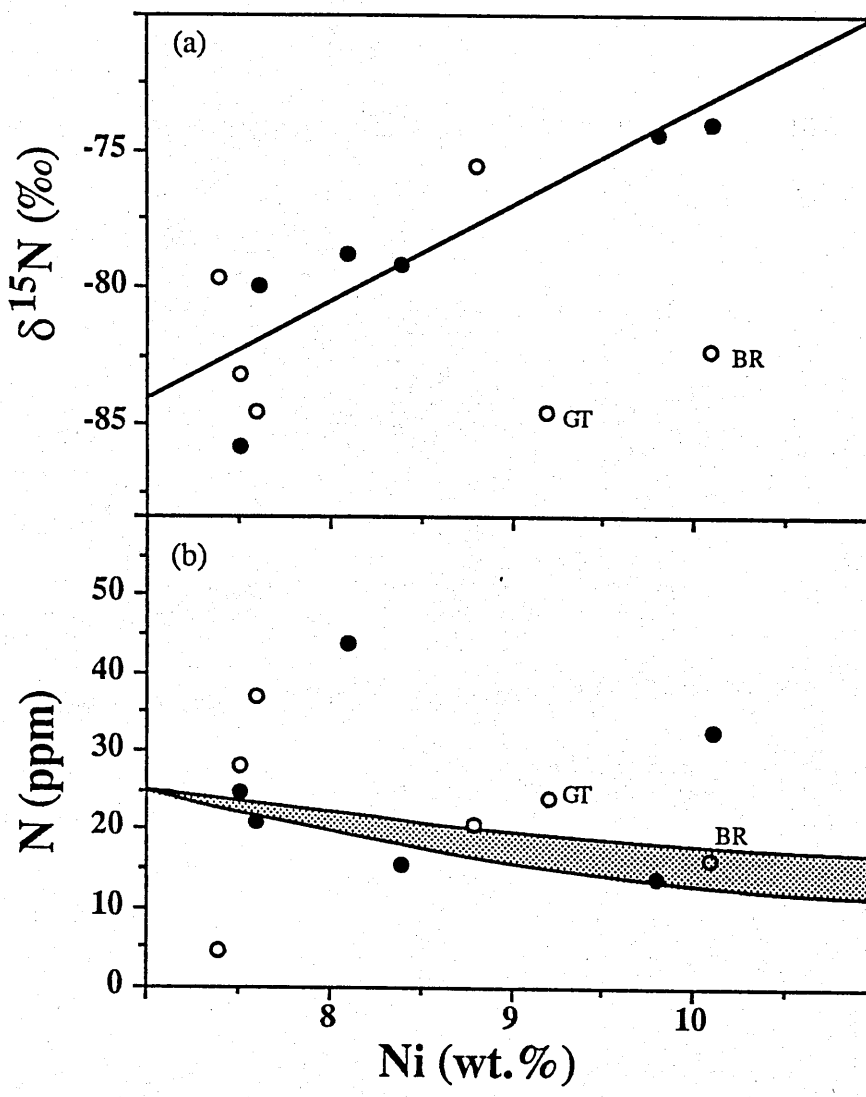

Figure 3.25 Plots of $\delta^{15}N$ value and nitrogen concentration versus Ni content in the IIIAB iron meteorites. The filled circles are the results of this study, the open circles from Prombo (1984). Meteorites which are present in both data sets are linked together. (a) The regression line drawn (r = 0.853 - significant at the 99.9% level) does not consider Bella Roca (BR) or Grant (GT) (see text). (b) The shaded area shows the variations in nitrogen concentration which would result if volatile loss were responsible for the variations in $\delta^{15}N$ value with Ni content defined by the line in the top half of the figure. The top boundary is for only diffusion of atomic nitrogen and the bottom boundary for only loss of molecular nitrogen.

therefore problems due to sampling of variable amounts of kamacite and taenite may be less severe.

The concentration of acid resistant nitrogen in the lowest Ni members of group IIIAB is the highest of that found in any iron meteorites (10.6ppm) but in irons with more than 8wt.% Ni the concentration falls to <0.2ppm (Figure 3.12 and Table 3.9). The high absolute nitrogen concentration of the Henbury residue (4.86wt.%) indicates that most of the nitrogen is present as a nitride, probably carlsbergite (CrN), which is common in this meteorite (Buchwald, 1975). The main nitrogen release between 800 and 1100°C closely resembles the release temperature of osbornite (TiN) (Grady *et al.*, 1986) which can be expected to decompose at similar temperatures to that of carlsbergite. The nitrogen release profile from the Cape York residue is rather puzzling, the high nitrogen concentration (up to 2900ppm) suggests that a nitride may be present yet the release temperature is considerably lower than that expected from nitrides. Analysis of the residue using an ATEM revealed only a number of Fe-Ni phosphides. Recently, Ash *et al.* (1987) have shown that at very small grainsizes (from 60 to 0.005μm) the grainsize has a large effect on the release temperature of nitrogen from diamonds when all other parameters are constant and therefore it may be that the nitrogen in the Cape York residue is bound in very small nitride crystals (<0.1μm) which were concealled from the ATEM by the phosphides.

The low concentrations of acid-resistant nitrogen in the high-Ni irons may simply be trace amounts of contamination as the absolute amounts of gas liberated (see Appendix 2) were generally only a few nanograms (close to blank levels) and the $\delta^{15}N$ values, up to 100‰ heavier than the corresponding whole-rock values, are close to that of terrestrial contamination. Sacramento Mountains has a Ni content of 7.8wt.%, intermediate between that of Cape York (7.6wt.%) and Thunda (8.1wt.%) and despite the effects of extreme secondary processes has an intermediate acid-resistant nitrogen concentration and isotopic composition (Figure 3.12).

3.4.2 Nitrogen in the IIIAB Parent Body

The well defined variation of the siderophile trace element abundances with the Ni content of the IIIABs suggest that these elements were at one stage homogeneously distributed within a single pool of molten metal, probably at the core the parent body (*e.g.* Scott and Wasson, 1975). It is probable therefore that nitrogen was similarly distributed throughout the liquid metal and should also imply at least an approximation to isotopic homogeneity. Although most of the data points display a relationship of increasing $\delta^{15}N$ value with increasing Ni content two of the high-Ni irons have $\delta^{15}N$ values similar to those with low-Ni contents. This indicates that the isotopic composition of the nitrogen may not have been homogeneous, some of the meteorites having evolved along separate, but possibly similar routes. If this is the case the heterogeneity could either be due to incomplete mixing in the core, or the structure of the IIIAB parent body was more akin to that of the raisin-bread structure (Figure 3.6). To account for the progressive nitrogen isotopic variation in the majority of IIIAB irons, a process which results in the nitrogen gradually being enriched in ^{15}N during cooling and solidification of the parent body core must have been operating. Two processes which could produce the observed $\delta^{15}N$ variations are:

(1) late-stage addition of metal containing heavy nitrogen or

(2) loss of nitrogen from the molten metal with an associated kinetic isotopic fractionation.

There are strong negative correlations between refractory siderophile elements (*e.g.* Ir, Ru, Re, Pt and Os) with Ni content except at the high-Ni end of group IIIAB. This may be due to small amounts of primitive metal melt from the overlying mantle being introduced into the residual liquid of the almost completely solidified core (Pernicka and Wasson, 1987). If this primitive metal contains nitrogen with a much heavier isotopic composition the bulk $\delta^{15}N$ value of the residual liquid in the core may be significantly altered. Pernicka and

Wasson (1987) calculated that the residual liquid in the core need only be contaminated with 0.1% primitive melt to produce the observed trace element abundances. If the nitrogen of this late stage melt has a $\delta^{15}N$ value of around 0‰ then its concentration must be more than 100 times that of the core metal to produce the observed shift in $\delta^{15}N$ value of the IIIABs. Alternatively, assuming a concentration of nitrogen in the primitive metal like 25ppm the observed shift in $\delta^{15}N$ values could be produced if the primitive metal had a $\delta^{15}N$ value of more than +10000‰. Either way, given the constraints imposed by the siderophile trace elements, it appears highly unlikely that the small observed ^{15}N enrichment with increasing Ni could be produced by addition of late-stage melts with a heavier nitrogen isotopic composition.

Fractionation of the isotopes of nitrogen during a degassing episode could occur when nitrogen diffuses through the metal as atomic nitrogen or during escape as molecular nitrogen. Assuming an initial nitrogen concentration of 25ppm when the crystallising phase contains 7.0wt.% Ni the curve shown in Figure 3.25a would be associated with a range of nitrogen concentrations depicted by the shaded area in Figure 3.25b if kinetic isotopic fractionation occurred during degassing. Despite the high degree of uncertainty ($\approx\pm30\%$) in the nitrogen concentration results (Table 3.8) most of the data points fall within, or close to, this region. In considering this interpretation it is noteworthy that the proposed mechanism appears successful for producing the observed nitrogen concentration and isotopic compositions observed in the closely related metal phase of the main group pallasites (see Section 3.3.8). If this is the correct interpretation it follows that $\delta^{15}N$ measurements are capable of discerning the location in the IIIAB parent body core sampled by individual iron meteorites.

The high concentrations of acid-insoluble nitrogen in Henbury, Cape York, and to a lesser extent Sacramento Mtns. is most probably linked to the differing solubility of nitrogen in kamacite and taenite. Kamacite can accommodate significantly less nitrogen than taenite (see Section 3.3.4) and as the metal cools

the kamacite exsolves the nitrogen which then combines with other exolved species such as Cr to form nitrides (Nielsen and Buchwald, 1981). Therefore, as the low-Ni irons are almost entirely kamacite (*i.e.* they have little or no taenite) the highest concentrations of nitride should be expected in these low-Ni irons with slow cooling rates as these are the conditions which will promote nitride growth.

3.4.3 Nitrogen in Group IAB Iron Meteorites

Whole-rock analyses of the IAB irons reveal a large range of nitrogen concentrations from 13.0 to 85.5ppm and $\delta^{15}N$ values from -64.4 to -42.8‰ (Table 3.7). With the exception of Bischtube all the other IAB irons have $\delta^{15}N$ values in the much narrower range of -64.4 to -55.0‰, which is very similar to the results of Prombo (1984) who reported nitrogen concentrations of 7.7 to 77.8ppm and $\delta^{15}N$ values of -63.7 to -57.0‰ (Table 3.4). With all the data on a plot of $\delta^{15}N$ value against Ni content no systematic variation of these two parameters is apparent (Figure 3.26a) although the lightest isotopic compositions ($\delta^{15}N$ = -64‰) are restricted to the more Ni-rich irons (Colfax at 10.4wt.% Ni and San Cristobal at 25.0wt.%) and a clustering of values around -60‰ for irons containing <7.5wt.% Ni. The three irons which have intermediate Ni contents (7.5 to 10wt.%) and display a wide range in $\delta^{15}N$ values - Four Corners (8.9wt.% Ni, $\delta^{15}N$ = -55.0‰), Bischtube (7.9wt.% Ni, $\delta^{15}N$ = -42.8‰) and Toluca (8.1wt.% Ni, $\delta^{15}N$ = -54.3 to -63.3‰) can however be subjected to closer scrutiny.

Toluca was analysed three times by Prombo and Clayton (1983) who reported $\delta^{15}N$ values of -54.3 to -61.9‰ (Table 3.8), with a mean of -57‰. This high degree of uncertainty could be due to either contamination problems or possibly sampling of variable proportions of kamacite and taenite (the same can also be said of Prombo and Clayton's analysis of the Canyon Diablo meteorite (Table 3.8)). The value obtained in this study and Prombo and Clayton's most

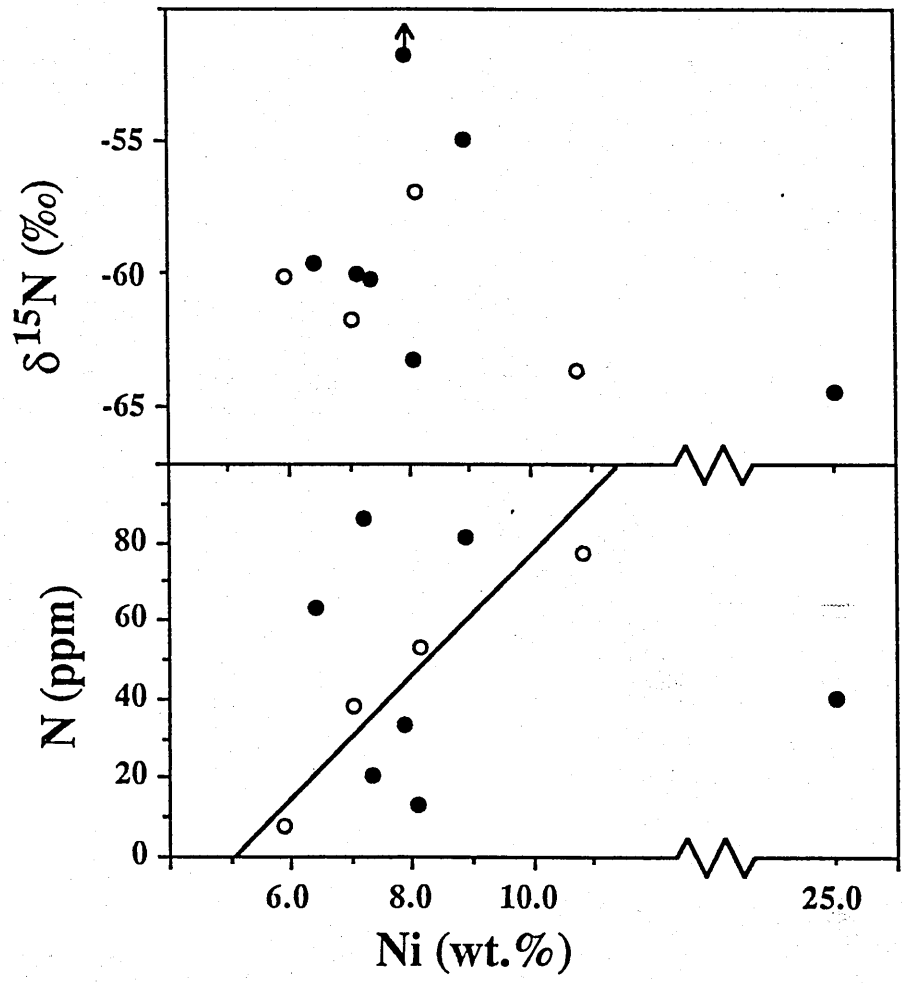

Figure 3.26 Plots of $\delta^{15}N$ value and nitrogen concentration versus Ni content in the IAB iron meteorites. The filled circles are the results of this study, the open circles from Prombo (1984). Iron meteorites which are present in both data sets are linked together. (a) The iron which plots off-scale is Bischtube ($\delta^{15}N$ = -42.8‰). (b) There is no identifiable systematic variation between nitrogen concentration and Ni content from the results of this study. However, the data of Prombo (1984), using samples up to 1000 times larger, reveal a positive correlation between these two parameters (r = 0.90 - significant at the 95% level).

extreme value are in good agreement and follow the trend of decreasing $\delta^{15}N$ with Ni content.

Four Corners acid residue contains many silicate inclusions (<0.1mm) which have small amounts of exceptionally heavy nitrogen ($\delta^{15}N >> +1000‰$). The concentration of this nitrogen is at least 0.5ppm, but because of the small amounts of gas liberated from each temperature step (≈0.5ng) accurate $\delta^{15}N$ value measurements were not possible. However, by assuming a cosmic ray exposure age of 700×10^6 years (the mean of 14 IAB iron meteorites (Voshage and Feldmann, 1979)) the $\delta^{15}N$ value of the silicates should be around +3000‰ due to spallogenic production of nitrogen. Although attempts were made to exclude most of the silicate inclusions from the whole-rock samples some were possibly included. Therefore, it would be possible to produce the measured $\delta^{15}N$ values of whole-rock samples of Four Corners if the the sample contained <20% silicate, assuming that the metal phase contained nitrogen with a $\delta^{15}N$ value comparable with the majority of IAB irons. The errors on this calculation are rather large due to analytical uncertainty on the small amounts of gas and the lack of a known exposure age for the meteorite; a longer exposure age would result in less silicate being required to produce the observed effect.

Bischtube also has a long cosmic ray exposure age of 895×10^9 years (Voshage and Feldmann, 1979) and therefore the ^{15}N-enrichment relative to other IAB irons could be due to spallogenic production of nitrogen. However, no silicates were visible in the piece of meteorite sampled during this study and none were observed in the acid residue. As no silicates are believed to be present spallogenic production of nitrogen in the metal must be considered. However, similar sized irons (10-30cm across) with long exposure ages do not appear to contain large concentrations of spallogenic ^{15}N compared to much larger members of the same group, *e.g.* Thunda (Voshage and Feldmann, 1979), suggesting that the production rate in metal is considerably lower than that in silicates. Therefore, the ^{15}N-enrichment in the metal phase of Bischtube cannot

be due to cosmic ray produced spallogenic nitrogen, although some other secondary process is probably involved as the acid residue contains nitrogen with a $\delta^{15}N$ value identical to that of the other IAB irons (Table 3.10). Analytical uncertainty is excluded as two analyses of this meteorite produced near identical results (Table 3.8).

From the total data set of this study there appears to be no co-variation of nitrogen concentration and Ni content in the IABs whereas the results of Prombo (1984) suggest that there is a positive correlation between N and Ni contents (Figure 3.26b). However, the uncertainty on some of the results from Prombo (1984) are rather large, two of the values being the mean of replicate analyses which were very widely separated *e.g.* the Toluca value of 53.0ppm is the mean of 41.5, 48.2 and 69.2ppm nitrogen and similarly the value of 38.0ppm for Canyon Diablo is the mean of 20.2, 45.0 and 48.8ppm nitrogen. The sample size employed by Prombo was approximately 1000 times greater than that used during this study yet the uncertainty on the concentration values appear to be no better. Therefore, with only four points with large errors on the nitrogen concentration data ($<\pm 40\%$) defining the positive correlation between nitrogen concentration and Ni content its significance is questionable.

In contrast to the magmatic irons of group IIIAB all the irons analysed from group IAB contain similar quantities of acid-resistant nitrogen with an isotopic composition similar to that obtained from whole-rock determinations, excluding cosmogenic components (Figure 3.13 and Table 3.10). The range in the concentration of acid resistant nitrogen is from 0.128 to 0.866ppm. In most samples this is contained in the magnetic fraction although Four Corners and ALH77250 contained considerable amounts in the non-magnetic fraction (mostly in graphitic carbon, which was common in the pieces of these meteorites which were sampled).

The isotopic compositions of the acid residues were relatively constant, most values falling in the range -59.7 to -63.7‰ (n = 7), very similar to the range

displayed by most of the whole-rock analyses. There were two main exceptions to this, the magnetic fraction of Toluca ($\delta^{15}N$ = -52.9‰) and the Odessa residue ($\delta^{15}N$ = -46.6‰). The latter is considered to be an erroneous result due to problems encountered separating small quantities of nitrogen (<6ng) from large amounts of CO_2 (>10^6ng) generated by the oxidation of the host carbide. However, similar problems were not encountered during the analysis of Toluca, the result of which remains to be understood. Interestingly, the non-magnetic fraction of the Toluca residue does contain nitrogen with a $\delta^{15}N$ value similar to that of the whole-rock sample (-62.8‰).

3.4.4 Nitrogen in the IAB Parent Body

When considering the preferred nitrogen data for the IAB samples, the most striking observation is that the variation in $\delta^{15}N$ values with Ni content (Figure 3.26a) is opposite to that displayed by the magmatic group IIIAB (Figure 3.25a) and suggests mutually incompatible formation processes for the two groups. It has been argued (see Section 3.4.2) that the nitrogen data for the IIIAB irons supports a model of fractional crystallisation, therefore it is unlikely that this process was responsible for the formation of the IAB iron meteorites. In the model of fractional crystallisation of a large pool of molten metal to produce the IAB irons advocated by Kracher (1985) the concentration of sulphur is required to be exceptionally high, necessary to alter the K_d values of the trace elements. Under such circumstances it may be that sulphur will interact with the nitrogen, drastically altering its behaviour. However, Gibson and Moore (1971) found that the behaviour of nitrogen was more chalcophile than siderophile, with nitrogen being concentrated in troilite (FeS) relative to the metal phase. As the IAB irons contain the highest concentrations of nitrogen in iron meteorites (Figure 3.17) it is unlikely that exceptionally large amounts of sulphide melt were intimately involved in their formation.

Rather than being the result of some major geological process it is possible that a minor secondary process is responsible for the limited range in $\delta^{15}N$ values (<5‰) displayed by the IABs (excluding Four Corners and Bischtube). The low-Ni IAB irons contain virtually no taenite, the Fe-Ni metal phase composed almost entirely of kamacite. The high-Ni members contain about 40% taenite, and San Cristobal, with 25wt.% Ni is approximately 95% taenite (Buchwald, 1975). From the analyses of Mount Edith, it has been shown that there is a higher concentration of nitrogen in taenite with a $\delta^{15}N$ value 4.5‰ lighter than that in the co-existing kamacite (see Section 3.3.4). It is noteworthy that it is the IAB irons which are predominantly composed of kamacite which have the lowest nitrogen concentrations and heaviest $\delta^{15}N$ values whereas those containing abundant taenite have the highest nitrogen concentrations and the lightest $\delta^{15}N$ values (Figure 3.26). Therefore, it is not inconceivable that some of the range of $\delta^{15}N$ values displayed by the IAB irons could simply be the product of kinetic isotopic fractionation brought about through nitrogen expulsion from kamacite.

The variation of $\delta^{15}N$ value with Ni content (≡kamacite:taenite ratio) in the IIIABs is in the opposite to that seen in the IAB iron meteorites. Therefore, the effect of isotopic fractionation during kamacite crystallisation will be to partly mask the underlying trend of increasing $\delta^{15}N$ value with Ni content produced during the crystallisation of the taenite from the molten metal (see Section 3.4.2).

Equally, processes operating in the parent body may have influenced the nitrogen isotopic composition. The uniform isotopic composition of the acid resistant nitrogen in group IAB irons suggests that a high degree of isotopic homogeneity was achieved (the larger range of whole-rock $\delta^{15}N$ values being the result of later processes such as spallogenic production of ^{15}N and cosmic reheating). It is necessary to consider that either the metal condensed with a homogeneous nitrogen isotopic composition or it was homogenised on the parent body. Most workers agree that the IAB irons formed as numerous small pools of metal dispersed throughout a parent body (McSween, 1987) which rules out

mechanical mixing of the metal as a homogenisation mechanism. However, volatile mobilisation during melting could produce a homogeneous reservoir of molecular nitrogen. Equilibration between the vapour phase and the metal droplets would then result in widespread homogenisation of the nitrogen isotopic composition of the metal.

Slow escape of nitrogen from the interior of the parent body would result in the residual nitrogen becoming enriched in ^{15}N. As the ^{129}I-^{129}Xe ages of silicate inclusions in the IABs show that 6 x 10^6 years elapsed between the formation of the high-Ni irons and the formation of the low-Ni irons (Niemeyer, 1979), the envisaged degassing scenario is consistent with the observed trend of increasing $\delta^{15}N$ value with decreasing Ni content. However, such a crystallisation sequence is the opposite to that predicted by the Fe-Ni phase diagram for a single pool of metal and so the IAB irons must have formed at different formation sites within the parent body. Regions which experienced less heating producing more Ni-rich melts and cooling to the closure temperature before hotter regions.

Most workers believe that the parental material which was melted to produce the iron meteorites was roughly chondritic in nature. The most primitive metal available are the inclusions in the C2 meteorites which show a wide range of Ni (4.0 to 9.3 wt.%), Co (0.17 to 0.74 wt.%), Cr (0.17 to 1.00 wt.%) and P (up to 3.16 wt.%) contents (Grossman and Olsen, 1974). Such a range in compositions must presumably affect their melting temperatures. With such a spread in major elements a large variation in the siderophile trace element abundances may also be expected. Mixing of multiple components has been used to try and model the formation of metre sized bodies in the solar nebula (Scott and Bild, 1974) but such models require a large number of components to account for all the trace element/Ni trends observed in the IABs. However, partial melting of small grains within a parent body will produce relatively large ranges of possible compositions from a relatively narrow range of initial compositions.

The presence of a number of components with different melting temperatures and nitrogen isotopic compositions would also produce a range of $\delta^{15}N$ values during melting of the parent body. The low-Ni irons have near chondritic trace element/Ni ratios, suggesting near total melting of a chondritic source rock (Wasson *et al.*, 1980). The Ni-rich irons have non-chondritic trace element/Ni ratios and they may be the product of small amounts of partial melts (Kelly and Larimer, 1977). If the source region contained components with more than one nitrogen isotopic composition, then preferential partial melting of the one containing lighter nitrogen could produce the high-Ni IABs, near complete melting of all the components producing the low-Ni irons with the heavier $\delta^{15}N$ values.

Two different models of the formation of the IAB irons relying on melting of a chondritic source have been proposed. Kelly and Larimer (1977) assumed that the IABs formed by melting within the interior of the parent body. In contrast, Wasson *et al.* (1980) have proposed that the IABs formed near the surface of a parent body in a "mega-regolith", the main heat source being derived from impacts on the surface. Both models require that the irons formed as small, dispersed, partially molten pools of metal. In the near-surface environment the pressures, temperatures and cooling rates experienced by each pool will be strongly influenced by specific impact events. However, the IABs show a very small range in cooling rates (1 to 5K My^{-1}), even compared to the magmatic groups (Wood, 1979). Because of the variety of shock pressures and temperatures, as well as fracture structures associated with different impacts it would be expected that the nitrogen in each metal pool in a near-surface environment would suffer varying degrees of degassing and thus isotopic fractionation. However, the $\delta^{15}N$ values are all quite similar. These characteristics are more in keeping with formation deep in the interior of a parent body where specific events on the surface have far less pronounced local effects.

The acid residues of the IAB irons all contained similar quantities of acid resistant nitrogen, although this tended to be concentrated in only one of the magnetic or non-magnetic separates. The magnetic separates were predominantly composed of phosphides and occasionally carbides, with trace amounts of nitride present in the Youndegin residue. The non-magnetic fraction was normally dominated by graphitic carbon although the Four Corners residue was predominantly silicates. Trace amounts of silicate may also have been present in the Youndegin and ALH77250 residues although they were not observed. The non-magnetic fraction of both of these meteorites contain small amounts of nitrogen with a $\delta^{15}N$ value considerably heavier than the rest of the high temperature releases, similar, although much less pronounced to the release above 1100°C from the Four Corners non-magnetic fraction. These features simply reflect the well documented high abundance of inclusions in the IAB irons (*e.g.* Buchwald, 1975) and the high cosmic ray exposure ages of these meteorites (Voshage and Feldmann, 1979).

3.5 SUMMARY

On the basis of their nitrogen concentration and isotopic composition the iron meteorite groups can be divided into four clusters. Groups IC, IIAB, IIIAB and IIIE have $\delta^{15}N$ values between -95 and -75‰, groups IAB and IIICD, the two main non-magmatic groups, have values between -65 and -55‰ and group IIC ranges from +125 to +155‰. All the remaining groups (IID, IIE, IIF, IIIF, IVA and IVB) and most of the ungrouped irons have $\delta^{15}N$ values around 0‰. The variations in $\delta^{15}N$ value suggest that nitrogen, present in its molecular form, in the solar nebula at high temperatures (>600K) existed as a number of reservoirs with distinct isotopic compositions and that nitrogen was not isotopically fractionated during condensation of the metal phase. The co-variation of $\delta^{15}N$ value with the cooling rate of iron meteorites may be due to injection of

radioactive ^{26}Al with large amounts of ^{15}N-rich nitrogen immediately prior to the formation of the solar nebula.

The variation of nitrogen within the main magmatic (IIIAB) and non-magmatic (IAB) groups, is quite different. In the case of the IIIAB parent body, nitrogen is slowly lost from the molten core(s) of the parent body, resulting in an enrichment of ^{15}N in the residual nitrogen. Towards the end of the crystallisation of group IIIAB the violent formation of the pallasites may have caused the severe depletion of nitrogen in the metal phase of these meteorites, and the associated ^{15}N enrichment. A small amount of scatter on the $\delta^{15}N$ values of the IIIABs suggests that the parent body may have had a raisin-bread structure.

The variation of $\delta^{15}N$ value with Ni content for the group IAB irons is in the opposite sense to that displayed by the IIIAB irons. This rules out fractional crystallisation models as possible explanations of the trace element abundances in these meteorites. The uniformity of the $\delta^{15}N$ values indicates that the IABs formed at depth and not in a near-surface regolith as suggested by Wasson *et al.* (1980). A model involving partial melting of a number of different components within a parent body is preferred.

A number of secondary processes also affect the nitrogen content and isotopic composition. Recrystallisation of shocked iron meteorites during cosmic reheating causes a major loss of nitrogen from the Fe-Ni metal, once again with an associated isotopic composition. However, there is little production of spallogenic nitrogen in the Fe-Ni metal phase of these meteorites due to cosmic ray exposure, although considerable production can still occur in any silicate inclusions. The growth of kamacite from taenite at sub-solidus temperatures also causes a loss of nitrogen, although whether the nitrogen is lost from the meteorite or simply diffuses from the kamacite into the taenite is not established.

Most of the nitrogen in iron meteorites is dissolved in the metal phases, kamacite and taenite, although up to 30% can be accommodated in nitrides. Taenite contains up to three times more nitrogen with a $\delta^{15}N$ value 4.5‰ lighter

than that in co-existing kamacite. Small amounts of nitrogen are also concentrated in phosphides and graphite but carbides are depleted in nitrogen. The sampling technique employed in this study, despite using much smaller samples than earlier studies, successfully copes with these variations to allow reproducible measurements to be made, at least comparable with, if not superior to previous results.

CHAPTER FOUR
THE ^{15}N ENRICHMENT IN THE BENCUBBIN METEORITE

4.1 THE BENCUBBIN METEORITE

The Bencubbin meteorite is a very unusual stony-iron meteorite which belongs to neither of the more common groups of this type, the pallasites and mesosiderites. The first mass (54kg) was found near the hamlet of Bencubbin, Western Australia in 1930 (Simpson and Murray, 1932). A second mass (64.5kg) was found in 1959 nearby at Mandinga, and is believed to be part of the Bencubbin fall (McCall, 1968). Four distinct petrographic units can be recognised in the meteorite: - the Fe-Ni metal clasts, the silicate clasts*, the chondritic clasts and the matrix.

4.1.1 Petrography and Geochemistry

The metal and silicate clasts of the Bencubbin meteorite are typically no larger than 1 to 2 cm across, are angular to sub-angular in form and constitute >90% of the meteorite, although with a somewhat uneven distribution. In a number of large samples of the meteorite Simpson and Murray (1932) reported 64 to 74% metal and Newsom and Drake (1979) found approximately equal amounts of metal and silicate clasts. The remaining 10% of the meteorite is matrix plus the

*Footnote - The achondritic clasts (Lovering, 1962) have been described using a number of different, often misleading, terms by previous workers. Hutchison (1986), amoung others, used the term "aubritic", however the unfractionated composition (see Section 4.1.1) of the clasts is different from all other achondritic meteorites and therefore use of the term aubritic may be misleading. Kallemeyn *et al.* (1978) described these clasts as "host silicates" but this term is too specific as there is no consensus on which clast type represents the host rock. Therefore, the more simple term "silicate clast" will be used herein, consistent with the terminology used by Newsom and Drake (1979).

rare chondritic clast. The formation locations and processes which could produce Fe-Ni metal, silicate and chondritic clasts differ quite markedly (*e.g.* Wasson, 1985), collisions between parent bodies, or pieces of parent bodies bringing such compositionally distinct materials together in these brecciated meteorites (Clayton and Mayeda, 1978b). Previous workers, when studying Bencubbin (*e.g.* Kallemeyn *et al.*, 1978), have dealt with each clast type (*i.e.* Fe-Ni metal, silicate, chondritic) separately, as it is difficult to determine the genetic relationships between different types of clast in a polymict breccia. The following summary description of the different clasts will also adopt this approach.

The metal clasts

The Fe-Ni metal clasts have a granular texture with a grain size typically around 100μm (Newsom and Drake, 1979). Jain and Lipshutz (1973) suggested that this texture was the result of intense shock, in excess of 130kbar followed by reheating to a temperature not above 550-650°C, the γ-α transformation temperature (Goldstein and Doan, 1972), causing recrystallisation of the stressed metal. Newsom and Drake (1979) reported even larger grain sizes in some clasts (up to 300μm) which they suggested indicates prolonged local heating of the clasts. The presence of the fused metal and glass matrix shows that parts of the meteorite attained exceptionally high temperatures beyond the melting point of the metal (1500°C) (Chuang *et al.*, 1986).

The metal clasts display a range in compositions, Ni varying from 5.3 to 7.5wt.% between clasts, although each clast is chemically homogeneous. The composition of the metal is quite distinct from that of most iron meteorites, particularly for the minor elements, but similar to the composition of metal in CM chondrites (Grossman and Olsen, 1974). Compared to the iron meteorites the Cr content is more than an order of magnitude greater whereas Co is lower. Phosphorus, however, is present in concentrations similar to that displayed by most iron meteorites (Newsom and Drake, 1979). Some siderophile trace

element/Ni ratios (Au, As, Cu, Ga and Ge) are similar to the iron meteorite group IIIF (Kallemeyn *et al.*, 1978). However, the match between the Bencubbin metal and the IIIFs is not perfect. Instead Newsom and Drake (1979) argue that the metal in Bencubbin has experienced no secondary, or parent body processing other than a shock heating event. Indeed, the trace element data of Kallemeyn *et al.* (1978) confirms minimal amounts of planetary processing with Ga, Au, Ir and Re/Ni ratios all consistent with predicted equilibrium condensation models (Newsom and Drake, 1979). The variation of the Co/Ni and P/Ni ratios in the metal clasts are in good agreement with that expected for equilibrium condensation (Grossman and Olsen, 1974; Wai and Wasson, 1977) although the Cr/Ni ratio, and indeed the Co/Ni ratio, can also be produced by fractional partial melting (Newsom and Drake, 1979).

In some of the metal clasts troilite is present with Cr concentrations up to 30wt.%, although this is more typically less than 5wt.% Cr (Newsom and Drake, 1979). The sulphide is often concentrated along the grain boundaries within the metal clasts (Figure 4.1). The presence of large amounts of troilite in some of the metal clasts suggests that if the metal is a primitive condensate then conditions in the solar nebula were far from equilibrium. Under equilibrium conditions sulphide precipitates by reaction of H_2S with Fe-Ni metal at temperatures about 600K lower than the condensation temperature of the metal. To explain the presence of troilite in the large metal clasts within the context of an equilibrium condensation model Newsom and Drake (1979) suggested a number of possible mechanisms including;

(1) the metal clasts represent a late accretionary stage of metal and sulphide grains,

(2) the metal condensed or aggregated with a porous structure, which was subsequently obliterated after condensation of sulphide or

(3) the sulphide has a presolar origin, possibly a supernova condensate, Cr- and Ti-rich iron sulphides having been predicted as condensates

upon cooling of the Si-burning zone of a supernova (Clayton and Ramadurai, 1977).

The silicate clasts

A detailed survey of the silicate clasts in Bencubbin has not been reported. However, it is known that each silicate clast in Weatherford, a meteorite almost identical to Bencubbin (see Section 4.1.3), is chemically homogeneous whereas the population as a whole displays a range in compositions (Mason and Nelen, 1968). The silicate clasts in Bencubbin, despite their achondritic texture display unfractionated rare earth and refractory trace element abundances. This indicates that the silicate clasts have not experienced any large scale igneous processes as these invariably result in fractionation of the trace element abundances. Kallemeyn *et al.* (1978) suggest that the silicate clasts formed by shock melting of a regolith with a composition related to that of the CI-CM-CO clan of carbonaceous chondrites.

The silicate clasts are composed mainly of clinoenstatite and forsterite with some interstitial glass (Lovering, 1962; Newsom and Drake, 1979). The texture of these clasts is rather unusual as they are generally very similar to those of coarse, barred-olivine chondrules found in ordinary chondrites, although finer textures, also similar to chondrules, are to be found (Weisberg *et al.*, 1987). The similarity of the composition and texture between the silicate clasts and chondrules suggests that a similar formation process is responsible for the production of both. However, one possibly significant difference is that chondrules are rarely larger than 2mm (Wasson, 1985) whereas the silicate clasts can be as large as 2cm across and their fragmentary nature indicates that their initial size was even larger (Weisberg *et al.*, 1987).

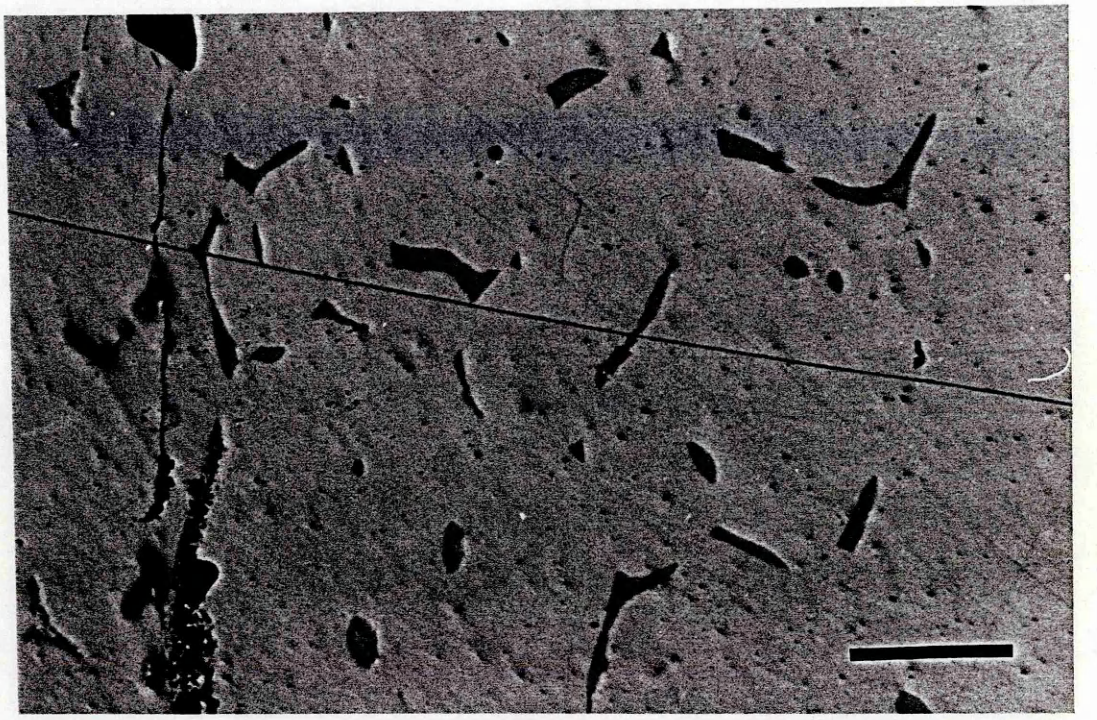

Figure 4.1 Sulphides in metal clasts. The sulphides marked define patterns characteristic of the triple junction between three metal grains. Reflected light. Scale bar = 300μm.

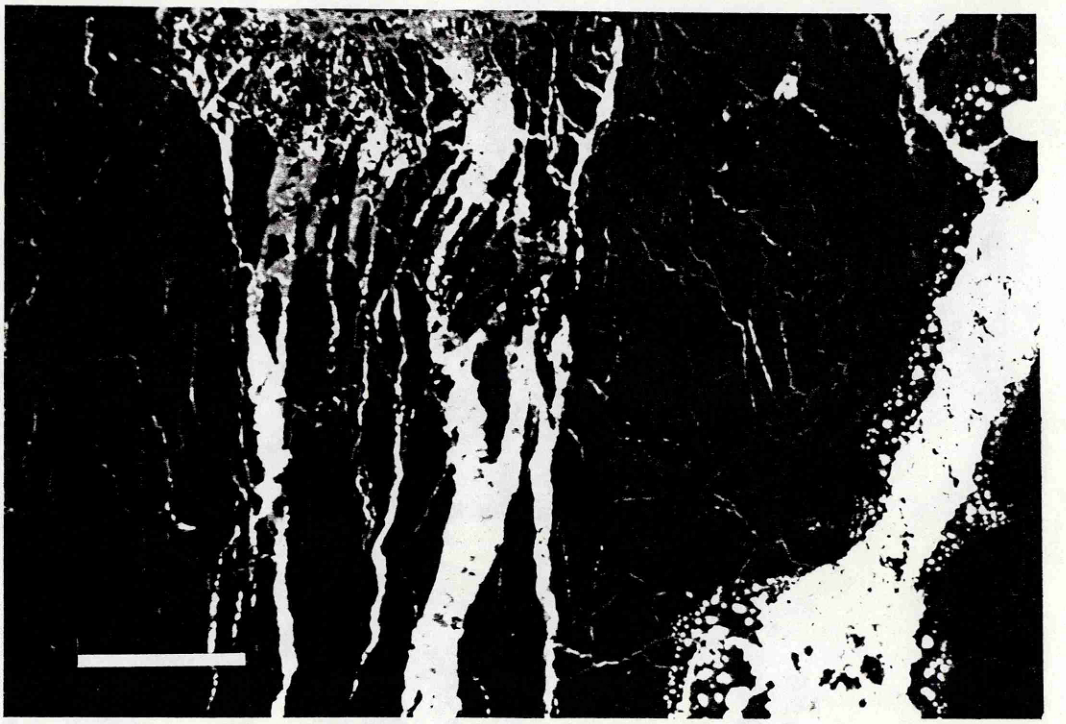

Figure 4.2 Metal-rich veins in silicate clast. Displays the locally disruptive and penetrative nature of the matrix material. Reflected light. Scale bar = 300μm.

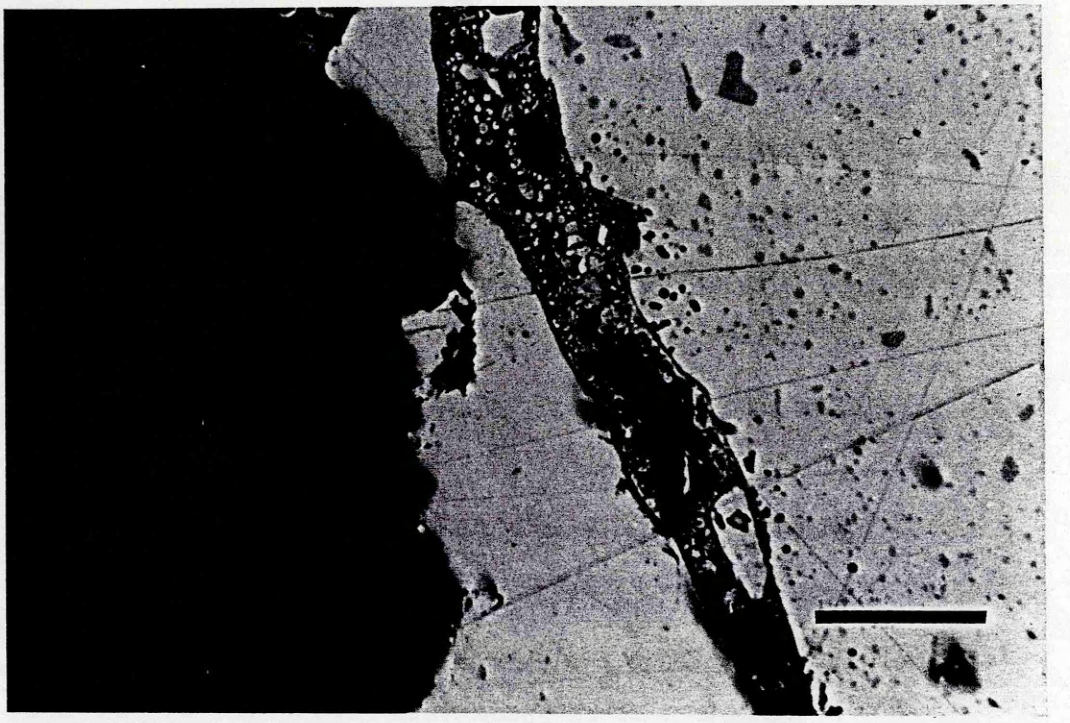

Figure 4.3 Metal and silicate matrix. The matrix here was completely molten and was composed of a mixture of immiscible metal and silicate. The metal clasts to the right of the matrix is rich in small troilite inclusions but the metal clast to the left is almost devoid of such inclusions. Reflected light. Scale bar = 300μm.

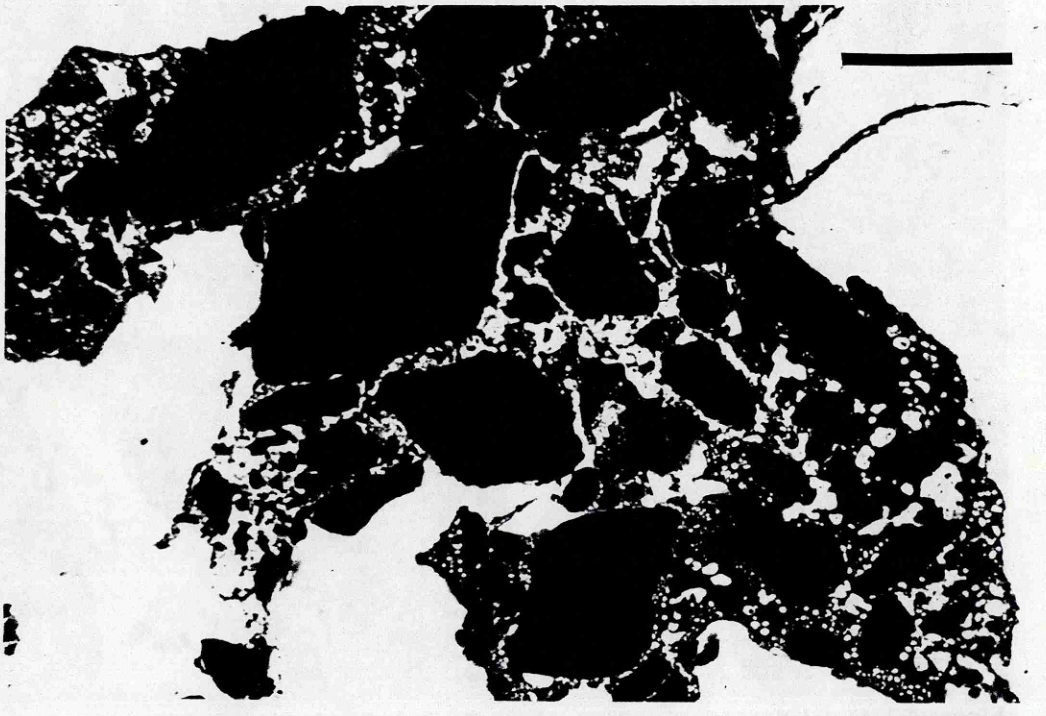

Figure 4.4 Silicate fragment-rich matrix. The matrix in this are has suffered relatively little melting, being composed primarily of unmelted fragments of the silicate clasts. Reflected light. Scale bar = 300μm..

The chondritic clasts

To date only four chondritic clasts have been reported;

(1) an ordinary chondrite, classified as LL4±1 by Kallemeyn *et al.* (1978),

(2) a carbonaceous chondrite, with a highly deformed texture (Lovering, 1962). Kallemeyn *et al.* (1978) suggested that this clast is related to the CI-CM-CO clan of carbonaceous chondrites,

(3) one similar to a type 3 ordinary chondrite, although it may be more closely related to the silicate inclusions of the IIE iron meteorites or Suwahib (Buwah) (Hutchison, 1986) and

(4) a dark metamorphosed chondrite, containing more than 10% metal, but which was too small for detailed examination (Lovering, 1962).

These four clasts constitute a very minor part of the meteorite, their wide range in compositions contrasting markedly with the restricted ranges of the much more abundant metal and silicate clasts. The oxygen isotopic composition of the LL4 and the carbonaceous chondritic clasts have been determined and they are distinct from that of the silicate clasts. This has been interpreted as indicating that they must have formed in different locations within the solar nebula and that they were incorporated into a regolith of metal and silicate material (Clayton *et al.*, 1978b). Although the occurrence of meteorites containing fragments with a range of primitive compositions is not unusual (*e.g.* the LL group breccia St. Mesmin - with LL6 and LL7 clasts in an LL5 matrix (Dodd, 1981)) the occurrence of such clasts in a meteorite primarily composed of Fe-Ni metal and non-chondritic silicate clasts is exceptional.

The matrix

The matrix in Bencubbin is composed of Fe-Ni metal, troilite and silicates, either as fragments or melts of the main types of clast and is largely confined to the interclast regions, although it is often observed cutting through clasts as veins

(Figure 4.2). The melted fractions of the matrix show almost no crystallinity, the silicates being glass, indicating rapid cooling (Newsom and Drake, 1979; Hutchison, 1986). The nature of the matrix ranges from roughly equal amounts of melted metal and silicate (Figure 4.3) through to fragments of silicate clasts surrounded by metal (Figure 4.4). The composition of the metal and silicate portions of the matrix tend to reflect that of adjacent clasts indicating that the matrix material, once melted was not able to flow any distance (Newsom and Drake, 1979). Ramdohr (1973) describes matrix as having a "spontaneous fusion" texture, the result of rapid melting of the main parts of the rock. The lack of any large scale mobilization of the matrix material and the mixing of metal and silicate components, together with the manner in which the matrix cuts through the clasts implies that the breccia existed prior to the shock melting event which produced the matrix rather than the breccia and the matrix forming in a single event.

4.1.2 Nitrogen and Noble Gases

The nitrogen contents and isotopic compositions of a metal clast, two silicate clasts and two whole-rock samples of Bencubbin (Table 4.1) were reported by Prombo and Clayton (1985). The silicate clasts contained 5.7 and 44.0ppm nitrogen with $\delta^{15}N$ values of +414.3 to +489.1‰ and the metal clast 53.3ppm with a $\delta^{15}N$ value of +829.3‰. At the time these results were published they were up to 500‰ heavier than any previous $\delta^{15}N$ measurement. The results of two whole-rock analyses are noteworthy because their $\delta^{15}N$ values are considerably heavier than those measured for individual clasts (+923 and +973‰) yet their nitrogen concentrations of 59.3 and 48.0ppm respectively are similar to those in the clasts. At face value therefore, it seemed to Prombo and Clayton (1985) that another nitrogen component must exist in the meteorite, other than that seen in the metal and silicate clasts, with a considerably heavier isotopic composition. However, they were unable to identify this postulated component,

	N (ppm)	$\delta^{15}N$ (‰)	Sample wt. (g)
Bencubbin			
Metal clast	53.3	+829.3	0.772
		+819.2	
Silicate clast#1	5.7	+414.3	0.440
Silicate clast#2	44.0	+489.1	1.217
		+479.1	
Whole rock#1	48.0	+973.0	2.10
Whole rock#2	59.3	+923.0	0.85
Weatherford			
Silicate clast	34.7	+462.5	0.20

Table 4.1 Nitrogen content and $\delta^{15}N$ value of Bencubbin and Weatherford. The analyses for these samples were performed using a dynamic mass spectrometer, with the operation modified because of problems measuring such unusual isotopic compositions. Taken from Prombo and Clayton (1985).

partly due to sample size limitations, and therefore could only outline some possible mechanisms to account for the origin of the ^{15}N enrichment. The scale of the enrichment suggests a primordial heterogeneity rather than processes operating in the solar nebula. The presolar process could have been a nucleosynthetic event, probably a nova, although fractionation during processing in an interstellar cloud could also have produced the enrichment in ^{15}N (Prombo and Clayton, 1985).

The noble gases in Bencubbin show no evidence of isotopic effects comparable with those of nitrogen. The metal and silicate samples analysed contain large amounts of primordial noble gases whose isotopic composition suggest an association with gas-rich meteorites, *i.e.* solar type noble gases (Begemann *et al.*, 1976). Lewis (1985) has shown that large elemental

fractionations exist, producing a noble gas abundance pattern similar to that of the subsolar component found in the enstatite chondrites. The isotopic composition of the noble gases suggest that it is unlikely that they have a common origin with the ^{15}N-rich nitrogen (Lewis, 1985).

^{40}Ar - ^{39}Ar dating using a laser microprobe extraction technique established that the clasts formed at 4.5Ga but that the final shock-melting event did not occur until 3.7Ga (Kelley and Turner, 1987). The high spatial resolution of the laser microprobe technique showed that large losses of argon due to this heating event were restricted to a 400μm zone around the the margins of each silicate clast, indicating a short heating period. Another feature detected was a high concentration of argon with a solar wind isotopic signature in the matrix whereas the centres of the clasts have a near planetary $^{20}Ne/^{36}Ar$ ratio. This is consistent with the clasts having spent some time in a regolith environment, their rims becoming enriched in solar wind implanted noble gases and the final shock melting event causing melting of the clast rims to produce the gas rich matrix.

4.1.3 Relationships to Other Meteorites

Like Bencubbin, the Weatherford meteorite is composed of Fe-Ni metal and silicate clasts plus the occasional chondritic clast welded together by a metal and silicate glass matrix. The composition of the metal and silicate clasts are essentially identical to those in Bencubbin, although displaying a slightly broader range in Ni contents (Mason and Nelen, 1968). The oxygen isotopic composition of the silicate clasts from the two meteorites are identical (Clayton *et al.*, 1978b). However, the unusual composition of these meteorites makes identifying genetic links with other meteorites very difficult.

The oxygen isotopic composition of Bencubbin, Kakangari, the mafic chondrule component of Renazzo and the silicate portion of the Tucson iron all fall on, or close, to a single mass fractionation line, slope 0.52, on an oxygen three isotope plot (Figure 4.5) suggesting that there may be some relationship

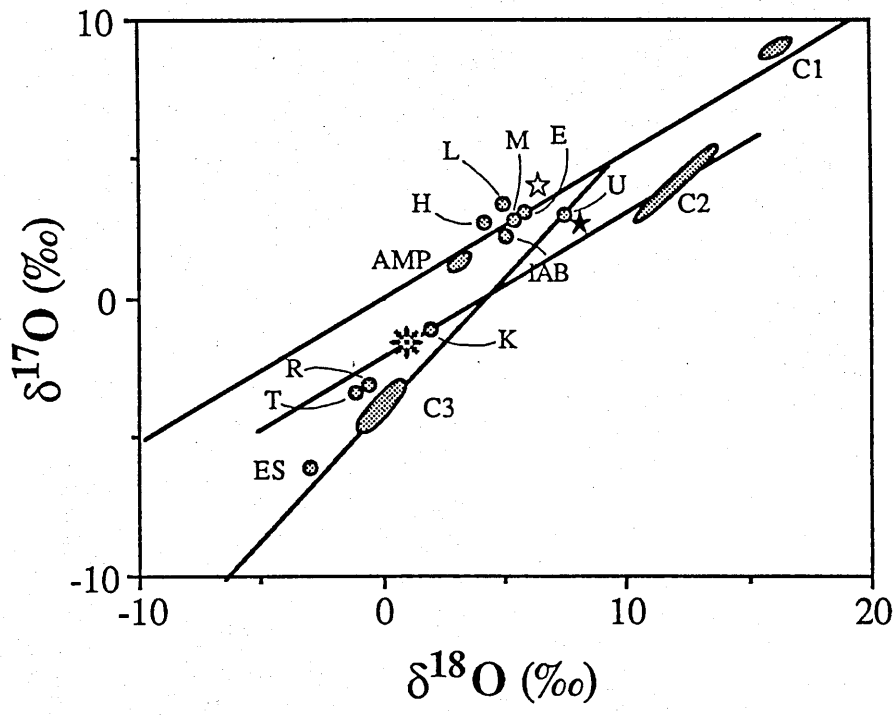

Figure 4.5 Oxygen isotopic composition of Bencubbin clasts. The silicate clasts from Weatherford have an identical isotopic composition to those in Bencubbin (✵). The chondritic clasts are also shown - ☆ = ordinary chondrite clast, ★ = carbonaceous chondrite clast. The three meteorites Prinz *et al.* (1987) suggested are related to Bencubbin are shown, Kakangari (K), Renazzo (R) and Tucson (T). The oxygen isotopic composition of other types of meteorites are shown for comparison; C1, C2, C3 = carbonaceous chondrites, AMP = howardites, eucrites, diogenites, mesosiderites and pallasites, E = enstatite chondrites and achondrites, U = ureilites, IAB = IAB iron meteorites, ES = Eagle station, M = Moon. After Clayton *et al.* (1978b).

between these meteorites (Prinz *et al.*, 1987). Kakangari is an unusual chondritic meteorite with a mineralogy and composition intermediate between that of the enstatite and ordinary chondrites (Graham and Hutchison, 1974). The CR2 meteorites Renazzo, Al Rais and Yamato 790112 are a "grouplet" of unusual carbonaceous chondrites, all containing heavy nitrogen with a $\delta^{15}N$ value of up to +175‰ (Kerridge, 1985), consistent with an association with Bencubbin. The Tucson meteorite is also rather unusual, with an anomalous composition and structure, including a high Cr content (≈2000ppm), and appears to be unrelated to

any other iron meteorite (Buchwald, 1975). However, due to the very diverse nature of formation conditions required to produce these very different types of meteorite the relationships between the 4 meteorites is unknown.

As mentioned in section 4.1.1 Kallemeyn *et al.* (1978) suggested that the metal clasts in Bencubbin were related to the IIIF iron meteorite group. Although the trace element ratios are not a perfect fit, two of the IIIFs have additional features which suggest that they may be closely related to Bencubbin. Clark County contains 1565ppm Cr (Smales *et al.*, 1967), which is high relative to other iron meteorites, but comparable to the concentrations observed by Newsom and Drake (1979) in Bencubbin metal. Another IIIF, Nelson County displays evidence of extreme cold working, the result of a violent shock event (Buchwald, 1975), which could be related to the event responsible for the formation of the Bencubbin breccia or the matrix.

Although the oxygen isotopic composition of the chondritic clasts in Bencubbin are similar to those of known chondritic meteorite groups, there are significant differences (Clayton *et al.*, 1978b). The determination of the nitrogen and carbon content and isotopic composition of these clasts may be of considerable use in establishing whether the oxygen results are significant or purely coincidental. Therefore, the use of the isotopic composition of nitrogen and carbon in these components in Bencubbin may help determine the relationship with other meteorites.

4.2 NITROGEN AND CARBON IN THE BENCUBBIN METEORITE

4.2.1 Nitrogen in the Clasts

The nitrogen extraction technique in which oxygen for each combustion step is generated from CF#3 (Figure 2.2), *i.e.* a single aliquot of oxygen is supplied to the combustion section at the start of each step (see Section 2.3.2), was used

for all whole rock samples of the meteorite except the matrix#2 sample which was heated in the presence of a continuous oxygen supply. High resolution stepped combustions have been performed on a metal clast, a silicate clast, the chondritic clast described by Hutchison (1986), the carbonaceous chondrite clast reported by Lovering (1962) and two samples of the matrix. The results from each stepped heating extraction are given in Appendix 2.

The metal and silicate clasts

The release profile and the isotopic composition of the nitrogen from the metal and silicate clast samples are remarkably similar (Figure 4.6). In both samples the $\delta^{15}N$ value of nitrogen released below 600°C tends towards 0‰, typical of trapped atmospheric nitrogen or possibly terrestrial organic or inorganic contamination (Boyd *et al.*, 1988). The two samples liberate most of their nitrogen in a single release around 1000°C with similar isotopic compositions. The main release from the metal clast (Figure 4.6a) is between 900 and 1125°C with a maximum $\delta^{15}N$ value of +887‰ and from the silicate clast (Figure 4.6b)

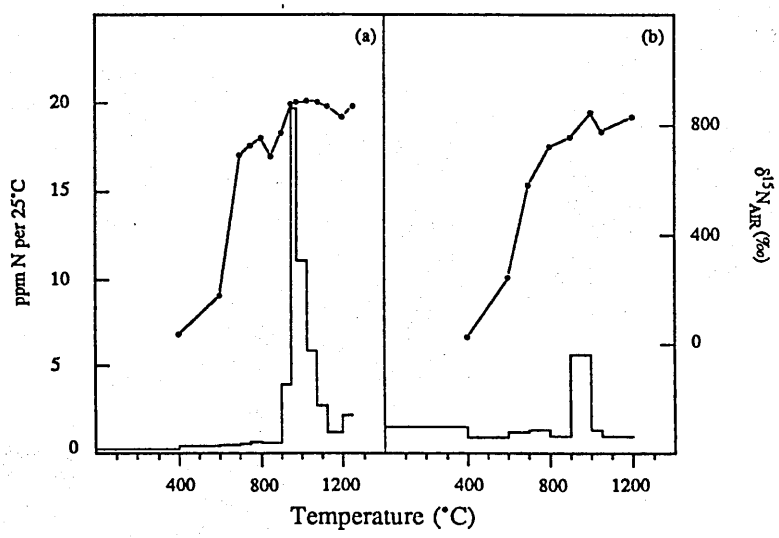

Figure 4.6 Stepped combustion profiles for nitrogen of a metal clast and a silicate clast from Bencubbin. (a) Metal clast; (b) silicate clast.

is over the slightly narrower range of 900 to 1050°C with a peak $\delta^{15}N$ value of +847‰. At lower temperatures, between 700 and 800°C, there is a second, smaller release of nitrogen from both clasts. The isotopic composition of the nitrogen from the two minor releases is slightly lighter than that from the main releases, with $\delta^{15}N$ values of +754 and +720‰ from the metal and silicate clasts respectively. The major and minor releases of nitrogen from these samples may be different components with different isotopic compositions. Alternatively, they may simply be the result of an admixture of absorbed atmospheric nitrogen ($\delta^{15}N$ = 0‰) and the indigenous nitrogen ($\delta^{15}N$ = +890‰). There is a small release of heavy nitrogen between 1200 and 1250°C from the metal clast but as the silicate clast was not heated above 1200°C the presence of this component in the silicate clast cannot be established.

The total amount of nitrogen in the two samples is also similar, 88.6ppm in the metal and 77.0ppm in the silicate clast (Table 4.2). However, as stated above some of the nitrogen is terrestrial contamination, predominantly that released at low temperatures. If only nitrogen released above 600°C is considered then the metal clast contains 81.6ppm nitrogen with a $\delta^{15}N$ value of +868‰ and the silicate clast 44.9ppm nitrogen with a $\delta^{15}N$ value of +789‰. The isotopic composition of nitrogen in the metal clast is comparable with that obtained by Prombo and Clayton (1985) ($\delta^{15}N$ = +829‰) but the isotopic composition of the silicate clast studied here is noticeably heavier.

The original purpose of stepped heating techniques was to resolve contamination components from gas indigenous to the sample (Chang *et al.*, 1974). Although they sometimes discard gas evolved below 800°C (*e.g.* Prombo and Clayton, 1983), Prombo and Clayton (1985) do not specify the procedure employed for their study of Bencubbin. It is therefore noteworthy that the summed $\delta^{15}N$ value of the nitrogen liberated between room temperature and 1250°C from the metal and silicate clasts, +809 and +493‰ respectively, are within a few per mil of the values reported by Prombo and Clayton (1985). This

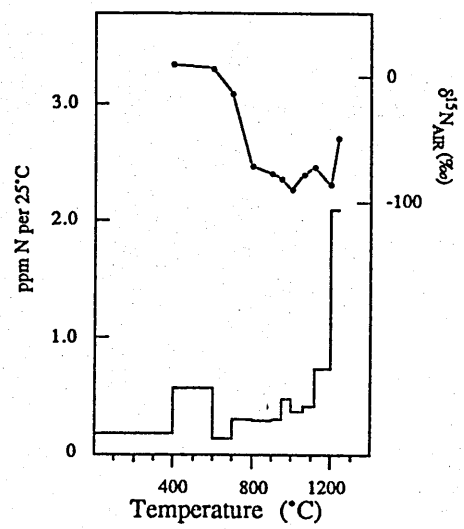

Figure 4.7 Stepped combustion profile for nitrogen of the iron meteorite Uwet. This sample was combusted in the same manner as the Bencubbin metal clast. Unlike the Bencubbin metal the nitrogen was difficult to extract, requiring multiple extractions at 1250°C.

suggests that either they did not employ a clean-up step at 800°C or they experienced problems resolving the indigenous nitrogen from contamination if they did use a stepped heating program.

The release temperature of the nitrogen from the Bencubbin metal clast is different to that released from iron meteorites using the same extraction technique. Figure 4.7 shows the nitrogen release profile from Uwet, a group IIAB iron meteorite which contains 13.9ppm nitrogen with a $\delta^{15}N$ value of -95.6‰. The main release of nitrogen from Uwet is not until 1250°C, over 200°C higher than that from the Bencubbin metal clast, although there is a small release of nitrogen at 1000°C corresponding with the main release from the metal clast. The distribution of nitrogen in Uwet is fairly typical of iron meteorites, with approximately 90% of the nitrogen dissolved in the kamacite, the remainder concentrated in nitrides and phosphides (see Figure 2.9 and Section 3.3.4). Therefore, it appears that the carrier or location of nitrogen in the Bencubbin

Sample	Total Nitrogen		High Temp. Nitrogen		
	N (ppm)	$\delta^{15}N$ (‰)	Temp.	N (ppm)	$\delta^{15}N$ (‰)
Metal Clast	88.6	+809	600	81.6	+868
Silicate Clast	77.0	+493	600	44.9	+789
Matrix#1	35.8	+492	700	14.0	+878
Matrix#2	122.5	+714	750	93.6	+888
Ordinary Chond.	35.8	+181	400	21.3	+285
Carb. Chond.	62.0	+166	400	44.7	+209

Table 4.2 Summary of nitrogen content and δ^{15}N value of clast and matrix from Bencubbin. The first two columns show the total nitrogen values extracted from room temperature up to 1200 or 1300°C. The last three columns show the totals for indigenous nitrogen, extracted at high temperatures, the exact cut off indicated in the third column.

metal is either thermally unstable or more accessible to oxygen compared to its location in iron meteorites.

Another unusual feature of the nitrogen in the metal clast is the high concentration of 81.6ppm, *cf.* the range of values from iron meteorites is from 0.4 to 85.5ppm nitrogen (Figure 3.9), with only 2 out of 68 iron meteorites containing >80ppm nitrogen. Although the concentration of nitrogen in the Bencubbin metal is just within the range of iron meteorites, 81.6ppm is unprecedented for iron meteorites which have a granular texture (indicative of recrystallisation of the stressed metal). The range of nitrogen concentrations from shocked and recrystallised iron meteorites is only 1.4 to 5.8ppm, the shock and recrystallisation having causied up to 90% loss of nitrogen (see Section 3.3.3). Therefore, Bencubbin metal either contained an exceptionally high concentration of nitrogen prior to the shock and recrystallisation, in excess of several hundred ppm or the nitrogen is concentrated in a minor phase which remains unaffected by shock and recrystallisation.

The matrix

The high degree of similarity in the nitrogen release profiles from the metal and silicate clasts suggests that if a minor phase contains the ^{15}N-enriched nitrogen it must be present in both types of clasts. No minerals have been reported which are common to both the metal and silicate clasts. However, dark matrix surrounds all the clasts, and is often observed as veins cutting through the clasts (Newsom and Drake, 1979). When the clasts were sampled for analysis care was taken to avoid adhering matrix, although it is concievable that small amounts may have been included. However, even allowing for 10% of the clast samples being matrix the concentration of nitrogen in the matrix is required to be in excess of 800ppm if this is the host of the ^{15}N-rich nitrogen.

Two samples of matrix material from Bencubbin have been analysed, matrix#1 and matrix#2. Neither sample reveals the exceptionally high concentration of heavy nitrogen necessary if the matrix is the carrier of the heavy nitrogen, although the concentration of the isotopically heavy nitrogen in the

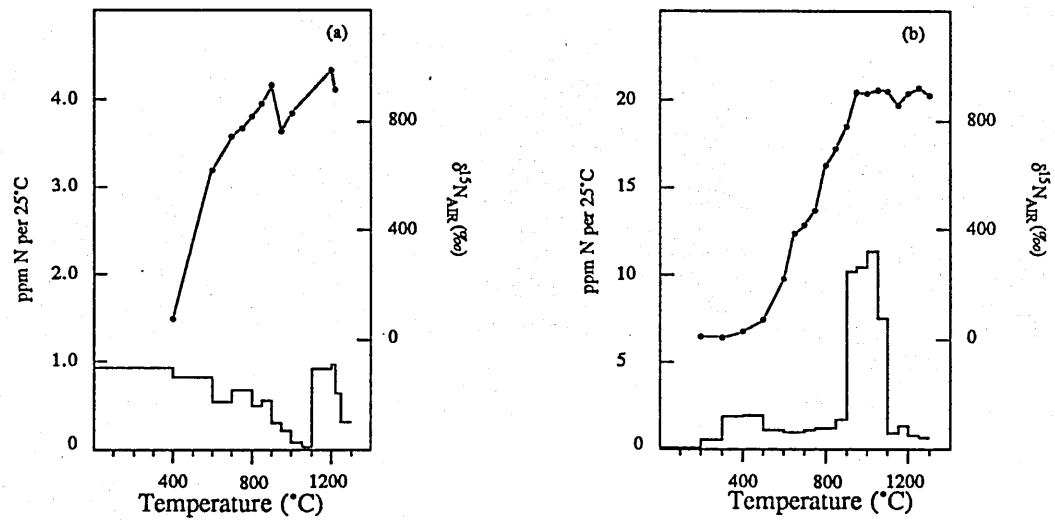

Figure 4.8 Stepped combustion profiles for nitrogen of two matrix samples from Bencubbin. (a) matrix#1 is mostly melted metal and silicate similar to that shown in Figure 4.3; (b) matrix#2 is dominated by fragments of silicate clasts similar to that in Figure 4.4.

matrix is variable, matrix#1 containing 14.0ppm ($\delta^{15}N$ = +878‰) and matrix#2 93.6ppm ($\delta^{15}N$ = +888‰). Respectively, these are the lowest and highest concentrations of nitrogen found in whole-rock specimens from the meteorite during this study (Table 4.2). The release profiles of the two matrix samples are also different (Figure 4.8). Matrix#1 liberates very little nitrogen between 900 and 1100°C, the temperature range of the main releases from the metal and silicate clasts. There is, however, a release of heavy nitrogen between 1100 and 1300°C with a $\delta^{15}N$ value of +973‰. This release may be related to the main release from the metal and silicate clasts, possibly shielded by the silicate glass or the melted metal of the matrix observed in a split of this sample taken for electron microprobe analysis (R. Hutchison, 1986 pers. comm.). A slightly smaller release of nitrogen between 700 and 900°C, with a peak $\delta^{15}N$ value of +929‰, coincides with the release temperature of the minor components in the metal and silicate clasts.

Nitrogen from the matrix#2 sample (Figure 4.8b) is liberated in a single release between 900 and 1100°C, the same range as the main release from the metal and silicate clasts. The lower release temperature compared to the matrix#1 sample may be due to the use of a continuous oxygen supply during the heating of this sample, which often has the effect of lowering the release temperature of a combustible carrier phase. However, the difference in release temperatures may be related to the nature of the two samples, which may also have a bearing on their respective nitrogen contents. The matrix#1 sample is almost entirely fused silicate and metal (*e.g.* Figure 4.3), whereas the matrix#2 sample is predominantly fine grained, unmelted fragments of the clasts and contains very little glass (*e.g.* Figure 4.4). Melting of matrix material could cause a major loss of nitrogen and encapsulation of the remaining nitrogen carriers by the molten metal and silicate would result in elevated release temperatures. The much lower nitrogen concentration in the matrix#1 sample is probably due to the higher degree of melting in this sample than that experienced by matrix#2. The high

concentration of nitrogen in matrix#2 implies that some of the clasts must have nitrogen concentrations in excess of 100ppm.

The chondritic clasts

The nitrogen in two chondritic clasts has been analysed. The type 3 ordinary chondrite (described by Hutchison, 1986) and the carbonaceous chondrite clasts (described by Lovering, 1962) have much lighter $\delta^{15}N$ values than the metal or silicate clasts (Table 4.2). Both clasts display a complex pattern of releases with distinct isotopic compositions. The type 3 clast has two releases of heavy nitrogen (Figure 4.9a). Between 400 and 650°C there is a large release with a peak $\delta^{15}N$ value of +395‰ but the second peak $\delta^{15}N$ value (+403‰) coincides with a minimum in the release profile at 1000°C. A small release of nitrogen between 700 and 850°C coincides with a minimum $\delta^{15}N$ value of +195‰. Lighter $\delta^{15}N$ values are found below 400°C but this is likely to be predominantly absorbed atmospheric nitrogen.

Atmospheric nitrogen is also the main component liberated from the carbonaceous chondrite clast below 400°C but the main release between 450 and

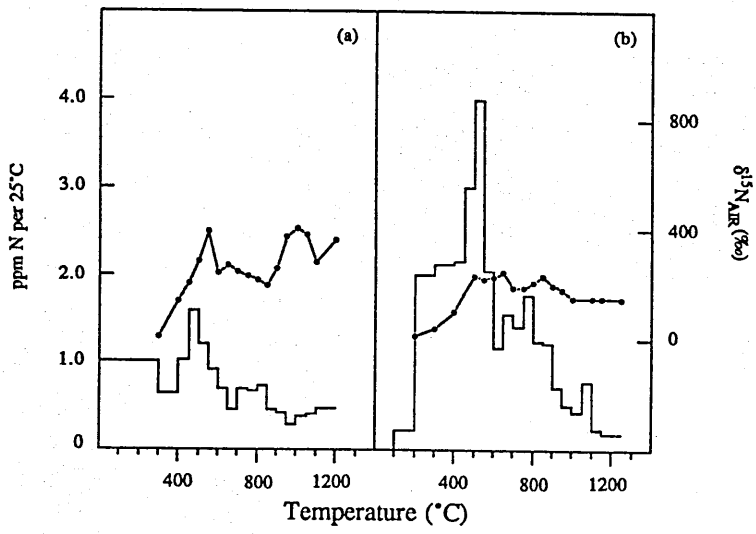

Figure 4.9 Stepped combustion profiles for nitrogen of the chondritic clasts in Bencubbin.
(a) the type 3 ordinary chondrite clast; (b) the carbonaceous chondrite clast.

600°C coincides with a peak $\delta^{15}N$ value of +245‰ (Figure 4.9b). Following the main release there is a small release of nitrogen which is associated with a minimum in the isotopic profile, only for the $\delta^{15}N$ value to rise back to its initial peak value. Finally, at high temperatures the isotopic composition is relatively constant at around +150‰.

The complex release profiles and the relatively low $\delta^{15}N$ values from the two chondritic clasts indicate that there are at least two components with different isotopic compositions in each clast. The simplest scenario which can be used to explain the $\delta^{15}N$ value variations is that the chondritic clasts initially contained nitrogen with a typical solar system isotopic composition ($\delta^{15}N$ = -100 to +50‰)* and that a heavier component with a $\delta^{15}N$ value of around +900‰, derived from another part of the Bencubbin meteorite, was introduced at some late stage. Mixing of the two components could easily occur during the shock heating event by one of two mechanisms. The heavy nitrogen could have been incorporated into the chondritic clasts either as a gas or in the molten matrix material seen to vein the clasts. That only intermediate $\delta^{15}N$ values were resolved by the high resolution stepped heating extractions (suggesting partial isotopic equilibration of the nitrogen) and the lack of extensive veining of the chondritic clasts favours a scheme where the heavy nitrogen is introduced as a gas, although this may be problematic without some confining trap to prevent the gas being lost to space.

4.2.2 Carbon in the Clasts

Over the years a variety of exotic components have been discovered in meteoritic material, the nature of the carrier phase often being carbonaceous or associated with isotopically anomalous carbon (*e.g.* Anders, 1988). Therefore, it

* Footnote - the range of whole-rock $\delta^{15}N$ values displayed by most meteorites, with the exception of the rare CR2 carbonaceous chondrites (see Figure 1.4) and the IIC iron meteorites (see Figure 3.17).

was decided to determine the distribution and isotopic composition of carbon in the Bencubbin meteorite to investigate any possible association with the isotopically heavy nitrogen, as such information may help constrain further the origin of the ^{15}N enrichment. Figures 4.10 and 4.11 show the results of high resolution stepped combustions for the extraction of carbon on splits of all the samples analysed for nitrogen (Section 4.2.1) except for the matrix#2 sample. All the carbon analyses of clasts in Bencubbin, except for the carbonaceous chondrite clast were performed by Dr. D. W. McGarvie. It is apparent that Bencubbin does not contain substantial quantities of carbon with unusual isotopic compositions on the scale of those displayed by nitrogen (Table 4.3). A common feature of all the analyses is that the low temperature carbon has a $\delta^{13}C$ value of between -30 and -25‰, characteristic of terrestrial organic contamination (Swart *et al.*, 1983a) although some carbon below 600°C may be indigenous to the sample.

The metal clast contains a number of carbon components released above 600°C with the $\delta^{13}C$ values becoming progressively heavier (Figure 4.10a). The main release of carbon is between 620 and 1020°C with a $\delta^{13}C$ value of -10‰. This release is much broader than any of the nitrogen releases, possibly due to the larger temperature increments and larger chip size of the sample. Consequently this release overlaps the temperature range of both the main nitrogen release and the minor release at 700 to 850°C. The release at 1220°C ($\delta^{13}C$ = +1‰) may correspond with the release of nitrogen at 1250°C. The concentration of carbon in the metal (98ppm) is within the range of values for iron meteorites (20 to 1850ppm) reported by Moore *et al.* (1969) and the $\delta^{13}C$ value of -10.2‰ is within the range of $\delta^{13}C$ values from iron meteorites (-30.3 to -4.0‰) reported by Deines and Wickman (1973).

The silicate clast contains a total of 1776ppm carbon. 188ppm carbon is released above 600°C, 94% of which is released between 600 and 800°C with a $\delta^{13}C$ value of -9.6‰ (Figure 4.10b). The temperature of this release

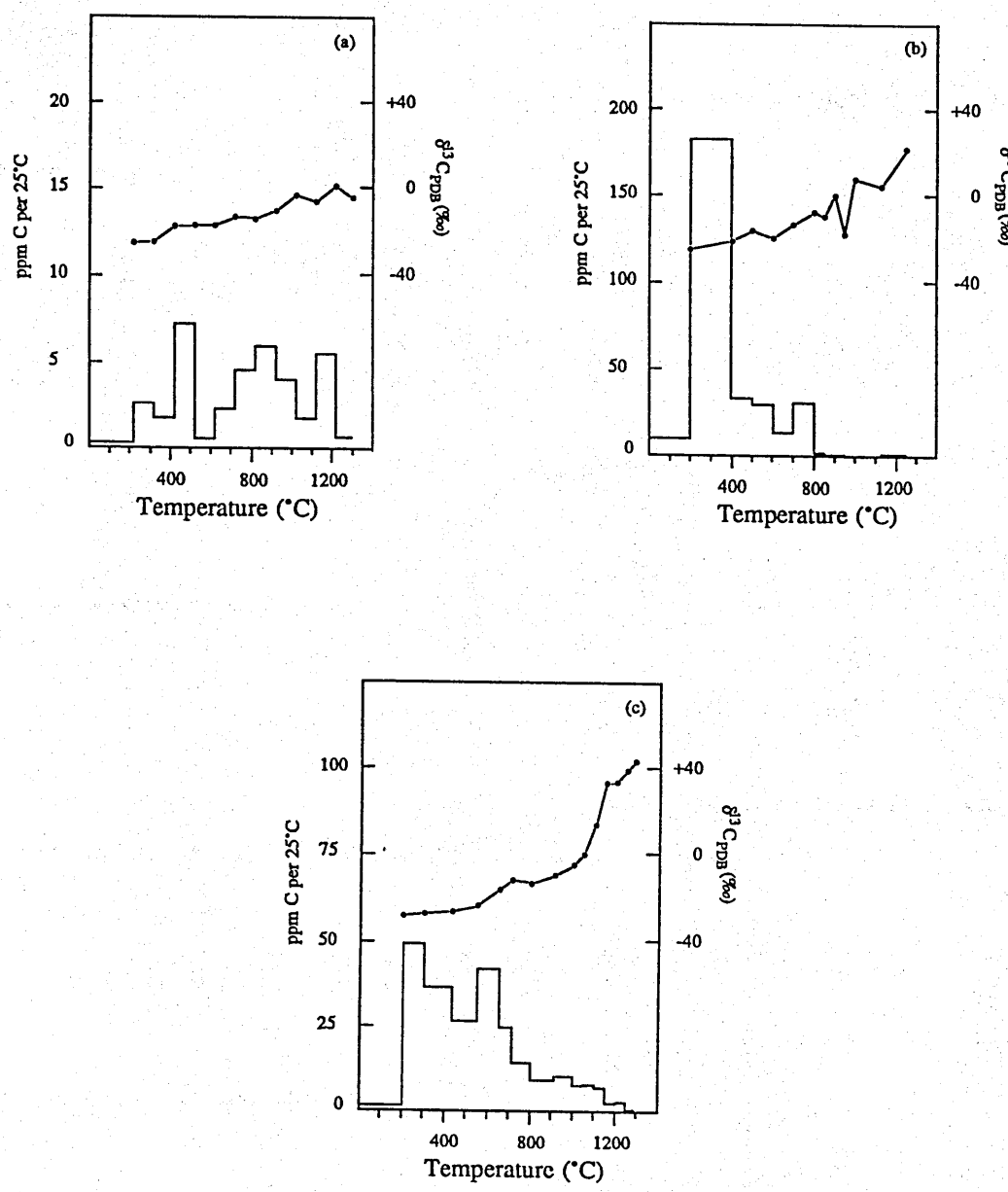

Figure 4.10 Stepped combustion profiles for carbon for samples used for nitrogen analysis. (a) metal clast; (b) the silicate clast; (c) matrix#1.

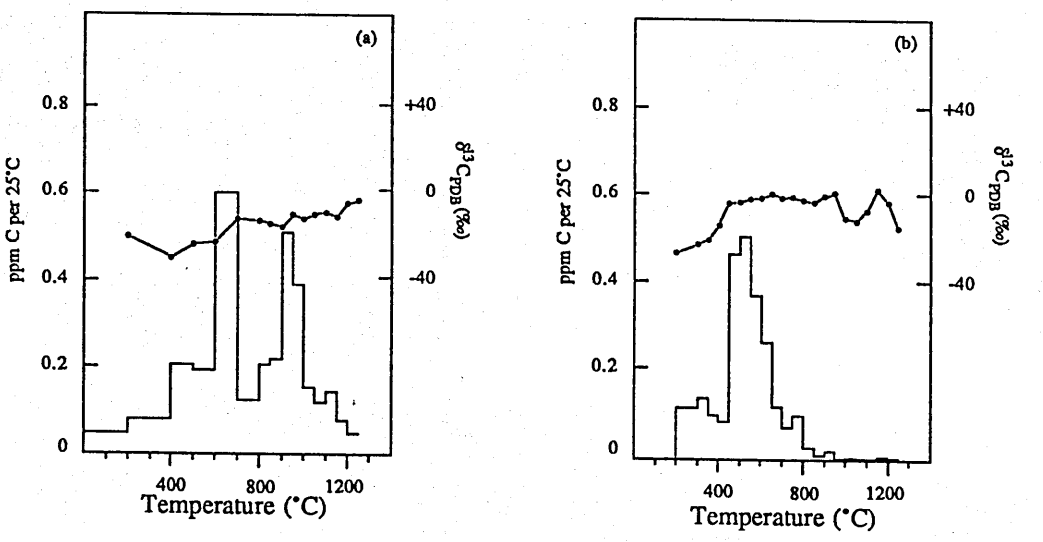

Figure 4.11 Stepped combustion profiles for carbon of the two chondritic lasts analysed for nitrogen. (a) the ordinary chondrite clast; (b) the carbonaceous chondrite clast.

corresponds very well with that of the minor release of nitrogen from the silicate clast and the $\delta^{13}C$ value is identical to that of the main carbon release from the metal clast. Heavy nitrogen may therefore be in some way linked to a carbon phase in the meteorite. At higher temperatures there is almost no carbon released until the 1125 to 1250°C step which yielded 5ppm carbon with a $\delta^{13}C$ value of +22‰. The most important feature is the lack of carbon between 900 and 1100°C, the temperature range of the main nitrogen release, implying that there is almost no carbon associated with the majority of the isotopically heavy nitrogen.

The matrix sample (Figure 4.10c) did not reveal any distinct releases of carbon at high temperature, the profile being dominated by what appears to be low temperature carbon, possibly contamination, persisting to high temperatures. However, above 1100°C the carbon becomes progressively enriched in ^{13}C reaching a maximum $\delta^{13}C$ value of +43‰. This relatively heavy carbon may be associated with the release of heavy nitrogen liberated between 1100 and 1300°C from the matrix#1 sample (Figure 4.8a).

The presence in Bencubbin of small amounts of isotopically heavy carbon combustible above 800°C is very similar to the carbonaceous chondrites, particularly the CM2s (*e.g.* Halbout *et al.*, 1986). Kallemeyn *et al.* (1978) have shown that the trace element abundances in the silicate clasts are chondritic, and very similar to the CI-CM-CO carbonaceous chondrite clan. The isotopic composition of the carbon liberated above 600°C from the silicate clast ($\delta^{13}C$ = -8.6‰) is consistent with such an origin. However, carbon isotopic variation in whole-rock samples of meteoritic material is somewhat limited, most meteorites falling in the range -30 to -5‰, and a value of $\delta^{13}C$ value of -8.6‰ is not exclusive to any specific group (Carr, 1985). Therefore, the $\delta^{13}C$ value of the silicate clasts cannot be considered conclusive evidence for them having a carbonaceous chondrite origin.

The carbon concentration (813ppm) and the isotopic composition of the type 3 ordinary chondritic clast ($\delta^{13}C$ = -13.0‰) are within the ranges reported for the ordinary chondrite finds (100 to 9500ppm; -29.7 to -11.0‰), although the $\delta^{13}C$ value is outside the more restricted range of -29.7 to -20.6‰ for the observed falls (Grady *et al.*, 1982). On the basis of mineral chemistry Hutchison (1986) suggested that this clast may be related to the H3 chondrite Suwahib (Buwah). However, Suwahib (Buwah) contains 0.07wt.% carbon with a $\delta^{13}C$ value of

Sample	Total Carbon		High Temp. Carbon		
	C (ppm)	$\delta^{13}C$ (‰)	Temp.	C (ppm)	$\delta^{13}C$ (‰)
Metal Clast	172	-9.8	600	98	-7.2
Silicate Clast	1776	-19.8	600	188	-8.6
Matrix#1	934	-18.6	800	133	+3.8
Ordinary Chond.	1132	-16.6	600	813	-13.0
Carb. Chond.	10115	-5.5	400	8246	-2.1

Table 4.3 Summary of carbon content and $\delta^{13}C$ value of clasts and matrix from Bencubbin.

-18.9‰ (Grady, 1982) which is 6‰ lighter than that of the clast. The technique used by Grady (1982) was one of bulk combustion, *i.e.* all the carbon was extracted in a single step from room temperature to 1050°C. However, since then Swart *et al.* (1983a) have shown that samples invariably contain small amounts of terrestrial contamination ($\delta^{13}C \approx -25‰$) and so it is probable that the true $\delta^{13}C$ value of the indigenous carbon in Suwahib (Buwah) is slightly heavier than that reported by Grady (1982). If all the carbon extracted from the clast is included in the $\delta^{13}C$ summation the isotopic composition becomes lighter ($\delta^{13}C = -18.6‰$), due to the inclusion of small amounts of organic contamination with a $\delta^{13}C$ value of -30 to -25‰. Such a result brings the isotopic evidence into agreement with the petrographic evidence of Hutchison (1986) although more evidence is required to be more specific, particularly information such as the oxygen isotopic composition of the clast.

The carbon release profile of the carbonaceous chondrite clast is similar to that of other carbonaceous chondrites (*e.g.* Grady *et al.*, 1983) and the concentration (0.82wt.%) is within the range of published values (Kerridge, 1985). The whole-rock isotopic composition of the carbonaceous chondrite clast is also within the range displayed by other carbonaceous chondrites (Kerridge, 1985). However, the uniform isotopic composition across the release profile (Figure 4.11) is not characteristic of the carbonaceous chondrites, typical release profiles displaying evidence of light organic carbon ($\delta^{13}C \approx -15‰$) and heavy carbonate carbon ($\delta^{13}C \approx +40‰$) (*e.g.* Halbout *et al.*, 1986). Indeed, on a plot of $\delta^{13}C$ versus carbon content the clast is quite distinct from all other carbonaceous chondrites (Figure 4.12). The oxygen isotopic composition of this clast is also distinct from all other carbonaceous chondrites. Although it plots close to the C2 matrix array on an oxygen three isotope plot (Clayton *et al.*, 1978b) it is nearer to the ureilite meteorites than anything else (Figure 4.5).

Kallemeyn *et al.* (1978) suggested that the carbonaceous clast was related to the CI-CM-CO clan of carbonaceous chondrites on the basis of its trace element

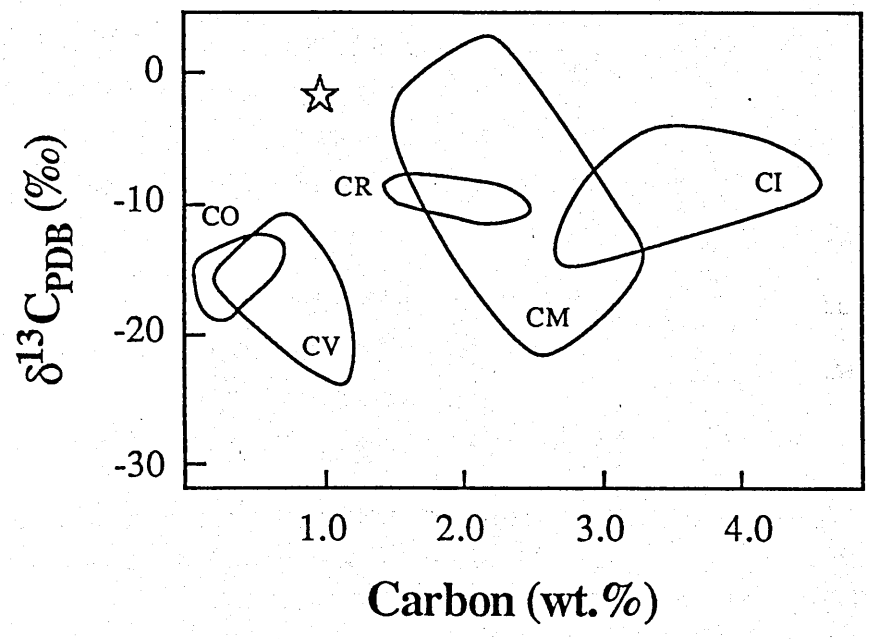

Figure 4.12 $\delta^{13}C$ versus carbon content of the carbonaceous chondrites.. The fields of the four main types of carbonaceous chondrites and the CR2 "grouplet" are shown to compare with the carbonaceous chondrite clast from Bencubbin (star symbol). Carbonaceous chondrite data taken from Kerridge (1985).

abundances. However, the isotopic composition of carbon and oxygen are not consistent with such an affinity, but instead indicate a closer relationship with the ureilites, which are themselves believed to be derived from carbonaceous chondrite material (*e.g.* Berkley *et al.*, 1980). The ureilites display a wide range of oxygen isotopic compositions, with the more ^{16}O-poor members falling very close to the carbonaceous chondrite clast of Bencubbin in $\delta^{17}O/\delta^{18}O$ space, and these same meteorites predominantly have $\delta^{13}C$ values in the range -3.4 to -0.7‰ (Grady *et al.*, 1985; Clayton and Mayeda, 1988). Such values are rather unusual for meteoritic material and therefore, as the carbonaceous chondrite clast has a $\delta^{13}C$ value of -2.1‰, there is good evidence that this clast is related to the ureilites.

4.3 PREPARATION AND ANALYSES OF ACID RESIDUES

A comparison of stepped extraction profiles of the metal clast and iron meteorites indicate that the nitrogen in Bencubbin is not trapped directly in the kamacite (see Section 4.2.1). The heavy nitrogen must therefore be located in a minor phase; identification and analysis of which may help establish the origin of the ^{15}N enrichment. The chemical instability of kamacite allows large amounts of the meteorite to be dissolved without recourse to strong reagents permitting an attempt to be made in concentrating the carrier phases. To explore this aspect a 2g sample of the meteorite was treated with 6M HCl.

Kamacite and FeS readily dissolve in HCl, whereas most of the trace phases found in achondritic and iron meteorites are resistant to this acid (*e.g.* nitrides, phosphides, most silicates, a few sulphides, carbides, graphite, diamonds, *etc.*). The bulk of the silicate clast (clinoenstatite) would only dissolve in much stronger acids, *e.g.* HF/HCl. Therefore, the sample chosen for acid treatment was one dominated by metal clasts as this would achieve the greatest mass loss using the weakest acid. Unfortunately, it was impossible to extract a large sample of pure metal clast from the parental 4.8kg slab without resorting to extensive sawing and therefore a sample of metal clasts and matrix was used.

4.3.1 The Acid Treatments

A flow chart of the various acid treatments performed on the 2g sample of metal and matrix is shown in Figure 4.13. A polished surface of a block 2.0 x 1.0 x 0.5cm showed there to be approximately 40% matrix but inspection of the unpolished reverse side of the block suggested it contained much less matrix. A rough average on the basis of examining both sides of the slab suggests that it is about 80% metal clast. The surface of the sample was cleaned with a corundum abrasive unit to remove any adhering foreign material and washed with methanol agitated by ultrasound for 5 minutes. The sample was dried and weighed in a

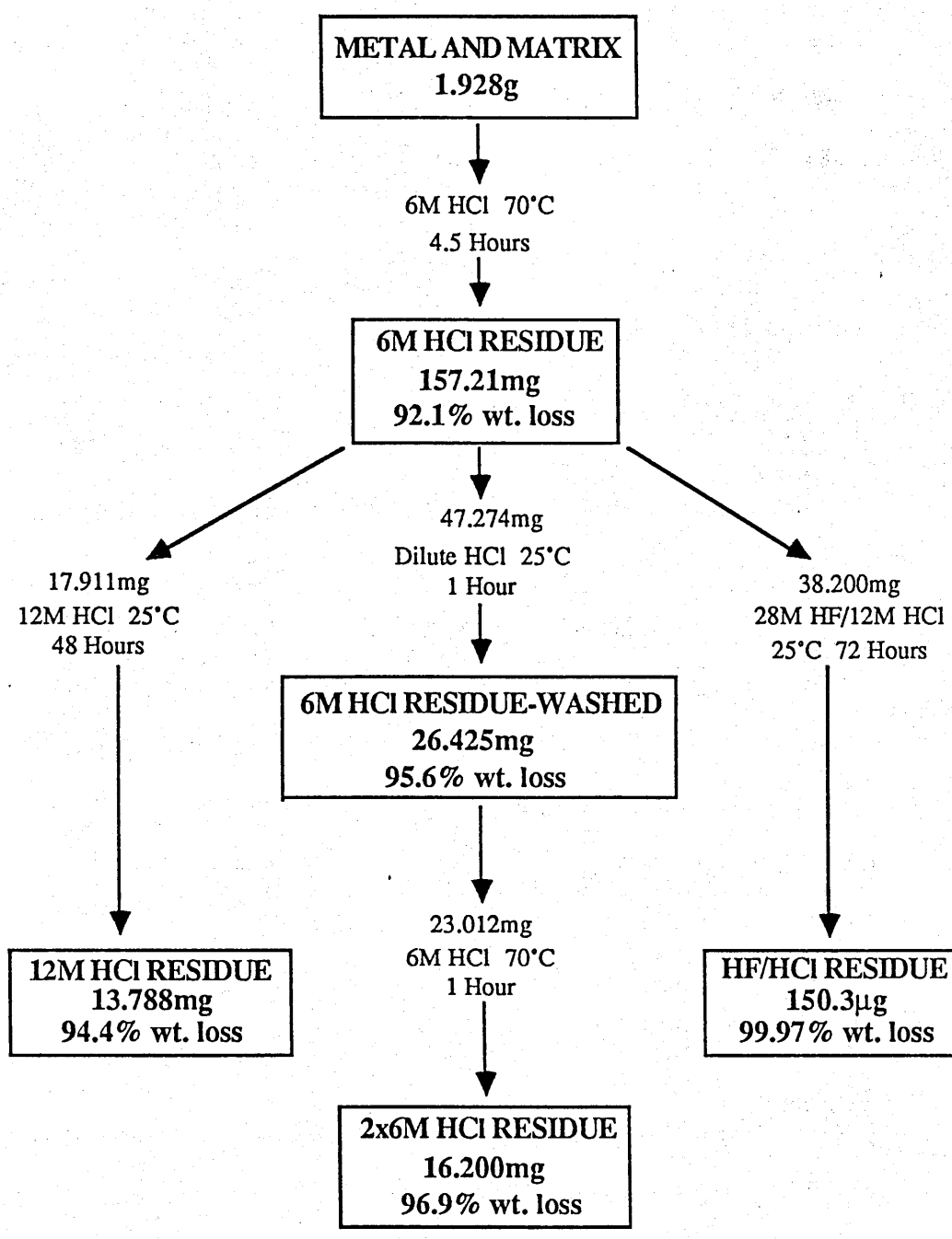

Figure 4.13 Flow chart of the acid residue treatments.

PTFE beaker and 20.544g (18.7ml) of 6M HCl added; after 150 minutes under an infra-red heat lamp all visible reaction had ceased. The treatment was continued for a further 120 minutes to ensure that all the metal had dissolved. The sample and acid were then centrifuged and the solution pipetted off. The sample was rinsed once in distilled water, dried and weighed. The resultant weight loss from the treatment was 92.1%.

Although no problems were encountered when performing the stepped heating extractions for nitrogen, when the 6M HCl residue was analysed for carbon large amounts of a gas (other than CO_2) were liberated, causing extreme instability in the readings from the capacitance manometer. Analysis of the residue by x-ray diffraction revealed considerable quantities of haematite (Fe_2O_3) and nickel chloride ($NiCl_2.6H_20$). It is believed that chlorine gas generated from the decomposition of the nickel chloride was responsible for the instability of the manometer. Washing the 6M HCl residue with dilute HCl had little effect on the two phases but a further wash in 6M HCl for 60 minutes at 70°C removed both compounds. The residue was then rinsed with distilled water until the solution was neutral, then dried and weighed. This residue is called the 2x6M HCl residue. The weight loss incurred in the preparation of this residue from the 6M HCl residue was 61.1%, bringing the total loss up to 96.9%.

A second aliquot of the 6M HCl residue was treated with 12M HCl for 48 hours at 25°C after which it was rinsed with distilled water until the solution was neutral, dried and then weighed. The weight loss introduced at this stage was 23.0%, giving a total weight loss of 94.4% for the 12M HCl residue. A third aliquot of the 6M HCl residue was subjected to 72 hours in a 50:50 mixture of 28M HF and 12M HCl at 25°C, after which is was rinsed in 12M HCl and then as for the 12M HCL residue. This produced a further weight loss of 99.6%, which makes a total of 99.97% for the HF/HCl residue, which is equivalent to 312ppm of the original whole-rock sample of metal plus matrix.

4.3.2 Nitrogen and carbon in the 6M HCl resistant residues

The results of the stepped heating extractions of the 6M HCl residue for nitrogen are shown in Figure 4.14. Pyrolysis of the residue released 734ppm nitrogen, equivalent to 58ppm in the original sample of metal plus matrix, with a $\delta^{15}N$ value of +979‰ (Table 4.4). The average concentration of nitrogen in whole rock material from Bencubbin is around 60ppm and thus it is considered that the 58ppm present in the acid resistant phase(s) accounts for a large proportion of the nitrogen in the original sample. As the bulk $\delta^{15}N$ value of the residue (+979‰) is considerably heavier than the highest bulk values of the clasts (+868‰) this suggests that a component of isotopically lighter nitrogen has been lost during the acid dissolution. Almost 60% of all iron meteorites have $\delta^{15}N$ values of between -90 and -60‰ and so if a $\delta^{15}N$ value of -70‰ is assumed for the component which has been lost it need only be present at the 6ppm level in the metal clast to produce the observed $\delta^{15}N$ values. The concentration of nitrogen

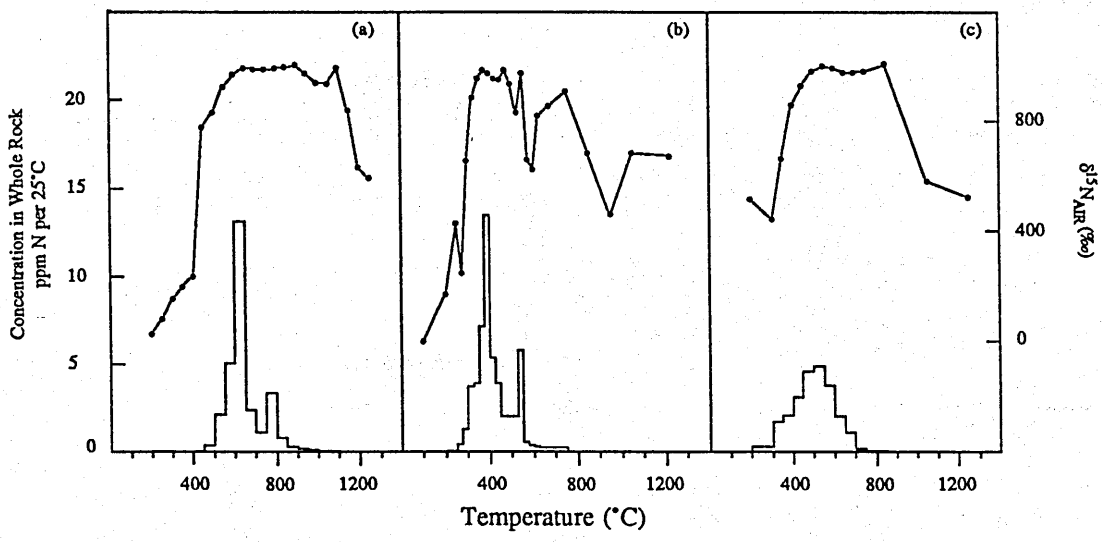

Figure 4.14 Stepped heating profiles for nitrogen extracted from the 6M and 2x6M HCl residues. The yield axis shows the concentration of nitrogen in the initial whole-rock sample, note that the scale is the same as that used in Figures 4.6 and 4.8b. (a) stepped pyrolysis of the 6M HCl residue; (b) stepped combustion of the 6M HCl residue; (c) stepped combustion of the 2x6M HCl residue.

Sample	Total Nitrogen		High Temp. Nitrogen			
	N conc. (ppm)	$\delta^{15}N$ (‰)	Temp.	N conc. (ppm)	N conc. (w.r) (ppm)	$\delta^{15}N$ (‰)
6M HCl	680	+931	275	672	53	+938
6M HCl (pyrol.)	741	+972	400	734	58	+979
2x6M HCl	1571	+927	300	1518	47	+943
12M HCl	211	+983	300	197	11	+998
HF/HCl	8047	+711	375	5875	2	+857
HF/HCl (pyrol.)	6466	+903	400	6053	2	+903

Table 4.4 Summary of nitrogen content and $\delta^{15}N$ value from acid residues of Bencubbin. The second last column shows the calculated concentration of indigenous nitrogen in the original metal and matrix sample after correction for the appropriate mass loss.

present in iron meteorites with kamacite which has been shocked and recrystallised ranges from 1.4 to 5.8ppm (see Section 3.3.3) and so a concentration of 6ppm for this postulated isotopically light component is not unreasonable.

The pyrolysis of the 6M HCl residue produced a bimodal release of nitrogen, with a major release between 450 and 750°C and a minor release between 750 and 850°C (Figure 4.14a). The isotopic composition across both releases is relatively constant, varying only slightly within the range +988 to +1003‰. The major component has a concentration of 608ppm nitrogen and the minor component 105ppm. For convenience the major release of nitrogen from the 6M HCl residue will be called N_α, and the minor release N_β, following the terminology of Franchi *et al.* (1986b).

It would be extremely difficult to establish whether the major and minor releases observed in the whole rock samples are N_α and N_β or simply mixtures of the two trapped in different sites because they have indistinguishable isotopic compositions and encapsulation in the acid soluble phases affects the release

temperatures. The concentration of nitrogen liberated during the major release from the metal clast was 66.9ppm and from the minor release between 700 and 850°C 5.6ppm, giving a ratio for the major : minor release of 12. In the glassy matrix sample (matrix#1) the equivalent ratio is approximately 1; a mixture of metal clast and matrix would be expected to produce a ratio intermediate between 12 and 1. Therefore, a ratio of 6 for N_α : N_β in the 6M HCl residue is consistent with the two releases seen in the clasts being N_α and N_β. However, due to the heterogeneous distribution of nitrogen in the matrix (see Section 4.2.1) there is a high degree of uncertainty in the relative abundances of N_α and N_β in a large sample. More evidence is required, such as the simultaneous release of another element from one or other of the components, before the nitrogen releases from the whole-rock samples can be identified as being N_α or N_β.

Combustion of the 6M HCl residue produces a yield which is marginally lower at 672ppm (equivalent to 53ppm nitrogen in the original sample) and an isotopic composition which is slightly lighter than the pyrolysis, the $\delta^{15}N$ value

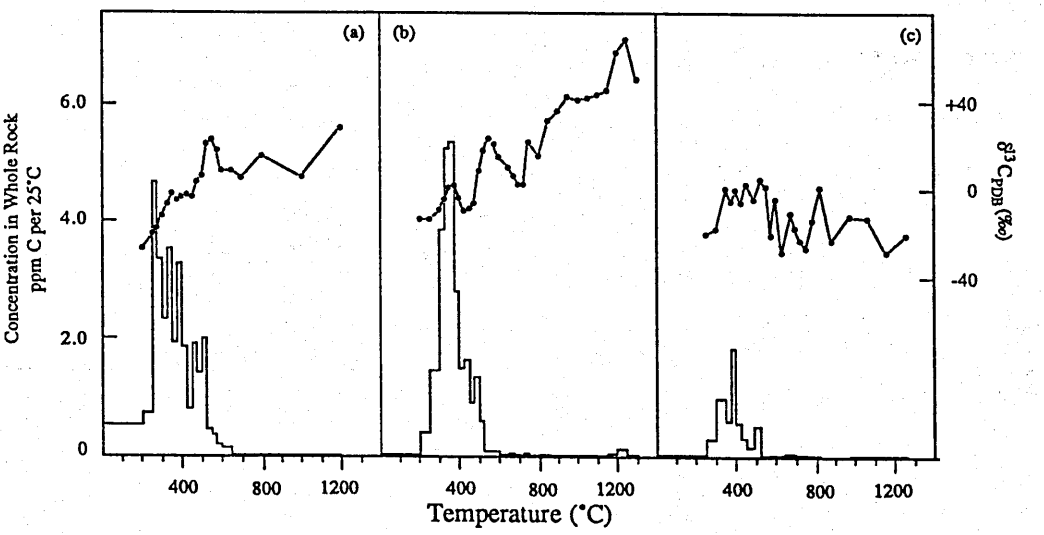

Figure 4.15 Stepped combustion profiles for carbon of the acid residues. Yield axis shows concentration of carbon in initial whole-rock sample. (a) 2x6M HCl residue; (b) 12M HCl residue; (c) HF/HCl residue.

being +938‰. The decrease in the $\delta^{15}N$ value appears to be due to trace amounts of light nitrogen released between 500 and 600°C producing a 350‰ dip in the isotopic profile. This light component is not evident in the pyrolysis, suggesting that it is not indigenous to the sample, and therefore is most probably some form of contamination introduced during sample handling. The presence of oxygen during the stepped heating has the effect of lowering the release temperature of both N_α and N_β so that N_α is liberated between 350 and 525°C and N_β between 500 and 575°C (Figure 4.14b). The release temperature of N_α during combustion and pyrolysis is almost 600 and 400°C respectively lower than the main release of nitrogen during combustion of the metal clast. This indicates that the component is located within a material which prevents decomposition until it is dissolved in 6M HCl. It is considered that the only phase which satisfies these requirements is the Fe-Ni metal.

The nature of the heavy nitrogen carrier phase is far from obvious. Acid-resistant meteoritic material which combusts below 600°C and pyrolyses at higher temperatures is usually carbonaceous, either as macromolecular organic molecules (Swart *et al.*, 1982) or very small diamonds (Lewis *et al.*, 1987; Ash *et al.*, 1987). However, analysis of the 2x6M HCl residue for carbon* only released a total of 1110ppm carbon (Figure 4.15a, Table 4.5). Such a low concentration of carbon argues against the nitrogen carrier being carbonaceous

* Footnote - Analytical problems prevented carbon measurements being performed on the 6M HCl residue (see Section 4.3.1) but a stepped combustion for nitrogen of the 2x6M HCl residue (Figure 4.14c) shows that little or no nitrogen was lost in the 60.8% weight loss incurred during its preparation. The nitrogen concentration of 1518ppm is equivalent to 47ppm in the original sample, which is 10% less than the concentration obtained from the combustion of the 6M HCl residue (Table 4.4). The release of nitrogen from this residue is unimodal, with no evidence of the minor release N_β. However, the release temperature of N_α from the 2x6M HCl residue (300 to 700°C) is higher and broader than that from the 6M HCl residue and thus is smeared out across the release temperature of N_β (500 to 575°C). This may be due to the larger step sizes employed in this extraction which may also be responsible for the increased release temperature

Sample	Total Carbon		High Temp. Carbon			
	C conc. (ppm)	$\delta^{13}C$ (‰)	Temp.	C conc. (ppm)	C conc. (w.r) (ppm)	$\delta^{13}C$ (‰)
2x6M HCl	594	-5.8	300	669	21	+2.6
12M HCl	508	+0.3	300	438	24	+1.9
HF/HCl	26003	-4.3	300	21565	7	-0.8

Table 4.5 Summary of carbon content and $\delta^{13}C$ value from acid residues of Bencubbin. The second last column shows the calculated concentration of indigenous carbon in the original metal and matrix sample after correction for the appropriate mass loss.

because, even assuming that all the carbon is associated with the isotopically heavy nitrogen, the maximum C/N ratio would only be 0.7. The true C/N ratio is more probably even lower as it is very likely that some of the carbon is terrestrial contamination.

The peak release temperature of SO_2 from troilite is the 400 to 500°C step during stepped combustion (Burgess, 1987). This temperature range coincides with that of N_α (300 to 450°C) indicating a possible association. Although pure troilite is soluble in HCl the troilite in Bencubbin is very chromium rich, the chromium content reaching as high as 30wt.% (Newsom and Drake, 1979). As the chromium-rich sulphide daubréelite is resistant to attack by HCl, it is possible that the chromium-rich troilite in Bencubbin is also stable in acid.

The main release of carbon (Figure 4.15a) is over the temperature range of N_α (300 to 450°C) but the analysis of the silicate clast showed that no carbon was associated with the majority of the heavy nitrogen, *i.e.* N_α. Between 500 and 575°C, the release temperature of N_β, the $\delta^{13}C$ value reaches a maximum of +24‰, but no discrete release of carbon can be identified because of the "tail" of the much larger release between 250 and 500°C. Therefore, this component cannot be present in very high concentrations, with a maximum C/N ratio of 1.

Although such low C/N ratios are not typical of carbonaceous material found in meteorites some of the organic materials extracted from the carbonaceous chondrites are exceptionally rich in nitrogen, *e.g.* the purine base adenine ($C_5H_5N_5$) and guanine ($C_5H_5N_5O$) (Anders *et al.* 1973), with C/N ratios of around 1. Although such minerals display considerable thermal stability (e.g. guanine decomposes at 360°C), it is not evident how such compounds could survive to almost 600°C (the release temperature of N_β) in the presence of oxygen. It is possible that the N_β carrier is shielded by a more refractory phase.

4.3.3 Nitrogen and Carbon in the 12M HCl Residue

As in the combustion of the 6M HCl residue, a high resolution stepped combustion of the 12M HCl residue produced a bimodal release of isotopically heavy nitrogen (Figure 4.16a). The release temperatures of the two components are 300 to 400°C and 425 to 600°C - very similar to the range of temperatures displayed by N_α and N_β in the 6M HCl residue. However, the concentration of nitrogen in the 12M HCl residue (197ppm) is much less than that of the 6M HCl residue (734ppm); the release profiles showing that N_α is severely depleted in the 12M HCl residue. The concentration of N_α in the residue is 63ppm (equivalent to 48ppm in the 6M HCl residue) implying that >90% of N_α has been removed upon treatment with the stronger acid. The concentration of N_β on the other hand is equivalent to 100ppm in the 6M HCl residue which compares with measured concentrations of N_β in the 6M HCl residue of 91 and 105ppm. It seems therefore that none of N_β has been lost during the 12M HCl dissolution.

The bulk isotopic composition of the 12M HCl residue is +998‰, 20‰ heavier than the bulk value from the 6M HCl residue. This is not considered significant because of the relatively small amounts of gas (<14ng) liberated from each temperature step from this residue. Because of the large difference in the isotopic composition of nitrogen in the blank and the sample any variations in the blank are magnified in the final $\delta^{15}N$ value when the measured ratios are

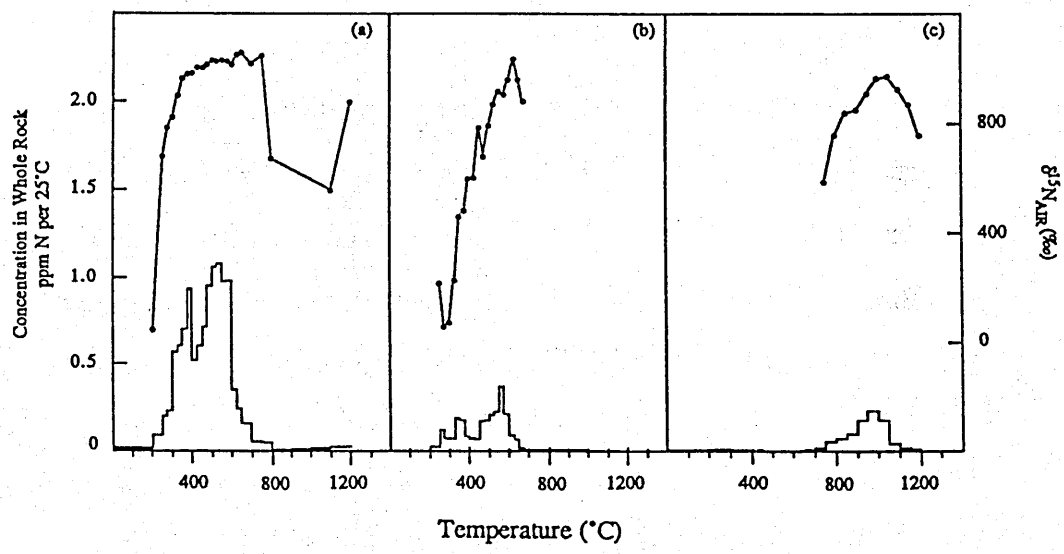

Figure 4.16 Stepped heating extraction profiles for nitrogen of the 12M HCl and HF/HCl residues. Yield axis shows concentration of nitrogen in initial whole-rock sample. (a) stepped combustion of 12M HCl residue; (b) stepped combustion of HF/HCl residue; (c) stepped pyrolysis of HF/HCl residue.

corrected for the blank contribution. The much larger amounts of gas liberated from the 6M HCl residue samples (up to 830ng per step) swamp any contribution from the blank (typically <1ng) and therefore errors which could be introduced through the blank are negligible.

Analysis of the 12M HCl residue for carbon yielded only 438ppm carbon with a $\delta^{13}C$ value of +1.9‰ (Table 4.5). Over the temperature range 300 to 600°C (corresponding to where N_α and N_β are liberated) the release profile and the isotopic composition are very similar to that of the 2x6M HCl residue (Figure 4.15b). Between 250 and 500°C there is a release of carbon, comparable in size to that released over the same temperature range from the 2x6M HCl residue, with a peak $\delta^{13}C$ value of +3‰ and over the temperature range of N_β the isotopic composition rises sharply to +24‰ before falling to 0‰ by 700°C. Therefore, both carbon components seen in the 2x6M HCl residue appear to still be present after treatment with 12M HCl. As 12M HCl removes N_α but not any carbon it is

possible to state that there are no detectable quantities of carbon associated with N_α . The release of relatively heavy carbon over the temperature range 500 to 650°C is further indication that carbon may be associated with the N_β component. However, the maximum C/N ratio appears to be 0.5 (the release is still indistinct because of the "tail" of the much larger release at lower temperatures), placing even greater constraint on the identity of the carrier phase if it is an organic or carbonaceous material.

Above 600°C very little carbon is released but the $\delta^{13}C$ value rises steadily to reach a maximum of +69‰, coinciding with a small release (7.6ppm carbon) at 1250°C. Although this is the heaviest carbon found in Bencubbin it does not appear to be associated with any isotopically heavy nitrogen. This carbon may be the same component observed above 1100°C in the whole rock samples of the silicate clast and the matrix (see Section 4.3.2). The origin of this carbon is not known, but bears some resemblance to the heavy carbon observed in the residues of the carbonaceous chondrites (McGarvie *et al.*, 1987), and if so may be indicative of the presence of presolar material, the release characteristics of the carbon suggesting that it may be similar to $C\beta$ (SiC).

4.3.4 Nitrogen and Carbon in the HF/HCl Residue

A stepped combustion of the HF/HCl residue (Figure 4.16b) liberated a total of 8047ppm nitrogen, although 25% of this is isotopically light and probably results from contamination. There are three distinct releases of nitrogen from this residue. The first, between 200 and 300°C with a minimum $\delta^{15}N$ value of +59‰ is probably absorbed atmospheric nitrogen with trace amounts of heavy nitrogen. The second release, between 325 and 400°C has a $\delta^{15}N$ value of almost +500‰ and is the remnant of N_α plus some isotopically light contamination. The third, and main release, between 450 and 650°C has a peak $\delta^{15}N$ value of +1033‰ and is the N_β component.

The trend of increasing isotopic composition with increasing release temperature is a reflection of mixing between terrestrial contamination ($\delta^{15}N \approx 0‰$) at low temperature and N_α and N_β ($\delta^{15}N \approx +1000‰$) at higher temperatures. This mixing occurs because stepped heating has incompletely resolved the various components. By assuming that the contamination has a $\delta^{15}N$ value of 0‰ and the sample nitrogen +1000‰ the amount of indigenous nitrogen can be calculated for each temperature step (Figure 4.17a). A plot of the concentration of nitrogen with a $\delta^{15}N$ value of 0‰ (Figure 4.17b) shows that most of this nitrogen is liberated at temperatures below 350°C. However, small amounts of "contamination" at temperatures above 350°C indicate that either the assumed isotopic composition of the two components are in error or, more probably, that there is more than one form of contamination component. The most likely nature of the extra contaminants is organic material such as air borne dust.

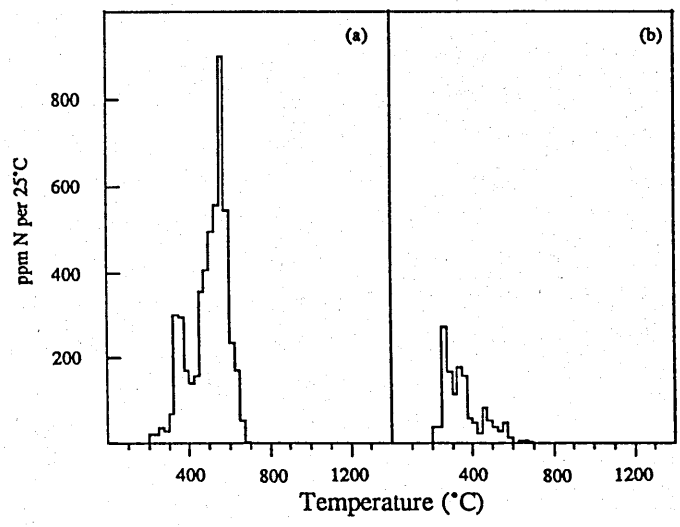

Figure 4.17 Calculated extraction profile of indigenous and contamination nitrogen in the HF/HCl residue. Assuming that the contamination has a $\delta^{15}N$ value of 0‰ and the indigenous nitrogen +1000‰ the relative proportions of each in every step of the combustion of the HF/HCl residue (Figure 4.16b) can be calculated. (a) release profile of nitrogen ($\delta^{15}N$ = +1000‰); (b) release profile of nitrogen ($\delta^{15}N$ = 0‰).

The concentration of nitrogen with a $\delta^{15}N$ value of +1000‰ is 6130ppm. A small release between 300 and 400°C shows that some N_α is still present but this represents <0.5% of the whole-rock abundance. Almost all the heavy nitrogen present is N_β but this is only present at a level equivelent to 24ppm in the 6M HCl residue, indicating that 75% has been lost during the HF/HCl treatment. Although this may be due to instability in 28M HF/12M HCl it is feared that during transfer of the residue, from the beaker in which it was dried to a receptacle in which it could be weighed accurately, some of the residue was not recovered. A poor recovery of the residue will exaggerate the weight loss and result in an apparent low yield for any components still present in the residue.

4.3.5 Sulphur in the residues and the metal clasts

As noted earlier, stepped heating of sulphides produces a sharp release of sulphur over the temperature range 300 to 500°C (Burgess, 1987), which corresponds with the release temperature of N_α (300 to 450°C). Although most common sulphides are soluble in HCl, the Cr-rich sulphide Daubréelite is stable in this acid. As the troilite in Bencubbin is known to be rich in Cr (Newsom and

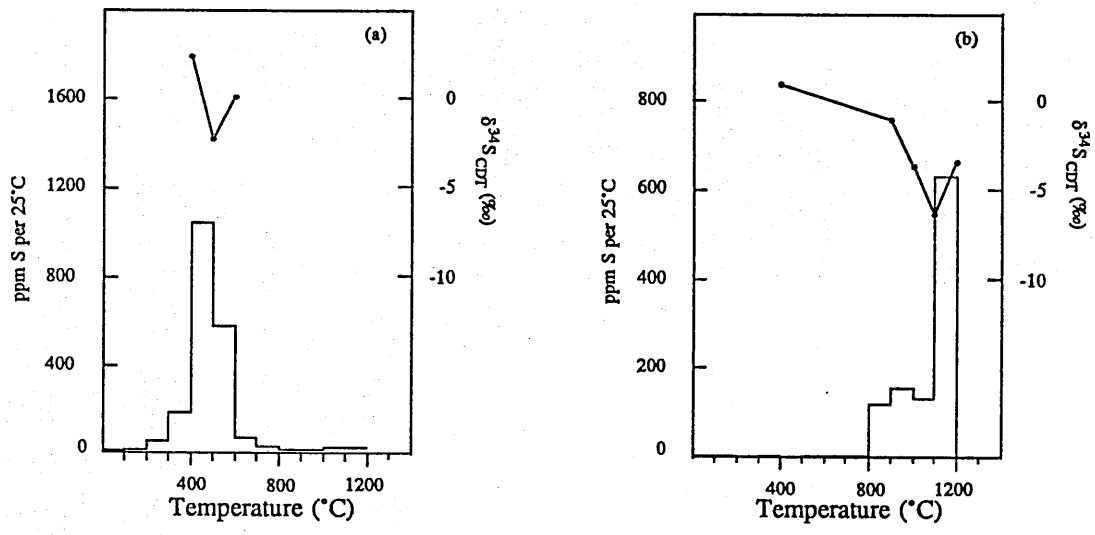

Figure 4.18 Stepped combustion profiles for sulphur. (a) 2x6M HCl residue; (b) bulk metal clast.

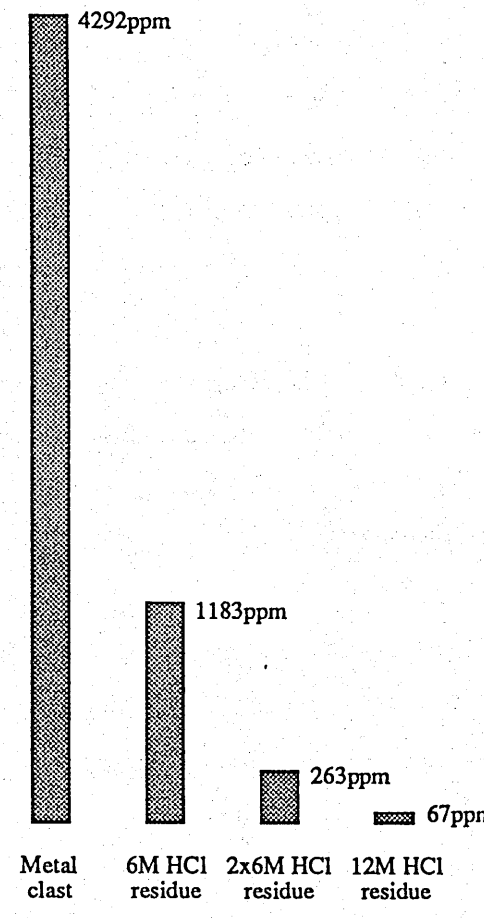

Figure 4.19 Relative sulphur abundances in the acid residues. The sulphur concentration in the 6M, 2x6M and 12M HCl residues are schematically shown as their concentration in the original whole-rock sample. The concentration of sulphur in the metal clast sample is shown for comparison.

Drake, 1979) it is possible that it is present in the residues resistant to 6M HCl. Trace amounts of daubréelite have also been reported from the meteorite (Ramdohr, 1973). If the nitrogen is associated with a sulphide then the isotopic composition of the sulphur may be of great use in establishing the origin of the ^{15}N enrichment.

Stepped combustion of the 2x6M HCl residue (Figure 4.18a) did indeed liberate sulphur over the temperature range characteristic of sulphides, 300 to 600°C. Although this is a slightly higher temperature than that at which N_α is

released this could be due to larger step sizes being employed in the sulphur extraction (100°C) than during the nitrogen extractions (25 and 50°C), larger steps generally causing an increase in the release temperature of a phase. The bulk concentration of sulphur in the 2x6M HCl residue was 0.84wt.% with a $\delta^{34}S$ value of -1.0‰, which is within the common range of meteorites, -1 to +1‰ (Kaplan and Hulston, 1966). However, due to problems associated with production of SO_3 at temperatures below 600°C the isotopic composition of sulphur liberated from free sulphide during stepped combustion is not reliable and can be *ca.* 2‰ low and the yield up to 25% down (Burgess, 1987).

Stepped combustion of a sample of a metal clast liberated 0.43wt.% sulphur with a $\delta^{34}S$ value of -3.4‰, the minimum value reached being -6.4‰ (Figure 4.18b). The release from the metal clast was above 800°C, due to shielding by the metal phase, and therefore the $\delta^{34}S$ values are not affected by SO_3 production. Such values are outside the normal range of meteorites but as only 6% of the sulphur in the clast is present in the 2x6M HCl residue (Figure 4.19) this isotopic signature may be that of an acid soluble sulphide. However, it is noteworthy that there was a dip in the $\delta^{34}S$ value across the release of sulphur from the 2x6M HCl residue.

A sample of the 6M HCl residue, analysed only for sulphur content, was found to contain much more sulphide (1.50wt.%), approximately 30% of that in the metal clast (Figure 4.19). The differences in the sulphur contents of the two 6M HCl resistant residues is considerable (a factor of 4) and may be the result of sample heterogeneity, poor sulphur yields during extraction due to SO_3 production or sulphide loss during the second 6M HCl treatment. As yet it is impossible to determine which of these three processes have caused the variable yields from the 6M HCl resistant residues, although loss during the second acid treatment is the most likely.

The sulphur content of the 12M HCl residue was determined by a bulk combustion. This sample liberated only 0.12wt.% sulphur, equivalent to

0.09wt.% sulphur in the 6M HCl residue. As this represents <8% of the sulphur in the 6M HCl residue the results of the sulphur analyses are consistent with the carrier of N_α being a sulphide as the 12M HCl treatment resulted in 90% of N_α being lost. Due to the small amount of sulphur recovered from the 12M HCl residue no isotopic measurement was possible.

4.3.6 Composition of the residues

Approximately 40% of the 2x6M HCl residue is large blebs or fragments (100μm or larger) of matrix silicate. The low release temperatures of N_α and N_β are not characteristic of nitrogen released from silicates or silicate glass and so these were excluded from any further analysis. To identify the sulphides in the Bencubbin residues, and any alternative carriers for N_α, the 2x6M HCl residue and the 12M HCl residue were analysed using an analytical transmission electron microscope (ATEM). The survey of the residues was restricted to only the finest material as the grains had to be less than 500nm thick in order that the electron beam could pass through; slightly larger grains could be analysed by targeting the

	2x6M HCl Residue	12M HCl Residue
Matrix Glass	≈75%	≈75%
Amorphous Silica	≈20%	≈25%
$(Cr,Fe)_2S_3$	5%	<1%
Graphite	trace	trace
Chromite ($FeCr_2O_4$)	trace	trace
Anatase (TiO_2)	trace	trace
Silicates*	trace	trace

Table 4.6 Composition of the 2x6M HCl and 12M HCl residues. These are the approximate amounts of the various phases in the two residues. The percentage silicate glass is very approximate as this was simply estimated visually, the approximate abundance of the other phases were determined by their frequency of occurrence on the copper grid in the ATEM. * The silicates were very rare and gave weak diffraction patterns and as a result could not be identified.

beam on the margins of a sample. Although the grain size limitations introduce a bias in the sampling, three samples of each residue were prepared in an attempt to minimise the errors.

The vast bulk of the fine material in each residue was an amorphous phase composed primarily of silicon (Table 4.6). The spectrometers on the ATEM could not detect low atomic mass elements (A≤23) and therefore it was impossible to determine if the silicon was in an elemental or oxidised form. An infrared spectrum of the 2x6M HCl residue (Figure 4.20) shows features at 1094, 800 and 470cm^{-1} characteristic of SiO_2 bonding (Moenke, 1974). These features could be due to either amorphous silica or the silicate glass from the matrix present in the sample. However a medium intensity feature at 950cm^{-1} is indicative of the presence of freshly prepared amorphous silica and is caused by stretching of the Si-O bond in Si-OH groups (Hino and Sato, 1971). Forsteritic olivine, present in the fragments of silicate clasts in the matrix is soluble in hot HCl and therefore is the most likely source of this silica, the silicate glass and the clinoenstatite being much more stable in HCl.

The other phase present in sufficient quantities to be considered as a possible host to N_α, and predicted from the results of the stepped heating experiments, is a sulphide with an approximate stoichiometery of $(Fe_{0.33},Cr_{0.67})_2S_3$. The chromium content of the sulphide is very high (>30wt.%) but quite constant, the Cr/Fe ratio being 2.2±0.31 (n=7) (Table 4.7). The stoichiometery is different to all other known sulphides, including daubréelite ($FeCr_2S_4$) which is deficient in sulphur compared to the sulphide in the Bencubbin residues. An electron diffraction pattern of the chromium-rich sulphide is distinctly different to that of daubréelite, but similar to the diffraction pattern of pyrrhotite, a pseudo-hexagonal sulphide with the stoichiometery $Fe_{(1-x)}S$ (x = 0 to 0.125) (Table 4.8).

A number of trace minerals were also found including chromite ($FeCr_2O_4$) and anatase (TiO_2). A few weakly diffracting silicate grains containing Mg and Al and small amounts of Fe and Ca were also present but could not be identified.

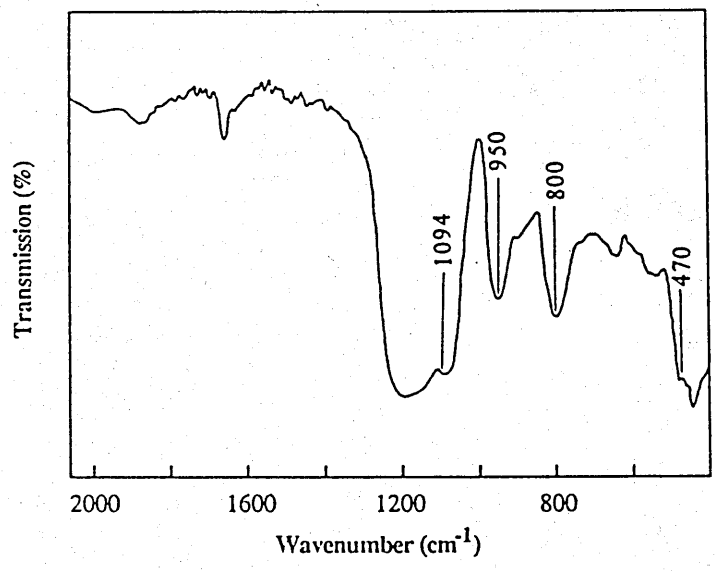

Figure 4.20 Infra-red transmission spectrum of 2x6M HCl residue. Prominent features at 1094, 800 and 470cm^{-1} are characteristic of amorphous silica, but could also be due to the silica glass in the sample. However, the feature at 950cm^{-1} is very characteristic of freshly prepared amorphous silica.

2x6M HCl Residue			12M HCl Residue			
Sample	Mole Fraction of Sulphur	Cr/Fe	Sample	Mole Fraction of Sulphur	Cr/Fe	Plus
CRS.01	0.60	2.6	CRS.03	0.63	2.6	3% Ni
CRS.02	0.60	2.0	CRS.04	0.70	-	
CRS.08	0.59	2.4	CRS.05	0.60	2.3	3% Ni
CRS.09	0.60	1.9	CRS.06	0.61	2.2	
CRS.10	0.61	2.5	CRS.07	0.62	3.0	
CRS.11	0.58	1.8	CRS.12	0.55	10.0	2% V*
CRS.15	0.60	2.1	CRS.13	0.52	2.4	10% V*
			CRS.14	0.62	0.2	
		mean = 2.2±0.31			mean** = 2.5±0.31	

Table 4.7 Composition of the Cr-rich sulphides in the acid residues. From the mean mole fraction of sulphur and the Cr/Fe ratio in the sulphides in the 2x6M HCl residue the stoichiometry can be estimated to be $(Cr_{0.67},Fe_{0.33})_2S_3$. * The vanadium abundances are very approximate. As there was no reference standard available for vanadium the concentrations were crudely estimated from the peak height in the ED spectrum. ** Mean value excludes CRS.04, CRS.12 and CRS.14 as their Cr/Fe ratios are more than 3σ from the mean.

Low atomic mass material in similar abundance to the Cr-rich sulphides were also detected, some of which were weakly diffracting indicating that it may be carbonaceous. However, a blank copper grid, on which the sample is normally mounted, contains similar quantities of this material. As the samples were mounted in a non-clean environment some of this material could be dust, predominantly organic in nature.

The mineralogy of the 12M HCl residue is very similar to that of the 2x6M HCl residue (Table 4.6). The majority of the fine material in the samples is once again amorphous silica but the amount of sulphide present is much lower (the sulphur analyses indicating a factor of 6). As >90% of N_{α} is removed by 12M HCl the amorphous silica is eliminated as a carrier phase, but the reduction of sulphide is consistent with the loss of N_{α}. The sulphides which remain after the 12M HCl treatment have a much more variable composition than those in the 2x6M HCl residue. The metal:sulphur ratio is approximately the same, around 2:3, but the Cr/Fe ratio is much more variable, although the majority of grains still have a similar Cr/Fe ratio (mean = 2.5±0.31 (n=5)). However, 5 out of the eight sulphides analysed in the 12M HCl residue had unusual compositions compared to those in the 2x6M HCl residue, with Cr contents ranging up to pure chromium sulphide and considerable concentrations of nickel and vanadium (Table 4.7). As the sulphides of both Ni and V are stable in HCl the presence of several wt.% Ni and V may explain the increased resistance to acid attack. Alternatively the range in compositions, particularly the sulphur content and the Cr/Fe ratio, could be due to leaching by the 12M HCl of sulphides which originally had a composition the same as those in the 2x6M HCl residue.

As the bulk sulphur abundance in the 2x6M HCl residue was only 0.84±0.21wt.% the concentration of the Cr-rich sulphide in the residue can only be 1.8wt.%. Therefore, with an N_{α} content of ≈1300ppm the concentration of nitrogen in the sulphide would be 7wt.%. An upper limit of 250ppm nitrogen has been reported for troilite from iron meteorites (Gibson and Moore, 1971).

$(Cr,Fe)_2S_3$	Pyrrhotite		Troilite
5.89	5.85		
5.70		5.74	
5.62			
			5.40
		5.27	
5.14	5.08		
4.97			
4.56			4.74
3.54			
3.49			
3.40			
2.96	2.98	2.98	2.98
2.92			
2.85	2.85	2.87	

Table 4.8 Diffraction pattern spacings of $(Cr;Fe)_2S_3$. The spacings are given in Å. For comparison the results of two analyses of pyrrhotite and one of troilite are also shown (taken from Alexander, 1987).

However, if the chromium sulphide does have a pseudo-hexagonal structure then approximately 30% of the lattice sites normally occupied by metal anions will be vacant which could then accommodate up to 7wt.% nitrogen. Thus a mechanism exists to accommodate the nitrogen in the Cr/Fe sulphide carrier.

An alternative explanation is that the excess sulphur in the sulphide, assuming a pseudo-hexagonal structure, is not part of the mineral structure. Instead this sulphur could be bound directly to the nitrogen forming some, as yet unidentified, sulphur nitride compound. Two of the more stable sulphur nitride compounds are S_4N_4 and SN_x (Greenwood and Earnshaw, 1984). The amount of excess sulphur in the sulphide would give a S/N ratio of 0.8, and therefore such compounds, or something similar are stoichiometrically feasible. However, these compounds are unstable at temperatures above 250°C, often decomposing explosively, particularly if heated rapidly or even subjected to shock (Labes *et al.*,

1979). Therefore, their presence in a meteorite which has suffered extensive shock heating, such as Bencubbin, is considered very unlikely.

The presence of so few phases with the appropriate thermal and chemical stability in concentrations other than trace amounts limits the possible host phases for N_α and N_β. The data so far available are consistent with the host of N_α being a chromium rich sulphide, $(Fe,Cr)_2S_3$, with a hexagonal structure. The only alternative carrier identified would be the amorphous silica, but as this was still present in abundance in the 12M HCl residue it is very unlikely that this could be the host of N_α. The constancy of the N_α:N_β ratio in the two analyses of the 6M HCl residue and the identical $\delta^{15}N$ value of the two components suggests that they are intimately associated. However, the host phase of N_β could not be identified because, due to insufficient sample, no characterisation of the HF/HCl residue was possible. It may be that the N_β host is trapped within the sulphide grains, which would explain the constant ratio of N_α:N_β concentrations in the same residue despite variations in the absolute concentrations.

4.4 THE LOCATION OF THE N_α CARRIER PHASE WITHIN THE METEORITE

Determining the distribution of the the heavy nitrogen within the meteorite may help constrain how the carriers were incorporated into the meteorite, thereby increasing our understanding of the timing of events and the possible origins of the ^{15}N enrichment. To conduct a general survey of the nitrogen in Bencubbin using conventional stepped heating techniques would be difficult and require a number of well characterised samples. A alternative approach would be to use the laser microprobe extraction technique (see Section 2.7). Although this technique is not yet sufficiently sensitive to detect and analyse nitrogen at <50ppm in unknown samples, it can be used to map out the distribution of

nitrogen in samples with a known isotopic composition. Each area sampled can be characterised immediately before each analysis and the laser extraction technique allows a high throughput of samples and results in minimal damage to the meteorite. A comparison with the Weatherford meteorite and any other meteorites may also yield information on the extent of the ^{15}N enrichment, as well as its possible origin.

4.4.1 Sample for Laser Microprobe Examination

A 6g sample of the meteorite containing metal and silicate clasts together with matrix was polished on one side for conventional petrographic examination. In order to minimise contamination the sample was not mounted in any resin (following laser extraction analyses this sample was used in the preparation of the acid residues). A series of potential target areas were identified for laser microprobe examination; these include sulphide-rich and sulphide-poor metal clasts (Figure 4.2) and the different types of matrix and veins (Figures 4.2 to 4.4).

Although the laser beam successfully produced large, roughly cylindrical pits in each of the target materials there was considerable variation in the size of the pits and particularly in the nature of the ejecta which was deposited around the rims. Using maximum laser energy output (5J) the depth of each pit was estimated to be approximately 150μm. The pit diameters in the metal clasts were 100μm (Figure 4.21) while those in the silicate clasts were smaller, around 80μm across (Figure 4.22). The matrix pit sizes were intermediate at approximately 90μm (Figure 4.23). Laser interaction with the target materials produced zones of spatter around each pit, extending up to 100μm from pits in the metal clasts (Figure 4.21) whereas for the silicate clasts extensive spatter was spread in zones around 500μm in diameter (Figure 4.22). The matrix was again intermediate forming spatter zones up to 350μm in diameter (Figure 4.23). Unfortunately, because the concentration of nitrogen in Bencubbin was low, multiple pulses of

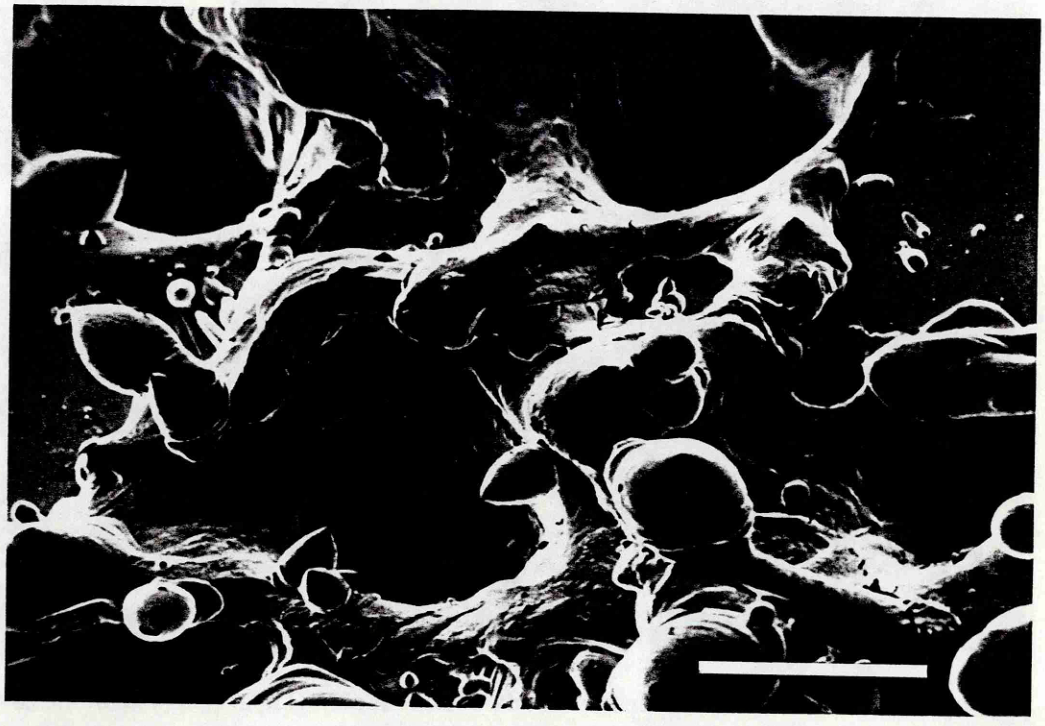

Figure 4.21 Laser pit produced in metal clast of Bencubbin. Output energy = 5J. Scale bar = 100μm.

Figure 4.22 Laser pit produced in silicate clast of Bencubbin. Output energy = 5J. Scale bar = 100μm.

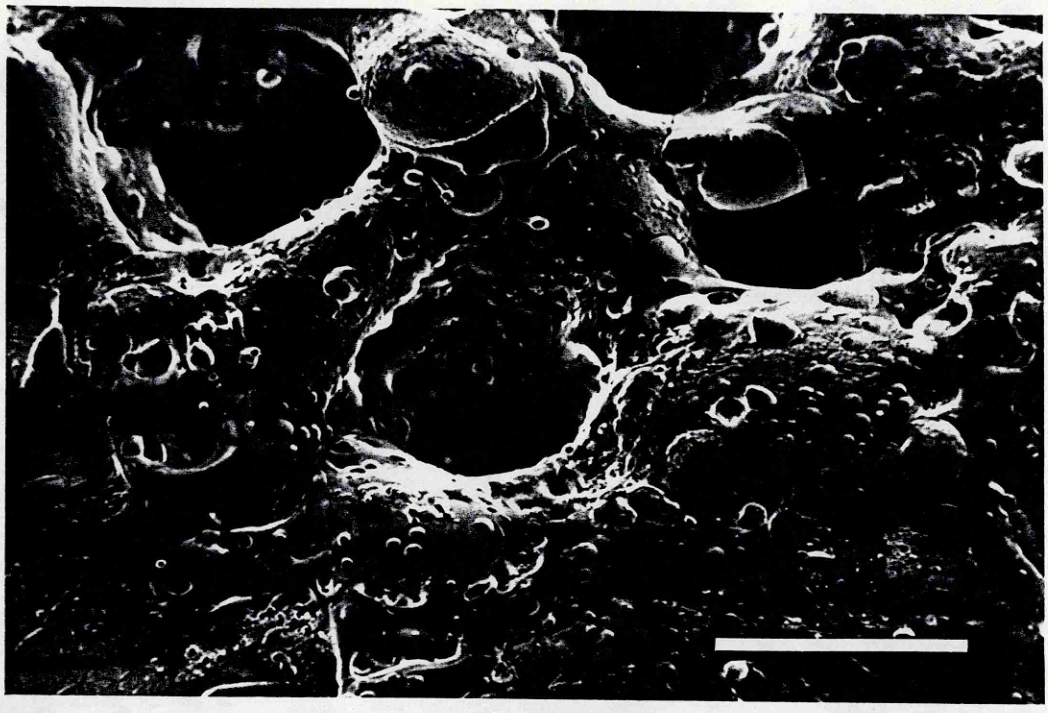

Figure 4.23 Laser pit produced in matrix of Bencubbin. Output energy = 5J. Scale bar = 100μm.

the laser were required in each target area to liberate sufficient gas to analyse; each successive pulse was targeted on a fresh piece of sample free of ejecta spatter.

4.4.2 Laser Microprobe Analyses

A total of 21 analyses of clasts and matrix were performed using the laser microprobe, the results of which are shown in Table 4.9. There is a considerable range in $\delta^{15}N$ values, from +190 to +958‰, and in nitrogen yields from 27 to 150pg $pulse^{-1}$. These variations are directly related to the nature of the target material. The silicate clasts have the lowest $\delta^{15}N$ values and the highest concentrations of nitrogen (Figure 4.24). The isotopic composition of the metal clasts and the matrix and vein material overlap but the metal clasts liberate less nitrogen than the matrix and veins. It would appear that there are significant differences in the nitrogen present in the various materials present in Bencubbin.

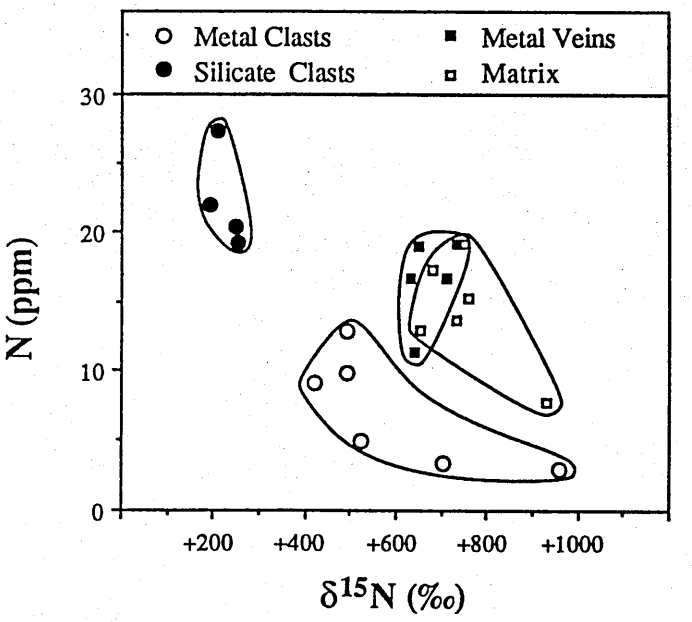

Figure 4.24 Nitrogen content versus $\delta^{15}N$ value plot of laser microprobe extractions of Bencubbin. The data has been split into metal clasts, silicate clasts and two types of matrix - metal-rich veins (*e.g.* Figure 4.2) and matrix containing unmelted fragments of the clasts (*e.g.* Figure 4.4).

Such results contrast with those obtained by the stepped heating extractions, which sampled on a larger scale.

There are a number of effects which will control the amount of nitrogen liberated by a laser pulse. The size of the laser pits (used to calculate the mass of material sampled) and the efficiency of nitrogen escape from material heated by the laser beam are the two most important parameters. The recovery of nitrogen from kamacite is not high (<30%) as experiments on Uwet have shown (see Section 2.7.2) and this effect certainly needs to be considered for the metal clasts. Such effects may also be significant for the other materials, although the results from the Murchison experiments indicate that recovery from silicate materials are much higher (see Section 2.7.2). The errors on the volume of the pits are probably less than 30% and therefore cannot account for the range in nitrogen concentration.

Target Area	No. of Pulses	$\delta^{15}N$ (‰)	Yield N (ng)	Conc. N (ppm)	$N_{(0‰)}$* (pg pulse^{-1})	$N_{(+1000‰)}$+ (ppm)
Metal Clast						
1	9	+420	0.76	9.1	49	3.8
11	20	+520	0.91	4.9	22	2.6
15	15	+958	0.41	2.9	1	2.8
16	20	+703	0.59	3.3	8	2.3
18	20	+492	1.82	9.9	46	4.9
19	18	+496	2.12	12.8	59	6.4
Silicate Clast						
3	14	+190	0.78	21.8	45	4.3
12	15	+206	1.05	27.3	55	5.8
14	15	+248	0.79	20.2	39	5.1
21	20	+253	0.99	19.1	37	4.7
Metal Vein						
2	8	+650	1.20	19.0	52	12.4
7	6	+632	0.79	16.7	48	10.5
8	9	+711	1.18	16.6	37	11.8
13	15	+732	1.90	19.1	34	13.9
20	12	+641	1.07	11.3	32	7.4
Matrix						
4	12	+680	1.10	17.2	29	7.8
5	10	+750	1.02	19.1	25	9.8
6	12	+655	0.83	12.9	24	5.7
10	12	+734	0.88	13.7	19	6.8
17	8	+758	0.65	15.2	20	7.7
22	18	+930	0.74	7.7	3	4.8

Table 4.9 Summary of results of laser microprobe investigation of Bencubbin. The concentrations are calculated using the estimated volumes of the laser pits. *The amount of contamination is expressed as the mass of nitrogen per pulse as this is related to the area of sample surface affected by the laser beam rather than the mass of sample excavated. + The amount of nitrogen with a $\delta^{15}N$ value of +1000‰ is expressed as ppm as this should be related to the volume of each laser pit.

However, despite these problems the most important feature of these results is that all the areas sampled contained detectable amounts of isotopically heavy nitrogen and generally within a factor of three. This effectively eliminates any one of the main components of the meteorite as the host of the heavy nitrogen carriers as postulated by Prombo and Clayton (1985). Therefore, it is most unlikely that the isotopically heavy nitrogen was added from an external source

during the brecciation event as this would produce very high concentrations in the interclast matrix relative to the clasts.

As the results from the laser extractions indicate a different distribution of nitrogen to that indicated by the stepped heating experiments a more detailed discussion of the results is warranted. A noticeable feature of the different target areas is the nature of the spatter zones around each pit. The nature of this ejected material could effect the escape of nitrogen. For instance, any gas trapped in the thin layer of ejecta from pits in the silicate clasts (Figure 4.22) should escape more easily than from the much thicker layers of ejecta produced from pits in the metal clasts (Figure 4.21). On the other hand, the matrix samples, which produce the thickest ejecta blankets (Figure 4.23), may have relatively high nitrogen yields as the ejecta falls as a mixture of small (≈5μm) metal and silicate blebs which could degas individually. Any gas liberated will then be able to escape along the metal-silicate boundaries. Another possibility is that after the laser pulse free nitrogen may react with the hot metal to form nitrides whereas in the silicates this will not be a problem (the metal is already oxidised). In the case of a metal and silicate mix sampled by the laser pulse the free metal is more likely to react with the oxygen derived from the silicate portions of the matrix.

The range in nitrogen isotopic compositions may also be a function of the size of the spatter zones around the pits. Even on a polished surface heated to 200°C adsorbed atmospheric gases and contaminant organics can still persist. Silicates polish to a much lesser degree than the metal (Figures 4.2 to 4.4) and therefore their total surface area and ability to accommodate contaminants is considerably larger. Optical examination of the ejecta blankets show that they were still molten when they landed on the sample surface, implying a temperature in excess of 1500°C. The effect of this hot material landing on the sample would be to heat up the sample surface, driving off the trapped gases and organic nitrogen. Because the silicate clasts have the largest total surface area also produce the largest ejecta blankets they should have the greatest contribution from this form of

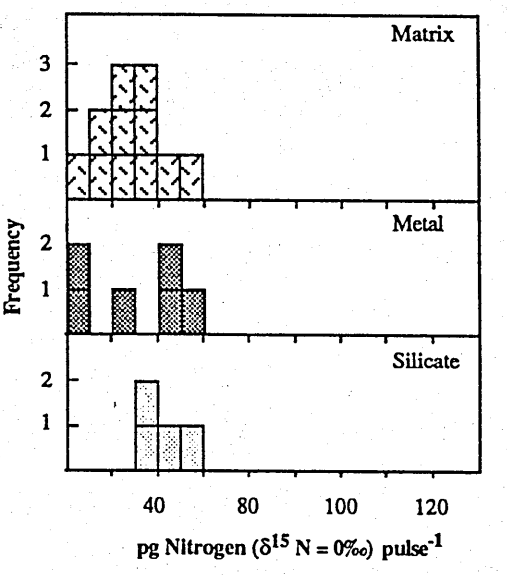

Figure 4.25 Histogram of calculated contamination nitrogen component in laser microprobe extractions. Shows the yield of nitrogen per pulse in each of the three main types of target areas. The yield is expressed as units mass as it is dependent on the area of sample affected by the laser beam rather than mass of material sampled.

contamination. This could account for the relatively high yields and light nitrogen derived from the silicate clasts.

Assuming the contamination to have a $\delta^{15}N$ value of 0‰ and the indigenous nitrogen to be +1000‰ the relative concentration of both components in each analysis can be calculated as was done for the HF/HCl residue (see Section 4.3.4), assuming no other nitrogen components are present. This last assumption may not necessarily be true as there appears to be an acid soluble nitrogen component with a relatively light $\delta^{15}N$ value. The amount of contamination calculated for target area ranged from 1 to 59pg pulse^{-1} (Table 4.9). Although the amount from metal clasts, silicate clasts and matrix all extend up to similar peak values the silicate clasts are strictly confined to the highest portion of the range (Figure 4.25), with a mean value of 44pg pulse^{-1}. The metal clast and the matrix/vein target areas display much wider ranges in contamination contents down to very low values, but give mean values of 31 and 29pg pulse^{-1}

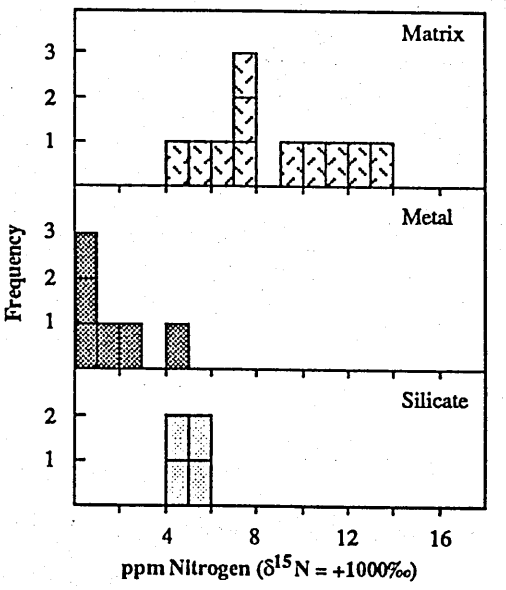

Figure 4.26 Histogram of calculated indigenous nitrogen concentration from laser microprobe extractions. Shows the concentration of nitrogen in each of the three main types of target areas expressed as ppm nitrogen.

respectively. As several days over the space of a week were required to perform the analyses (the laser-port was opened midway through to replace the glass coverslip) the variation in the contamination yields may be due to the degree of degassing of the sample at the time of analysis.

The yield of isotopically heavy nitrogen (Figure 4.26) from the metal and silicate clasts are considerably lower than those obtained using stepped heating, indicating a poor recovery of the nitrogen from these materials. The values for the matrix are higher, close to the yield obtained from matrix#1, although considerably less than that from matrix#2 (see Section 4.2.1). This may reflect either a high nitrogen concentration or a high recovery rate. The matrix target areas also display a wide range of heavy nitrogen concentrations, reflecting the very different nitrogen concentrations obtained by stepped heating of the two matrix samples (Table 4.2).

The last important result from the laser microprobe experiments was for the analysis of two adjacent metal clasts (shown in Figure 4.2). One clast contains numerous troilite inclusions 10 to 100μm across (Target Area 18) whereas the other clast is devoid of such inclusions (Target Area 19). However, the concentration and $\delta^{15}N$ value of the nitrogen in these two clasts is very similar, 9.9ppm and +492‰ from the the troilite-rich clast and 12.8ppm and +496‰ from the FeS-poor clast (Table 4.9). Therefore, the carrier phase of N_α, identified as a chromium-rich sulphide, is not uniquely associated with the main troilite phases in the meteorite but is more evenly distributed implying two distinct populations of sulphides in Bencubbin - one being the large sulphide grains readily identified in polished sections, the other the much smaller sulphides with very high Cr contents identified with the ATEM in the acid residues. Unfortunately, the polished surface was not of high enough quality to allow detection of the sub-micron sized sulphide grains observed in the acid residues (see Section 4.3.6). Detection, and identification, of the N_β component using the laser microprobewas not possible due to its low abundance and identical isotopic composition to N_α.

4.4.3 Comparison with Other Meteorites

Weatherford

The unusual structure, mineralogy and composition of Bencubbin is very similar to another meteorite - Weatherford (Mason and Nelen, 1968; McCall, 1968). More importantly, the achondritic silicate clasts from the two meteorites also have very similar oxygen isotopic compositions which are distinct from other meteorites (Clayton *et al.*, 1978b). Weatherford should therefore be expected to also contain isotopically heavy nitrogen. A sample of a metal clast from Weatherford was analysed by stepped heating (Figure 4.27a) but although isotopically heavy nitrogen was liberated above 800°C the maximum $\delta^{15}N$ value was only +257‰. It is possible that this only represents a minimum due to

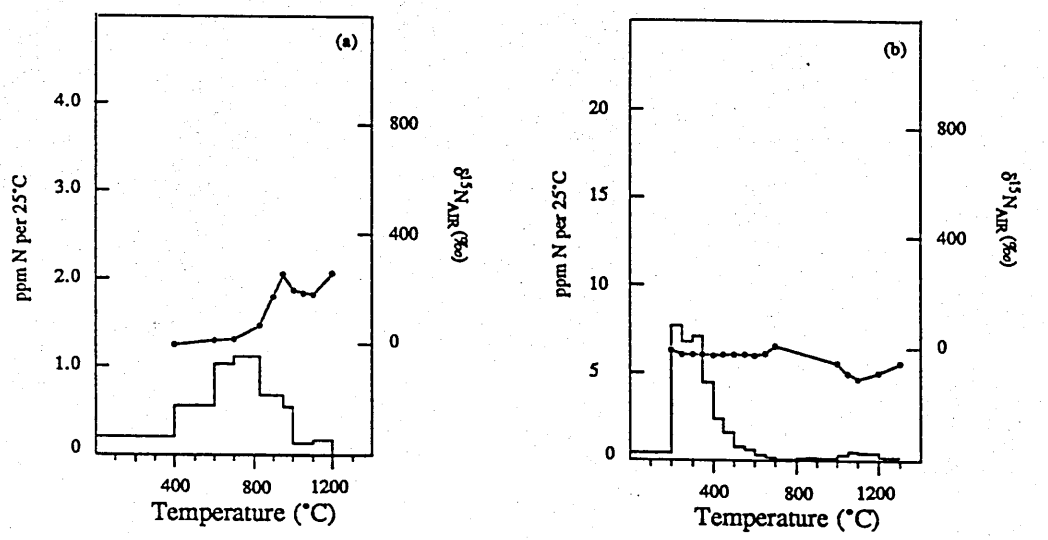

Figure 4.27 Stepped combustion profiles for nitrogen of Weatherford and Kakangari. (a) metal clast in Weatherford; (b) whole-rock sample of Kakangari.

masking by the relatively larger release (16ppm) of isotopically light nitrogen between 400 and 800°C tailing up to higher temperatures. Above 900°C only 5.5ppm nitrogen was liberated with a $\delta^{15}N$ value of +209‰ (compared to Bencubbin which liberated 73.7ppm nitrogen above 700°C with a $\delta^{15}N$ value of +879‰).

The low concentration and $\delta^{15}N$ values may be due to terrestrial weathering, as the sample used was considerably more weathered than any of the Bencubbin samples - a reflection of the condition of the meteorite in general. The uncharacteristically low release temperature of nitrogen from the metal clast in Bencubbin indicates that the carrier of N_α is not fully shielded by the kamacite; this should imply that the carrier is also similarly exposed to terrestrial weathering agents. Oxidation of the carrier phases may cause loss of indigenous nitrogen and any residual nitrogen may equilibrate with terrestrial nitrogen ($\delta^{15}N \approx 0$‰). The large release of isotopically light nitrogen between 400 and 800°C is considered to be a terrestrial component associated with the weathering products. Assuming two components are present in this sample, a terrestrial component

with a $\delta^{15}N$ value of 0‰ and an indigenous component at +1000‰ then above 600°C the metal clast sample of Weatherford liberates only 1.6ppm nitrogen with $\delta^{15}N$ value of +1000‰.

Keeling *et al.* (1987) reported low concentrations of nitrogen (5-10ppm) in metal clasts from Weatherford and, compared to Bencubbin, relatively low $\delta^{15}N$ values ranging from +250 to +440‰, comparable with the results above. Their analysis of the matrix of Wetherford however revealed nitrogen concentrations and $\delta^{15}N$ values much closer to those in Bencubbin. The highest values they reported for the matrix were 108ppm and +654‰. The nitrogen concentration (34.7ppm) and $\delta^{15}N$ value (+462‰) reported by Prombo and Clayton (1985) in a silicate clast from Weatherford are very similar to the values they obtained for Bencubbin silicate clasts, *i.e.* 5.7 and 44.0ppm and +414 to +489‰. Although this is much lighter than the value obtained by stepped heating this may be due to incomplete resolution of the contamination from indigenous nitrogen (see Section 4.2.1). It appears that in Weatherford the silicate clast and matrix contain nitrogen of similar concentration and isotopic composition to that in the same materials from Bencubbin while the metal clasts contain less nitrogen with a much lower $\delta^{15}N$ value. As there is evidence of considerable weathering of the metal clasts in Weatherford (Mason and Nelen, 1968) it is probable that such a process is responsible for the observed nitrogen contents and isotopic composition.

Assuming that the Bencubbin and Weatherford meteorites were originally similar in terms of their nitrogen inventory, a loss of nitrogen from the metal clasts in Weatherford due to weathering gives an indication of the exact location of the N_α carrier phase. The lowering of the release temperature of N_α once the metal had been dissolved by 6M HCl shows that the oxidation of the carrier phase was inhibited by the Fe-Ni metal, although the low release temperature from the metal clast relative to other Fe-Ni metal samples (*e.g.* iron meteorites) indicates that the main nitrogen carriers are not enclosed by the metal in the same way that nitrogen dissolved in the metal phase of iron meteorites is. Newsom and Drake

(1979) noted a number of phases along the grain boundaries in the metal clasts, including silicates, phosphates and vanadium-rich chromites. The release characteristics of N_α and its resistance to weathering reagents on Earth indicate that the Cr/Fe sulphide may also be concentrated along these grain boundaries. Such a distribution has already been noted for the more common Cr bearing troilite (containing little or no nitrogen) in this meteorite (Figure 4.1). During a prolonged period on the surface of the Earth weathering agents such as oxygen and water could also exploit these zones of weakness. Oxidation of the surrounding metal and the sulphides would allow the nitrogen to escape or be leached out of the structure of the sulphides.

Silicates are generally less reactive than highly reduced Fe-Ni metal to the oxidising weathering reagents normally active on the surface of the Earth. Therefore, the silicate clasts have been able to preserve their compliment of isotopically heavy nitrogen, consistent with the weathering in the Weatherford meteorite being largely confined to the metal clasts (Mason and Nelen, 1968). Even the metal within the matrix remains fresh as it is usually swathed in silicate glass, similar to that in Bencubbin (Figure 4.2).

Other meteorites

Three meteorites, Renazzo, Kakangari and Tucson have oxygen isotopic compositions and mineralogies which suggest affinities to Bencubbin (Prinz *et al.*, 1987). A high resolution stepped combustion of Kakangari (Figure 4.27b) revealed no isotopically heavy nitrogen, indeed, a small release of nitrogen (5.4ppm) between 1100 and 1300°C had a minimum $\delta^{15}N$ value of -106‰. Renazzo on the other hand does contain isotopically heavy nitrogen with a $\delta^{15}N$ value of around +175‰ (*e.g.* Grady *et al.*, 1983). However, high resolution stepped combustions of a magnetic and non-magnetic fraction of this meteorites failed to resolve any nitrogen components with a $\delta^{15}N$ value more than 20‰ away from the bulk value (Figure 4.28). However, it is noteworthy that the

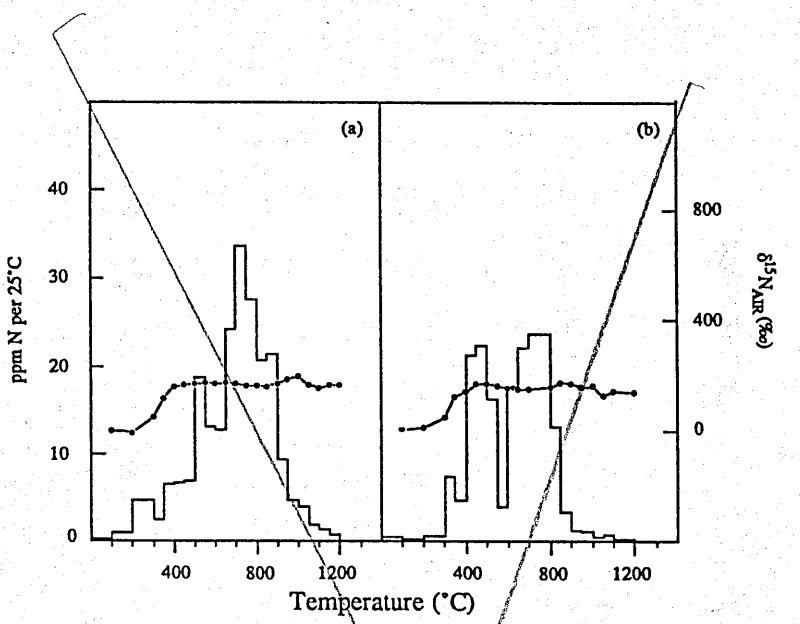

Figure 4.28 Stepped combustion profiles for nitrogen of Renazzo. (a) magnetic fraction of whole-rock sample; (b) non-magnetic fraction of whole-rock sample.

heaviest nitrogen released from Renazzo was in the 1000°C step of the magnetic fraction - almost identical to the peak release temperature of N_α in the whole rock samples of Bencubbin. The shape of the nitrogen release profile is also very unusual for a type 2 carbonaceous chondrite, in which most of the nitrogen is contained in organic molecules and so is liberated below 500°C during stepped combustion. In both Renazzo samples two distinct releases are visible, the low temperature one (400-55°C) undoubtedly being from organic molecules. However, the nature of the carrier which liberates nitrogen between 600 and 900°C and is concentrated in the magentic fraction is unknown.

The Tucson iron meteorite was not analysed as part of this study but contains only 0.3ppm nitrogen with a $\delta^{15}N$ value of +8.2‰ (Prombo, 1985). These nitrogen results indicate that the speculative relationship of Bencubbin, Kakangari, Renazzo and Tucson postulated by Prinz *et al.* (1987) is less than straightforward. Although some of the nitrogen in Renazzo may be from the same reservoir as the nitrogen in Bencubbin the uniformity of the isotopic

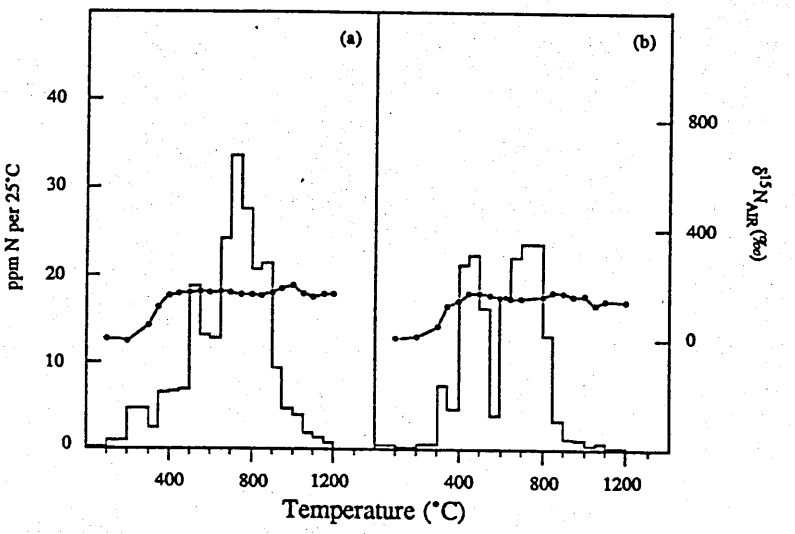

Figure 4.28 Stepped combustion profiles for nitrogen of Renazzo. (a) magnetic fraction of whole-rock sample; (b) non-magnetic fraction of whole-rock sample.

heaviest nitrogen released from Renazzo was in the 1000°C step of the magnetic fraction - almost identical to the peak release temperature of N_α in the whole rock samples of Bencubbin. The shape of the nitrogen release profile is also very unusual for a type 2 carbonaceous chondrite, in which most of the nitrogen is contained in organic molecules and so is liberated below 500°C during stepped combustion. In both Renazzo samples two distinct releases are visible, the low temperature one (400-55°C) undoubtedly being from organic molecules. However, the nature of the carrier which liberates nitrogen between 600 and 900°C and is concentrated in the magentic fraction is unknown.

The Tuscon iron meteorite was not analysed as part of this study but contains only 0.3ppm nitrogen with a $\delta^{15}N$ value of +8.2‰ (Prombo, 1985). These nitrogen results indicate that the speculative relationship of Bencubbin, Kakangari, Renazzo and Tuscon postulated by Prinz *et al.* (1987) is less than straightforward. Although some of the nitrogen in Renazzo may be from the same reservoir as the nitrogen in Bencubbin the uniformity of the isotopic

composition around +175‰ suggests that the nitrogen has been completely homogenised, either within the meteorite, or more probably in the solar nebula.

Kallemeyn *et al.* (1978) suggested that the metal clasts in Bencubbin may be related to the IIIF iron meteorite group on the basis of their siderophile-trace-element/nickel ratios. Clark County, a IIIF iron containing 1565ppm Cr liberated 5.1ppm nitrogen with a $\delta^{15}N$ value of -16.3‰ (see Table 3.7). A second IIIF iron meteorite, Nelson County, with extensive shock deformation contains 1.4ppm nitrogen with a $\delta^{15}N$ value of +8.6‰ (Prombo and Clayton, 1983). Thus, there is nothing in the $\delta^{15}N$ values to link the metal phases of Bencubbin with iron meteorites which other lines of evidence suggest may be related.

4.5 THE ORIGIN OF THE ^{15}N ENRICHMENT

4.5.1 The Origin of the ^{15}N-enrichment in a Regolith Environment

There are a large number of meteorites which have a brecciated or veined texture, although Bencubbin and Weatherford are unique with their unusual mineralogy of metal and silicate clasts. It is noteworthy that a number of brecciated meteorites contain nitrogen components enriched in ^{15}N. Abee, a polymict enstatite achondrite liberates up to 29ppm nitrogen with a maximum measured $\delta^{15}N$ value of +350‰ between 500 and 600°C during stepped pyrolysis, or 400 to 500°C during combustion (Grady *et al.*, 1986). Three polymict ureilites, EET83309, Nilpena and North Haig also release a component of isotopically heavy nitrogen at low temperatures (Grady and Pillinger, 1988). EET83309 liberates 11ppm nitrogen with a peak $\delta^{15}N$ value of +527‰ between 300 and 400°C during stepped combustion. Employing small temperature increments during a stepped pyrolysis revealed a bimodal release of nitrogen, the second, smaller release at slightly higher temperatures. Treatment with HF/HCl removes most of the major component released at the lower temperature. The physical characteristics of these two components are very similar to those of N_α

and N_β in the acid residues of Bencubbin. If all these heavy nitrogen components are related then the only difference between them is that in Bencubbin the components have somehow managed to find their way into protected sites within the meteorite.

As Grady *et al.* (1985) detected no heavy nitrogen in main group ureilites Grady and Pillinger (1988) favour a model in which the heavy nitrogen is introduced into the polymict ureilites during the brecciation event. This type of model does not extrapolate well to Bencubbin. Although the heavy nitrogen in Bencubbin is released at a higher temperature than from the polymict ureilites this could be explained by trapping of the nitrogen carriers within the glassy matrix. However, such a model would predict a much higher concentration of nitrogen in the matrix relative to the clasts. The observed concentration of nitrogen in the Bencubbin matrix is comparable with that in the clasts, and therefore inconsistent with a model similar to that proposed by Grady and Pillinger (1988) for the ureilites.

The clasts of brecciated meteorites are believed to have existed in a regolith type environment on a parent body surface, accounting for the high concentrations of solar wind implanted noble gases found in these meteorites (Wasson, 1974). The energy of solar wind particles is such that they penetrate the host material, although generally only to a depth of a few to a few hundred angstroms. They are therefore concentrated on the surface of grains (Wasson, 1985). The possibility that the heavy nitrogen is derived from solar wind implantation of nitrogen has to be considered. The concentration of solar wind ^{36}Ar in the matrix reaches peak values of 10^{-4}cc (STP)g^{-1} (S. Kelley, 1987, pers. comm.). Assuming that the efficiency of nitrogen retention is comparable with that of argon and using a solar $^{14}N/^{36}Ar$ abundance ratio of 28.2 (Anders and Ebihara, 1982) a maximum value of 45ppm solar wind implanted nitrogen could exist in the matrix. However, a number of factors argue against solar wind implantation being the origin of the ^{15}N enrichment;

(1) the laser microprobe experiments, similar to those of Kelley and Turner (1987), showed heavy nitrogen in the centre of the large clasts, not simply confined to the rims - which is where the solar wind argon is found,

(2) the $\delta^{15}N$ value of ancient solar wind nitrogen ranges down to -276‰ (Carr *et al.*, 1985) and up to +120‰ for recent solar wind nitrogen (Becker and Clayton, 1976). There is no evidence to suggest that at the time of formation of the Bencubbin regolith between 4.5 and 3.7Ga (Kelly and Turner, 1987) the solar wind had a $\delta^{15}N$ value of +1000‰.

(3) the solar wind argon is not liberated at the same temperature as the heavy nitrogen during stepped heating, and therefore cannot be present in the same location within the meteorite. This is consistent with the findings of Lewis (1985) who reported that there appeared to be no noble gas carriers in acid residues of the meteorite.

(4) as solar wind implanted nitrogen should be concentrated in the rims of the clasts, which preferentially melted during the shock event to produce the matrix, the matrix should contain the highest concentrations of nitrogen. However, once again, as the concentration of nitrogen in the matrix is comparable with those of the clasts this is inconsistent with a solar wind origin of the ^{15}N enrichment.

(5) concentration of the heavy nitrogen in a minor sulphide phase is certainly inconsistent with a solar wind origin, which should be present in more or less equal abundance of all exposed materials.

Because the concentration and isotopic composition of the nitrogen within the matrix is roughly comparable with that in the clasts all models involving late stage infall of nitrogen bearing phases (possibly from cometary material or grains from a dust cloud, *etc.*) into a pre-existing regolith seem to be excluded.

However, the fact that large amounts of solar wind implanted argon are present in the matrix is important, as assuming any reasonable Ar/N ratio in the

sun, large amounts of solar wind implanted nitrogen should be present in the matrix. But even in the relatively unmelted matrix#2 sample no nitrogen component other than the isotopically heavy nitrogen was evident. One possibility is that the light nitrogen lost upon acid treatment, accounting for the heavier $\delta^{15}N$ values in the acid residues compared to the whole-rock samples, may have a solar wind origin. However, the distribution of this component is not consistent with such an origin. There is no evidence for mechanisms which could dramatically alter the solar Ar/N ratio or cause selective loss of nitrogen relative to argon. The presence, or lack of presence, of solar wind implanted nitrogen in the Bencubbin meteorite remains an enigmatic problem.

4.5.2 The Origin of the ^{15}N-enrichment by Spallogenic Reactions

One process which could produce isotopically heavy nitrogen within the clasts and matrix in a regolith environment is that resulting from the interaction of high energy cosmic rays with appropriate target nuclei. Such a spallogenic origin results in production of roughly equal amounts of ^{15}N and ^{14}N, mainly through the loss of a proton or a proton and a neutron from ^{16}O (Kung and Clayton, 1978). Becker and Clayton (1976) determined the spallogenic production rate of ^{15}N in lunar soils to be 3.6pg of $^{15}Ng^{-1}$ m.y.$^{-1}$ which would be comparable with the production rate on the Bencubbin parent body assuming a similar cosmic ray flux at 4.5Ga. As the production rate for ^{14}N is similar (Armstrong and Alsmiller, 1971) then such a low rate would not have any measureable impact on the nitrogen abundance, even over the age of the solar system. However, as spallogenic nitrogen has a $^{14}N/^{15}N$ ratio of approximately 1 the isotopic composition of any indigenous nitrogen can be made significantly heavier.

Assuming an initial concentration of 50ppm nitrogen and $\delta^{15}N$ value of approximately 0‰, a present day cosmic ray flux would require at least 50×10^9 years (3-4 times the age of the universe) to produce a $\delta^{15}N$ value of +1000‰ in Bencubbin. However, on the basis of ^{36}Cl-^{36}Ar production rates Begemann *et*

al. (1976) determined a cosmic ray exposure age for Bencubbin of only 36.5 x 10^6 years. The production rates in the metal clasts would be considerably lower than those in the silicate clasts as the target nuclei are less suitable for nitrogen production, yet the concentration of nitrogen in the metal is higher than that in the silicates. Similarly, spallation reactions do not account for the concentration of nitrogen in a minor sulphide carrier when the troilite present in Bencubbin contains much lower concentrations of nitrogen. Production of spallogenic nitrogen in small precursor grains during an intense radiation flux in the early history of the solar system (such as a T-tauri phase (Lee, 1978)) is also unlikely as such an event should also be recorded by the noble gases - which show no such signature. Therefore, it is impossible to account for the ^{15}N enrichment in Bencubbin from additions to an originally isotopically normal nitrogen by spallogenic reactions during cosmic ray exposure.

4.5.3 The Origin of the ^{15}N-enrichment in the Solar Nebula

As processes which could operate during or after brecciation in a regolith have been ruled out as possible sources of the ^{15}N enrichment then events occurring during or before the formation of the clasts must be considered. Firstly, isotopic effects occurring within the solar nebula will be considered, namely kinetic and equilibrium fractionation during processes such diffusion, evaporation, condensation and chemical reaction as well as non-mass-dependent (NoMaD) effects.

Evaporation and diffusion

The simplest isotopic fractionation effect is one of kinetic fractionation during evaporation or diffusion processes. This is a temperature independent effect and is a function of molecules containing the different isotopes passing through phases or across phase boundaries at different rates due to the translational velocities of the two isotopes (O'Neil, 1986). Mechanism which could produce

such an effect include volatile loss from either dust grains, planetesimals, the meteorite parent body or the meteorite itself and would result in the remaining nitrogen becoming enriched in ^{15}N. However, assuming the volatile lost was molecular nitrogen with an initially normal solar system isotopic composition (around 0‰), an initial mass of $>10^{25}$g nitrogen would be required to produce 50ppm nitrogen with a $\delta^{15}N$ value of +1000‰ in the 118kg of Bencubbin so far recovered. Therefore, it is very unlikely that a single stage volatile loss mechanism could account for the isotopic composition of nitrogen in the Bencubbin meteorite. Larger isotopic effects are possible if the process is repeated many times, one possible sequence which could occur in the solar nebula is repeated diffusion and evaporation on growing condensates (Arrhenius and Alfven, 1971). However, it is unlikely that such processes could significantly increase the enrichment to a level approaching those observed in Bencubbin without each cycle proceeding to near completion, therefore still requiring a large mass of gas.

Chemical fractionation

There is usually an isotopic fractionation between different phases in equilibrium with each other (Richet *et al.*, 1977), but the effects for nitrogen are generally very small (Geiss and Bochsler, 1982). The main nitrogen bearing phase in the solar nebula over most temperatures and pressures is N_2 (Norris, 1980) and it is not until the lowest temperatures and highest pressures that small amounts of the condensible species NH_3, NO, HCN, *etc.* form (Geiss and Bochsler, 1982). Exchange between these species is temperature dependant, the largest isotopic effects occurring as the temperature approaches absolute zero (Hoefs, 1987). Isotopic exchange between any of the condensible species and molecular nitrogen produces an enrichment of ^{14}N in the condensible species, and therefore an enrichment of ^{15}N in the molecular nitrogen (Richet *et al.*, 1977). As the enrichment of ^{14}N in the condensible phases is only of the order

of a few tens of permil at 200K (Geiss and Bochsler, 1982) the enrichment of ^{15}N in the much more abundant N_2 will be proportionally less due to dilution in the much larger reservoir of molecular nitrogen. Geiss and Bochsler (1982) suggested that non-equilibrium fractionation could produce larger isotopic effects but that once again the main enrichments would be of ^{14}N in the minor, condensible species with the ^{15}N enrichment still diluted in the much larger reservoir of molecular nitrogen. Therefore, it is very unlikely that chemical fractionation under equilibrium or non-equilibrium conditions could produce the observed $\delta^{15}N$ values in Bencubbin from an initially homogeneous nitrogen reservoir in the solar nebula.

Non-Mass-Dependant Effects

(1) Dissociative recombination reactions

Fractionation of nitrogen isotopes in gas phase reactions involving interactions of energetic neutral and ionic species can produce considerable enrichments of ^{15}N. Electron impact dissociation of N_2

$$e^- + N_2 \rightarrow e^- + N + N$$

and dissociative recombination of N_2^+

$$N_2^+ + e^- \rightarrow N + N$$

in the exosphere of Mars can produce fast atoms capable of planetary escape; these are believed to be responsible for the pronounced enrichment of ^{15}N in the Martian atmosphere (McElroy *et al.*, 1976). The $\delta^{15}N$ value recorded by the Viking landers was about +770‰ (Nier *et al.*, 1976), comparable with that observed in Bencubbin. However, it is unlikely that such a process could have occurred in the early solar system on meteorite parent body sized planetesimals (<500km diameter). A large escape velocity is required to allow selective escape of ^{14}N, as the speed of atoms produced in the above reactions is around 5km sec^{-1} even at relatively low temperatures of 400K (McElroy *et al.*, 1976). However, due to the small size of the meteorite parent bodies the maximum

escape velocities would be around 0.3km sec^{-1}. The nitrogen loss process from the Martian atmosphere has been proceeding since the planet formed but as the clasts in Bencubbin closed to K/Ar system around 4.5Ga (Kelly and Turner, 1987) the time scale for such a process producing the ^{15}N enrichment in Bencubbin would be at least two orders of magnitude less, making such an origin very improbable.

(2) Extreme non-equilibrium reactions

Arrhenius *et al.* (1978) reported a ^{15}N enrichment of 420‰ in nitrogen oxide produced by a fractional dissociative recombination reaction between nitrogen and oxygen gas in a low temperature plasma. The powerful R.F. plasma raised the vibrational temperature of the reactants well above their kinetic temperature, greatly facilitating the reaction, and the nitrogen oxide produced was rapidly condensed at 77K. Similar enrichments, up to 210‰ were obtained by Manuccia and Clark (1976) in low temperature glow discharge reactions between N_2 and O_2 and similar experiments by Basov *et al.* (1977) obtained enrichments of 2000‰. However, Geiss and Bochsler (1982) argue that there is no evidence of a period in the early solar system which would be comparable with the severe conditions employed in these experiments. Therefore, although it is possible to produce large enrichments of ^{15}N such an environment is unlikely to have existed in the early solar system or solar nebula which could produce enrichments comparable with those in Bencubbin.

(3) Other NoMaD effects

Theimens and Heidenreich (1983) and Heidenreich and Theimens (1985) produced isotopic fractionations in oxygen which were inexplicable in terms of any mass dependant effect. The non-mass-dependant, or NoMaD effects, produced in the electrodissociation of O_2 to form O_3, and CO_2 to form O_2, appear to be specifically associated with the formation or relaxation of ozone in an

excited electronic state (Heidenreich and Theimens, 1985). However, whether similar effects could produce the ^{15}N enrichment observed in Bencubbin from a similar reaction sequence involving an excited intermediate species is not clear. The maximum enrichment of ^{18}O reported by Theimens and Heidenreich (1983) was only +40‰, a very minor effect compared to the ^{15}N enrichment observed in Bencubbin. As there is still considerable debate as to the significance of NoMaD effects in accounting for the small variations in oxygen isotopic composition of meteorites, it is unlikely that the large enrichments of ^{15}N could be produced in much less reactive molecular nitrogen.

4.5.4 The Origin of the ^{15}N-enrichment in a Pre-solar Environment

There are two broad categories of extra-solar locations where it is possible to produce large variations in the isotopic composition of the light elements;

(1) within stars during the synthesis of the elements

(2) in the interstellar medium (ISM), particularly in the dense molecular clouds.

Although early models of solar system formation assumed a homogeneous solar nebula there is now a wide body of evidence which necessitates that this was never achieved. The major and trace element geochemistry of the chondritic meteorites, generally believed to be the most primitive materials currently available, cannot be explained in terms of fractionation processes from a homogeneous reservoir (*e.g.* McSween, 1987). Similarly, the departures from a single fractionation line on a three isotope plot of the oxygen isotopic composition of meteorites (Figure 4.5) can only be satisfactorily explained by mixing of different reservoirs (Clayton *et al.*, 1976). Finally, inclusions and acid residues from chondritic meteorites, particularly groups C1 to C3 contain elements with large isotopic variations which cannot be explained in terms of fractionation from a single reservoir e.g. H, C, N, O, Ne, Mg, Ar, Ca, Ti, Cr, *etc.* (Clayton *et al.*, 1973; Eberhart *et al.*, 1981; Wasserburg and Papanastassiou, 1982; Swart *et al.*,

1983b; Wasson, 1985; Shima, 1986; Lewis *et al.*, 1987; Epstein *et al.*, 1987). Most workers interpret these isotopic anomalies as originating from a nucleosynthetic event.

However, some of the isotopic anomalies in specific phases are thought to have been produced in the ISM, where ion-molecule reactions are believed to dominate the local chemistry of the light elements (Herbst, 1985). Laboratory experiments have shown that these ion-molecule reactions could build up large organic molecules with considerable isotopic fractionation of the constituent elements (Smith and Adams, 1984) and they have been invoked to explain enrichments in D and ^{15}N in meteoritic organic material (McNaughton *et al.*, 1982; Epstein *et al.*, 1987). The presence of ^{15}N enriched nitrogen in a sulphide phase within an Fe-Ni metal clast which may contain nitrogen with a typical solar system isotopic composition dissolved in the metal strongly suggests that the sulphide grains predate the metal clasts. Models of equilibrium condensation predict that sulphides should condense from the nebula at least 600K below the condensation temperature of Fe-Ni metal (e.g. Grossman and Larimer, 1974) and therefore, either;

(1) the nebula was cool and the sulphide grains were early condensates or

(2) the sulphide grains have a presolar origin but the solar nebula was never hot enough to vaporise the grains or

(3) the solar nebula was in part hot but the sulphide grains resided in a cool part of the nebula and were not introduced to the metal which formed the Bencubbin metal clasts until that part of the nebula had cooled significantly.

The third possibility allows for the sulphide grains to be either presolar or early condensates. As there is a low probability of a strong presolar isotopic signature surviving in the solar nebula in the gaseous phase (Wasserburg and Papanastassiou, 1982) it is unlikely that the schemes involving the sulphides condensing from the solar nebula are correct. Therefore, the isotopic

composition of elements present in the chromium sulphide grains other than nitrogen could be of considerable assistance in determining the origin of the ^{15}N enrichment.

If the sulphide grains formed in the solar nebula, then a number of other possible scenarios exist in which the nitrogen is introduced to the solar nebula in a solid. It may be that N_β, with its relatively high thermal and chemical stability, is a presolar component and that the sulphide grains grew around that, as yet unidentified, carrier phase. Possibly the growth process or some subsequent event caused the decomposition of some N_β resulting in redistribution of the nitrogen throughout the sulphide (N_α). The worst possible scenario of this type, in terms of identifying the origin of the ^{15}N enrichment, would be that the heavy nitrogen was introduced to the solar nebula in a third, unidentified carrier (N_χ) which decomposed during or after the formation of the sulphide grains so that the nitrogen liberated from N_χ combined with normal solar system material to form N_α and N_β. In the latter of these two scenarios the isotopic composition of the sulphur and any other elements present would be independent of the origin of the ^{15}N enrichment. In the former scenario elements associated with N_β could still contain anomalous isotopic signatures. However, without a better understanding of the origin of N_β all that can be assumed is that both components are presolar. The unusual nature of the sulphides indicates that they may indeed have an exotic origin.

A nucleosynthetic origin for N_α and N_β

The two isotopes of nitrogen are primarily produced by the same sequence of nuclear reactions, commonly known as the CNO cycle (Figure 4.29). This cycle is basically a form of hydrogen burning, whereby four protons are merged to form a helium nucleus. The carbon, nitrogen and oxygen nuclei (products from an earlier He burning event) essentially perform a catalytic role in these reactions (Trimble, 1975). However, not every cycle is completed, resulting in production

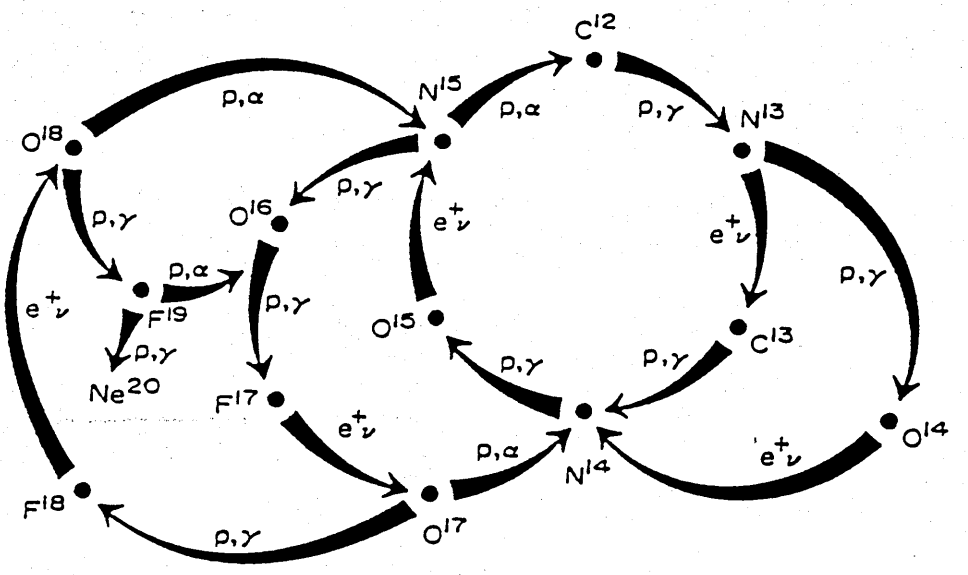

Figure 4.29 Schematic diagram of the CNO cycles. Shows the main reactions and decays in the hydrogen burning sequence involving CNO isotopes. From Caughlan (1977).

of new isotopes of carbon, nitrogen and oxygen. Different reaction cross sections and decay rates occurring at different temperatures will produce different proportions of products (Audouze and Vauclair, 1980) thereby producing different $^{14}N/^{15}N$ ratios.

^{14}N is believed to be produced by the "cold" CNO cycle operating at temperatures around 10^6K in hydrostatic equilibrium conditions within massive stars. In such an environment destruction of ^{14}N is the slowest reaction in the cycle ($^{14}N(p,\gamma)^{15}O$) due to the relatively small proton capture cross section of this nuclei (Trimble, 1975). $^{14}N/^{15}N$ ratios about 100 times larger than the solar system value of 272 have been calculated for such environments (Audouze and Vauclair, 1980). This nitrogen is returned to the ISM during the red giant phase of massive stars or the final stage of the red giant branch, when a planetary nebula is formed (Wannier and Werner, 1985).

Nucleosynthesis of ^{15}N will not reach appreciable levels until the temperature is in excess of 2×10^8K. At such temperatures the "hot" CNO cycle is operative,

where the reaction rates are so fast that the conditions are basically explosive. These conditions are normally only generated during nova or supernova events (Burbidge *et al.*, 1957). Under such conditions the nuclear fusion reactions (proton or positron capture) are very fast, leaving the temperature independent β^+ decays as the slowest reactions, the slowest decay being $^{15}O(\beta^+)^{15}N$ (Trimble 1975). During a stellar explosion the unstable nuclei are removed from the nucleosynthetic environment during a nova or supernova on a time scale comparable to the half life of ^{15}O decay ($t_{1/2}$ = 176sec for $^{15}O(\beta^+)^{15}N$) (Truran, 1982). Production of nitrogen with a $^{14}N/^{15}N$ ratio of up to 1.3 has been calculated for such events (Audouze and Vauclair, 1980).

Consideration of the isotopic composition of elements associated with the heavy nitrogen in Bencubbin is required to establish whether the ^{15}N enrichment is a signature of a nova or supernova event. The small amounts of carbon associated with the the N_β component has a $\delta^{13}C$ value of +24‰, which is heavier than the range of $\delta^{13}C$ values seen in whole rock samples of meteorites, -33 to 0‰ (Carr, 1985), although in acid residues $\delta^{13}C$ values extend from -50‰ (R.D. Ash, unpubl. data) to +7000‰ (Zinner *et al.*, 1987a). Some of the carbon in acid residues of meteorites, particularly carbonaceous chondrites, is associated with noble gas components displaying nucleosynthetic signatures (*e.g.* Pillinger, 1984). Carbon produced in nova or supernova from explosive hydrogen burning (the hot CNO cycle) is generally extremely enriched in ^{13}C relative to typical solar system carbon ($^{12}C/^{13}C$ = 90). However, the carbon liberated over the temperature range of N_β from the Bencubbin meteorite has a $^{12}C/^{13}C$ ratio of 88 - very close to typical solar system carbon. Although the maximum $\delta^{13}C$ value associated with the heavy nitrogen may be a minimum it is very unlikely that the ^{13}C enrichment is much greater than 100‰ making nucleosynthesis during explosive hydrogen burning appear an unrealistic possibility.

The isotopic composition of some of the sulphur associated with the N_α component may be slightly depleted in ^{34}S relative to normal solar system material, with a minimum $\delta^{34}S$ value of -6.3‰ recorded from a whole rock sample of the metal clast. If sulphur has been produced by the same nucleosynthetic event which produced the heavy nitrogen in Bencubbin then a nova outburst can be ruled out as a possibility. The heaviest nuclei which can be produced by explosive hydrogen burning during the CNO cycle is ^{20}Ne (Caughlan, 1977), whereas production of the isotopes of sulphur proceeds by explosive carbon, and more especially oxygen burning (Wannier, 1980; Audouze and Vauclair, 1980). In a star with an outer hydrogen burning zone it is possible that hydrostatic carbon and oxygen burning could be occurring in a zone in the interior of the star (Trimble, 1975). But as a nova outburst usually ejects only 10^{-3} to 10^{-4} solar masses from the surface of the star it will not disrupt the deeper carbon and oxygen burning zones. However, a supernova event will destroy most of the original star in a single event, leaving only a small percentage of the mass of the progenitor as a neutron star (Trimble, 1975), thereby ejecting high and low atomic mass elements in the same mass loss event.

In the zone of a massive star which has converted most of its hydrogen to helium nuclei the dominant reaction cycle will be one of helium burning, where helium nuclei are merged to produce ^{12}C (Burbidge *et al.*, 1957). During a supernova, explosive, or non-equilibrium helium burning is very similar to the processes of the hot CNO cycle, the CNO nuclei acting in a catalytic manner and the β^+ decays once again the slowest reactions and therefore such a process will produce nitrogen enriched in ^{15}N (Howard *et al.*, 1971; Arnould and Beelen, 1974). However, in contrast to explosive hydrogen burning relatively small amounts of ^{13}C are produced by this process (Audouze and Vauclair, 1980). The $^{32}S/^{34}S$ ratio of sulphur produced from the oxygen burning zone of a massive star during a supernova is very close to the solar ratio (Trimble, 1975), although

Clayton and Ramadurai (1977) predict that there may be a slight under abundance of the heavier isotopes.

It is clear that approximations to the isotopic composition of the nitrogen, carbon and sulphur present in the N_α and N_β components present in Bencubbin can be synthesised from a single supernova event with a massive progenitor star. This conveniently coincides with the prediction of Clayton and Ramadurai (1977) that Cr, Fe and Ti sulphides may condense from the oxygen burning zone of an expanding supernova shell. However, there is the problem of introducing the carbon and nitrogen produced in the helium burning zone with the products of the oxygen burning zone, without oxidising all the elemental sulphur. As yet no models have been reported which can achieve this, but possibly a major weakness in the models so far calculated for the condensation of grains from supernova shells is that they assume equilibrium condensation (*e.g.* Lattimer and Grossman, 1978). As the cooling time of supernova ejecta shells is very short (10^2 - 10^4 years) it is considered unlikely that equilibrium conditions were maintained. Therefore, mixing of different shells of a supernova prior to, or during condensation may not be an insurmountable problem.

Analysis of noble gases in HF/HCl residues of Bencubbin have shown a solar isotopic signature, with perhaps a small sub-solar component similar to that seen in the enstatite chondrites (Lewis, 1985). However, from this study it is known that the majority of the heavy nitrogen (N_α) would not be in the residue analysed as it is removed by concentrated HF and HCl acids (N_β should still be present). The results of Lewis (1985) were simply presented as bulk contents and isotopic compositions and therefore the only conclusions which can be drawn are that either;

(1) the noble gases associated with N_β have isotopic compositions similar to solar values, or

(2) no noble gases are associated with N_β .

The latter conclusion is probably correct as the low abundance of Xe in the residue (<3% of the original Xe) and the low Kr/Xe ratio suggest that the Xe in the HF/HCl residue is largely gas readsorbed during the acid dissolution (Lewis, 1985).

A cosmochemical origin for N_α and N_β

The dense molecular clouds of the ISM, one of which collapsed to form the solar nebula, contain a rich suite of complex organic molecules which are formed by ion-molecule reactions in the gas phase within the clouds (Winnewisser *et al.*, 1979). At the temperatures of the dense clouds (5 - 10K) isotopic exchange reactions can be significantly exothermic, producing large isotopic enrichments (Smith and Adams, 1984). Observation of the $^{14}N/^{15}N$ ratios in some molecules throughout the Milky Way shows that the ratio increases by a factor of two towards the galactic centre, although this is believed to be due to nuclear processing rather than chemical fractionation (Penzais, 1980; Wannier, 1980). However, laboratory studies have shown that ion-molecule reactions can produce large chemical fractionation effects in hydrogen, carbon, nitrogen and oxygen (Smith and Adams, 1984).

Adams and Smith (1981) calculated the forward and reverse reaction rate coefficients for the ion-molecule isotope exchange reaction

$$^{14}N_2H^+ + {}^{14}N^{15}N \leftarrow\rightarrow {}^{14}N^{15}NH^+ + {}^{14}N_2 + \Delta E$$

at 292K and 80 K. At room temperature there was no perceptible difference between the forward and reverse rates but at 80K a measurable enrichment of ^{15}N in N_2H^+ was obtained. Extrapolating the results to the temperature of dense clouds (10K) under equilibrium conditions they predict ^{15}N to be enriched by a factor of 2.5 ($\delta^{15}N = +1500‰$ relative to initial composition). The main loss of N_2H^+ is by proton transfer to CO, which should be non-selective isotopically

(Adams and Smith, 1981), and therefore if larger molecules are built up incorporating N_2H^+ the they will also carry a ^{15}N enrichment.

The isotopic composition of the carbon in the Bencubbin residues would also be consistent with an ISM origin. The near solar system values of the $^{12}C/^{13}C$ ratio of the carbon associated with N_β suggest a close relationship with normal solar nebula material. Although large ^{13}C enrichments have been achieved in laboratory experiments during ion-molecule reactions (Smith, 1981) the chemistry of carbon in these clouds is much more complex than that of nitrogen (Smith, 1988) and it is possible that isotopic effects would tend to cancel each other out in the larger molecules. For nitrogen on the other hand, most of the ^{14}N enrichments should be in the N_2 molecule, by far the most abundant and least reactive nitrogen bearing molecule, and therefore all the ^{15}N enrichments should be concentrated in the larger molecules.

Although it appears entirely feasible to produce complex organic molecules enriched in ^{15}N in the ISM they must be concentrated and protected prior to the formation of the solar nebula. If they existed in the gas phase during the collapse of the dense cloud the increased temperatures and turbulent convection found in the solar nebula would quickly homogenise them with lighter solar system nitrogen. However, the probability of an isotopic signature surviving in the solar nebula is much greater if it is locked in dust grains (Wasserburg and Papanastassiou, 1982). The only possible mechanism by which this could occur is by large organic molecules binding or condensing on to the surface of growing dust grains. However, the most abundant organic molecules present in the dense clouds (*i.e.* those most easily detected due to their high column densities) are carbon rich, with C/N ratios of up to 11 (Smith, 1988), yet the C/N ratio over the release temperature of N_α and N_β was <1 (and any heating events would tend to volatilize the nitrogen, increasing the C/N ratio). Therefore, it is unlikely that the organic molecules from an ISM could be the origin of the ^{15}N enrichment.

4.6 SUMMARY

It has been shown that the isotopically heavy nitrogen in Bencubbin is present as two components, N_α and N_β, with a uniform isotopic composition enriched in ^{15}N by a factor of two relative to average solar system values ($\delta^{15}N \approx +1000‰$). The carrier phase of the main component, N_α, appears to be a sulphide containing about 30wt.% chromium ($(Cr_{0.67},Fe_{0.33})_2S_3$) with a lattice structure similar to pseudo-hexagonal pyrrhotite. This sulphide contains up to 7wt.% nitrogen, probably located in the large number of vacant sites normally occupied by metal anions. The isotopic composition of the sulphur from the carrier of N_α is light, the lowest $\delta^{34}S$ value recorded being -6.3‰. The identity of the carrier phase of N_β is less well defined, the only possibility so far identified is that it is a carbonaceous phase with a low C/N ratio. The maximum measured $\delta^{13}C$ value of the carbon associated with N_β is +24‰.

The isotopically heavy nitrogen carriers are concentrated along grain boundaries in the metal clasts but how such a component gets to be in the silicate clasts is unknown. As the matrix is derived from melting and fragmentation of the clast material it also contains isotopically heavy nitrogen, but with a variable concentration, primarily dependant on the degree of melting. This is in contrast to the prediction of Prombo and Clayton (1985) who suggested that the matrix might be the primary ^{15}N carrier and contain a nitrogen component with a $\delta^{15}N$ value well in excess of +1000‰. There are also a number of nitrogen components with $\delta^{15}N$ values close to normal solar system values;

(1) adsorbed atmospheric nitrogen and terrestrial organic contamination,

(2) 5 - 10ppm nitrogen in the metal clasts released by dissolving the metal; there is possibly a similar component in the silicate clasts and

(3) the majority of the nitrogen present in chondritic clasts is isotopically heavy compared to normal solar system material, but significantly lighter than the other materials in Bencubbin. The release profile from

these clasts is also different to the rest of the meteorite. Therefore it is believed that the heavy nitrogen present was acquired during the shock melting event.

The distribution of heavy nitrogen within Bencubbin, concentrated in the metal and silicate clasts rules out processes operating during or after the formation of the regolith as a possible origin of the ^{15}N enrichment. The scale of the enrichment also excludes any processes operating in the solar nebula or on the parent body other than a few reactions under unfeasibly extreme non-equilibrium conditions. Therefore, the heavy nitrogen must be from presolar grains which did not mix with normal solar system nitrogen. The heavy nitrogen and associated carriers could have been produced in the dense molecular cloud from which the solar nebula formed but the C/N ratio may be too low for such an origin. A more likely scheme is that the isotopic composition of the nitrogen simply reflects its nucleosynthetic origin. The chromium rich sulphides may be condensates from a cooling supernova envelope, with non-equilibrium helium burning during the supernova explosion producing the isotopically heavy nitrogen and relatively light carbon.

The presence of presolar sulphides in metal which is believed to have suffered little processing since it condensed implies that conditions in the solar nebula were far from chemical equilibrium. The thermal stability of sulphides is relatively low and therefore either;

(1) the maximum temperature of the region of the solar nebula from which Bencubbin formed was never very hot (<1000K) or

(2) if the nebula was hot the sulphides were not introduced until the metal had condensed and the temperature dropped significantly.

CHAPTER 5
CONCLUSIONS

5.1 SUMMARY AND CONCLUSIONS

A study of the distribution and isotopic composition of nitrogen in metal rich meteorites has been undertaken using a high sensitivity static vacuum mass spectrometer, allowing analysis of samples 2-3 orders of magnitude smaller than that of conventional dynamic vacuum instruments. Further development of the stepped heating technique has also be accomplished, to quickly remove terrestrial contamination from metal samples and also for the characterisation of individual nitrogen components within a sample. An on-line laser microprobe was also developed for the extraction of carbon and nitrogen from solid samples. This technique is successful at releasing nitrogen from discrete target areas for $\delta^{15}N$ and nitrogen concentration measurements. For samples containing >100ppm nitrogen the uncertainty on $\delta^{15}N$ value measurements is almost comparable with those obtained by more conventional techniques.

Nitrogen in the solar nebula

In general the results are comparable, and in some cases superior, to previously published values. One of the main aspects of this study has been to investigate further the wide range of nitrogen isotopic variation in meteoritic material and why nitrogen should have been so apparently isotopically heterogeneous in the solar nebula.

Whole-rock samples of iron meteorites display a wide range of $\delta^{15}N$ values, from -96 to +156‰, although the variability in the isotopic composition from any genetic group is generally less than 20‰. The difference in $\delta^{15}N$ value between the groups appears to be due to isotopic variation in the solar nebula. The scale of the $\delta^{15}N$ variations together with the lack of any co-variation with primary

fractionation of other elements make the nitrogen isotopic variations difficult to explain by any fractionation process which may have been occurring in the solar nebula. Therefore, the range in $\delta^{15}N$ values in the iron meteorites is primarily controlled by primordial heterogeneity in the solar nebula.

There appears to have been four distinct nitrogen reservoirs in the region of the solar nebula sampled by the iron meteorite parent bodies. The lightest $\delta^{15}N$ values (-96 to -74‰) are characteristic of the majority of magmatic iron meteorites (groups IIAB, IIC, IIIAB and IIIE). The two main non-magmatic groups (IAB and IIICD) also have distinctive $\delta^{15}N$ values between -66 and -55‰, as do group IIC irons, with $\delta^{15}N$ values typically around +150‰. The remaining groups (IID, IIE, IIF, IIIF, IVA and IVB), all but one of which contain 15 or fewer members, together with a large proportion of the ungrouped irons analysed by Prombo (1984) have $\delta^{15}N$ values concentrated around 0‰.

A number of processes or sources of nitrogen must have contributed to the large nitrogen isotopic heterogeneity in the solar nebula. Two sources have been identified from this study. One may be associated with the observed trend of increasing $\delta^{15}N$ value with increasing metallographic cooling rate of the iron meteorites. Such a trend suggests that decay of a short lived radionuclide, probably ^{26}Al, was the primary heat source of at least some of the iron meteorite parent bodies. As one of the most likely sites of ^{26}Al synthesis is a nova explosions, injection of live ^{26}Al into the proto-solar nebula would be accompanied by large amounts of nitrogen enriched in ^{15}N. The time scale of these events, indicated by the short half-life of ^{26}Al, must have been rapid enough to prevent total equilibration of the nitrogen with normal solar nebula nitrogen.

Another source of isotopically heavy nitrogen has been identified through a detailed study of the Bencubbin meteorite. Two nitrogen components, both with a $\delta^{15}N$ value of about +990‰, have been found in this meteorite. The carrier of the more abundant component, N_α, on the evidence gathered during this

investigation is $(Cr_{0.67}Fe_{0.33})_2S_3$, with a structure similar to pseudo-hexagonal pyrrhotite. The identity of the minor component, N_β, is not well defined but appears to be associated with carbon with a $\delta^{13}C$ value >+24‰. If N_β is carbonaceous, as indicated by its resistance to acid attack and decomposition temperature, then it has a C/N ratio <1.

The abundance of these two components in the meteorite dominate the whole-rock $\delta^{15}N$ measurements. A light nitrogen component is also present in the meteorite, possibly indigenous to the metal and silicate clasts, which is lost upon acid dissolution. This component could not be resolved, but may be more typical of solar system nitrogen and if so is present at around the 6ppm level. The rare chondritic clasts present in this meteorite have $\delta^{15}N$ values (+209 and +285‰) which are much lighter than the metal clasts (+868‰), silicate clasts (+789‰) or matrix (+878 and +888‰). The release profiles indicate that the chondritic clasts acquired their heavy nitrogen from the other components during the shock heating event.

In the metal clasts N_α appears to be concentrated along the grain boundaries. Such a location precludes incorporation of the heavy nitrogen carriers into the clasts during or after the brecciation event and the scale of the enrichment suggests a presolar signature. The favoured origin for the ^{15}N enrichment is one of nucleosynthesis in a supernova. Explosive helium burning will produce large amounts of ^{15}N but little excess ^{13}C, and explosive oxygen burning should lead to condensation of Cr- and Ti-rich sulphides upon cooling. However, it is not clear how the products from the two non-adjacent shells of the supernova can be incorporated into the same mineral. The presence of a presolar sulphide is further evidence that at least part of the solar nebula did not achieve very high temperatures (≈1800K).

Nitrogen in the iron meteorite parent bodies

A relatively detailed study of group IIIAB, a typical magmatic iron meteorite group, has allowed an understanding of the behaviour of nitrogen during core formation. With increasing Ni content (a measure of the extent of crystallisation) the nitrogen concentration appears to fall and the $\delta^{15}N$ value becomes heavier. This indicates that as the core cools nitrogen is being lost from the molten metal with an associated fractionation such that the residual nitrogen is enriched in ^{15}N. Towards the end of crystallisation of the IIIAB core agitation of the metal during pallasite formation appears to have caused a major loss of nitrogen from the liquid metal, producing the wide range of relatively heavy $\delta^{15}N$ values and low nitrogen concentrations observed by Prombo (1984).

The IAB iron meteorites, a large non-magmatic group of irons, has also been studied in detail. These meteorites appear to define a trend of slightly decreasing $\delta^{15}N$ value, and possibly increasing nitrogen concentration, with increasing Ni content. Although there is a degree of uncertainty in the definition of these trends they are clearly in the opposite direction to that displayed by the IIIAB irons. Therefore, any model of their formation process which requires fractional crystallisation of a large pool of molten metal (*e.g.* Kracher, 1985) is precluded. The almost uniform $\delta^{15}N$ value of these meteorites suggest formation in the interior of a parent body rather than in a large shock heated regolith as the latter would probably produce a wide spectrum of $\delta^{15}N$ values due to the likelihood of different degassing histories for each iron.

Unlike carbon, no large isotopic fractionations between co-existing phases exist for nitrogen. However, there is a small fractionation between the kamacite and taenite portions of the Widmannstätten structure, with taenite containing 3 times more nitrogen and with a $\delta^{15}N$ value up to 4.6‰ lighter. The results of replicate analyses of a number of irons indicate that the sampling method employed coped with the isotopic heterogeneity but was less successful in obtaining representative measurements of the nitrogen content, particularly in

those irons with coarser grain size. The isotopic fractionation between the two phases may be due to either fractionation during preferential loss of nitrogen from cooling kamacite or isotopic equilibration between the two phases. It is possible that a combination of the these two processes is responsible. The small range in isotopic composition displayed by most members of group IAB may be due to loss of nitrogen from the kamacite as it is the IAB irons with the most kamacite which have the least amount of nitrogen and heaviest $\delta^{15}N$ values.

Four iron meteorites have low nitrogen concentrations and heavy $\delta^{15}N$ values (up to 40‰ heavier) compared to other members of their respective groups. Each of these meteorites displays evidence of extensive shock followed by cosmic reheating, resulting in recrystallisation of the metal. It is therefore concluded that one effect of recrystallisation is to cause up to a 90% loss of nitrogen from the metal. Nitrogen present in acid insoluble phases, *e.g.* graphite, phosphides, *etc.*, appears not to be affected and so retain the original isotopic signature.

5.2 FUTURE RESEARCH

Iron meteorites

To date only just over 6% of the known collection of iron meteorites have been analysed for their nitrogen isotopic composition in total. Therefore, the discussion in Chapter 3 and the resulting conclusions may not be based on a statistical sample. As more samples are analysed what at first appeared to be like simple processes may become more complicated or an apparently complex problem may turn out to have a simple solution. Three particular aspects of this study require further work in order to:

(1) constrain the 4 fields of nitrogen concentration and $\delta^{15}N$ values shown in Figure 3.17, with particular emphasis on including a large number of analyses from all the groups rather than just a few.

(2) confirm the trend of $\delta^{15}N$ value versus cooling rate as this may have significant cosmochemical implications.

(3) define the $\delta^{15}N$ value and nitrogen concentration variations with respect to Ni content, particularly for group IAB.

The presence of trends similar to those already identified in various magmatic and non-magmatic groups would be a good test of the explanations proposed in the case of groups IAB and IIIAB. Two of the IIIAB irons analysed by Prombo (1984) do not fall on the fractionation line defined by other members of the group, suggesting that either the core of this parent body was not homogeneous or that the parent body had, to some extent, a raisin-bread structure. If the latter is true, nitrogen may be used to investigate the structure of iron meteorite parent bodies.

The chemical classification of iron meteorites developed by Wasson and co-workers fails to classify 14% of all irons. As these irons are believed to represent approximately 50 different parent bodies (Scott, 1978) determination of their nitrogen content and $\delta^{15}N$ value could allow:

(1) a search for distinctive $\delta^{15}N$ values in those iron meteorites - are more than four nitrogen reservoirs sampled by the iron meteorite parent bodies, or will a full survey of the ungrouped irons reveal a broad spectrum of $\delta^{15}N$ values?

(2) some form of genetic classification where the chemical classification scheme fails, allowing trace element investigations of irons with similar $\delta^{15}N$ values.

Bencubbin

A number of problems remain unsolved in this unusual and complex meteorite. The origin of the ^{15}N enrichment, and its survival, could be investigated further by better characterisation of the N_β component, which was precluded during this study as the original residue was completely consumed in

performing the carbon and nitrogen analyses. Preparation of a larger amount of N_β would allow simultaneous extraction of carbon and nitrogen during a stepped combustion, yielding much more detailed information about any coupling of carbon and nitrogen. Should this component still prove to be carbonaceous further investigation with an array of analytical equipment (SEM, ion microprobe, pyrolysis GCMS) may allow a full identification of the nature of the carrier.

The proposed origin of the the ^{15}N enrichment of N_α, a chromium-rich sulphide, could be tested by measuring the isotopic composition of the chromium and the sulphur present. A search should also be made for titanium. As there are at least two populations of sulphides present in this meteorite, and possibly in the residues as well, the best technique for this study is the ion microprobe. A sample for this purpose has been provided to Dr. Ernst Zinner at the University of Washington, St. Louis.

Pallasites

The pallasites, meteorites composed of Fe-Ni metal and olivine-rich silicates, are believed to have formed at the core-mantle interface of the IIIAB parent body. Such samples offer the possibility of yielding information on the relative abundance and isotopic composition of nitrogen in co-existing core and mantle materials. Not only is such information important with regards to identifying genetic links between iron and stony meteorites but may also allow a better understanding of the nitrogen inventory of the Earth, its initial nitrogen isotopic composition and its volatile degassing history, there being no direct means of studying the core of the planet.

Prombo and Clayton (1984) analysed the metal and silicate portions of 5 pallasites. They found that the silicate portions of the meteorites had $\delta^{15}N$ values considerably heavier than the metal phase, by up to 80‰, due to the production of spallogenic nitrogen. The cosmic ray exposure age of only two pallasites has been determined, and the results of Prombo and Clayton (1984) indicate that the

samples they analysed were partially shielded. Correction for the spallogenic nitrogen could be made if the total flux of cosmic rays was accurately known for each sample.

Laser microprobe

The sensitivity of the static vacuum mass spectrometers available at the time of this study were such that their minimum sample size requirements were approximately 1ng for isotopic measurement of carbon or nitrogen. This excluded many low carbon or nitrogen samples from laser microprobe examination, and for the rest, multiple pulses of the laser were often required to liberate sufficient gas, thereby reducing the spatial resolution.

Recently, Dr. I. P. Wright and Mr. S. J. Prosser have designed and built a new mass spectrometer for the purpose of $\delta^{13}C$ measurements with a minimum sample size requirement 2-3 orders of magnitude smaller than that of previous instruments. Development of a facility with a similar capability for nitrogen isotopic measurements are also in hand. Such instruments should realise the possibility of light element stable isotope measurements on gas liberated from a single laser pulse on a wide range of extraterrestrial and geological materials. The following are just a few of the many experiments such a capability would allow:

(1) simultaneous determination of carbon and nitrogen from laser microprobe traverses of graphitic inclusions from iron meteorites is currently being considered using a laser sectioning technique described by Boyd *et al.* (1987) for diamonds. Deines and Wickman (1975) have shown that these inclusions have a variable carbon isotopic composition. Detailed mapping of the isotopic composition of carbon and nitrogen may yield more information of the origin of these inclusions. Also in the iron meteorites, detailed sampling in and around taenite fields may provide better information on the behaviour of nitrogen within the irons during cooling and kamacite growth.

(2) The work performed during this study on the Murchison meteorite using the laser microprobe showed that the refractory inclusions displayed a wide range in $\delta^{15}N$ values. The capability of single pulse analyses may help produce a better understanding of the true range in $\delta^{15}N$ values displayed by such materials. One problem which may be addressed is attempting to establish the distribution of the presolar components such as Cδ and Cβ.

(3) The distribution and carriers of the isotopically heavy nitrogen in the silicate clasts in Bencubbin has not been established, the reason being that to remove the bulk of the silicate material would require using reagents which would destroy any phases such as N_α. High resolution laser microprobe examination of the silicate clasts, using reduced output energies, may yield information on this subject. Similarly, the elusive solar wind nitrogen component mentioned in Section 4.5.1 may be revealed by carefully sampling unmelted clast margins.

(4) Detailed and quick isotopic mapping of carbonate cement growths in sedimentary rocks will be a powerful tool in understanding diagenesis processes. Such a technique is particularly important to the oil industry in identifying and evaluating possible reservoir and cap rocks.

APPENDIX 1
LIST OF SAMPLES STUDIED

The samples studied, their source and catalogue number. BM(NH) = British Museum (Natural History); Ariz. = Arizona Center for Meteorite Studies; AMWG = Antarctic Meteorite Working Group; Camb = Univ. of Cambridge.

SAMPLE	TYPE	SOURCE	CAT. No.
ALH77250	IRON - IAB	AMWG	
ALH77283	IRON - IAB	AMWG	
Barranca Blanca	IRON - IIE	BM(NH)	41187
Bencubbin	ACHANOM	BM(NH)	1931,536
Bischtube	IRON - IAB	BM(NH)	84372
Cape York	IRON - IIIAB	Ariz.	#403.1
Chihuahua City	IRON - IC	BM(NH)	1959,1011
Clark County	IRON - IIIF	BM(NH)	1959,949
Four Corners	IRON - IAB	BM(NH)	1924,331
Henbury	IRON - IIIAB	BM(NH)	1932,1430
Kumerina	IRON - IIC	BM(NH)	1938,220
Monahans	IRON - IIF	BM(NH)	910
Mount Edith	IRON - IIIAB	BM(NH)	1914,1570
Narraburra	IRON - IIIAB	BM(NH)	86997
Odessa	IRON - IAB	Ariz.	#D91.91
Putnam County	IRON - IVA	Ariz.	#246.2
Renazzo	CHOND CR2	Camb.	
Sacramento Mtns.	IRON - IIIAB	BM(NH)	81871
San Cristobal	IRON - IAB	BM(NH)	86763
Sanderson	IRON - IIIAB	BM(NH)	1959,964
Tamarugal	IRON - IIIAB	BM(NH)	1921,5
Thunda	IRON - IIIAB	BM(NH)	1927,1260
Tlacotepec	IRON - IVB	BM(NH)	1959,913
Toluca	IRON - IAB	BM(NH)	33747
Uwet	IRON - IIAB	BM(NH)	1908,171
Wallapai	IRON - IID	Ariz.	#586x
Weatherford	ACHANOM	BM(NH)	1959,987
Winona	CHANOM	BM(NH)	1930,974
Willow Creek	IRON - IIIE	BM(NH)	1937,391
Youndegin	IRON - IAB	BM(NH)	56150

APPENDIX 2
RESULTS OF STEPPED HEATING EXPERIMENTS

Results of stepped combustions for nitrogen of acid residues of iron meteorites from group IAB.

Sample wt.(mg)	ALH77250 magnetic 4.556		ALH77250 non-magnetic 0.864		Bischtube magnetic 5.623	
Temp °C	ppm N	$\delta^{15}N$ (‰)	ppm N	$\delta^{15}N$ (‰)	ppm N	$\delta^{15}N$ (‰)
200	1.4	-11.2	5.2	-8.0	0.3	-4.4
250	4.2	+0.8	26.5	0.0	0.2	-10.7
300	9.3	+5.3	92.9	+5.8	0.2	-4.2
350	10.9	+6.8	99.4	+2.6	0.2	-7.2
400	7.9	+11.1	96.3	+5.0	0.1	-16.5
450	4.2	+10.3	37.8	+0.2	0.1	-23.0
500	2.6	+4.6	25.0	+3.9	-	-
550	2.0	-5.9	21.2	-21.6	0.1	-17.6
600	3.3	-22.9	30.3	-46.5	-	-
650	5.1	-46.5	159.0	-57.0	0.4	-49.4
700	6.8	-62.0	181.5	-62.6	0.5	-60.6
750	10.5	-63.8	148.4	-63.2	0.7	-66.3
800	13.4	-67.3	108.7	-64.4	0.8	-64.1
850	15.0	-67.6	61.5	-60.5	1.0	-64.1
900	11.7	-67.0	30.0	-58.3	1.1	-65.3
950	10.6	-64.0	17.6	-44.0	0.9	-64.3
1000	6.3	-53.3	7.6	-29.0	-	-
1050	0.5	-35.8	-	-	-	-
1100	0.1	nm	8.7	-18.0	-	-
1150	-	-	-	-	-	-
1200	-	-	18.0	-13.9	-	-
1300	-	-	-	-	-	-
total	125.8	-38.9	1175.6	-37.8	6.6	-54.2

Sample wt.(mg)	Four Corners magnetic 6.132		Four Corners non-magnetic 2.251		Odessa 6.936	
Temp °C	ppm N	$\delta^{15}N$ (‰)	ppm N	$\delta^{15}N$ (‰)	ppm N	$\delta^{15}N$ (‰)
200	1.3	+10.7	0.9	-10.0	0.7	-6.5
250	0.8	-6.0	2.0	-31.3	-	-
300	0.5	-4.9	0.7	-14.1	0.9	-6.6
350	-	-	-	-	-	-
400	0.3	-3.6	0.9	-21.1	1.5	-15.1
450	-	-	-	-	0.5	-15.1
500	0.4	+2.5	1.0	-24.5	0.2	nm
550	-	-	-	-	0.3	-15.7
600	0.3	+5.2	1.0	-39.2	0.2	nm
650	-	-	-	-	0.1	nm
700	-	-	4.0	-61.3	0.1	nm
750	-	-	4.4	-69.1	0.1	nm
800	0.6	+14.8	2.8	nm	0.1	nm
850	-	-	0.8	-47.5	0.1	nm
900	0.7	-23.1	nm	nm	0.2	nm
950	0.1	nm	-	-	0.4	-26.9
1000	0.1	nm	nm	nm	0.4	-41.1
1050	-	-	-	-	0.8	-48.2
1100	-	-	nm	nm	0.8	-55.6
1150	-	-	-	-	0.5	-46.9
1200	-	-	0.3	+420	-	-
1300	-	-	0.2	+1200	0.8	-47.9
total	5.1	+0.7	19.0	-26.5	8.6	-28.8

Sample wt.(mg)	Toluca magnetic 8.875		Toluca non-magnetic 0.113	
Temp °C	ppm N	$\delta^{15}N$ (‰)	ppm N	$\delta^{15}N$ (‰)
200	1.5	-10.5	17.7	-10.4
250	0.6	-14.7	-	-
300	1.3	-5.8	101.0	-9.5
350	3.2	-12.2	-	-
400	2.7	-5.9	172.7	nm
450	4.0	-14.6	-	-
500	1.2	-9.4	123.1	-16.5
550	0.9	-13.9	-	-
600	0.5	-18.1	99.2	-6.2
650	0.4	-28.7	-	-
700	0.7	-34.8	163.0	-11.1
750	1.2	-30.3	-	-
800	1.5	-52.8	25.7	-60.5
850	1.0	-52.3	-	-
900	1.0	-53.3	20.4	-62.0
950	1.2	-52.5	-	-
1000	0.4	-55.7	13.3	-68.3
1100	-	-	0.9	nm
1200	-	-	0.9	nm
1300	-	-	-	-
total	23.2	-22.3	737.8	-16.6

Sample wt.(mg)	Youndegin magnetic 4.683		Youndegin non-magnetic 0.385	
Temp °C	ppm N	$\delta^{15}N$ (‰)	ppm N	$\delta^{15}N$ (‰)
200	0.6	-15.9	1.3	nm
250	0.4	-23.8	6.2	-23.0
300	1.4	-23.5	26.5	-20.9
350	3.9	-31.8	64.9	-23.9
400	3.9	-31.2	42.3	-22.0
450	4.2	-39.5	31.4	-23.9
500	1.7	-51.8	33.5	-23.6
550	1.4	-54.0	37.7	-24.4
600	2.3	-58.9	71.4	-28.0
650	3.1	-64.6	109.1	-29.8
700	3.7	-64.8	40.8	-63.3
750	3.2	-62.3	41.6	-65.1
800	2.3	-65.5	30.4	-64.2
850	1.8	-62.1	17.4	-64.0
900	1.7	-57.0	11.7	-64.0
950	1.2	-54.7	-	-
1000	3.0	-54.6	7.3	-67.6
1050	0.8	-48.7	-	-
1100	0.3	nm	1.6	nm
1150	-	-	-	-
1200	-	-	5.7	+17.0
1300	-	-	-	-
total	41.0	-50.1	580.8	-35.2

Results of stepped combustions for nitrogen of iron meteorites from group IIIAB and Uwet from group IIAB.

Sample	Cape York		Henbury magnetic	
wt.(mg)	0.350		0.194	
Temp °C	ppm N	$\delta^{15}N$ (‰)	ppm N	$\delta^{15}N$ (‰)
200	19.2	-8.9	33.5	-44.6
250	-	-	61.3	-32.4
300	21.7	-28.2	47.9	-60.7
350	26.0	-44.4	216.0	-35.1
375	19.7	-65.2	-	-
400	23.4	-82.5	285.6	-42.6
425	32.5	-82.8	-	-
450	35.7	-85.8	268.6	-42.1
475	68.6	-85.8	-	-
500	93.7	-86.6	270.1	-47.1
525	89.1	-86.9	-	-
550	83.7	-84.9	366.0	-58.4
575	66.0	-86.5	-	-
600	70.6	-86.8	542.8	-57.5
625	75.4	-86.2	-	-
650	73.7	-86.1	960.8	-77.0
675	67.4	-84.5	-	-
700	58.6	-85.2	1529.9	-84.5
725	59.1	-85.8	-	-
750	51.7	-83.8	1935.0	-84.2
775	42.9	-86.9	-	-
800	31.4	-85.8	2792.8	-84.5
850	52.9	-83.3	5105.3	-85.2
900	53.7	-87.5	9285.7	-86.5
950	40.0	-86.3	8009.4	-86.4
1000	24.9	-83.6	7711.4	-85.9
1050	14.3	-86.6	6898.0	-86.7
1100	1.7	nm	2041.2	-88.6
1150	-	-	271.1	-78.8
1200	1.4	nm	25.2	-68.7
1300	-	-	-	-
total	1299.1	-82.4	48657.7	-84.2

Sample wt.(mg)	Narraburra magnetic 5.417		Sacramento Mtns. non-magnetic 1.935		Sanderson magnetic 3.237	
Temp °C	ppm N	$\delta^{15}N$ (‰)	ppm N	$\delta^{15}N$ (‰)	ppm N	$\delta^{15}N$ (‰)
200	1.9	+29.9	3.8	-20.0	1.9	+21.8
250	0.3	+24.9	10.8	-19.0	0.5	+11.2
300	0.4	+8.9	31.9	-14.8	0.3	+7.7
350	0.3	+8.4	45.2	-29.4		-
400	0.1	nm	64.0	-27.4	0.6	+10.8
450	-	-	45.7	-35.1		-
500	0.1	nm	32.8	-43.5	0.3	nm
550	-	-	31.7	-36.3		-
600	0.2	nm	28.2	-48.1	0.4	nm
650	-	-	18.3	-50.0	-	
700	0.3	nm	23.3	-36.8	0.6	nm
750	-	-	13.3	-39.7	-	-
800	0.6	+31.1	10.4	-38.2	0.5	nm
850	-	-	8.1	-36.0	-	-
900	0.3	+34.6	6.9	-31.6	0.3	nm
950	-	-	-	-	0.2	nm
1000	-	-	11.3	-24.8	0.1	nm
1050	-	-	-	-	-	-
1100	-	-	6.2	-12.9	-	-
1150	-	-	-	-	-	-
1200	-	-	24.5	-8.0	-	-
1300	-	-	0.5	nm	-	-
total	4.6	+28.6	417.0	-31.6	5.6	+17.0

Sample wt.(mg)	Thunda magnetic 2.100		Thunda non-magnetic 0.157		Uwet 4.281	
Temp °C	ppm N	$\delta^{15}N$ (‰)	ppm N	$\delta^{15}N$ (‰)	ppm N	$\delta^{15}N$ (‰)
200	53.6	-22.5	74.5	-10.7	-	-
250	32.7	-7.2	75.8	-1.2	-	-
300	20.1	+2.5	67.5	-1.6	-	-
350	39.5	+9.1	99.4	-3.1	29.3	-0.6
400	17.1	+10.0	117.8	+0.4	5.0	-9.2
450	8.7	+8.7	53.5	+2.6	17.2	nm
500	4.1	+2.7	27.4	+8.3	29.5	-0.5
550	3.9	+2.0	14.6	+4.7	2.5	-24.6
600	3.0	+5.6	18.5	+4.8	4.3	-41.4
650	2.5	+7.8	-	-	7.2	-73.3
700	2.7	+4.4	28.0	+9.2	21.9	-89.5
750	-	-	-	-	32.4	-94.8
800	3.8	+4.9	29.9	+7.3	22.6	-94.8
850	-	-	-	-	14.9	-94.5
900	7.2	+7.8	17.2	+8.2	13.7	-96.9
950	-	-	-	-	44.1	-98.0
1000	2.1	+12.6	7.0	nm	5.4	-92.0
1050	-	-	-	-	-	-
1100	0.6	nm	1.3	nm	3.1	-78.1
1150	-	-	-	-	-	-
1200	0.2	nm	-	-	0.1	nm
1300	-	-	-	-	0.2	nm
total	201.8	-3.1	632.5	-0.2	253.5	-62.8

Results of stepped combustions for nitrogen of clasts and matrix from Bencubbin.

Sample wt.(mg)	Metal Clast 6.807		Silicate Clast 2.227		Matrix#1 3.894	
Temp °C	ppm N	$\delta^{15}N$ (‰)	ppm N	$\delta^{15}N$ (‰)	ppm N	$\delta^{15}N$ (‰)
400	3.6	+35.9	24.5	+26.9	15.0	+75.9
600	3.4	+179.8	7.6	+245.8	6.6	+622.8
700	1.9	+689.5	4.8	+583.9	2.2	+743.9
750	1.1	+726.1	-	-	1.4	+775.7
800	1.4	+754.4	5.4	+720.5	1.4	+819.5
850	1.2	+687.6	-	-	0.9	+863.6
900	1.2	+773.2	4.0	+756.9	1.1	+928.8
950	7.9	+878.7	-	-	0.6	+762.9
975	19.7	+886.0	-	-	-	-
1000	-	-	22.4	+846.8	0.4	+830.9
1025	22.1	+888.6	-	-	-	-
1050	-	-	2.6	+778.0	0.2	nm
1075	11.7	+885.7	-	-	-	-
1100	-	-	-	-	0.1	nm
1125	5.4	+867.7	-	-	-	-
1200	3.6	+828.6	5.7	+830.0	3.7	+984.2
1220	-	-	-	-	0.8	+913.7
1250	4.3	+870.8	-	-	0.8	+996.4
1300	-	-	-	-	0.6	+952.1
total	88.6	+809.3	77.0	+492.8	35.8	+492.1

Sample wt.(mg)	Matrix#2 4.809		Ord. Chondrite Clast 3.368		Carb. Chond. Clast. 4.661	
Temp °C	ppm N	$\delta^{15}N$ (‰)	ppm N	$\delta^{15}N$ (‰)	ppm N	$\delta^{15}N$ (‰)
200	1.0	+9.9	-	-	0.9	+8.8
300	2.3	+8.2	12.0	+5.2	7.9	+36.9
400	7.5	+28.0	2.5	+137.1	8.4	+98.4
450	-	-	2.0	+202.0	4.3	nm
500	7.7	+70.7	3.1	+285.6	6.0	+229.5
550	-	-	2.4	+394.5	8.0	+221.2
600	4.3	+219.2	1.8	242.6	4.0	228.9
650	1.9	+386.0	1.4	+268.9	2.3	+228.9
700	1.9	+416.6	0.9	+247.3	3.1	+189.4
750	2.2	+469.6	1.4	+229.5	2.8	+186.6
800	2.4	+638.6	1.3	+214.8	3.5	+205.9
850	2.4	+699.2	1.4	+194.8	2.4	+230.5
900	3.3	+778.6	0.9	+257.5	2.4	+197.8
950	20.2	+902.6	0.8	+372.2	1.4	+179.8
1000	20.6	+898.1	0.6	+403.0	1.0	+150.3
1050	22.4	+911.6	0.7	+381.9	0.9	nm
1100	14.9	+909.1	0.8	+279.6	1.5	+147.8
1150	1.8	+859.1	-	-	0.5	+148.6
1200	2.7	+901.2	1.8	+364.2	-	-
1250	1.6	+918.5	-	-	0.7	+146.6
1300	1.3	+893.6	-	-	-	-
total	122.5	+713.8	35.8	+181.0	62.0	+165.7

Results of stepped combustions for carbon of clasts and matrix from Bencubbin.

Sample wt.(mg)	Metal Clast 2.727		Silicate Clast 2.329		Matrix#1 4.835	
Temp °C	ppm C	$\delta^{13}C$ (‰)	ppm C	$\delta^{13}C$ (‰)	ppm C	$\delta^{13}C$ (‰)
200	2.4	-25.8	77.9	-25.4	12.6	-28.6
300	10.5	-25.0	-	-	195.9	-27.6
400	7.0	-17.8	1458.6	-21.2	-	-
430	-	-	-	-	188.7	-26.5
500	28.7	-17.6	132.0	-16.5	-	-
550	-	-	-	-	126.0	-23.7
600	2.1	-17.3	118.9	-20.1	-	-
650	-	-	-	-	167.6	-16.6
700	9.1	-13.7	52.5	-13.5	58.8	-12.0
800	10.2	-14.6	123.8	-7.9	51.3	-13.4
850	-	-	3.3	-9.9	-	-
900	23.8	-10.4	1.6	0.0	39.6	-9.7
950	-	-	0.8	-17.9	-	-
1000	16.1	-3.3	0.4	+7.8	37.1	-4.9
1050	-	-	-	-	15.4	+0.1
1100	7.0	-6.5	-	-	15.8	+13.4
1125	-	-	0.8	+4.4	-	-
1150	-	-	-	-	13.8	+32.9
1200	22.0	+1.0	-	-	4.7	+33.1
1250	-	-	4.9	+21.7	5.2	+38.6
1300	2.1	-4.6	-	-	1.0	+43.1
total	141.0	-11.5	1975.6	-19.8	933.5	-18.6

Sample wt.(mg)	Ord. Chond. Clast 10.200		Carb. Chond. Clast 2.816	
Temp °C	ppm C	$\delta^{13}C$ (‰)	ppm C	$\delta^{13}C$ (‰)
200	46.7	-21.6	4.8	-26.6
300	-	-	920.1	-23.0
350	-	-	549.4	-20.8
400	77.5	-31.3	394.5	-14.0
450	-	-	337.7	-4.0
500	100.7	-25.1	1858.0	-3.5
550	-	-	2007.1	-2.0
600	94.9	-24.0	1478.0	-1.5
650	-	-	1058.9	+0.3
700	296.2	-13.4	479.4	-1.5
750	-	-	292.2	-1.0
800	60.7	-14.0	400.2	-2.5
850	50.0	-	111.5	-3.5
900	53.1	-17.1	42.2	-0.6
950	124.9	-11.5	80.2	+0.8
1000	95.7	-13.5	14.6	-10.9
1050	37.2	-11.3	17.8	-12.2
1100	29.0	-10.6	14.6	-7.2
1150	35.4	-12.6	9.6	+2.2
1200	18.5	-6.3	25.9	-3.4
1250	11.8	-5.0	18.1	-15.1
total	1132.3	-16.6	10114.8	-5.5

Results of stepped heating* for nitrogen of acid residues of Bencubbin.
*stepped combustion unless otherwise indicated.

Sample wt.(mg)	6M HCl pyrol. 2.515		6M HCl 0.857		2x6M HCl 0.609	
Temp °C	ppm N	$\delta^{15}N$ (‰)	ppm N	$\delta^{15}N$ (‰)	ppm N	$\delta^{15}N$ (‰)
200	2.5	+24.8	1.0	+169.7	9.1	+517.4
250	1.8	+79.3	1.9	+428.8	-	-
275	-	-	5.2	+247.8	-	-
300	1.1	+153.2	16.0	+654.7	43.3	+445.3
325	-	-	46.7	+882.8	-	-
350	0.6	+197.8	48.9	+953.2	109.0	+664.4
375	-	-	89.8	+984.1	-	-
400	0.5	+233.1	169.9	+974.3	133.3	+856.7
425	-	-	67.4	+952.2	-	-
450	1.0	+776.3	48.8	+949.6	201.1	+925.6
475	-	-	25.7	+985.5	-	-
500	10.0	+831.8	25.3	+936.4	293.3	+982.4
525	-	-	25.1	+828.5	-	-
550	53.3	+924.5	72.3	+974.8	312.5	+999.5
575	-	-	7.2	+661.0	-	-
600	126.7	+968.3	4.6	+626.7	242.0	+991.3
625	-	-	3.6	+820.2	-	-
650	330.2	+992.0	-	-	129.2	+976.8
675	-	-	6.8	+855.4	-	-
700	59.8	+990.4	-	-	71.9	+979.2
750	28.0	+988.7	8.6	+906.5	10.8	+982.8
800	84.5	+992.0	-	-	-	-
850	20.5	+997.4	1.8	+685.1	6.4	+1006.8
900	8.5	+1003.0	-	-	-	-
950	4.0	+971.9	1.2	+462.6	-	-
1000	2.9	+937.4	-	-	-	-
1050	1.9	+936.7	0.8	+683.7	4.8	+582.6
1100	1.1	+994.2	-	-	-	-
1150	0.7	+838.9	-	-	-	-
1200	0.6	+632.8	1.1	+672.5	-	-
1250	0.5	+592.7	-	-	4.3	+524.0
total	740.7	+971.6	679.7	+930.8	1571.0	+926.7

Sample wt.(mg)	12M HCl 0.697		HF/HCl 0.040		HF/HCl pyrol. 0.009	
Temp °C	ppm N	$\delta^{15}N$ (‰)	ppm N	$\delta^{15}N$ (‰)	ppm N	$\delta^{15}N$ (‰)
100	-	-	2.5	nm	-	-
200	2.6	+751.3	25.0	nm	190.9	nm
250	3.2	+680.7	147.5	+215.4	-	-
275	3.6	+782.9	380.0	+58.6	-	-
300	4.2	+824.6	240.0	+73.8	136.4	nm
325	10.2	+900.1	225.0	+227.2	-	-
350	10.8	+963.5	592.5	+457.5	-	-
375	12.5	+978.5	560.0	+480.9	-	-
400	16.6	+980.4	280.0	+600.2	85.2	nm
425	9.3	+1001.2	230.0	+602.5	-	-
450	10.8	+999.7	222.5	+782.0	38.6	nm
475	12.8	+1013.7	542.5	+680.1	-	-
500	16.9	+1026.2	567.5	+792.1	19.3	nm
525	18.9	+1023.8	660.0	+867.4	-	-
550	19.2	+1027.3	722.5	+914.6	15.9	nm
575	17.4	+1025.7	1175.0	+903.0	-	-
600	17.5	+1012.0	690.0	+956.3	9.1	nm
625	6.3	+1047.2	292.5	+1032.6	-	-
650	4.3	+1055.2	215.0	+958.1	27.3	nm
675	-	-	70.0	+880.2	-	-
700	5.7	+1014.4	-	-	53.4	nm
725	-	-	40.0	nm	-	-
750	1.9	+1044.1	-	-	130.7	+587.8
800	1.7	+672.2	52.5	nm	370.4	+755.7
850	-	-	-	-	481.8	+837.0
900	0.6	nm	-	-	637.5	+849.3
950	-	-	-	-	1144.3	+908.8
1000	0.7	nm	107.5	nm	1504.5	+961.0
1050	-	-	-	-	1131.8	+970.9
1100	1.3	+557.4	-	-	294.3	+923.5
1150	-	-	-	-	112.5	+869.1
1200	1.7	+877.1	7.5	nm	81.8	+757.9
total	210.6	+983.0	8047.5	+711.1	6465.7	+902.9

Stepped combustions for carbon of acid residues of Bencubbin.

Sample wt.(mg)	2x6M HCl 0.028		12M HCl 6.407		HF/HCl 1.448	
Temp °C	ppm C	$\delta^{13}C$ (‰)	ppm C	$\delta^{13}C$ (‰)	ppm C	$\delta^{13}C$ (‰)
200	136.0	-26.0	4.1	-12.4	1647.0	-28.3
250	46.7	-19.3	14.5	-12.4	936.4	-19.3
275	150.6	-17.0	-	-	-	-
300	107.4	-11.0	51.6	-8.4	1855.1	-16.8
325	75.1	-6.0	68.5	-3.3	-	-
350	113.4	-1.0	93.6	+1.7	6173.1	+1.3
375	62.2	-3.9	95.4	+2.8	1922.2	-4.3
400	105.5	-2.6	49.8	-2.8	5823.3	+0.9
425	59.6	-1.3	26.7	-8.6	1773.8	-4.9
450	25.7	-2.4	29.1	-8.0	978.8	+3.5
475	61.3	+4.1	16.1	-5.5	-	-
500	45.5	+7.4	23.8	+9.7	837.4	-3.3
525	64.6	+21.8	10.7	+18.6	2247.3	+5.7
550	14.5	+23.7	1.8	+24.3	84.8	+2.4
575	11.5	+18.7	1.7	+15.7	70.7	-19.7
600	6.6	+9.4	1.7	+15.7	120.1	-3.3
630	-	-	-	-	102.5	-27.4
650	9.9	+9.7	1.6	+11.0	113.1	nm
675	-	-	1.0	+7.0	176.7	-9.8
700	1.6	+6.4	0.6	+3.4	155.5	-16.4
725	-	-	0.5	+3.4	120.1	-22.5
750	-	-	0.9	+22.7	95.4	-25.6
800	1.9	+16.6	0.9	+16.4	53.0	-13.1
850	-	-	1.1	+32.4	88.3	+2.0
900	-	-	0.6	+36.7	74.2	-22.2
950	-	-	0.9	+42.9	102.5	-11.0
1000	3.4	+6.6	1.0	+41.3	-	-
1050	-	-	0.5	+42.6	148.4	-12.2
1100	-	-	0.7	+44.1	-	-
1150	-	-	0.9	+46.0	141.3	-27.8
1200	6.6	+28.9	1.8	+62.6	-	-
1250	-	-	4.3	+68.5	162.5	-19.8
1300	-	-	1.5	+50.5	-	-
total	1109.8	-5.8	2507.9	+0.3	6003.5	-4.3

Results of stepped combustions for sulphur of a metal clast and an acid residue of Bencubbin.

Sample wt.(mg)	Metal Clast 23.826		2x6M HCl 2.107	
Temp °C	ppm S	$\delta^{34}S$ (‰)	ppm S	$\delta^{34}S$ (‰)
100	7.8	nm	42.7	nm
200	9.6	nm	71.2	nm
300	3.4	nm	227.8	nm
400	65.1	+1.0	754.6	+2.5
500	2.1	nm	4285.7	-2.2
600	12.2	nm	2363.5	+0.2
700	9.6	nm	284.8	nm
800	7.1	nm	118.6	nm
900	488.5	-1.0	-	-
1000	625.3	-3.6	118.6	nm
1100	528.8	-6.3	-	-
1200	2532.5	-3.4	185.1	nm
total	4292.0	-3.5	8452.6	-1.0

Results of stepped combustions for nitrogen of other meteorites analysed during this study.

Sample wt.(mg)	Renazzo magnetic 4.541		Renazzo non-magnetic 2.465		Winona 6.078	
Temp °C	ppm N	$\delta^{15}N$ (‰)	ppm N	$\delta^{15}N$ (‰)	ppm N	$\delta^{15}N$ (‰)
100	1.1	-0.7	1.9	+7.3	-	-
200	3.9	-7.5	1.1	+18.0	4.4	-10.3
300	18.4	+50.2	2.5	+55.2	46.4	-35.4
350	5.0	+118.0	14.5	+129.9	-	-
400	13.0	+161.7	9.3	+147.8	63.0	nm
450	13.1	+168.6	42.6	+174.5	-	-
500	13.7	+173.7	44.7	+175.0	11.8	-21.2
550	37.3	+174.6	32.5	+169.3	-	-
600	26.0	+173.8	7.9	+160.5	15.9	-10.2
650	25.3	+175.0	35.5	+155.6	-	-
700	48.2	+173.7	44.4	+156.7	2.5	nm
750	67.2	+164.6	-	-	-	-
800	55.1	+165.5	94.7	+164.7	0.6	-0.8
850	41.2	+162.4	26.2	+179.4	-	-
900	42.6	+172.2	6.6	+176	0.4	+22.8
950	18.4	+188.1	2.3	+165.6	-	-
1000	9.3	+201.2	2.1	+169.3	0.4	+26.1
1050	7.7	+166.5	1.1	+132.8	-	-
1100	3.7	+158.0	1.4	+150.5	0.4	+12.6
1150	2.7	+168.8	-	-	-	-
1200	1.6	+166.5	1.1	+144.6	-	-
total	454.5	+163.9	372.4	+162.9	148.8	-25.9

Sample wt.(mg)	Kakangari 2.853		Uwet 11.404		Weatherford metal 6.189	
Temp °C	ppm N	$\delta^{15}N$ (‰)	ppm N	$\delta^{15}N$ (‰)	ppm N	$\delta^{15}N$ (‰)
200	3.4	-2.4	-	-	-	-
250	15.2	-16.5	-	-	-	-
300	13.4	-17.5	-	-	-	-
350	14.0	-16.8	-	-	-	-
400	8.9	-19.2	2.9	+8.6	3.4	-2.9
450	4.8	-15.1	-	-	-	-
500	3.2	-16.3	-	-	-	-
550	1.6	-17.9	-	-	-	-
600	1.2	-21.8	4.5	+5.7	4.4	+14.0
650	0.6	-12.2	-	-	-	-
700	0.4	+16.1	0.6	-13.8	4.1	+19.8
800	0.3	nm	1.2	-71.0	-	-
830	-	-	-	-	5.8	+69.3
850	0.3	nm	-	-	-	-
900	0.4	nm	1.2	-77.2	1.9	+173.2
950	-	-	0.6	-80.8	1.4	+254.0
1000	0.4	-48.2	0.9	-89.4	1.1	+196.8
1050	0.6	-87.4	-	-	0.2	+185.3
1060	-	-	0.9	-78.2	-	-
1100	1.0	-106.2	-	-	0.2	+181.7
1120	-	-	1.0	-71.5	-	-
1200	1.7	-81.2	2.3	-85.6	0.7	+256.7
1240	-	-	3.3	-49.0	-	-
1300	0.8	-48.1	-	-	-	-
total	72.2	-20.1	19.4	-39.4	23.2	+72.8

LIST OF REFERENCES

Adams N. G. and Smith D. (1981) $^{14}N/^{15}N$ Isotope fractionation in the reaction $N_2H^+ + N_2$: interstellar significance. Astrophys. J. **247**, L123-L125.

Alexander C. M. O. (1987) The rims and matrices of unequilibrated ordinary chondrites: origin, metamorphism and alteration. Ph.D. Thesis, Univ. of Essex.

Alexander C. M. O., Arden J. W., McGarvie D. W., Schelhaas N., Ott U., Wright I. P. and Pillinger C. T. (1988) Stable isotopes in the ordinary chondrites: characterisation of isotopically anomalous phases. Lunar Planet. Sci. **XIX**, 5.

Anders E. and Ebihara M. (1982) Solar system abundances of the elements. Geochim. Cosmochim. Acta **46**, 2363-2380.

Anders E. (1980) Local and exotic components of primitive meteorites, and their origin. Phil. Trans. R. Soc. Lond. A **323**, 287-304.

Anders E., Hayatsu R. and Studier M. H. (1973) Organic compounds in meteorites. Science **182**, 781-790.

Armstrong T. M. and Alsmiller R. G. (1971) Calculation of cosmogenic radionuclides in the Moon and comparison with Apollo measurements. Proc. Lunar Sci. Conf. **2nd**, 1729-1745.

Arnould M. (1988) Nucleosynthesis contributions to the solar nebula. Phil. Trans. R. Soc. Lond. A **323**, 251-267.

Arnould M. and Beelen W. (1974) More about the nucleosynthesis of the nuclei between carbon and neon. Astron. Astrophys. **33**, 215-230.

Arrhenius G. and Alfven H. (1971) Fractionation and condensation in space. Earth Planet. Sci. Lett. **10**, 253-267.

Arrhenius G., Fitzgerald R., Markus S. and Simpson C (1978) Isotope fractionation under simulated space conditions. Astrophys. Space Sci. **55**, 285-297.

Ash R. D., Wright I. P., Pillinger C. T., Lewis R. S. and Anders E. (1987) An investigation of carbon and nitrogen isotopes in Cδ and the effects of grain size upon combustion temperature. Meteoritics **22**, In Press.

Audouze J. and Vauclair S. (1980) Introduction to nuclear astrophysics. Reidel, Dordrecht , 167pp.

Basov N. G., Belenov E. M., Isakov V. A., Markin E. P., Oraevskii A. N. and Romaneko V. I. (1977) New methods of isotope separation. Sov. Phys. Usp. **20**, 209-225.

Becker R. H. (1987) Heavy nitrogen in the Bells carbonaceous chondrite. Lunar Planet. Sci. **XVII**, 52-53.

Becker R. H. and Clayton R. N. (1975) Nitrogen abundances and isotopic compositions in lunar samples. Proc. Lunar Sci. Conf. **6th**, 2131-2149.

Becker R. H. and Epstein S. (1982) Carbon, hydrogen and nitrogen isotopes in solvent-extractable organic matter from carbonaceous chondrites. Geochim. Cosmochim. Acta **46**, 97-103.

Becker R. H. and Pepin R. O. (1984) The case for a Martian origin for the shergottites: nitrogen and noble gases in EETA79001. Earth Planet. Sci. Lett. **69**, 225-242.

Becker R. H., Clayton R. N. and Mayeda T. K. (1976) Characterisation of lunar nitrogen components. Proc. Lunar Sci. Conf. **7th**, 441-458.

Begemann F., Weber H. W., Vilcsek E. and Hintenberger H. (1976) Rare gases and ^{36}Cl in stony-iron meteorites: cosmogenic elemental production rates, exposure ages, diffusion losses and thermal histories. Geochim. Cosmochim. Acta **40**, 353-368.

Berkley J. L., Taylor G. J., Keil K., Harlow G. E. and Prinz M.(1980) The nature and origin of ureilites. Geochim. Cosmochim. Acta **44**, 1579-1597.

Bild R. W. (1977) Silicate inclusions in group IAB irons and a relation to the anomalous stones Winona and Mt. Morris. Geochim. Cosmochim. Acta **41**, 1439-1458.

Bowman C. T. (1976) Kinetics of pollutant formation and destruction in combustion. Prog. Energy Combust. Sci. **1**, 33-45.

Boyd S. R., Mattey D. P., Pillinger C. T., Milledge H. J., Mendelssohn M. J. and Seal M. (1987) Multiple growth events during diamond genesis: an integrated study of carbon and nitrogen isotopes and nitrogen aggregation state in coated stones. Earth Planet. Sci. Lett. **86**, 341-353.

Boyd S. R., Wright I. P., Franchi I. A. and Pillinger C. T. (1988) Preparation of sub-nanomole quantities of nitrogen gas for stable isotopic analysis. J. Phys. E.: Sci. Instrum., In Press.

Brown P. W. and Pillinger C. T. (1981) Nitrogen concentrations and isotopic ratios from separated lunar soils. Meteoritics **16**, 298.

Buchwald V. (1961) The iron meteorite "Thule", North Greenland. Geochim. Cosmochim. Acta **25**, 95-98.

Buchwald V. (1975) Handbook of iron meteorites. Univ. Calif. Press, Berkley, 3 vols., 1418pp.

Buchwald V. (1977) The mineralogy of iron meteorites. Phil. Trans. R. Soc. Lond. A **286**, 453-491.

Buchwald V. and Scott E. R. D. (1971) First nitride (CrN) in iron meteorites. Nat. Phys. Sci. **233**, 113-114.

Burbidge E. M., Burbidge G. R., Fowler W. A. and Hoyle F. (1957) Synthesis of the elements in stars. Rev. Mod. Phys. **29**, 547-650.

Burgess R. (1987) An investigation of sulphur in carbonaceous and enstatite chondrites by stepped combustion. Ph.D. Thesis,. Open Univ.

Cameron A. G. W. (1982) Elemental and nuclide abundances in the solar system. In: Essays in Nuclear Astrophysics (ed. C. A. Barnes, D. D. Clayton and D. N. Schramm), Camb. Univ. Press, Cambridge, 23-43.

Carr L. P., Wright I. P. and Pillinger C. T. (1985) Nitrogen content and isotopic composition of lunar breccia 79035: a high resolution study. Meteoritics **20**, 622-623.

Carr R. H. (1985) High sensitivity stable carbon isotope ratio mass spectrometer: instrument development and applications. Ph.D Thesis, Univ. Cambridge.

Carr R. H., Wright I. P., Joines A.W. and Pillinger C. T. (1986) Measurement of carbon stable isotopes at the nanomole level: a static mass spectrometer and sample preparation technique. J. Phys. E.: Sci. Instrum. **19**, 798-808.

Caughlan C. (1977) The CNO cycles. In: CNO Isotopes in Astrophysics (ed. J. Audouze). Reidel, Dordrecht , 121-131.

Chang S., Lawless J., Romiez M., Kaplan I. R., Petrowski C., Sakai H. and Smith J. W. (1974) Carbon, nitrogen and sulphur in lunar fines 15012 and 15013: abundances, distribution and isotopic compositions. Geochim. Cosmochim. Acta **38**, 853-872.

Chuang Y. Y., Hsieh K. C. and Chang Y. A. (1986) A thermodynamic analysis of the phase equilibria of the Fe-Ni system above 1200K. Metal. Trans. A **17**, 1373-1380.

Clarke R. S., Jarosewich E., Goldstein J. I. and Baedecker P. A. (1980) Antarctic iron meteorites from Allan Hills and Purgatory Park. Meteoritics **15**, 273-274.

Clayton D. D. and Ramaduri S. (1977) On presolar meteoritic sulphides. Nature **265**, 427-428.

Clayton R. N. and Mayeda T. K. (1978a) Genetic relations between iron and stony meteorites. Earth Planet. Sci. Lett. **40**, 168-174.

Clayton R. N. and Mayeda T. K. (1978b) Multiple parent bodies of polymict brecciated meteorites. Geochim. Cosmochim. Acta **42**, 325-327.

Clayton R. N. and Thiemens M. H. (1980) Lunar nitrogen: evidence for secular change in the solar wind. In: The Ancient Sun (ed. R. O. Pepin, J. A. Eddy and R. B. Merril), 463-473.

Clayton R. N. and Mayeda T. K. (1988) Ureilites are not igneous differentiates. Lunar Planet. Sci. **XIX**, 197-198.

Clayton R. N., Grossman L. and Mayeda T. K. (1973) A component of primitive nuclear composition in carbonaceous meteorites. Science **182**, 485-488.

Clayton R. N., Onuma N. and Mayeda T. K. (1976) A classification of meteorites based on oxygen isotopes. Earth Planet. Sci. Lett. **30**, 10-18.

Clayton R. N., Mayeda T. K., Olsen E. J. and Prinz M. (1983) Oxygen isotopic relationships in iron meteorites. Earth Planet. Sci. Lett. **65**, 229-232.

Clayton R. N., Mayeda T. K., Prinz M., Nehru C. E. and Delany J. S. (1986) Oxygen isotopic confirmation of a genetic association between achondrites and IIIAB iron meteorites. Lunar Planet. Sci. **XVII**, 141.

Comerford M. F. (1969) Phosphide and carbide inclusions in iron meteorites. In: Meteorite Research (ed. P. Millman). Reidel, Dordrecht , 780-795.

Craig H. (1953) The geochemistry of the stable carbon isotopes. Geochim. Cosmochim. Acta **3**, 53-92.

Deines P. and Wickman F. E. (1973) The isotopic composition of "graphitic" carbon from iron meteorites and some remarks on the troilitic sulphur of iron meteorites. Geochim. Cosmochim. Acta **37**, 1295-1319.

Deines P. and Wickman F. E. (1975) A contribution to the stable carbon isotope geochemistry of iron meteorites. Geochim. Cosmochim. Acta **39**, 547-557.

Des Marais D. J. (1978) Carbon, nitrogen and sulphur in Apollo 15, 16 and 17 Rocks. Proc. Lunar Sci. Conf. **9th**, 2451-2467.

Doan A. S. and Goldstein J. I. (1969) The formation of phosphides in iron meteorites. In: Meteorite Research (ed. P. Millman). Reidel, Dordrecht, 763-779.

Dodd R. T. (1981) Meteorites: a petrologic-chemical synthesis. Camb. Univ. Press, Cambridge, 368pp.

Dole M., Lane G. A., Rudd D. P. and Zaukelies D. A. (1954) Isotopic composition of atmospheric oxygen and nitrogen. Geochim. Cosmochim. Acta **6**, 65-78.

Eberhardt P., Jungck M. H. A., Meier F. O. and Niederer F. R. (1981) A neon-E rich phase in Orgueil: results obtained on density separates. Geochim. Cosmochim. Acta **45**, 1515-1528.

Epstein S., Krishnamurthy R. U., Cronin J. R., Pizzarello S. and Yuen G. U. (1987) Unusual stable isotope ratios in amino acids and carboxylic acid extracts from the Murchison meteorite. Nature **326**, 477-479.

Exley R. A., Boyd S. R., Mattey D. P. and Pillinger C. T. (1987) Nitrogen isotope geochemistry of basaltic glasses: implications for mantle degassing and structure? Earth Planet. Sci. Lett. **81**, 163-174.

Fallick A. E., Gardiner L. R., Jull A. J. T. and Pillinger C. T. (1980) Instrumental effects in the application of static mass spectrometery to high sensitivity carbon isotope measurements. Adv. Mass Spectrm. **8A**, 309-317.

Fast J. D. (1965) Interaction of metals and gases. Vol. 1. Thermodynamics and phase relations. Philips, Eindhoven

Fish R. A., Goles G. G. and Anders E. (1960) The record in the meteorites III. On the development of meteorites in asteroidal bodies. Astrophys. J. **132**, 243-258.

Franchi I. A., Wright I. P., Gibson E. K. and Pillinger C. T. (1986a) The laser microprobe: a technique for extracting carbon, nitrogen, and oxygen from solid materials for isotopic measurement. Proc. Lunar Sci. Conf. **16th**, 514-524.

Franchi I. A., Wright I. P. and Pillinger C. T. (1986b) Heavy nitrogen in Bencubbin - a light-element isotopic anomaly in a stony-iron meteorite. Nature **323**, 138-140.

Frick U. and Pepin R. O. (1981) Microanalysis of nitrogen isotope abundances:- association of nitrogen with noble gas carriers in Allende. Earth Planet. Sci. Lett. **56**, 64-81.

Fuchs L. H., Olsen E. and Jensen K. J. (1973) Mineralogy, mineral-chemistry, and composition of the Murchison (C2) meteorite. Smithsonian Contrib. Earth Sci. **10**, 1-39.

Ganapathy R. and Larimer J. W. (1980) A meteoritic component rich in volatile elements: its characterisation and implications. Science **207**, 57-59.

Gardiner L. R. and Pillinger C. T. (1979) Static mass spectrometric analysis of active gases. Anal. Chem. **51**, 1230-1236.

Gardiner L. R., Woodcock M. R., Pillinger C. T. and Stepheson A. (1977) Carbon chemistry and magnetic properties of bulk and agglutinate size fractions from soil 15601. Proc. Lunar Sci. Conf. **8th**, 2817-2839.

Geiss J. and Bochsler P. (1982) Nitrogen isotopes in the solar system. Geochim. Cosmochim. Acta **46**, 529-548.

Gibson E. K. and Moore C. B. (1971) The distribution of total nitrogen in iron meteorites. Geochim. Cosmochim. Acta **35**, 877-890.

Gilmour I., Wright I. P. and Pillinger C. T. (1986) Carbon and nitrogen isotopic variations in the organic matter of CM2 carbonaceous chondrites. Lunar Planet. Sci. **XVII**, 995-996.

Goel P. S. (1986) Variable $^{190}Os/^{184}Os$ ratios in acid residues of iron meteorites. Proc. Indian Acad. Sci. (Earth Planet. Sci.) **96**, 81-102.

Goldstein J. I. and Doan A. S. (1972) The effect of phosphorus on the formation of the Widmannstätten pattern in iron meteorites. Geochim. Cosmochim. Acta **36**, 51-69.

Grady M. M. (1982) The content and isotopic composition of carbon in stony meteorites. Ph.D. Thesis, Univ. of Cambridge.

Grady M. M. and Pillinger C. T. (1986) Carbon isotope relationships in winonaites and forsterite chondrites. Geochim. Cosmochim. Acta **50**, 255-264.

Grady M. M. and Pillinger C. T. (1988) ^{15}N-enriched nitrogen in polymict ureilites and its bearing on their formation. Nature **331**, 321-323.

Grady M. M., Swart P. K. and Pillinger C. T. (1982) The variable carbon isotopic composition of type 3 ordinary chondrites. Proc. Lunar Sci. Conf. **13th**, 289-296.

Grady M. M., Wright I. P., Fallick A. E. and Pillinger C. T. (1983) The stable isotopic composition of carbon, nitrogen and hydrogen in some Yamato meteorites. Proc. Eighth Symposium on Antarctic meteorites, 292-305.

Grady M. M., Wright I. P., Swart P. K. and Pillinger C. T. (1985) The carbon and nitrogen isotopic composition of ureilites: implications for their genesis. Geochim. Cosmochim. Acta **49**, 903-916.

Grady M. M., Wright I. P., Carr L. P. and Pillinger C. T. (1986) Compositional differences in enstatite chondrites based on stable carbon and nitrogen isotope measurements. Geochim. Cosmochim. Acta **50**, 2799-2813.

Graham A. L. and Hutchison R. (1974) Is Kakangari a unique chondrite? Nature **251**, 128-129.

Graham A. L., Bevan A. W. R. and Hutchison R. (1985) Catalogue of meteorites. British Museum (Natural History), 460pp.

Greenwood N. N. and Earnshaw A. (1984) Chemistry of the elements. Pergamon Press, Oxford, 1542pp.

Grossman L. and Larimer J. W. (1974) Early chemical history of the solar system. Rev. Geophys. Space Phys. **12**, 71-101.

Grossman L. and Olsen E. (1974) Origin of the high-temperature fraction of C2 chondrites. Geochim. Cosmochim. Acta **38**, 173-187.

Halbout J., Mayeda T. K. and Clayton R. N. (1986) Carbon isotopes and light element abundances in carbonaceous chondrites. Earth Planet. Sci. Lett. **80**, 1-18.

Heidenreich J. E. and Thiemens M. H. (1985) The non-mass-dependant oxygen isotope effect in the electrodissociation of carbon dioxide: a step toward understanding NoMaD chemistry. Geochim. Cosmochim. Acta **49**, 1303-1306.

Hennecke E. W. and Manuel O. K. (1977) Argon, Krypton and Xenon in iron meteorites. Earth Planet. Sci. Lett. **36**, 29-43.

Herbst E. (1985) Chemical evolution in the interstellar medium. In: Cosmic History of the Biogenic Elements and Compounds (ed. J. A. Wood-and S. Chang). NASA, Washington , 43-59.

Hino M. and Sato T. (1971) Infrared absorption spectra of silica gel - $H_2{}^{16}O$, $D_2{}^{16}O$ and $H_2{}^{18}0$ systems. Bull. Chem. Soc. Japan **44**, 33-37.

Hoefs J. (1987) Stable isotope geochemistry. Springer-Verlag, New York, 241pp.

Hoffman J. H., Hodges R. R., McElroy M. B., Donahue T. M. and Kolpin M. (1979) Composition and structure of the Venus atmosphere - results from Pioneer Venus. Science **205**, 49-52.

Howard W. M., Arnett W. D. and Clayton D. D. (1971) Explosive nucleosynthesis in helium zones. Astrophys. J. **165**, 495-507.

Hutchison R. (1986) New data on the Bencubbin polymict stony-iron breccia. Lunar Planet. Sci. **XVII**, 374-375.

Injerd W. G. and Kaplan I. R. (1974) Nitrogen isotopic distribution in meteorites. Meteoritics **9**, 352-353.

Irako M., Oguri T. and Kanomata I. (1975) The static operation mass spectrometer. Japan. J. App. Phys. **14**, 533-543.

Jain A. V. and Lipshutz M. E. (1973) Shock history of mesosiderites. Nat. Phys. Sci. **242**, 26-28.

Javoy M. and Pineau F. (1986) Nitrogen isotopes in mantle materials. Terra Cognita, ICOG VI **6**, 103

Javoy M., Pineau F. and Demaiffe D. (1984) Nitrogen and carbon isotopic composition in the diamonds of Mbuji Mayi (Zaïre). Earth Planet. Sci. Lett. **68**, 399-412.

Jones J. H. and Drake M. J. (1983) Experimental investigations of trace element fractionation in iron meteorites, II: the influence of sulphur. Geochim. Cosmochim. Acta **47**, 1199-1209.

Junk G. and Svec H. J. (1958) The absolute abundance of the nitrogen isotopes in the atmosphere and compressed gas from various sources. Geochim. Cosmochim. Acta **14**, 234-243.

Kallemeyn G. W., Boynton W. V., Willis J. and Wasson J. T. (1978) Formation of the Bencubbin polymict meteorite breccia. Geochim. Cosmochim. Acta **42**, 507-515.

Kaplan I. R. (1975) Stable isotopes as a guide to biogeochemical processes. Proc. R. Soc. Lond. B **189**, 183-211.

Kaplan I. R. and Hulston J. R. (1966) The isotopic abundance and content of sulphur in meteorites. Geochim. Cosmochim. Acta **30**, 479-496.

Keeling D. C., Marti K. and Newsom H. E. (1987) Nitrogen anomalies in Weatherford metal clasts. Meteoritics **22**, In press.

Kelley S. and Turner G. (1987) Laser probe ^{40}Ar-^{39}Ar investigation of the "unique" meteorite Bencubbin. Meteoritics **22**, In Press.

Kelly W. R. and Larimer J. W. (1977) Chemical fractionations in meteorites - VIII. Iron meteorites and the cosmochemical history of the metal phase. Geochim. Cosmochim. Acta **41**, 93-111.

Kerridge J. F. (1982a) Whence so much ^{15}N? Nature **295**, 643-644.

Kerridge J. F. (1982b) Nitrogen isotope systematics in meteorites. Meteoritics **17**, 235-236.

Kerridge J. F. (1985) Carbon, hydrogen and nitrogen in carbonaceous chondrites: abundances and isotopic compositions in bulk samples. Geochim. Cosmochim. Acta **49**, 1707-1714.

Kothari B. K. and Goel P. S. (1974) Total nitrogen in meteorites. Geochim. Cosmochim. Acta **38**, 1493-1507.

Kracher A. (1982) Crystallisation of a S-saturated Fe, Ni melt, and the origin of iron meteorite groups IAB and IIICD. Geophys. Res. Lett. **9**, 412-415.

Kracher A. (1985) The evolution of partially differentiated planetesimals: evidence from iron meteorite groups IAB and IIICD. Proc. Lunar Sci. Conf. **15th**, 689-698.

Kracher A. and Wasson J. T. (1982) The role of S in the evolution of the parental cores of the iron meteorites. Geochim. Cosmochim. Acta **46**, 2419-2426.

Kracher A., Willis J. and Wasson J. T. (1980) Chemical classification of iron meteorites - IX. A new group (IIF), revision of IAB and IIICD, and data on 57 additional irons. Geochim. Cosmochim. Acta **44**, 773-787.

Kung C. C. and Clayton R. N. (1978) Nitrogen abundances and isotopic compositions in stony meteorites. Earth Planet. Sci. Lett. **38**, 421-435.

Labes M. M., Love P. and Nichols L. F. (1979) Polysulphur nitride - a metallic superconducting polymer. Chem. Revs. **79**, 1-15.

Larimer J. W. (1975) The effect of C/O ratio on the condensation of planetary material. Geochim. Cosmochim. Acta **39**, 389-392.

Lattimer J. M. and Grossman L. (1978) Chemical condensation sequences in supernova ejecta. Moon and Planets **19**, 169-184.

Lee T. (1978) A local proton irradiation model for isotopic anomalies in the solar system. Astrophys. J. **224**, 217-226.

Leslie W. C., Hornbogen E. and Dieter G. E. (1962) The structure of shock-hardened iron before and after annealing. J. Iron Steel Inst. **200**, 622-633.

Letolle R. (1980) Nitrogen-15 in the natural environment. In: Handbook of Environmental Isotope Geochemistry, Vol. I (ed. P. Fritz and J. C. Fontes). Elsevier, Amsterdam , 407-433.

Lewis R. S. (1985) Noble gases in the unique breccia, Bencubbin. Meteoritics **20**, 698-699.

Lewis R. S., Anders E., Wright I. P., Norris S. J. and Pillinger C. T. (1983) Isotopically anomalous nitrogen in primitive meteorites. Nature **305**, 767-771.

Lewis R. S., Tang M., Wacker J. F., Anders E. and Steel E. (1987) Interstellar diamonds in meteorites. Nature **236**, 160-162.

Lovering J. F. (1962) The evolution of the meteorites - evidence for the co-existence of chondritic, achondritic and iron meteorites in a typical parent meteorite body. In: Researches on Meteorites (ed. C. B. Moore). Wiley, New York , 179-197.

Malvin D. J., Wang D. and Wasson J. T. (1984) Chemical classification of iron meteorites - X. Multielement studies of 43 irons, resolution of group IIIE from IIIAB, and evaluation of Cu as a taxonomic parameter. Geochim. Cosmochim. Acta **48**, 785-804

Manuccia T. J. and Clark M. D. (1976) Enrichment of ^{15}N by chemical reactions in a glow discharge at 77K. App. Phys. Lett. **28**, 372-374.

Mariotti A. (1983) Atmospheric nitrogen is a reliable standard for natural ^{15}N abundance measurements. Nature **303**, 685-687.

Mariotti A. (1984) Natural ^{15}N abundance measurements and atmospheric nitrogen standard calibration. Nature **311**, 251-252.

Mason B. and Jarosewich E. (1967) The Winona meteorite. Geochim. Cosmochim. Acta **31**, 1079-1099.

Mason B. and Nelen J. (1968) The Weatherford meteorite. Geochim. Cosmochim. Acta **32**, 661-664.

McCall G. J. H. (1968) The Bencubbin meteorite: further details, including microscopic character of host material and two chondrite enclaves. Mineral. Mag. **36**, 726-739.

McElroy M. B., Yung Y. L. and Nier A. O. (1976) Isotopic composition of nitrogen: implications for the past history of Mars' atmosphere. Science **194**, 70-72.

McGarvie D. W., Wright I. P., Grady M. M., Pillinger C. T. and Gibson E. K. (1987) A stable carbon isotopic study of types 1 and 2 carbonaceous chondrites. Proc. Eleventh Symposium on Antarctic meteorites, 179-195.

McKeegan K. D., Walker R. M. and Zinner E. (1985) Ion microprobe isotopic measurements of individual interplanetary dust particles. Geochim. Cosmochim. Acta **49**, 1971-1987.

McNaughton N. J., Fallick A. E. and Pillinger C. T. (1982) Deuterium enrichments in type 3 ordinary chondrites. Proc. Lunar Sci. Conf. **13th**, 297-302.

McNaughton N. J., Abell P. I., Wright I. P., Fallick A. E. and Pillinger C. T. (1983) Preparation of nanogram quantities of deuteromethane for stable carbon isotope analysis. J. Phys. E.: Sci. Instrum. **16**, 505-511.

McSween H. Y. (1984) SNC meteorites: are they Martian rocks? Geology **12**, 3-6.

McSween H. Y. (1987) Meteorites and their parent bodies. Cambridge Univ. Press, Cambridge, 237pp.

Minagawa M., Winter D. A. and Kaplan I. R. (1984) Comparison of Kjeldahl and combustion methods for measurement of nitrogen isotope ratios in organic matter. Anal. Chem. **56**, 1859-1861.

Moenke H. H. W. (1974) Silica, the three-dimensional silicates, borosilicates and beryllium silicates. In: The Infrared Spectra of Minerals (ed. V. C. Farmer). Min. Soc. Monograph **4**, 365-382.

Moore C. B., Lewis C. F. and Nava D. (1969) Superior analysis of iron meteorites. In: Meteorite Research (ed. P. Millman). Reidel, Dordrecht, 738-748.

Moren A. E. and Goldstein J. I. (1978) Cooling rate variations of group IVA iron meteorites. Earth Planet. Sci. Lett. **40**, 151-161.

Murty S. V. S., Goel P. S., Minh D. V. and Shukolyukov Y. A. (1983) Nitrogen and xenon in acid residues of iron meteorites. Geochim. Cosmochim. Acta **47**, 1061-1068.

Narayan C. and Goldstein J. I. (1985) A major revision of iron meteorite cooling rates - an experimental study of the growth of the Widmannstätten pattern. Geochim. Cosmochim. Acta **49**, 397-410.

Nash L. K. and Baxter G. P. (1947) The determination of the gases in meteoritic and terrestrial irons and steels. J. Amer. Chem. Soc. **69**, 2534-2544.

Newsom H. E. and Drake M. J. (1979) The origin of metal clasts in the Bencubbin meteoritic breccia. Geochim. Cosmochim. Acta **43**, 689-707.

Nielsen H. P. and Buchwald V. (1981) Roaldite, a new nitride in iron meteorites. Proc. Lunar Sci. Conf. **12th**, 1343-1348.

Niemeyer S. (1979) I-Xe dating of silicate and troilite from IAB iron meteorites. Geochim. Cosmochim. Acta **43**, 843-860.

Nier A. O. (1947) A mass spectrometer for isotope and gas analysis. Rev. Sci. Instrum. **18**, 398-411.

Nier A. O., McElroy M. B. and Yung Y. L. (1976) Isotopic composition of the Martian atmosphere. Science **194**, 68-70.

Norris S. J., Brown P. W. and Pillinger C. T. (1981) Laser pyrolysis for light element stable isotope studies. Meteoritics **16**, 369.

Norris S. J., Swart P. K., Wright I. P., Grady M. M. and Pillinger C. T. (1983) A search for correlatable carbon and nitrogen components in lunar soils and breccias. Proc. Lunar Sci. Conf. **14th**, 200-210.

Norris T. L. (1980) Kinetic model of ammonia synthesis in the solar nebula. Earth Planet. Sci. Lett. **47**, 43-50.

O'Neil J. R. (1986) Theoretical and experimental aspects of isotopic fractionation. In: Stable Isotopes in High Temperature Geological Processes (ed. J. W. Valley, H. P. Taylor and J. R. O'Niel). Revs. Min. **16**, 1-40.

Penzais A. A. (1980) Nuclear processing and isotopes in the Galaxy. Science **208**, 663-669.

Pepin R. O. and Becker R. H. (1982) Nitrogen isotopes in iron meteorites. Meteoritics **17**, 269.

Pernicka E. and Wasson J. T. (1987) Ru, Re, Os, Pt and Au in iron meteorites. Geochim. Cosmochim. Acta **51**, 1717-1726.

Pillinger C. T. (1984) Light element stable isotopes in meteorites - from grams to picograms. Geochim. Cosmochim. Acta **48**, 2739-2766.

Prinz M., Weisberg M. K., Nehru C. E. and Delany J. S. (1987) Bencubbin, Kakangari, Tuscon and Renazzo: a speculative connection between some of their major components. Lunar Planet. Sci. **XVIII**, 800-801.

Prombo C. A. (1984) Nitrogen contents and isotopic composition of metal rich meteorites. Ph.D Thesis, Univ. Chicago.

Prombo C. A. and Clayton R. N. (1983) Nitrogen isotopes in iron meteorites. Meteoritics **18**, 377-379.

Prombo C. A. and Clayton R. N. (1984) Nitrogen abundances and isotopes in co-existing metal and silicates. Lunar Planet. Sci. **XV**, 655-656.

Prombo C. A. and Clayton R. N. (1985) A striking nitrogen isotopic anomaly in the Bencubbin and Weatherford meteorites. Science **230**, 935-937.

Ramdohr P. (1973) The opaque minerals in stony meteorites. Elsevier, Berlin.

Reynolds J. H. (1956) High sensitivity static mass spectrometer for noble gas analysis. Rev. Sci. Instrum. **27**, 928-934.

Richet P., Bottinga Y. and Javoy M. (1977) A review of hydrogen, carbon, nitrogen oxygen, sulphur and chlorine stable isotope fractionation among gaseous molecules. Ann. Rev. Earth Planet. Sci. **5**, 65-110.

Saikumar V. and Goldstein J. I. (1987) An evaluation of the methods for the determining cooling rates of iron meteorites. Meteoritics **22**, In press.

Schaudy R., Wasson J. T. and Buchwald V. F. (1972) The chemical classification of iron meteorites. VI. A reinvestigation of irons with Ge concentrations lower than 1ppm. Icarus **17**, 174-129.

Schultz L., Funk H., Nyquist L. and Signer P. (1971) Helium, neon and argon in separated phases of iron meteorites. Geochim. Cosmochim. Acta **35**, 77-88.

Scott E. R. D. (1972) Chemical fractionation in iron meteorites and its interpretation. Geochim. Cosmochim. Acta **36**, 1205-1236.

Scott E. R. D. (1977) Pallasites - metal composition, classification and relationships with iron meteorites. Geochim. Cosmochim. Acta **41**, 349-360.

Scott E. R. D. (1978) Primary fractionation of elements among iron meteorites. Geochim. Cosmochim. Acta **42**, 1447-1458.

Scott E. R. D. and Bild R. W. (1974) Structure and formation of the San Cristobal meteorite, other IAB irons and group IIICD irons. Geochim. Cosmochim. Acta **38**, 1379-1391.

Scott E. R. D. and Wasson J. T. (1975) Classification and properties of iron meteorites. Revs. Geophys. Space Sci. **13**, 527-546.

Scott E. R. D. and Wasson J. T. (1976) Chemical classification of iron meteorites - VIII. Groups IC, IIE, IIIF and 97 other irons. Geochim. Cosmochim. Acta **40**, 103-115.

Scott E. R. D., Wasson J. T. and Buchwald V. (1973) The chemical classification of iron meteorites - VII. A reinvestigation of irons with Ge concentrations between 25 and 80ppm. Geochim. Cosmochim. Acta **37**, 1957-1983.

Sears D. W. (1978) Condensation and the composition of iron meteorites. Earth Planet. Sci. Lett. **41**, 128-138.

Shima M. (1986) A summary of extremes of isotopic variations in extra-terrestrial materials. Geochim. Cosmochim. Acta **50**, 577-584.

Shukla P. N. and Goel P. S. (1981) Total nitrogen in iron meteorites. Earth Planet. Sci. Lett. **52**, 251-258.

Simpson E. S. and Murray D. G. (1932) A new siderolite from Bencubbin, Western Australia. Mineral. Mag. **23**, 33-37.

Smales A. A., Mapper D. and Fouche K. F. (1967) The distribution of some trace elements in iron meteorites, as determined by neutron activation. Geochim. Cosmochim. Acta **31**, 673-720.

Smith D. (1981) Laboratory studies of isotope exchange in ion-molecule reactions: interstellar implications. Phil. Trans. R. Soc. Lond. A **303**, 535-542.

Smith D. (1988) Interstellar molecules. Phil. Trans. R. Soc. Lond.A **323**, 269-286.

Smith D. and Adams N. G. (1984) Isotope exchange in ion-molecule reactions. In: Ionic Processes in the Gas Phase (ed. M. A. Almoster Ferreira). Reidel, Dordrecht , 41-66.

Sonnet C. P. and Reynolds R. T. (1979) Primordial heating of asteroidal parent bodies. In: Asteroids (ed. T. Gehrels). Univ. Arizona Press, Tuscon, 822-848.

Swart P. K., Grady M. M. and Pillinger C. T. (1983a) A method for the identification and elimination of contamination during carbon isotopic analysis of extraterrestrial samples. Meteoritics **18**, 137-154.

Swart P. K., Grady M. M., Pillinger C.T., Lewis R. S. and Anders E. (1983b) Interstellar carbon in meteorites. Science **202**, 406-410.

Sweeney R. E., Liu K. K. and Kaplan I. R. (1978) Oceanic nitrogen isotopes and their uses in determining the source of sedimentary nitrogen. Dept. Sci. Ind. Res. Bull. **220**, 9-26.

Tang M., Anders E. and Zinner E. (1988) Noble gases, C, N and Si isotopes in interstellar SiC from the Murchison carbonaceous chondrite. Lunar Planet. Sci. **XIX**, 1177-1178.

Thiemens M. H. and Heidenreich J. E. (1983) A mass-independent fractionation of oxygen: a novel isotope effect and its possible cosmochemical implications. Science **219**, 1073-1075.

Tokunaga A. T., Kacke R. F., Ridgway S. T. and Wallace L. (1979) High resolution spectra of Jupiter in the 744-980 inverse centimeter spectral range. Astrophys. J. **232**, 603-615.

Trimble V. (1975) The origin and abundance of the chemical elements. Rev. Mod. Phys. **47**, 877-976.

Truran J. W. (1982) Nuclear theory of novae. In: Essays in Nuclear Astrophysics (ed. C. A. Barnes, D. D. Clayton and D. N. Schramm). Camb. Univ. Press, Cambridge, 467-493.

Voshage H. (1967) Bestrahlungsalter und Herkunft der Eisenmeteorite. Z. Naturforschg. **22a**, 477-506.

Voshage H. and Feldmann H. (1979) Investigations on cosmic-ray-produced nucleides in iron meteorites, 3. Exposure ages, meteoroid sizes and sample depths determined by mass spectrometric analysis of potassium and rare gases. Earth Planet. Sci. Lett. **45**, 293-308.

Wai C. M. and Wasson J. T. (1979) Nebular condensation of Ga, Ge and Sb and the chemical classification of iron meteorites. Nature **282**, 790-793.

Wannier P. G. (1980) Nuclear abundances and evolution of the interstellar medium. Ann. Rev. Astron. Astrophys. **18**, 399-437.

Wannier P. G. and Werner M. W. (1985) Nucleosynthesis and ejection to the interstellar medium of the biogenic elements. In: Cosmic History of the Biogenic Elements and Compounds (ed. J. A. Wood and S. Chang). NASA, Washington, 11-19.

Wasserburg G. J. and Papanastassiou D. A. (1982) Some short-lived nuclides in the early solar system - a connection with the placental ISM. In: Essays in Nuclear Astrophysics (ed. C. A. Barnes, D. D. Clayton and D. N. Schramm). Camb. Univ. Press, Cambridge, 77-140.

Wasson J. T. (1969) The chemical classification of iron meteorites. III. Hexahedrites and other irons with germanium concentrations between 80 and 200ppm. Geochim. Cosmochim. Acta **33**, 859-876.

Wasson J. T. (1970a) Ni, Ga, Ge and Ir in metal of iron-meteorites-with-silicate-inclusions. Geochim. Cosmochim. Acta **34**, 957-964.

Wasson J. T. (1970b) The chemical classification of iron meteorites IV. Irons with Ge concentrations greater than 190ppm and other meteorites associated with group I. Icarus **12**, 407-423.

Wasson J. T. (1974) Meteorites, Classification and properties. Springer-Verlag, New York, 316pp.

Wasson J. T. (1985) Meteorites: their record of early solar-system history. Freeman, New York, 267pp.

Wasson J. T. and Schaudy R. (1971) The chemical classification of iron meteorites - V. Groups IIIC and IIID and other irons with germanium concentrations between 1 and 25ppm. Icarus **14**, 59-70.

Wasson J. T. and Wang J. (1986) A non-magmatic origin of group-IIE iron meteorites. Geochim. Cosmochim. Acta **50**, 725-732.

Wasson J. T., Willis J., Wai C. M. and Kracher A. (1980) Origin of iron meteorite groups IAB and IIICD. Z. Naturforsch. **35**, 781-795.

Weins R. C., Becker R. H. and Pepin R. O. (1986) The case for a martian origin of the shergottites, II. Trapped and indigenous gas components in EETA79001 glass. Earth Planet. Sci. Lett. **77**, 149-158.

Weisberg M. K., Prinz M., Nehru C. E. and Delaney J. S. (1987) Barred olivine-textured Bencubbin major silicates: a ureilite connection. Meteoritics **22**, In press.

Willis J. and Goldstein J. I. (1982) The effects of C, P and S on trace element partitioning during solidification in Fe-Ni alloys. Proc. Lunar Sci. Conf. **13th**, 435-445.

Winnewisser G., Churchwell E. and Walmsley C. M. (1979) Astrophysics of interstellar molecules. In: Modern Aspects of Microwave Spectroscopy (ed. G. W. Chantry). Academic Press, London, 313-435.

Wlotzka F. (1974) Nitrogen In: Handbook of Geochemistry (ed. K. H. Wedepohl). Springer-Verlag, Berlin, P7A-7O.

Wood J. A. (1964) The cooling rates and parent bodies of several iron meteorites. Icarus **3**, 429-459.

Wood J. A. (1979) Review of the metallographic cooling rates of meteorites and a new model for the planetesimals in which they formed. In: Asteroids (ed. T. Gehrels). Univ. Arizona Press, Tuscon, 849-891.

Wright I. P., Boyd S. R., Franchi I. A. and Pillinger C. T. (1988) Determination of high precision nitrogen stable isotope ratios at the sub-nanomole level. J. Phys. E.: Sci. Instrum., In Press.

Zinner E., Tang M. and Anders E. (1987a) Large isotopic anomalies of Si, C, N and noble gases in interstellar silicon carbide from the Murray meteorite. Nature **330**, 730-732.

Zinner E., Fahey A. J., Goswami J. N. and McKeegan K. D. (1987b) Isotopic structures in Murchison hibonites: O, Ca and Ti. Meteoritics **22**, In Press.